frontiers | Research Topics

Uterine fibroid surgery in gynecology and obstetrics and reproduction: lights and shadows

Edited by
Andrea Tinelli, Safak Hatirnaz and Radmila Sparic

Published in
Frontiers in Medicine
Frontiers in Surgery

ISSN 1664-8714
ISBN 978-2-8325-6970-2
DOI 10.3389/978-2-8325-6970-2

Generative AI statement
Any alternative text (Alt text) provided alongside figures in the articles in this ebook has been generated by Frontiers with the support of artificial intelligence and reasonable efforts have been made to ensure accuracy, including review by the authors wherever possible. If you identify any issues, please contact us.

About Frontiers

Frontiers is more than just an open access publisher of scholarly articles: it is a pioneering approach to the world of academia, radically improving the way scholarly research is managed. The grand vision of Frontiers is a world where all people have an equal opportunity to seek, share and generate knowledge. Frontiers provides immediate and permanent online open access to all its publications, but this alone is not enough to realize our grand goals.

Frontiers journal series

The Frontiers journal series is a multi-tier and interdisciplinary set of open-access, online journals, promising a paradigm shift from the current review, selection and dissemination processes in academic publishing. All Frontiers journals are driven by researchers for researchers; therefore, they constitute a service to the scholarly community. At the same time, the *Frontiers journal series* operates on a revolutionary invention, the tiered publishing system, initially addressing specific communities of scholars, and gradually climbing up to broader public understanding, thus serving the interests of the lay society, too.

Dedication to quality

Each Frontiers article is a landmark of the highest quality, thanks to genuinely collaborative interactions between authors and review editors, who include some of the world's best academicians. Research must be certified by peers before entering a stream of knowledge that may eventually reach the public - and shape society; therefore, Frontiers only applies the most rigorous and unbiased reviews. Frontiers revolutionizes research publishing by freely delivering the most outstanding research, evaluated with no bias from both the academic and social point of view. By applying the most advanced information technologies, Frontiers is catapulting scholarly publishing into a new generation.

What are Frontiers Research Topics?

Frontiers Research Topics are very popular trademarks of the *Frontiers journals series*: they are collections of at least ten articles, all centered on a particular subject. With their unique mix of varied contributions from Original Research to Review Articles, Frontiers Research Topics unify the most influential researchers, the latest key findings and historical advances in a hot research area.

Find out more on how to host your own Frontiers Research Topic or contribute to one as an author by contacting the Frontiers editorial office: frontiersin.org/about/contact

Uterine fibroid surgery in gynecology and obstetrics and reproduction: lights and shadows

Topic editors
Andrea Tinelli — Veris delli Ponti Hospital, Italy
Safak Hatirnaz — Medicana Hospital, Türkiye
Radmila Sparic — University of Belgrade, Serbia

Citation
Tinelli, A., Hatirnaz, S., Sparic, R., eds. (2025). *Uterine fibroid surgery in gynecology and obstetrics and reproduction: lights and shadows*. Lausanne: Frontiers Media SA.
doi: 10.3389/978-2-8325-6970-2

Table of contents

frontiers | Frontiers in Surgery

TYPE Editorial
PUBLISHED 25 September 2025
DOI 10.3389/fsurg.2025.1698612

OPEN ACCESS

EDITED AND REVIEWED BY
Stefano Cianci,
University of Messina, Italy

*CORRESPONDENCE
Radmila Sparić
radmila@rcub.bg.ac.rs

RECEIVED 03 September 2025
ACCEPTED 08 September 2025
PUBLISHED 25 September 2025

CITATION
Sparić R, Hatirnaz S and Tinelli A (2025) Editorial: Uterine fibroid surgery in gynecology and obstetrics and reproduction: lights and shadows.
Front. Surg. 12:1698612.
doi: 10.3389/fsurg.2025.1698612

Editorial: Uterine fibroid surgery in gynecology and obstetrics and reproduction: lights and shadows

Radmila Sparić[1,2]*, Safak Hatirnaz[3] and Andrea Tinelli[4]

[1]Faculty of Medicine University of Belgrade, Belgrade, Serbia, [2]Clinic for Gynecology and Obstetrics, University Clinical Center of Serbia, Belgrade, Serbia, [3]School of Health Sciences, Kent University, Istanbul, Türkiye, [4]Department of Obstetrics and Gynecology, CERICSAL (CEntro di RIcerca Clinico SALentino), "Veris Delli Ponti Hospital", Scorrano, Italy

KEYWORDS

fibroid, STUMP (smooth muscle tumours of uncertain malignant potential), cesarean myomectomy, surgery, artificial inteligence

Editorial on the Research Topic
Uterine fibroid surgery in gynecology and obstetrics and reproduction: lights and shadows

The most prevalent benign tumors in women of reproductive age are uterine fibroids. The mainstay for treating symptomatic fibroids that don't respond to less invasive or medicinal treatments is still surgery. Myomectomy, which entails surgically removing fibroids while leaving the uterus intact, is the recommended course of action for women who want to preserve their fertility. Nevertheless, it doesn't stop new fibroids from growing (1–5). Women who have severe disease or no desire for conception may benefit from a hysterectomy, the final therapy that involves removing the uterus and resolves symptoms permanently. The benefit of a hysterectomy is that there is no subsequent recurrence of fibroids, despite the risks involved with major surgery (3, 6). Minimally invasive alternatives include uterine artery embolization (UAE), which deprives fibroids of their blood supply causing shrinkage but may carry pregnancy-related risks. Other noninvasive options such as magnetic resonance-guided focused ultrasound (MRgFUS) or high-intensity focused ultrasound (HIFU) offer thermal ablation of fibroids with symptom relief and uterine preservation. These modalities exhibit low complication rates and suit patients seeking uterus-sparing treatments (1, 3, 7).

Given the prevalence of uterine fibroids and the serious complications they can cause, this research topic consists of excellent, thought-provoking studies that are primarily focused on improving the diagnosis and treatment of these conditions. This work is essential and extremely valuable to both clinical practice and scientific research.

It has long been recognized that acupuncture exerts positive effects on human health and symptoms of various diseases, including uterine fibroids. Chen et al. demonstrated that traditional acupuncture and Chinese herbal medicine are more effective than herbal therapy alone; they reduce uterine and fibroid size, relieve symptoms, improve hormone balance, and improve general quality of life (8).

Enhanced recovery after surgery (ERAS) protocols aim to reduce perioperative discomfort and accelerate recovery. A clinical trial by Mao et al. applied acupuncture as an integral component of ERAS, finding it safe and well tolerated, effectively controlling visceral, incisional, and shoulder pain, and exerting anxiolytic effects when

applied preoperatively. These benefits reduced opioid requirements and adverse effects, shortened hospitalization, and lowered treatment costs (9).

The clinical appearance and fibroid features dictate the unique indications for each therapy approach. Optimizing efficacy and safety requires careful monitoring of fibroid characteristics and how they respond to treatment. Xue et al. identified predictive factors for successful HIFU ablation, noting higher ablation rates —and thus lower resistance—in larger, highly echogenic, irregularly shaped fibroids, as well as those with attenuation bands, anterior wall lesions, or subserosal locations. Conversely, fibroids with necrotic foci exhibited greater resistance to ablation.

Furthermore, tracking fibroid pathogenesis-related biomarkers both before and after surgery is essential for assessing results and recurrence risk. The protocol proposed by Aimagambetova et al. explores correlations between angiogenic factors (e.g., VEGF), fibrotic growth factors (e.g., TGF-β), and clinical parameters such as menorrhagia score and quality of life following organ-preserving uterine artery embolization (10).

Cesarean myomectomy may present certain risks, potentially deterring clinicians. However, research by Güler et al. indicates that cesarean myomectomy, performed via either transendometrial or serosal approaches, does not significantly differ in obstetric, perinatal, or surgical outcomes compared to cesarean section alone. This supports its safety and efficacy as a durable management option for fibroids at delivery.

The advent of new technologies significantly enhances fibroid diagnosis and decision-making by reducing subjectivity. Chen et al. introduced an AI algorithm based on machine and deep learning that improves MRI interpretation objectivity, procedural planning, reduces hysteroscopy duration, intraoperative blood loss, and accelerates postoperative recovery.

Five fascinating case studies that highlight uncommon and difficult clinical situations are included in this edition. There are significant risks for both the mother and the fetus in a twin pregnancy after laparoscopic adenomyomectomy, such as placenta accreta spectrum and uterine rupture. With careful patient screening, Ota et al. reported a successful dichorionic diamniotic twin pregnancy delivered by elective cesarean at 32 weeks.

Dong et al. presented a rare and severe case of a giant 27 cm fibroid causing prolapse through the cervix, deep venous thrombosis, pulmonary embolism, cardiac and renal failure, and shock. Following inferior vena cava filter placement and extensive hysterectomy, the patient fully recovered.

Bićanin-Ilić et al. described a smooth muscle tumor of uncertain malignant potential (STUMP) progressing rapidly to high-grade leiomyosarcoma with uterine rupture, hemoperitoneum, and widespread metastases, highlighting risks of malignant transformation.

Huang et al. reported a case initially diagnosed as a benign leiomyoma that was later identified as endometrial stromal sarcoma with mixed grades and a rare mutation, underscoring how malignancies may masquerade as benign lesions; metastases were found in the pelvis and inferior vena cava.

Hu et al. encountered a rare benign metastasizing leiomyoma with metastases to the anterior abdominal wall involving fascia and muscle, illustrating that histologically benign tumors can sometimes display unusual metastatic patterns.

The collection of material included in this issue shows how uterine fibroids are being managed, from non-invasive, holistic approaches to innovative therapeutics and careful oncologic evaluation. Even though there is a lot of hope due to advancements, problems including imprecise diagnosis, risky surgery, and possible malignant transformation still exist. Future studies must keep improving tailored strategies that strike a compromise between safety, efficacy, preserving fertility, and incorporating new technology.

Author contributions

RS: Methodology, Conceptualization, Project administration, Supervision, Formal analysis, Investigation, Writing – original draft, Resources. AT: Conceptualization, Writing – review & editing, Investigation. SH: Resources, Conceptualization, Writing – review & editing.

Conflict of interest

The authors declare that the research was conducted in the absence of any commercial or financial relationships that could be construed as a potential conflict of interest.

The author(s) declared that they were an editorial board member of Frontiers, at the time of submission. This had no impact on the peer review process and the final decision.

Generative AI statement

The author(s) declare that no Generative AI was used in the creation of this manuscript.

Any alternative text (alt text) provided alongside figures in this article has been generated by Frontiers with the support of artificial intelligence and reasonable efforts have been made to ensure accuracy, including review by the authors wherever possible. If you identify any issue please contact us.

Publisher's note

References

1. Zhang J, Go VA, Blanck JF, Singh B. A systematic review of minimally invasive treatments for uterine fibroid-related bleeding. *Reprod Sci*. (2022) 29(10):2786–809. doi: 10.1007/s43032-021-00722-z

2. Strong SM, Sideris M, Magama Z, Rouabhi S, Odejinmi F. Surgical intervention for uterine fibroids. Our 4-year experience and literature review: is it time to centralise care provision via specialist fibroid centres? *In Vivo*. (2020) 34(2):695–701. doi: 10.21873/invivo.11826

3. Micić J, Macura M, Andjić M, Ivanović K, Dotlić J, Micić DD, et al. Currently available treatment modalities for uterine fibroids. *Medicina (Kaunas)*. (2024) 60(6):868. doi: 10.3390/medicina60060868

4. Lazaridis A, Hirsch M, Pistofidis G, Odejinmi F. Surgical management of uterine fibroids. *Curr Opin Obstet Gynecol*. (2023) 35(5):440–5. doi: 10.1097/GCO.0000000000000903

5. Cianci S, Gulino FA, Palmara V, La Verde M, Ronsini C, Romeo P, et al. Exploring surgical strategies for uterine fibroid treatment: a comprehensive review of literature on open and minimally invasive approaches. *Medicina (Kaunas)*. (2023) 60(1):64. doi: 10.3390/medicina60010064

6. Gurusamy KS, Vaughan J, Fraser IS, Best LMJ, Richards T. Medical therapies for uterine fibroids - A systematic review and network meta-analysis of randomised controlled trials. *PLoS One*. (2016) 11(2):e0149631. doi: 10.1371/journal.pone.0149631

7. Morris JM, Liang A, Fleckenstein K, Singh B, Segars J. A systematic review of minimally invasive approaches to uterine fibroid treatment for improving quality of life and fibroid-associated symptoms. *Reprod Sci*. (2023) 30(5):1495–505. doi: 10.1007/s43032-022-01120-9

8. Liu T, Yu J, Kuang W, Wang X, Ye J, Qiu X, et al. Acupuncture for uterine fibroids: protocol for a systematic review of randomized controlled trials. *Medicine (Baltimore)*. (2019) 98(8):e14631. doi: 10.1097/MD.0000000000014631

9. Chen Y, Fu M, Huang G, Chen J. Effect of the enhanced recovery after surgery protocol on recovery after laparoscopic myomectomy: a systematic review and meta-analysis. *Gland Surg*. (2022) 11(5):837–46. doi: 10.21037/gs-22-168

10. Navarro A, Bariani MV, Yang Q, Al-Hendy A. Understanding the impact of uterine fibroids on human endometrium function. *Front Cell Dev Biol*. (2021) 9:633180. doi: 10.3389/fcell.2021.633180

frontiers | Frontiers in Oncology

TYPE Original Research
PUBLISHED 08 December 2023
DOI 10.3389/fonc.2023.1325179

OPEN ACCESS

EDITED BY
Andrea Tinelli,
Veris delli Ponti Hospital, Italy

REVIEWED BY
Michael Stark,
New European Surgical Academy (NESA), Germany
Moamar Al-Jefout,
United Arab Emirates University, United Arab Emirates

*CORRESPONDENCE
Wenpei Bai
baiwp@bjsjth.cn
Haixia Pan
haixiapan@buaa.edu.cn

†These authors have contributed equally to this work and share first authorship

RECEIVED 20 October 2023
ACCEPTED 24 November 2023
PUBLISHED 08 December 2023

CITATION
Chen M, Kong W, Li B, Tian Z, Yin C, Zhang M, Pan H and Bai W (2023) Revolutionizing hysteroscopy outcomes: AI-powered uterine myoma diagnosis algorithm shortens operation time and reduces blood loss.
Front. Oncol. 13:1325179.
doi: 10.3389/fonc.2023.1325179

Revolutionizing hysteroscopy outcomes: AI-powered uterine myoma diagnosis algorithm shortens operation time and reduces blood loss

Minghuang Chen[1†], Weiya Kong[1†], Bin Li[2], Zongmei Tian[3], Cong Yin[1], Meng Zhang[4], Haixia Pan[4*] and Wenpei Bai[1*]

[1]Department of Obstetrics and Gynecology, Beijing Shijitan Hospital, Capital Medical University, Beijing, China, [2]Department of Magnetic Resonance Imaging (MRI), Beijing Shijitan Hospital, Capital Medical University, Beijing, China, [3]Information Center, Beijing Shijitan Hospital, Capital Medical University, Beijing, China, [4]College of Software, Beihang University, Beijing, China

Background: The application of artificial intelligence (AI) powered algorithm in clinical decision-making is globally popular among clinicians and medical scientists. In this research endeavor, we harnessed the capabilities of AI to enhance the precision of hysteroscopic myomectomy procedures.

Methods: Our multidisciplinary team developed a comprehensive suite of algorithms, rooted in deep learning technology, addressing myomas segmentation tasks. We assembled a cohort comprising 56 patients diagnosed with submucosal myomas, each of whom underwent magnetic resonance imaging (MRI) examinations. Subsequently, half of the participants were randomly designated to undergo AI-augmented procedures. Our AI system exhibited remarkable proficiency in elucidating the precise spatial localization of submucosal myomas.

Results: The results of our study showcased a statistically significant reduction in both operative duration (41.32 ± 17.83 minutes vs. 32.11 ± 11.86 minutes, p=0.03) and intraoperative blood loss (10.00 (6.25-15.00) ml vs. 10.00 (5.00-15.00) ml, p=0.04) in procedures assisted by AI.

Conclusion: This work stands as a pioneering achievement, marking the inaugural deployment of an AI-powered diagnostic model in the domain of hysteroscopic surgery. Consequently, our findings substantiate the potential of AI-driven interventions within the field of gynecological surgery.

KEYWORDS

artificial intelligence (AI), submucosal myomas, instance segmentation, hysteroscopic myomectomy, magnetic resonance imaging (MRI)

1 Introduction

Uterine fibroids, also known as myomas, are the most common benign tumors affecting the female reproductive system. They are most prevalent among patients aged 30-50 years (1). By the age of 50, the cumulative incidence of myomas in women can reach up to 70%—80%. Among all myomas, submucosal myomas account for approximately 5.5%-10% (2). Submucosal myomas often lead to abnormal uterine bleeding, infertility, recurrent pregnancy loss, and pelvic pain (3).

Submucosal myomas were divided into three subtypes. In 1993, Wamsteker et al. introduced a classification system for submucosal myomas based on the degree of intramural extension during hysteroscopic myomectomy (4). According to this system, submucosal myomas are categorized as type 0, 1, or 2. This classification system was adopted by the European Society of Hysteroscopy and served as the basis for the myoma subclassification system established by the International Federation of Gynecology and Obstetrics (FIGO) (5). Hysteroscopic myomectomy is considered the optimal method for type 0 myomectomy, and the slicing technique is now widely accepted as the standard approach (6). However, the International Society for Gynecologic Endoscopy (ISGE) suggests intrauterine morcellation (IUM) as an alternative option due to its advantages in terms of learning curve and operative time (7, 8).

However, the FIGO subclassification system also has clinical limitations. Uterine myomas will usually distort uterine structure. It will increase the difficulty to distinguish the extent of myometrial invasion, reducing the accuracy of FIGO system (9). Magnetic resonance imaging (MRI) has become an essential imaging modality for assessing myomas. In the clinical management of myomas, MRI T2-weighted images, particularly sagittal images, are commonly utilized. MRI has demonstrated significant advantages in terms of accurately determining the number, size, and location of uterine myomas (10). Conventional MRI can clearly differentiate from uterine myomas, myometrium, and endometrial layers. Myomas exhibit low signal intensity in T2-weighted images, allowing for a clear demarcation of their boundaries from the surrounding myometrium. Study by Wilde, S. and S. Scott-Barrett has indicated that MRI exhibits higher sensitivity in detecting small submucosal myomas measuring less than 5 mm (11). And MRI images were obtained in a more objective way, not dependent on the operator's experience.

Traditional imaging diagnosis heavily relies on the expertise and experience of physicians. However, artificial intelligence (AI), based on machine learning and deep learning techniques, offers significant advantages in terms of image feature extraction, repeatability, and objectivity, thus aiding in decision-making process (12).

The approaches powered by AI can enhance the efficiency and reliability of diagnoses, ultimately benefiting patient care and outcomes. AI has demonstrated promising results in the diagnosis of breast cancer (13), prostate cancer (14), and brain glioma (15) using MRI. However, its application in the diagnosis of gynecological tumors is still in its early stage. Robin Wang et al. conducted a study that they utilized AI and MRI data to differentiate between benign and malignant ovarian tumors (16). They developed a deep learning model that outperformed primary radiologists in terms of accuracy and specificity. Moreover, the AI model enhanced the specificity of diagnosis for both junior and senior radiologists. Tang et al. proposed a new segmentation network using deep learning based on T2-weighted sagittal MRI data, exhibiting high sensitivity and specificity in the diagnosis of uterine diseases (17). They modified a convolutional neural network to achieve automatic segmentation of uterine MRI images based on T2-weighted signatures, covering uterine endometrial cancer, uterine cervical cancer, and uterine myomas. This approach demonstrated the feasibility of diagnosing uterine myomas through a deep learning approach (17, 18). But the existing studies mostly focused on the semantic segmentation, limiting the identification among the myomas, uterine wall and uterine cavity.

Our team has successfully constructed a large-scale uterine myoma MRI dataset that covers all FIGO types. This dataset comprises a substantial number of T2-weighted sagittal images of myomas, along with corresponding annotation files. Additionally, we have developed an instance MRI segmentation model based on deep learning, which significantly contributes to myoma classification and facilitates surgical decision-making through precise instance segmentation of myomas, uterine wall, and cavity (19).

This research represents the first endeavor to introduce AI technology into the realm of operative decision-making for submucosal myomas. By utilizing AI model based on MRI, surgeons could be better prepared. Consequently, patients can benefit from various advantages, such as less bleeding and shorter operation duration, highlighting the potential of AI applications in hysteroscopic myomectomy.

2 Methods

2.1 Participants and study design

Participants in this study were enrolled from January 2022 to January 2023 at Beijing Shijitan Hospital. 56 patients were included with age ranging form 39 to 46 years old and in size 2.43± 0.77 cm. This study was conducted in accordance with the World Medical Association's Declaration of Helsinki. And it was approved by the scientific research ethics committee of Beijing Shijitan Hospital, Capital Medical University (code: sjtkyll-lx-2022 (1)). This study would not violate the rights and interests of patients. The ethics committee clearly stated that specific consent procedures were not required for this study.

Participants met the followed inclusion criteria: 1) with symptoms such as abnormal uterine bleeding, infertility, and recurrent pregnancy loss; 2) diagnosed with submucosal myomas by magnetic resonance imaging (MRI); 3) The postoperative pathology was submucosal myoma. The exclusion criteria were as follows: 1) with severe comorbidities; 2) acute stage of pelvic inflammation and vaginal inflammation, or body temperature >37.5°C; 3) uterine active massive bleeding, severe anemia; 4) normal pregnancy status; 5) history of uterine perforation within

3 months; 6) invasive cervical cancer; 7) genital tuberculosis without anti-tuberculosis treatment; 8) with MRI contraindications, such as febrile convulsions, active foreign bodies in the eyes, cardiac pacemakers, metal intrauterine devices, metal joints and metal dentures; 9) postoperative pathology excluded uterine myomas.

All eligible subjects underwent MRI examination. All eligible subjects were equally divided into 2 groups with the method of random number table. Half of them were divided into group MRI-AI, and the other half were divided into group MR. Bipolar electrosurgical system was employed and intrauterine pressure was set at 100 mmHg during hysteroscopic myomectomy in this study. The surgical procedure in both groups was performed by the same surgeon with abundant experience.

2.2 MRI image acquisition

MRI examination in this study was completed in the PHILIPS INGENIA magnetic resonance imaging system with 3.0T ultra-high field. The MRI scan parameters were as follows: repetition time 4200ms, echo time 130ms, voxel 0.8x0.8x4.0cm3, field of view 24x24cm, reverse angle 90°. MRI provided multiple images from the sagittal, coronal and axial scans and from various sequences including T1W, T2W, mDIXON and DWI. The image resolution was larger than 512x512 pixel. T2W sagittal images were finally collected for the followed image processing.

2.3 MRI image instance segmentation

MRI image was processed based on the instance segmentation model which has been published by our team (19).

MRI images are characterized by the presence of offset fields, low contrast and blurred uterine tissue boundaries, which increasing difficulty in AI automatic segmentation. In order to solve this problem, adaptive histogram equalization was used to adjust the contrast between uterine tissues, especially for uterine myomas and uterine wall with slightly similar signal intensity. The N4ITK method was used to correct the offset field problem, and the Z-Score method was used to normalize the MRI images to the same range.

A specialized network architecture was designed for image processing. Firstly, HRNetv2p was used for high-resolution feature extraction and multi-scale feature fusion operations in the backbone section, so that small scale targets in the uterine region can also be extracted effectively. And DCN was used to address the issue of diverse organ shapes, to extract true feature information from different shapes, and to reduce the loss of shape information. CBAM modules were used to assist in feature extraction, filter out irrelevant and interfering feature information, and enhance the feature expression ability of the AI model. An anchor-based approach was used to assist in target localization.

The size of the myoma, uterine wall and uterine cavity within the uterine region varies considerably so that conventional size settings are no longer suitable. Our previous work conducted distribution statistics on the length, width, and aspect ratio of the target minimum peripheral bounding box on our dataset, providing reference for MR image processing. K-Means clustering method was used to calculate the number of clusters in the target bounding box and output the box size. Simultaneously, it is applied to different feature layers for better detection of small-scale targets in the shallow layer and large-scale targets in the deep layer. Finally, the PointRend module was introduced in the segmentation task to continuously optimize the segmentation edges between adjacent targets using an iterative segmentation strategy. This algorithm reduced jaggies and rough edges, resulting in smoother and more detailed edges for various objects within the uterine region. Since the model contains multiple subtasks, the loss function also consists of multiple parts. The classification loss function tested the accuracy of target classification by using cross entropy loss. The bounding box loss function detected the accuracy of target localization by using smooth L1. The segmentation loss function consists of two parts, CoarseMaskHead and MaskPointRend, which are mainly calculated by binary cross-entropy loss.

2.4 Measurement methods

The clinical data, including age, weight, height, pregnancy times, abortion times, clinical symptoms, preoperative hemoglobin value, operation time, bleeding, and fluid deficit, were analyzed in this study. The size, type and position of submucosal myomas were measured using MRI and AI models we built. And the final hysteroscopic myomectomy was the gold standard according to the FIGO system. A graduated plastic bag was placed under the participant to collect the effluent fluid during operation, contributing to get the fluid deficit. Cervical dilatation time was not included in the operation time.

2.5 Statistical analysis

Statistical analysis was realized using the SPSS software (version 29.0, SPSS Inc., Chicago, IL, USA). Quantitative data that conform to normal distribution were expressed as mean ± standard deviation (SD). Comparisons between the data were performed with *t* test. Quantitative data that do not fit a normal distribution are expressed as percentiles. Comparisons between the data were performed with Mann-Whitney U test. Qualitative data were expressed as number and percentage. And chi-square test was performed to analyze the difference of the two groups. Probability values of $p<0.05$ were considered significant.

3 Results

3.1 General clinical characteristics

The clinical characteristics were similar in both groups MRI and MRI-AI. No significant differences in terms of age, height, weight, BMI, time of pregnance, and the level of hormone ($p>0.05$, Table 1) were found. The symptoms, such as abnormal menstruation and

TABLE 1 General clinical characteristics.

	Total	MRI	MRI-AI	*p*-value
patients(n)	56	28	28	–
Age	43(39-46)	43.50(39.25-47)	42(38.25-45)	0.13
height(cm)	161.43 ± 4.89	160.93 ± 5.29	161.93 ± 4.49	0.45
weight(kg)	62(56-67)	62.50(55.25-71.75)	62.00(56.25-66.50)	0.94
BMI(kg/m^2)	23.73(21.47-26.16)	23.97(21.10-26.48)	23.20(21.54-25.82)	0.86
pregnance	2(1-3)	2(1-3)	2(1-3)	0.72
vaginal delivery	1(0-1)	1(0-1)	1(0-1)	0.29
cesarean section	0(0-0)	0(0-0)	0(0-0.75)	0.81
aborion	1(0-2)	1(0-2)	1(0-2)	0.84
prolonged menstruation(n[%])	22[39.29]	10[35.71]	12[42.86]	0.55
menorrhagia(n[%])	31[55.36]	16[57.14]	15[53.57]	0.50
anaemia(n[%])	10[17.86]	4[14.29]	6[21.43]	0.36
giddy(n[%])	20[35.71]	8[28.57]	12[42.86]	0.20
HGB(g/l)	121.50(93.75-130.50)	122.50(97.00-130.00)	122.00(84.00-130.50)	0.56
myoma size(cm)	2.43 ± 0.77	2.44 ± 0.64	2.43 ± 0.90	0.99
type-0(n[%])	18[32.14]	10[35.71]	8[28.57]	0.39
type-1(n[%])	27[48.21]	13[46.43]	14[50.00]	0.50
type-2(n[%])	11[19.64]	5[17.86]	6[21.43]	0.50
progesterone(ng/ml)	0.88(0.31-4.56)	0.58(0.31-5.48)	1.23(0.31-2.74)	0.90
estrogen(pg/ml)	83.33(57.75-156.06)	78.79(30.21-175.32)	93.06(63.67-135.85)	0.59

anaemia, caused by myoma were also similar in the two groups (p>0.05). Besides, there are no significant differences in the size (2.44 ± 0.64cm vs. 2.43 ± 0.90cm, p=0.99) and type ((type 0:10 [35.71%] vs. 8[28.57%], p=0.39; type 1: 13[46.43%] vs. 14[50.00%], p=0.50; type 2: 5[17.86%] vs.6[21.43%], p=0.50) of each myoma between group MRI and group MRI-AI.

3.2 MRI image instance segmentation

Figure 1 showed the results of the instance segmentation of AI model. MRI images of submucosal myomas, including type 0, type 1 and type 2, were segmented by AI model. Inference masks were covered on the original MRI images, representing myomas, uterine cavity and uterine wall. The left side represents original MRI image, and the middle side represents the inference masks generated by our AI model. And the right side represents the intraoperative view. The inference masks clearly showed the position of myomas, uterine cavity and uterine wall in relation to each other. And it was verified by the intraoperative view. A, B and C showed that the myoma is attached to the lower part of the uterine cavity by a stalk(green narrow), representing the type 0 myoma. D, E and F showed that the intrauterine penetration of myoma exceeded 1/2, which represented it is type 1 myoma. G, H and I showed the bigger myoma is <50% submucosal and≥50% intramural, representing the type 2 myoma.

3.3 Myoma type matching and perioperative data

Table 2 showed the myoma type consistency and perioperative data in group MRI and group MRI-AI. The type consistency rate in group MRI-AI was higher than that in group MRI, but not statistically significant (24[85.71] vs. 26[92.86], p=0.34). Although no significant differences in terms of fluid in, fluid out and fluid deficit were found(p>0.05), the difference in operation time (41.32 ± 17.83min vs. 32.11 ± 11.86min, p=0.03) and bleeding (10.00(6.25-15.00) ml vs. 10.00(5.00-15.00) ml, p=0.04) was reported to be statistically significant.

4 Discussion

The application of AI powered algorithm in clinical decision-making is globally popular among clinicians and medical scientists (20). Artificial intelligence, especially machine learning, reinforcing repetition learning and deep learning, are particularly well-suited to deal with challenges in healthcare industry. Decision trees are common tools used by clinicians, which aim to make accurate decision in daily practice (21). Convolution neural networks, role as a deep learning model, aim to decipher various clinic images to help make diagnosis (22). Some machine learning models that can risk-

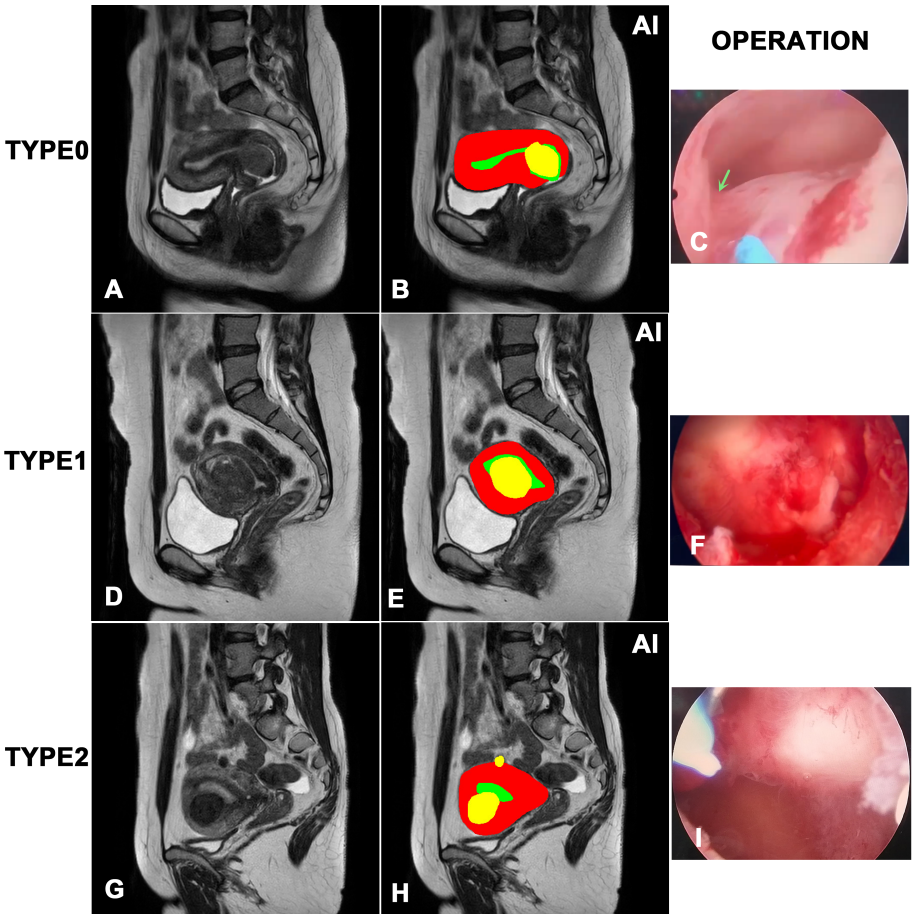

FIGURE 1
Visualization of the instance segmentation of our AI model. The left side represents original MRI image, and the right side represents the inference masks generated by our AI model. In the masks of model inference, yellow represents myomas, red represents the uterine wall, green represents the uterine cavity. **(A, B)** and **(C)** represents type 0 myoma. **(D, E)** and **(F)** represents type 1 myoma. **(G, H)** and **(I)** represents type 2 myoma.

stratify patients in preparation for surgery will help clinicians identify high-risk factors and optimize the healthcare progress (23, 24). There are still many challenges. The adoption of AI has the potential of making unsound decision and inadvertent bias, which means the training curricula renewal and the update of knowledge are necessary (25). Moreover, the black-box process which most AI models present make it hard for clinicians to trust and explain to the patients, which restrict their application in healthcare practice. In this article, to make it more acceptable in practice, we explain our AI algorithm in detail rather than simply give out the figure and data. We are willing to construct an accurate, locally calibrated and clinically accessible AI powered algorithm to risk-stratify patients with submucosal uterine myoma and to optimize patients' care process.

Uterine myomas, occurring in 70% of women in their reproductive years, are the most common benign, solid, pelvic tumors in women. The minimally invasive operations choice for uterine myomas includes laparoscopy and hysteroscopy, which is the common indication for the submucosal myomas. A meta-analysis showed that, compared with infertile women without

TABLE 2 Type matching and Perioperative data.

	Total	MRI	MRI-AI	*p*-value
type consistency(n[%])	50[89.29]	24[85.71]	26[92.86]	0.34
operation time(min)	36.71 ± 15.70	41.32 ± 17.83	32.11 ± 11.86	0.03
fluid in(ml)	2000.00(1000.00-3000.00)	2250.00(1500.00-3000.00)	2000.00(1000.00-2750.00)	0.16
fluid out(ml)	1600.00(762.50-2500.00)	1850.00(1100.00-2650.00)	1400.00(712.50-2325.00)	0.11
fluid deficit(ml)	392.86 ± 179.76	408.93 ± 182.09	376.79 ± 179.24	0.51
bleeding(ml)	10.00(5.00-15.00)	10.00(6.25-15.00)	10.00(5.00-15.00)	0.04

submucosal myomas, those who are infertile women with submucosal myomas showed significantly lower pregnancy and delivery rates (26). Consequently, the resection of submucosal myomas led to a significant increase in the pregnancy rate. Research also indicates that the operation effectively decrease the patients' blood loss (27). Submucosal myomas, which grouped as type0,1 and 2, are almost removable only with hysteroscopy, which means the preoperative recognition and classification of myoma is meaningful and decisive in clinical practice.

In a retrospective cohort study designed by Mayo Clinic, preoperative MRI FIGO myoma staging read by experts is not completely consistent with surgical description, the variation of which is clinically significant. The author concluded that additional validation of FIGO staging is needed, however, in the other way, it means that even experts' ability to map the lesion is not always stable and liable (9).

However, only preoperative myoma mapping is not enough. The image character also make difference. In a prospective study, according to the signal intensity of T2-weighted MR images, myomas are classified into 3 types: low intensity; intermediate intensity; high intensity, which kinds of classification method is totally different from the method we mentioned before which is classified by the positional relationship between uterine myoma and myometrium (28). In conclusion, the researchers assumed that the myomas with the high intensity in T2-weighted MR images should be exempted from a kind of specific myoma surgery, the magnetic resonance-guided focused ultrasound surgery, because the postoperative outcome is unfavorable. It hints us that not only the positional relationship between uterine myoma and myometrium is meaningful, the MR signal intensity also makes the difference, which our AI algorithm will take into account.

The time of operation influence the preoperative recovery, as well as the loss of blood. Our data firmly proved that the AI algorithm group experienced shorter operation time and less loss of blood. The concept of prehabilitation or enhanced recovery after surgery (ERAS) is frequently mentioned and quoted by the clinicians, which aim to speed up the progress of postoperative recovery. The AI algorithm can also help to make the patients who experienced hysteroscopy recover faster, because its application shortens the operation time. In a prospective randomized controlled trail, researchers reported that intracervical vasopressin injection during hysteroscopy reduces intraoperative bleeding (29). In another RCT study, oxytocin drip during hysteroscopy showed the similar effect. However, hypotension, arrhythmia, hyponatremia, might occur after administration of oxytocin and vasopressin, which seriously restrict the medication administration. The AI algorithm help to showed the same result but not lead to any side effect.

In addition to fluid overload and hyponatremia, hysteroscopy is associated with several other immediate complications, including uterine perforation, air embolism, transient blood oxygen desaturation, hypercapnia, and coagulopathy (29–31). However, it is noteworthy that none of these complications were observed among the participants in our study. The absence of these complications could be attributed, in part, to the relatively modest sample size of our study.

Our prior research introduced a deep learning-based instance segmentation model capable of automatically generating output encompassing the class, location, and masks related to the uterine wall, uterine cavity, and uterine myomas (19). Although MRI has been proved to be a useful technique to diagnose uterine myoma and enable clinicians to select appropriate management (32, 33), there are few similar studies with limited transformation and application. In 2017, Korean researchers proposed a 3D reconstruction method with uterine MRI templates enables 3D visualization of myomas (34). This article exclusively focuses on the methodology aspect, without delving into real-world applications or providing a comparison with operative foundations. As a result, its practical applicability might be viewed with skepticism. Furthermore, three dimensional printed uterine model from MRI was constructed to guide the operation and choose the uterine incision in a pregnancy woman, at the same time with caesarean section (35), which is just a case report with restricted clinical evidence. The author asserts that the expense and complexity associated with producing the three-dimensional model were comparatively modest. This emphasizes the attainability of employing 3D models within the realm of myoma operations. In another research, a 3D MRI model was drawn preoperatively and taken into application in clinical practice (36). The deduction that the present study surpasses conventional 2-dimensional MRI in accurately identifying the locations of uterine myomas and endometrium was based on a web-based survey distributed to gynecologists. However, this conclusion lacks precise data on factors such as blood loss or operation time. Based on our current accomplishment, our future research endeavors will extend beyond refining the methodology of 3D reconstruction. In addition to methodological advancements, we aim to harness the visual representations derived from MRI images of uterine myomas for widespread clinical applications. We intend to explore advanced algorithms, machine learning techniques, or innovative image processing methodologies that could further elevate the quality of our 3D models.

Our goal is to bridge the gap between research and practical clinical applications. To achieve this, we plan to collaborate with healthcare institutions and practitioners to implement our 3D uterine myoma models in various clinical scenarios.

This integration will encompass a wide range of applications, including but not limited to:

Preoperative Planning: We aim to provide surgeons with comprehensive 3D models that assist in surgical planning and decision-making. This includes the precise localization of myomas, estimation of surgical complexities, and selection of optimal incision sites.

Intraoperative Guidance: We will explore the real-time use of 3D models during surgeries, particularly in scenarios such as cesarean sections and myomectomy procedures, to aid surgeons in navigating complex anatomical structures.

Patient Education: We intend to develop educational tools that utilize 3D models to communicate with patients, helping them understand their condition and the proposed surgical interventions.

In summary, our forthcoming research endeavors will encompass a multifaceted approach, encompassing

methodological enhancements, clinical integration, and rigorous validation. We aspire to translate our current achievements into tangible benefits for both patients and healthcare providers in the realm of uterine myoma diagnosis and treatment.

5 Conclusion

This study, applying an AI-powered uterine myoma diagnosis algorithm created by our team based on MRI, revealed a promising prospect on improving the efficiency of hysteroscopic myomectomy. The further stage needs more patients to refine the diagnosis algorithm and realize the achievements in clinical widely application.

Data availability statement

The original contributions presented in the study are included in the article/Supplementary Material. Further inquiries can be directed to the corresponding authors.

Ethics statement

The studies involving humans were approved by the scientific research ethics committee of Beijing Shijitan Hospital, Capital Medical University. The studies were conducted in accordance with the local legislation and institutional requirements. Written informed consent for participation was not required from the participants or the participants' legal guardians/next of kin in accordance with the national legislation and institutional requirements.

Author contributions

MC: Data curation, Investigation, Writing – original draft, Writing – review & editing. WK: Data curation, Formal analysis, Writing – review & editing. BL: Methodology, Resources, Writing – review & editing. ZT: Data curation, Resources, Writing – review & editing. CY: Data curation, Writing – review & editing. MZ: Data curation, Software, Writing – review & editing. HP: Software, Validation, Visualization, Writing – review & editing. WB: Funding acquisition, Project administration, Resources, Supervision, Validation, Writing – original draft, Writing – review & editing.

Funding

The author(s) declare financial support was received for the research, authorship, and/or publication of this article. This research was funded by the Beijing Hospitals Authority's Ascent Plan (grant no. DFL20190701).

Conflict of interest

The authors declare that the research was conducted in the absence of any commercial or financial relationships that could be construed as a potential conflict of interest.

Publisher's note

All claims expressed in this article are solely those of the authors and do not necessarily represent those of their affiliated organizations, or those of the publisher, the editors and the reviewers. Any product that may be evaluated in this article, or claim that may be made by its manufacturer, is not guaranteed or endorsed by the publisher.

Supplementary material

The Supplementary Material for this article can be found online at: https://www.frontiersin.org/articles/10.3389/fonc.2023.1325179/full#supplementary-material

References

1. Baird DD, Dunson DB, Hill MC, Cousins D, Schectman JM. High cumulative incidence of uterine leiomyoma in black and white women: ultrasound evidence. *Am J obstet gynecol* (2003) 188(1):100–7. doi: 10.1067/mob.2003.99

2. American Association of Gynecologic Laparoscopists (AAGL): Advancing Minimally Invasive Gynecology Worldwide. Aagl practice report: practice guidelines for the diagnosis and management of submucous leiomyomas. *J minimal invasive gynecol* (2012) 19(2):152–71. doi: 10.1016/j.jmig.2011.09.005

3. Emanuel MH. Hysteroscopy and the treatment of uterine fibroids. *Best Pract Res Clin obstet gynaecol* (2015) 29(7):920–9. doi: 10.1016/j.bpobgyn.2015.03.014

4. Wamsteker K, Emanuel MH, de Kruif JH. Transcervical hysteroscopic resection of submucous fibroids for abnormal uterine bleeding: results regarding the degree of intramural extension. *Obstet gynecol* (1993) 82(5):736–40.

5. Munro MG, Critchley HOD, Fraser IS. The two figo systems for normal and abnormal uterine bleeding symptoms and classification of causes of abnormal uterine bleeding in the reproductive years: 2018 revisions. *Int J gynaecol obstet* (2018) 143 (3):393–408. doi: 10.1002/ijgo.12666

6. Friedman JA, Wong JMK, Chaudhari A, Tsai S, Milad MP. Hysteroscopic myomectomy: A comparison of techniques and review of current evidence in the management of abnormal uterine bleeding. *Curr Opin obstet gynecol* (2018) 30(4):243–51. doi: 10.1097/gco.0000000000000475

7. Loddo A, Djokovic D, Drizi A, De Vree BP, Sedrati A, van Herendael BJ. Hysteroscopic myomectomy: the guidelines of the international society for gynecologic endoscopy (Isge). *Eur J obstet gynecol Reprod Biol* (2022) 268:121–8. doi: 10.1016/j.ejogrb.2021.11.434

8. van Dongen H, Emanuel MH, Wolterbeek R, Trimbos JB, Jansen FW. Hysteroscopic morcellator for removal of intrauterine polyps and myomas: A randomized controlled pilot study among residents in training. *J minimal invasive gynecol* (2008) 15(4):466–71. doi: 10.1016/j.jmig.2008.02.002

9. Laughlin-Tommaso SK, Hesley GK, Hopkins MR, Brandt KR, Zhu Y, Stewart EA. Clinical limitations of the international federation of gynecology and obstetrics (Figo) classification of uterine fibroids. *Int J gynaecol obstet* (2017) 139(2):143–8. doi: 10.1002/ijgo.12266

10. Hossain MZ, Rahman MM, Ullah MM, Mukthadira M, Akter FA, Jahan AB, et al. A comparative study of magnetic resonance imaging and transabdominal ultrasonography for the diagnosis and evaluation of uterine fibroids. *Mymensingh Med J MMJ* (2017) 26(4):821–7.

11. Wilde S, Scott-Barrett S. Radiological appearances of uterine fibroids. *Indian J Radiol Imaging* (2009) 19(3):222–31. doi: 10.4103/0971-3026.54887

12. Hosny A, Parmar C, Quackenbush J, Schwartz LH, Aerts H. Artificial intelligence in radiology. *Nat Rev Cancer* (2018) 18(8):500–10. doi: 10.1038/s41568-018-0016-5

13. Lu W, Li Z, Chu J. A novel computer-aided diagnosis system for breast mri based on feature selection and ensemble learning. *Comput Biol Med* (2017) 83:157–65. doi: 10.1016/j.compbiomed.2017.03.002

14. Wang X, Yang W, Weinreb J, Han J, Li Q, Kong X, et al. Searching for prostate cancer by fully automated magnetic resonance imaging classification: deep learning versus non-deep learning. *Sci Rep* (2017) 7(1):15415. doi: 10.1038/s41598-017-15720-y

15. Cui S, Mao L, Jiang J, Liu C, Xiong S. Automatic semantic segmentation of brain gliomas from mri images using a deep cascaded neural network. *J healthc Eng* (2018) 2018:4940593. doi: 10.1155/2018/4940593

16. Wang R, Cai Y, Lee IK, Hu R, Purkayastha S, Pan I, et al. Evaluation of a convolutional neural network for ovarian tumor differentiation based on magnetic resonance imaging. *Eur Radiol* (2021) 31(7):4960–71. doi: 10.1007/s00330-020-07266-x

17. Kurata Y, Nishio M, Kido A, Fujimoto K, Yakami M, Isoda H, et al. Automatic segmentation of the uterus on mri using a convolutional neural network. *Comput Biol Med* (2019) 114:103438. doi: 10.1016/j.compbiomed.2019.103438

18. Tang C-m, Liu D, Yu X. Mri image segmentation system of uterine fibroids based on ar-unet network. *Am Sci Res J Eng Technol Sci(ASRJETS)* (2020) 71:1–10.

19. Pan H, Zhang M, Bai W, Li B, Wang H, Geng H, et al. An instance segmentation model based on deep learning for intelligent diagnosis of uterine myomas in mri. *Diagnos (Basel Switzerland)* (2023) 13(9). doi: 10.3390/diagnostics13091525

20. Giordano C, Brennan M, Mohamed B, Rashidi P, Modave F, Tighe P. Accessing artificial intelligence for clinical decision-making. *Front digital Health* (2021) 3:645232. doi: 10.3389/fdgth.2021.645232

21. Azar AT, El-Metwally SM. Decision tree classifiers for automated medical diagnosis. *Neural Comput Appl* (2013) 23:2387–403. doi: 10.1007/s00521-012-1196-7

22. Martín Noguerol T, Paulano-Godino F, Martín-Valdivia MT, Menias CO, Luna A. Strengths, weaknesses, opportunities, and threats analysis of artificial intelligence and machine learning applications in radiology. *J Am Coll Radiol JACR* (2019) 16(9 Pt B):1239–47. doi: 10.1016/j.jacr.2019.05.047

23. Corey KM, Kashyap S, Lorenzi E, Lagoo-Deenadayalan SA, Heller K, Whalen K, et al. Development and validation of machine learning models to identify high-risk surgical patients using automatically curated electronic health record data (Pythia): A retrospective, single-site study. *PloS Med* (2018) 15(11):e1002701. doi: 10.1371/journal.pmed.1002701

24. Hyer JM, Ejaz A, Tsilimigras DI, Paredes AZ, Mehta R, Pawlik TM. Novel machine learning approach to identify preoperative risk factors associated with super-utilization of medicare expenditure following surgery. *JAMA Surg* (2019) 154 (11):1014–21. doi: 10.1001/jamasurg.2019.2979

25. Mehrabi N, Morstatter F, Saxena N, Lerman K, Galstyan A. A survey on bias and fairness in machine learning. *ACM Comput Surv* (2021) 54(6):115. doi: 10.1145/3457607

26. Pritts EA. Fibroids and infertility: A systematic review of the evidence. *Obstet gynecol survey* (2001) 56(8):483–91. doi: 10.1097/00006254-200108000-00022

27. Vercellini P, Zàina B, Yaylayan L, Pisacreta A, De Giorgi O, Crosignani PG. Hysteroscopic myomectomy: long-term effects on menstrual pattern and fertility. *Obstet gynecol* (1999) 94(3):341–7. doi: 10.1016/s0029-7844(99)00346-4

28. Funaki K, Fukunishi H, Funaki T, Kawakami C. Mid-term outcome of magnetic resonance-guided focused ultrasound surgery for uterine myomas: from six to twelve months after volume reduction. *J minimal invasive gynecol* (2007) 14(5):616–21. doi: 10.1016/j.jmig.2007.04.009

29. Goldenberg M, Zolti M, Bider D, Etchin A, Sela BA, Seidman DS. The effect of intracervical vasopressin on the systemic absorption of glycine during hysteroscopic endometrial ablation. *Obstet gynecol* (1996) 87(6):1025–9. doi: 10.1016/0029-7844(96)00063-4

30. Papadopoulos NP, Magos A. First-generation endometrial ablation: roller-ball vs loop vs laser. *Best Pract Res Clin obstet gynaecol* (2007) 21(6):915–29. doi: 10.1016/j.bpobgyn.2007.03.014

31. Bongers MY, Mol BW, Brölmann HA. Current treatment of dysfunctional uterine bleeding. *Maturitas* (2004) 47(3):159–74. doi: 10.1016/j.maturitas.2003.08.002

32. Stamatopoulos CP, Mikos T, Grimbizis GF, Dimitriadis AS, Efstratiou I, Stamatopoulos P, et al. Value of magnetic resonance imaging in diagnosis of adenomyosis and myomas of the uterus. *J minimal invasive gynecol* (2012) 19 (5):620–6. doi: 10.1016/j.jmig.2012.06.003

33. Hatta K, Terai Y, Okuda K, Nakamura Y, Yoo S, Tanaka Y, et al. Preoperative assessment by magnetic resonance imaging is useful for planning the treatment of an enlarged uterus by total laparoscopic hysterectomy. *J obstet gynaecol Res* (2013) 39 (4):814–9. doi: 10.1111/j.1447-0756.2012.02065.x

34. Lee SR, Kim YJ, Kim KG. A fast 3-dimensional magnetic resonance imaging reconstruction for surgical planning of uterine myomectomy. *J Korean Med Sci* (2018) 33(2):e12. doi: 10.3346/jkms.2018.33.e12

35. Mackey A, Ng JI, Core J, Nguyen L, Cross D, Lim P, et al. Three-dimensional-printed uterine model for surgical planning of a cesarean delivery complicated by multiple myomas. *Obstet gynecol* (2019) 133(4):720–4. doi: 10.1097/aog.0000000000003107

36. Kim YJ, Kim KG, Lee SR, Lee SH, Kang BC. Preoperative 3-dimensional magnetic resonance imaging of uterine myoma and endometrium before myomectomy. *J minimal invasive gynecol* (2017) 24(2):309–14. doi: 10.1016/j.jmig.2016.10.021

frontiers | Frontiers in Oncology

TYPE Case Report
PUBLISHED 15 February 2024
DOI 10.3389/fonc.2024.1354032

OPEN ACCESS

EDITED BY
Safak Hatirnaz,
Medicana Hospital, Türkiye

REVIEWED BY
Seda Şahin Aker,
Kayseri Education and Research Hospital, Türkiye
İsmail Bıyık,
Kutahya Health Sciences University, Türkiye

*CORRESPONDENCE
Peiling Zhai
ZPL198109@163.com
Xinbo Wang
13370681899@189.cn
Shuai Wang
sdwftcmws@163.com

†These authors have contributed equally to this work

RECEIVED 11 December 2023
ACCEPTED 29 January 2024
PUBLISHED 15 February 2024

CITATION
Huang W, Zhang T, Wang H, Liu Z, Zhai P, Wang X and Wang S (2024) Intravenous metastasis of unexpected uterine sarcoma in the context of uterine fibroids: case report and literature review.
Front. Oncol. 14:1354032.
doi: 10.3389/fonc.2024.1354032

Intravenous metastasis of unexpected uterine sarcoma in the context of uterine fibroids: case report and literature review

Wenying Huang[1†], Tianwei Zhang[1,2†], Hui Wang[3], Zhengchun Liu[1], Peiling Zhai[3*], Xinbo Wang[3*] and Shuai Wang[4*]

[1]School of Clinical Medicine, Weifang Medical University, Weifang, Shandong, China, [2]Department of Hematology and Radiotherapy, Zibo 148 Hospital, Zibo, Shandong, China, [3]Department of Gynecology, Affiliated Hospital of Weifang Medical University, Weifang, Shandong, China, [4]Department of Radiotherapy, School of Medical Imaging, Affiliated Hospital of Weifang Medical University, Weifang Medical University, Weifang, Shandong, China

Objective: Endometrial stromal tumors are rare and complex mesenchymal tumors that often present with clinical symptoms similar to uterine leiomyomas. Due to their atypical nature, they are prone to be misdiagnosed or overlooked by healthcare professionals. This study presents a case report of an incidentally discovered endometrial stromal sarcoma with venous metastasis, which was initially misdiagnosed as a uterine leiomyoma. In addition, this study reviews previously documented cases of similar tumors.

Case report: During a routine medical examination in 2016, a 50-year-old woman was diagnosed with uterine fibroids. In June 2020, she began experiencing moderate, irregular vaginal bleeding. Nevertheless, a histopathological examination indicated an endometrial stromal sarcoma with a striking amalgamation of both low-grade and high-grade features. Molecular analysis identified a rare *MED12* gene mutation. The patient underwent total hysterectomy, bilateral salpingectomy, and resection of the metastatic lesions. Postoperative management included radiotherapy, chemotherapy, and hormone therapy. After completion of chemotherapy, the patient was followed up for 27 months with no evidence of tumor recurrence.

Conclusion: This case report highlights the importance of pathological, immunohistochemical, and molecular aspects of this rare tumor involving the inferior vena cava and showing the presence of atypical gene mutations. The successful treatment outcome further emphasizes the importance of advances in diagnostic modalities for managing rare tumors like this.

KEYWORDS

high-grade endometrial stromal sarcoma (HG-ESS), *MED12*, venous metastasis, unexpected uterine sarcoma, low-grade endometrial stromal sarcoma (LGESS)

1 Introduction

Endometrial stromal and associated neoplasms are a rare and complex group of mesenchymal tumors that develop within the uterus. Endometrial stromal sarcoma (ESS) is an aggressive tumor arising from endometrial stromal cells, representing about 1% of uterine malignancies and <10% of uterine stromal tumors (1). Most patients with uterine sarcoma have no specific symptoms, with approximately 25% of the patients being asymptomatic or presenting with symptoms similar to uterine fibroids (2). In some cases, uterine sarcoma is found during intraoperative frozen section examination or postoperative pathological diagnosis after myomectomy or total hysterectomy, which is known as "unexpected uterine sarcoma" in some academic circles (3). In the most recent classification by the World Health Organization (WHO, 2020), endometrial stromal and associated tumors have been classified into four distinct groups: endometrial stromal nodule (NST), low-grade endometrial stromal sarcoma (LGESS), high-grade endometrial stromal sarcoma (HGESS), and undifferentiated uterine sarcoma (UUS) (4). This classification is based on gross morphological characteristics, histological observations, immunophenotype, and the expression of genetic abnormalities associated with the tumor.

The patient was diagnosed with uterine fibroids during a routine medical examination in December 2016. Because of the absence of any discomfort or irregular vaginal bleeding, the patient did not maintain regular follow-ups or seek further medical consultation. In June 2020, the patient attributed the irregular vaginal bleeding to menopausal manifestations and opted to forego medical attention. In December 2020, the patient finally sought care at our institution, where she underwent a diagnostic hysteroscopy. The postoperative diagnosis was LGESS which was an incidental finding of uterine sarcoma. The National Comprehensive Cancer Network (NCCN) guidelines (5) recommend advancing imaging modalities to gain a more thorough understanding of the lesion and its anatomical relationship with surrounding pelvic and abdominal organs. This helps to assess the lymph node involvement and the presence of suspicious extrauterine metastases. In this case, unsuccessful removal of the intrauterine device because of the adhesions contraindicates the use of magnetic resonance imaging (MRI) for the investigation. Therefore, we adopted a combination of plain and contrast-enhanced computed tomography (CT) scans as an alternative. An abdominal CT scan of the woman showed adenomyosis involving both adnexa, multiple leiomyomas with partial cystic changes, and significant dilatation of the bilateral uterine arteries and veins. Furthermore, dilation was noticeable in the inferior vena cava, left iliac vein, and pelvic veins, indicating the possibility of venous leiomyoma. Two weeks following the hysteroscopic biopsy, she underwent major abdominal surgery including total hysterectomy, bilateral salpingectomy, and resection of tumor from the inferior vena cava, the left common iliac vein, and the left internal iliac vein. The conclusive pathological diagnosis revealed the presence of an HGESS with intravascular metastases.

The patient was diagnosed with uterine fibroids during a routine medical examination in December 2016. Despite the absence of any discomfort or irregular vaginal bleeding, the patient did not maintain regular follow-ups or seek further medical consultation. It was not until June 2020 when irregular vaginal bleeding occurred that the patient attributed this symptom to menopausal manifestations and opted to forego medical attention. Only in December 2020 did the patient finally seek care at our institution, where she underwent a diagnostic hysteroscopy. The postoperative diagnosis was low-grade endometrial stromal sarcoma (LGESS), which was an incidental finding of uterine sarcoma. The National Comprehensive Cancer Network (NCCN) guidelines (5) recommend enhancing imaging examinations to gain a more thorough understanding of the lesion and its anatomical relationship with surrounding pelvic and abdominal organs. This helps to assess lymph node involvement and the presence of suspicious extrauterine metastases. In this case, due to the unsuccessful removal of the intrauterine device caused by adhesions, magnetic resonance imaging (MRI) is contraindicated. Therefore, we have chosen a combination of plain and contrast-enhanced computed tomography (CT) scans as an alternative. Abdominal CT scan of the woman showed adenomyosis involving both adnexa, multiple leiomyomas with partial cystic changes and significant dilatation of bilateral uterine arteries and veins. Furthermore, dilation was noticeable in the inferior vena cava, left iliac vein and pelvic veins, indicating the possibility of venous leiomyoma. Two weeks following the hysteroscopic biopsy, she underwent major abdominal surgery including total hysterectomy, bilateral salpingectomy, resection of tumor from the inferior vena cava, resection of tumor from the left common iliac vein and resection of tumor from the left internal iliac vein. The conclusive pathological diagnosis revealed the presence of a high-grade endometrial stromal sarcoma (HGESS) with intravascular metastases.

2 Methods and results

2.1 Case presentation

The patient, a 50-year-old female, was diagnosed with uterine fibroids during a routine medical examination in 2016. In June 2020, she experienced moderate-intensity irregular vaginal bleeding, occasionally accompanied by dark red blood clots. In December 2020, the patient came to our hospital for consultation and underwent a gynecological ultrasound examination. The ultrasound revealed an anteverted uterus measuring approximately 10.5×8.3×9.0 cm. Multiple hypoechoic lesions were found within the myometrium. The largest fibroid, approximately 2.6×1.4 cm in size, was found in the anterior wall. Additionally, a 7.3×5.5×7.0 cm solid cystic echo was observed in the anterior wall muscle. These findings suggest the presence of multiple uterine fibroids and possible changes in the endometrium. Moreover, it was noted that the intrauterine contraceptive device had descended. During the gynecological examination, a significant amount of dark red blood clot tissue was found in the vagina of the patient, accompanied by a foul-smelling discharge. The cervix was difficult to expose, and the uterus appeared to be the size of a 4-month-old pregnancy. It had a firm consistency, irregular shape, and was mobile. No tenderness was observed upon palpation, and no abnormalities were detected in the bilateral adnexa.

The patient denied any family history of similar diseases. The findings of auxiliary examinations revealed the levels of tumor markers as follows: carbohydrate antigen 125 (CA125) 22.48 U/mL (normal range: 0-35 U/mL), carbohydrate antigen 19-9 (CA19-9) <0.600 U/mL (normal range: 0-27 U/mL), and human epididymis protein 4 (HE4) 73.69 pmol/L (normal range: 0-140 pmol/L). Owing to the enlarged uterus and poor exposure of the cervix, diagnostic dilation and curettage was difficult to perform, severely reducing the accuracy of the biopsy. Therefore, on December 21, 2020, an intrauterine mass biopsy was performed on the patient after a comprehensive evaluation. The postoperative pathological examination revealed a "spindle cell tumor of the uterine cavity," with immunohistochemistry indicating a tendency toward an LGESS. To further assess the interplay between the lesion and adjacent tissues, the patient underwent chest and abdominal CT scans. The abdominal CT revealed adenomyosis along with multiple leiomyomas, some of which exhibited partial cystic degeneration. There was substantial thickening of the bilateral vasculature, including the arterial and venous systems. In addition, there were lesions within the uterine cavity (Figure 1A), and there was evident dilation of the inferior vena cava, left iliac vein, and pelvic veins, indicative of venous leiomyoma (Figure 1C). The chest CT did not reveal any major abnormalities. The preoperative diagnosis revealed "LGESS" and "Intravascular tumor". After a comprehensive evaluation of the patient's condition, on January 4, 2021, she underwent a "complete abdominal hysterectomy with bilateral salpingo-oophorectomy and tumor resection from the inferior vena cava, left common iliac vein, and left internal iliac vein." The diagnosis of "HGESS with intravascular metastases" was established based on the postoperative pathology findings.

2.2 Gross examination

In surgery, tumor emboli were palpable within the left common iliac vein and inferior vena cava, with margins extending approximately 2 cm above the renal veins. Grayish-white tumor tissue measuring 5 x 3.5 x 1 cm was successfully extracted from within the blood vessels (Figure 2A). Upon dissection of the enlarged uterus and adnexa (Figure 2B), the following findings were observed: the uterine volume measured 14.5 x 10 x 7 cm, the cervical length was 8.5 cm, the external cervical uterine diameter was 5 cm, and the internal cervical uterine diameter was 2.5 cm. The uterine wall anteriorly showed hypertrophy, measuring approximately 3 cm in thickness. The uterine cavity contained an elevated mass, which appeared grayish-white in cross-section and measured 8 x 4 x 4 cm. Additionally, multiple grayish-white nodules, ranging in diameter from 0.5 to 1.5 cm, were observed within the uterine wall. No significant abnormalities were identified in the bilateral adnexa.

2.3 Microscopic examination of tumor cells

An Olympus (CX43) optical microscope was used for observation. Localization of the intracavitary mass showed distinct borders (Figure 3A X40). In certain areas, the cells were densely packed and showed active growth. The tumor tissue invaded the deep muscular layer of the uterine wall, reaching the serosal surface, and extended into the cervical canal. In addition, tumor tissue was present at the cut end of the cervix with evidence of neural invasion and intravascular tumor thrombi. Cancer cells are abundant but irregular in size and shape, with most of them appearing ovoid (Figure 3B X200). The cytoplasm is

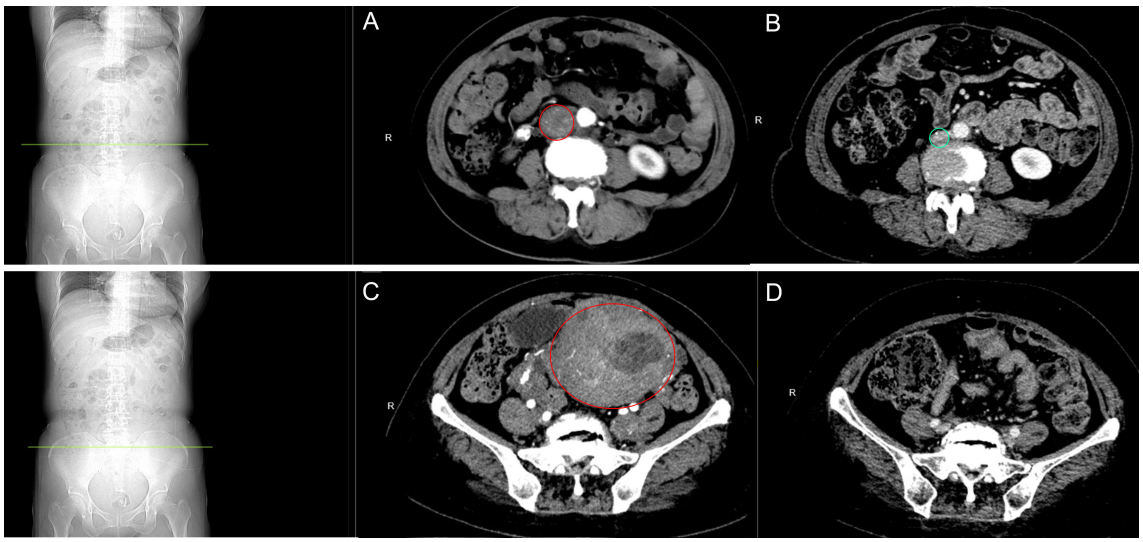

FIGURE 1
Abdominal CT scan. **(A)** Preoperative image of the inferior vena cava: The inferior vena cava was observed to be dilated, suggestive of smooth muscle leiomyoma. **(B)** Follow-up image of the inferior vena cava: Following the completion of chemotherapy after 27 months, no abnormalities were detected. **(C)** Preoperative image of the uterus: Multiple smooth muscle leiomyomas are present in the uterus and bilateral adnexa, with partial cystic degeneration. **(D)** Follow-up pelvic examination: 27 months after chemotherapy, changes indicative of postoperative alterations in the uterus were observed.

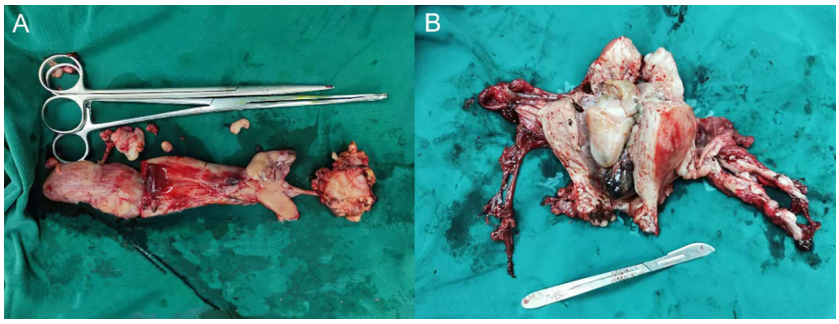

FIGURE 2
Gross examination. **(A)** Intravascular tumor tissue: a mass of grayish-white tissue measuring 5 × 3.5 × 1 cm in volume. **(B)** Uterus and bilateral adnexal tissue: The uterus has a volume of 14.5 × 10 × 7 cm, with a cervical length of 8.5 cm. The external cervical orifice is 5 cm in diameter and the internal cervical orifice is 2.5 cm in diameter. The anterior uterine wall is approximately 3 cm thick. A protruding mass with a total volume of 8 × 4 × 4 cm is present within the uterine cavity. The dimensions of the left ovary are 4 × 3 × 1.5 cm, and the fallopian tube has a length of 5 cm and a maximum diameter of 1 cm. The right ovary measures 3.5 × 2.5 × 1 cm, and the fallopian tube has a length of 6.5 cm and a maximum diameter of 0.8 cm.

either sparse or vacuolated and the nuclei are enlarged with an increased nuclear to cytoplasmic ratio. Moderate-to-severe anisokaryosis was observed with visible nuclear division (8/10 high-power fields) (Figure 3C X400). Within the mass, small arteries, thin-walled vessels, and numerous thick-walled vessels were observed. In addition, within the vasculature, the tumor was wrapped around the small arteries in a vortex-like pattern (Figure 3D X200). The results indicate conformity with HGESS (Figure 3E X400).

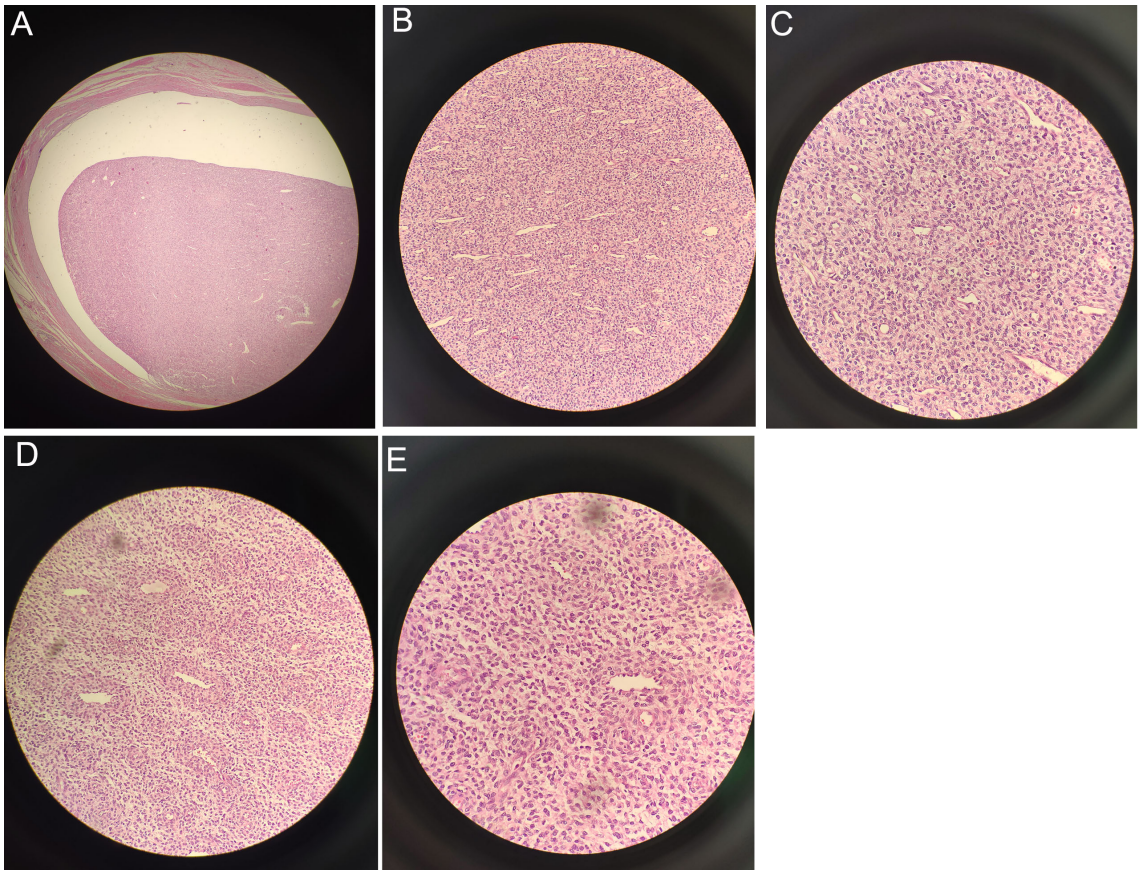

FIGURE 3
Under the microscope: **(A)** Localization of the intracavitary mass revealed distinct borders (X40). **(B)** Most of the cells appeared ovoid (X200). **(C)** Visible nuclear division with moderate-to-severe anisokaryosis (X400). **(D)** Tumor wrapped around small arteries in a whirlpool-like pattern (X200). **(E)** Consistent with high-grade endometrial stromal sarcoma (X400).

2.4 Immunohistochemistry

On December 21, 2020, the results of the biopsy of tumor tissue demonstrated partial positivity for CD10 and a Ki-67 proliferation index of 20-30%. They further exhibit positivity for Wilms Tumor 1 (WT-1) and smooth muscle actin (SMA), but negativity for h-Caldesmon staining.

On January 4, 2021, the tumor cells located within the uterine cavity displayed positive CD10 immunohistochemical staining results (Figure 4A X400), with an approximate 40% positive rate of Ki-67 (Figure 4B X400). In addition, the cells demonstrated positive SMA (Figure 4C X400), negative h-Caldesmon (Figure 4D X400), positive estrogen receptor (ER) (Figure 4E X400), and weakly positive progesterone receptor (PR) (Figure 4F X400) and cyclin D1 (Figure 4G X400). The WT-1 and Vimentin markers were positive whereas EMA and HMB45 were negative.

2.5 Next-generation sequencing testing

Next-generation sequencing (NGS) is used to extract and sequence tumor samples that are embedded in paraffin wax. The raw sequencing data is filtered and then subjected to bioinformatic analysis. The reference sequence used for NGS testing was GRCh37/

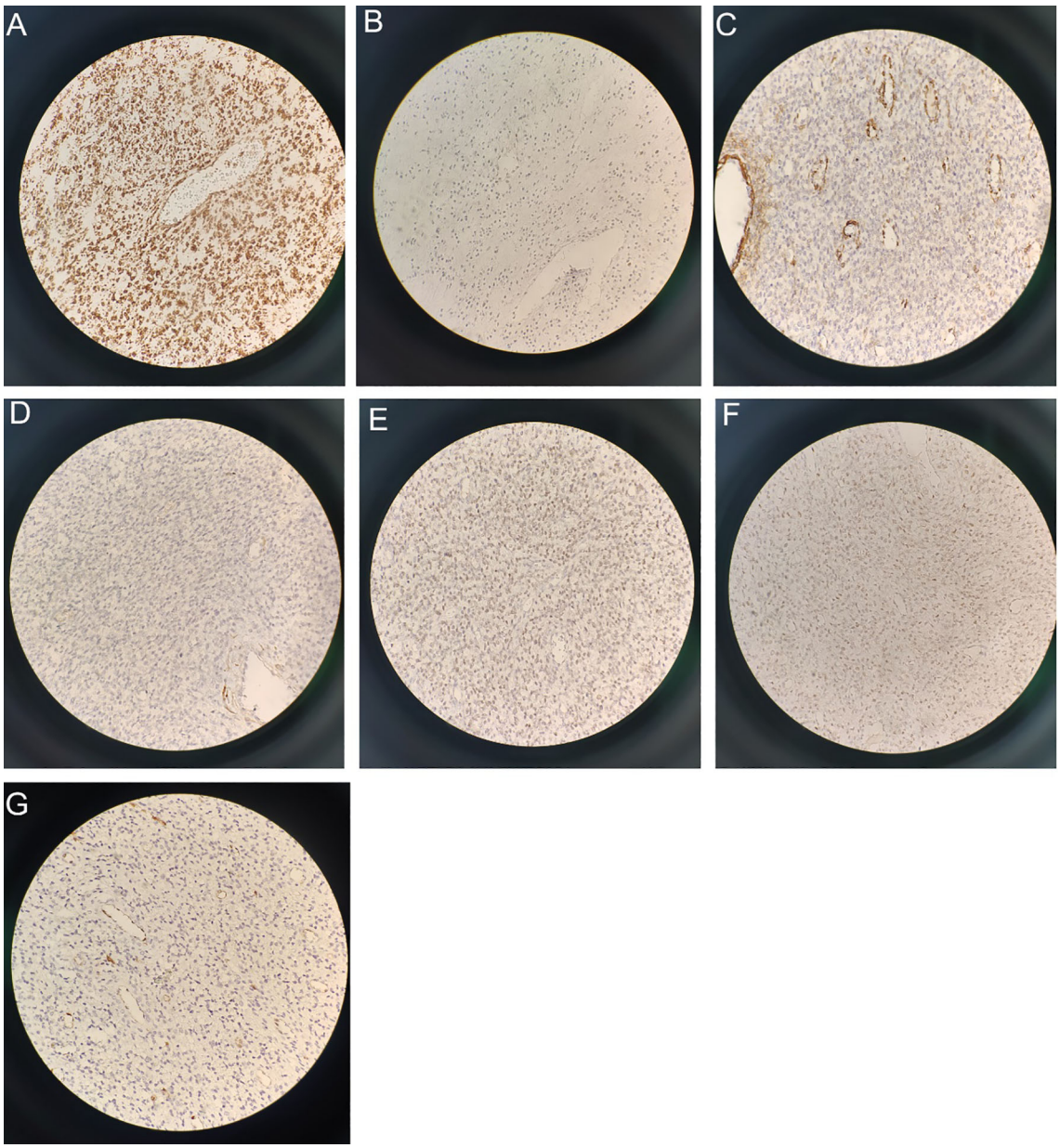

FIGURE 4
Immunohistochemical staining results (X400): **(A)** Immunohistochemical staining revealed CD10 positivity. **(B)** Ki-67 demonstrated a positive rate of approximately 40%. **(C)** SMA shows positivity. **(D)** h-Caldesmon staining is negative. **(E)** ER staining is positive. **(F)** PR staining exhibits weak positivity. **(G)** Cyclin D1 shows weak positivity.

hg19 (Supplementary Figure 1: Gene mutations). The detected types of gene variants included fusion mutations, point mutations, insertion/deletion mutations, and copy number variations. A frameshift mutation, p. T920Lfs*36, was discovered in the 20th exon of the *MED12* gene. The mutation identified was c.2757del (p. T920Lfs*36) and had a variant abundance of 40.38%. Furthermore, the *RB1* gene experienced a loss in copy number (CN) with a CN of 0.39. Finally, a missense mutation, p.Y251C (c.752A>G), was observed in the 3rd exon of the *VEGFA* gene with an abundance of 1.26%. Moreover, a heterozygous polymorphism, namely c.313A>G (p.I105V), was present in the *GSTP1* gene. However, the fusion genes associated with HGESS, including YWHAE-NUTM2A, YWHAE-NUTM2B, and ZC3H7B-BCOR were not detected in this case.

2.6 Treatment and follow-up results

According to the 2023 International Federation of Gynecology and Obstetrics (FIGO) staging criteria and treatment recommendations for uterine sarcoma (6, 7), the patient in this case was classified as stage IVB. The treatment involved a total abdominal hysterectomy with bilateral salpingo-oophorectomy, as well as the removal of a tumor from the inferior vena cava, the left common iliac vein, and the left internal iliac vein. Following the surgery, the patient is taking letrozole orally 2.5 mg daily. Moreover, one month after the surgery, the patient underwent intensity-modulated radiotherapy (IMRT) for a total of 25 times with a dose of 2 Gy each time, followed by post-loading radiotherapy for a total of 6 times with a dose of 5 Gy each time. The patient underwent six cycles of chemotherapy with ifosfamide (2 g on days 1-3 every 21 days), etoposide (60 mg on days 1-2 every 21 days), and cisplatin (30 mg on days 1-3 every 21 days) simultaneously. After completing systemic treatment, the patient will undergo routine physical examinations and repeat serum CA125 testing every 3 months for 3 years. The chest, abdomen, and pelvic CT scans will be conducted every 6 months. In case of suspicion of tumor metastasis, a comprehensive positron emission tomography (PET)-CT examination will be performed for further evaluation. As per the most recent follow-up, which occurred 27 months after the completion of chemotherapy, the echocardiography assessment indicated the absence of any focal mass within the ventricle. Furthermore, a follow-up CT scan of the abdomen and pelvis, enhanced with contrast, revealed no abnormal masses (Figures 1B, D).

3 Discussion

Endometrial stromal sarcoma is a rare tumor type, comprising only 0.2% of all malignant uterine tumors. Nevertheless, ESS represents approximately 7-25% of all uterine sarcomas (8). The annual incidence rate is 0.19 cases per 100,000 females, showing a gradual increase over the past decade. ESS is regarded as the second most prevalent uterine mesenchymal tumor after uterine leiomyoma (9),. The worldwide median age for the diagnosis of ESS diagnosis is 55 years (10). Most of the patients do not experience specific symptoms, and up to 25% of the patients may remain asymptomatic (2). Owing to the absence of clear clinical manifestations and the resemblance of symptoms to uterine fibroids, most patients with ESS are initially misdiagnosed to have uterine fibroids, leading to the term “unexpected uterine sarcoma” being applied in these cases. The diagnostic challenges associated with ESS are related to its morphological features, clinical behavior, and genetic abnormalities. The condition is categorized into two types based on these characteristics: LGESS and HGESS. According to a large-scale study, 86% of all ESS cases are LGESS, whereas the remaining 14% are categorized as HGESS (11). Nevertheless, the complexity and heterogeneity of these tumors go beyond this diagnostic classification.

LGESS is the dominant subtype of ESS. It is characterized by late recurrence and has an indolent nature. The tumor grows slowly and has a favorable prognosis. LGESS is typically identified within the uterus during an investigation of hysterectomy specimens (9). In this case report, the clinical presentation together with abdominal ultrasound and CT scans suggested the presence of uterine fibroids. However, postoperative pathology revealed the coexistence of both LGESS and HGESS. LGESS commonly presents in perimenopausal women and is rarely reported in young women and adolescents (12). Risk factors shared among these age groups include obesity, diabetes, early menarche, and the use of tamoxifen and estrogen medications (9, 13, 14). The woman in this case study had a BMI >28 kg/m^2, indicating an obesity level, and a 7-year history of diabetes.

Pathologically, LGESS comprises uniform tumor cells with features resembling proliferative endometrial stroma. Its histological features include uniform and densely packed stromal cells accompanied by mild nuclear atypia (<5 per 10 high-power fields) and occasional mitotic activity. Immunohistochemically, positive staining can be observed for CD10, WT-1, vimentin, interferon-induced transmembrane protein 1 (IFITM1), ER, androgen receptor (AR), and PR. Nevertheless, Cyclin D1 and desmin yield negative or focally positive results. Some researchers have pointed out that the immunohistochemical profile of LGESS is characterized by positive staining for CD10, ER, and PR (15). LGESS can be distinguished based on the presence of IFITM1, providing a level of specificity in its detection (16). CD10 as a marker of mesenchymal tumors exhibits high sensitivity and is the most commonly used immunohistochemical antibody for distinguishing LGESS from HGESS (1). However, it is worth noting that in clinical practice, a few cases of LGESS may be negative, weakly positive, or focally positive for CD10. Therefore, positive CD10 staining alone does not suffice as a specific marker for LGESS. The diagnosis of LGESS requires a combination of CD10, cyclin D1, ER, PR, h-Caldesmon, SMA, and desmin. In certain cases, molecular genetic alterations can also establish a definitive diagnosis. Common fusion genes identified in LGESS comprise JAZF1-SUZ12, JAZF1-PHF1, EPC1-PHF1, and MEAF6-PHF1 fusions. Other fusion genes, including MBTD1-CXorf67, BRD8-PHF1, EPC2-PHF1, and EPC1-SUZ12, have been detected in LGESS (17). Nevertheless, it is worth noting that approximately one-third of LGESS cases, including this case, do not exhibit any identified fusion genes. This implies the possible presence of other undefined genetic molecular alterations (18).

Compared with LGESS, HGESS has a worse prognosis and more aggressive biological behavior. It has a recurrence rate of one

year. Clinically, it has similarities with LGESS. Pathologically, HGESS has a uniform population of round and/or spindle-shaped cells, occasionally including low-grade spindle cells, displaying moderate-to-severe nuclear atypia (>10/10 high-power fields). In addition, focal components of LGESS may be observed. In immunohistochemistry, HGESS typically does not exhibit expression of CD10, ER, PR, and smooth muscle markers. Nevertheless, cyclin D1, a cell cycle protein, displays a diffuse marked positivity (>70% of cell nuclei). Furthermore, HGESS shows a high Ki-67 proliferation index. One study demonstrated that approximately half of HGESS cases may have a low-grade spindle cell component (19). In addition, there are some instances where HGESS can exhibit positive staining for ER, PR, and CD10 (18). HGESS cases without *YWHAE* gene rearrangement may show weak or even negative staining for cyclin D1 (20). Research suggests that positive nuclear staining of the β-catenin protein may serve as an immunohistochemical marker for HGESS (21). As for molecular diagnostics, fusion genes such as *YWHAE-NUTM2A*, *YWHAE-NUTM2B*, *ZC3H7B-BCOR*, and *BCOR ITD* have been observed. No fusion genes associated with HGESS were detected in this particular case.

Compared with LGESS, HGESS has a worse prognosis and more aggressive biological behavior. It has a recurrence rate of one year. Clinically, it has similarities with LGESS. Pathologically, HGESS has a uniform population of round and/or spindle-shaped cells, occasionally including low-grade spindle cells, displaying moderate-to-severe nuclear atypia (>10/10 high-power fields). In addition, focal components of LGESS may be observed. In immunohistochemistry, HGESS typically does not exhibit expression of CD10, ER, PR, and smooth muscle markers. Nevertheless, cyclin D1, a cell cycle protein, displays a diffuse marked positivity (>70% of cell nuclei). Furthermore, HGESS shows a high Ki-67 proliferation index. One study demonstrated that approximately half of HGESS cases may have a low-grade spindle cell component (19). In addition, there are some instances where HGESS can exhibit positive staining for ER, PR, and CD10 (18). HGESS cases without *YWHAE* gene rearrangement may show weak or even negative staining for cyclin D1 (20). Research suggests that positive nuclear staining of the β-catenin protein may serve as an immunohistochemical marker for HGESS (21). As for molecular diagnostics, fusion genes such as *YWHAE-NUTM2A*, *YWHAE-NUTM2B*, *ZC3H7B-BCOR*, and *BCOR ITD* have been observed. No fusion genes associated with HGESS were detected in this particular case.

This patient sought medical attention for uterine fibroids and was unexpectedly diagnosed with ESS (Supplementary Figure 2: Development of the disease). The tumor displays highly invasive behavior, infiltrating the deep muscle layer near the serosal surface and involving the cervical canal. Its biological behavior is consistent with that of HGESS in terms of invasiveness. Cytologically, the tumor exhibits a coexistence of low-grade spindle-shaped cells and high-grade round cells. Furthermore, the presence of pathological nuclear division (8/10 high-power fields) is more consistent with the characteristics of HGESS. Immunohistochemically, the tumor is positive for CD10 and ER and weakly positive for PR (15). These findings are consistent with immunological expression of LGESS. However, it should be noted that in certain cases, HGESS can also exhibit positive staining for ER, PR, and CD10 (18). Considering the concurrent immunohistochemical expression of HGESS, such as low positivity for cyclin D1 and a Ki-67 proliferation index of approximately 40%, the diagnosis of HGESS with concurrent LGESS is plausible. Further precision of the diagnosis can be achieved by genetic profiling for validation.

Although fusion genes associated with HGESS were not detected in this case, a frameshift mutation in exon 20 of the *MED12* gene was identified in the patient. This mutation differs from most of the previously reported *MED12* mutations, which predominantly occur in exon 2 and intron 1 (22, 23). MED12 is a constituent of the mediator complex, which acts as a key regulatory factor for the transcription of numerous genes (24, 25). Somatic mutations in *MED12* have been identified in approximately 70% of uterine leiomyomas and 10% of leiomyosarcomas (26). Studies have shown that *MED12* mutations in fibroadenomas are associated with dysregulation of estrogen signaling (27). This suggests that *MED12* mutations may play a crucial oncogenic role in estrogen-related ESS (28). The study reveals that mutations in exon 2 of *MED12* have been identified in ESS carrying the *JAZF1-SUZ12* or *JAZF1-PHF1* fusion genes. These mutations may confer additional oncogenic advantages (28).

The *MED12* mutations identified in ESS are novel and lack distinct pathological characteristics. There is no evidence of an adverse prognosis associated with the mutation status. In this case, the presence of partially high-grade areas within a low-grade ESS in combination with the *MED12* gene mutation is considered. Thus far, there has been no recurrence observed during follow-up. Given the existence of other rare types of ESS with genetic features that are not yet widely recognized, continuous monitoring of the patient is necessary to further gain experience and knowledge.

4 Conclusions

This study presents a case report of incidentally discovered ESS, which was initially misdiagnosed as uterine leiomyoma with tumor metastasis to the inferior vena cava. The pathological diagnosis was a combination of both LGESS and HGESS. Surprisingly, molecular analysis did not reveal any mutations commonly associated with LGESS or HGESS but instead identified a rare *MED12* mutation within the ESS. The patient underwent total hysterectomy, bilateral salpingectomy, and resection of the metastatic lesions after consulting the gynecological and surgical specialists. Postoperative management included radiotherapy, chemotherapy, and hormone therapy. Currently, the patient shows no signs of recurrence, and her condition is being closely monitored during follow-up.

Data availability statement

The original contributions presented in the study are included in the article/Supplementary Material. Further inquiries can be directed to the corresponding authors.

Ethics statement

Written informed consent was obtained from the individual(s) for the publication of any potentially identifiable images or data included in this article.

Author contributions

WH: Visualization, Writing – original draft, Writing – review & editing. TZ: Conceptualization, Methodology, Writing – original draft, Writing – review & editing. HW: Conceptualization, Investigation, Methodology, Project administration, Resources, Writing – review & editing. ZL: Formal analysis, Methodology, Visualization, Writing – review & editing. PZ: Formal analysis, Project administration, Resources, Supervision, Writing – review & editing. XW: Project administration, Resources, Writing – review & editing. SW: Conceptualization, Funding acquisition, Methodology, Project administration, Supervision, Writing – review & editing.

Funding

The author(s) declare financial support was received for the research, authorship, and/or publication of this article. The study was supported by Weifang Municipal Health Commission Research Program Project (No. WFWSJK-2023-032); Weifang Science and Technology Development Project(No.2023YX053); Wu Jieping Medical Foundation (No.320.6750.2021-21-12).

Conflict of interest

The authors declare that the research was conducted in the absence of any commercial or financial relationships that could be construed as a potential conflict of interest.

Publisher's note

All claims expressed in this article are solely those of the authors and do not necessarily represent those of their affiliated organizations, or those of the publisher, the editors and the reviewers. Any product that may be evaluated in this article, or claim that may be made by its manufacturer, is not guaranteed or endorsed by the publisher.

Supplementary material

The Supplementary Material for this article can be found online at: https://www.frontiersin.org/articles/10.3389/fonc.2024.1354032/full#supplementary-material

SUPPLEMENTARY FIGURE 1
Gene Mutations: **(A)** *MED12* gene frameshift mutation. **(B)** *RB1* gene copy number loss. **(C)** *VEGFA* gene missense mutation.

SUPPLEMENTARY FIGURE 2
Development of the disease: the progression of the condition.

References

1. de Almeida BC, Dos Anjos LG, Dobroff AS, Baracat EC, Yang Q, Al-Hendy A, et al. Epigenetic features in uterine leiomyosarcoma and endometrial stromal sarcomas: an overview of the literature. *Biomedicines*. (2022) 10(10):2567. doi: 10.3390/biomedicines10102567

2. Roy M, Kumar S, Bhatla N, Ray MD, Kumar L, Jain D, et al. Androgen receptor expression in endometrial stromal sarcoma: correlation with clinicopathologic features. *Int J Gynecol Pathol*. (2017) 36:420–7. doi: 10.1097/PGP.0000000000000353

3. Hosh M, Antar S, Nazzal A, Warda M, Gibreel A, Refky B. Uterine sarcoma: analysis of 13,089 cases based on surveillance, epidemiology, and end results database. *Int J Gynecol Cancer*. (2016) 26:1098–104. doi: 10.1097/IGC.0000000000000720

4. *Female Genital Tumours WHO Classification of Tumours. 5th ed*. Lyon, France: IARC Publications (2020).

5. Abu-Rustum N, Yashar C, Arend R, Barber E, Bradley K, Brooks R, et al. Uterine neoplasms, version 1.2023, NCCN clinical practice guidelines in oncology. *J Natl Compr Canc Netw*. (2023) 21:181–209. doi: 10.6004/jnccn.2023.0006

6. Berek JS, Matias-Guiu X, Creutzberg C, Fotopoulou C, Gaffney D, Kehoe S, et al. FIGO staging of endometrial cancer: 2023. *Int J Gynaecol Obstet*. (2023) 162:383–94. doi: 10.1002/ijgo.14923

7. Matsuo K, Klar M, Song BB, Roman LD, Wright JD. Validation of the 2023 FIGO staging schema for advanced endometrial cancer. *Eur J Cancer*. (2023) 193:113316. doi: 10.1016/j.ejca.2023.113316

8. Gorostidi M, Yildirim Y, Macuks R, Mancari R, Achimas-Cadariu P, Ibañez E, et al. ASO visual abstract: impact of hospital case volume on uterine sarcoma prognosis: SARCUT study subanalysis. *Ann Surg Oncol*. (2023) 30:7667–8. doi: 10.1245/s10434-023-14209-5

9. Hoang L, Chiang S, Lee C-H. Endometrial stromal sarcomas and related neoplasms: new developments and diagnostic considerations. *Pathology*. (2018) 50:162–77. doi: 10.1016/j.pathol.2017.11.086

10. Surace A, Baù MG, Privitera S, Botta G, Danese S, Plazzotta C, et al. Risk of unexpected uterine leiomyosarcoma during laparoscopic procedures: Experience from a single tertiary institute in Italy. *Int J Gynaecol Obstet*. (2022) 156:236–9. doi: 10.1002/ijgo.13701

11. Abeler VM, Røyne O, Thoresen S, Danielsen HE, Nesland JM, Kristensen GB. Uterine sarcomas in Norway. A histopathological and prognostic survey of a total population from 1970 to 2000 including 419 patients. *Histopathology*. (2009) 54:355–64. doi: 10.1111/j.1365-2559.2009.03231.x

12. Piątek S, Szymusik I, Dańska-Bidzińska A, Ołtarzewski M, Trojan G, Bidziński M. Fertility-sparing management may be considered in young women with uterine sarcoma. *J Clin Med*. (2022) 11(16):4761. doi: 10.3390/jcm11164761

13. Leary AF, Quinn M, Fujiwara K, Coleman RL, Kohn E, Sugiyama T, et al. Fifth Ovarian Cancer Consensus Conference of the Gynecologic Cancer InterGroup (GCIG): clinical trial design for rare ovarian tumours. *Ann Oncol*. (2017) 28:718–26. doi: 10.1093/annonc/mdw662

14. Porter AE, Kho KA, Gwin K. Mass lesions of the myometrium: interpretation and management of unexpected pathology. *Curr Opin Obstet Gynecol*. (2019) 31:349–55. doi: 10.1097/GCO.0000000000000569

15. Rebegea LF, Firescu D, Anghel RM, Gales L, Ilie AM, Dumitru ME, et al. Clinical, histological and therapeutical aspects in the management of uterine and extrauterine stromal sarcomas: Case reports. *Exp Ther Med*. (2021) 22:1456. doi: 10.3892/etm.2021.10891

16. Busca A, Gulavita P, Parra-Herran C, Islam S. IFITM1 outperforms CD10 in differentiating low-grade endometrial stromal sarcomas from smooth muscle neoplasms of the uterus. *Int J Gynecol Pathol*. (2018) 37:372–8. doi: 10.1097/PGP.0000000000000424

17. Yoshida H, Kikuchi A, Tsuda H, Sakamoto A, Fukunaga M, Kaku T, et al. Discrepancies in pathological diagnosis of endometrial stromal sarcoma: a multi-institutional retrospective study from the Japanese clinical oncology group. *Hum Pathol*. (2022) 124:24–35. doi: 10.1016/j.humpath.2022.03.007

18. Akaev I, Yeoh CC, Rahimi S. Update on endometrial stromal tumours of the uterus. *Diagnostics (Basel)*. (2021) 11(3):429. doi: 10.3390/diagnostics11030429

19. Sciallis AP, Bedroske PP, Schoolmeester JK, Sukov WR, Keeney GL, Hodge JC, et al. High-grade endometrial stromal sarcomas: a clinicopathologic study of a group of tumors with heterogenous morphologic and genetic features. *Am J Surg Pathol*. (2014) 38:1161–72. doi: 10.1097/PAS.0000000000000256

20. Zou Y, Turashvili G, Soslow RA, Park KJ, Croce S, McCluggage WG, et al. High-grade transformation of low-grade endometrial stromal sarcomas lacking YWHAE and BCOR genetic abnormalities. *Mod Pathol*. (2020) 33:1861–70. doi: 10.1038/s41379-020-0535-y

21. Dall GV, Hamilton A, Ratnayake G, Scott C, Barker H. Interrogating the genomic landscape of uterine leiomyosarcoma: A potential for patient benefit. *Cancers*. (2022) 14(6):1561. doi: 10.3390/cancers14061561

22. Markowski DN, Bartnitzke S, Löning T, Drieschner N, Helmke BM, Bullerdiek J. MED12 mutations in uterine fibroids–their relationship to cytogenetic subgroups. *Int J Cancer*. (2012) 131:1528–36. doi: 10.1002/ijc.27424

23. Piscuoglio S, Burke KA, Ng CKY, Papanastasiou AD, Geyer FC, Macedo GS, et al. Uterine adenosarcomas are mesenchymal neoplasms. *J Pathol*. (2016) 238:381–8. doi: 10.1002/path.4675

24. Clark AD, Oldenbroek M, Boyer TG. Mediator kinase module and human tumorigenesis. *Crit Rev Biochem Mol Biol*. (2015) 50:393–426. doi: 10.3109/10409238.2015.1064854

25. Buyukcelebi K, Chen X, Abdula F, Elkafas H, Duval AJ, Ozturk H, et al. Engineered MED12 mutations drive leiomyoma-like transcriptional and metabolic programs by altering the 3D genome compartmentalization. *Nat Commun*. (2023) 14:4057. doi: 10.1038/s41467-023-39684-y

26. Mehine M, Mäkinen N, Heinonen H-R, Aaltonen LA, Vahteristo P. Genomics of uterine leiomyomas: insights from high-throughput sequencing. *Fertil Steril*. (2014) 102:621–9. doi: 10.1016/j.fertnstert.2014.06.050

27. Lim WK, Ong CK, Tan J, Thike AA, Ng CCY, Rajasegaran V, et al. Exome sequencing identifies highly recurrent MED12 somatic mutations in breast fibroadenoma. *Nat Genet*. (2014) 46:877–80. doi: 10.1038/ng.3037

28. Yuan C-T, Huang W-C, Lee C-H, Lin M-C, Lee C-H, Kao Y-C, et al. Comprehensive screening for MED12 mutations in gynaecological mesenchymal tumours identified morphologically distinctive mixed epithelial and stromal tumours. *Histopathology*. (2017) 70:954–65. doi: 10.1111/his.13156

frontiers | Frontiers in Oncology

TYPE Case Report
PUBLISHED 17 May 2024
DOI 10.3389/fonc.2024.1391850

OPEN ACCESS

EDITED BY
Andrea Tinelli,
Veris delli Ponti Hospital, Italy

REVIEWED BY
Nasuhi Engin Aydin,
Izmir Kâtip Çelebi University, Türkiye
Francesk Mulita,
General University Hospital of Patras, Greece

*CORRESPONDENCE
Yonghong Yu
yuyonghong8379@126.com

RECEIVED 26 February 2024
ACCEPTED 06 May 2024
PUBLISHED 17 May 2024

CITATION
Hu J, Tian S, Pan Q and Yu Y (2024) Multiple benign metastasizing leiomyoma in the abdominal wall: a case report and literature review.
Front. Oncol. 14:1391850.
doi: 10.3389/fonc.2024.1391850

Multiple benign metastasizing leiomyoma in the abdominal wall: a case report and literature review

Jiaqi Hu[1], Shuyuan Tian[1], Qing Pan[2] and Yonghong Yu[1]*

[1]Department of Ultrasound Medicine, Tongde Hospital of Zhejiang Province, Hangzhou, China,
[2]Department of Pathology, Tongde Hospital of Zhejiang Province, Hangzhou, China

Benign metastasizing leiomyoma (BML) is a rare disease that results from metastasis of uterine leiomyoma to distant sites with benign pathologic features. The lung is the most common metastatic site for BML. This report describes the case of a 49-year-old woman who presented with a mass in the abdominal wall with a surgical history of uterine myomectomy. Ultrasound and Magnetic resonance imaging (MRI) revealed multiple mass lesions. The histopathology of the mass specimen indicated BML. The imaging and clinical features of BML are discussed based on the characteristics of this case and related literature reports.

KEYWORDS

benign metastasizing leiomyoma, myomectomy, abdominal wall, smooth muscle cell, CEUS

Introduction

BML is a rare disease, first described by Steiner in 1939 (1). Although the disease appears benign in histomorphology, the biological behavior of the tumor is invasive. The most commonly involved organ is the lung, and others include lymph nodes, heart, skeletal muscle and pelvic cavity (2–4). BML is usually associated with a history of hysterectomy or myomectomy (5). A patient with BML in the abdominal wall is described in this study.

Case presentation

A 49-year-old woman, gravida 1 para 1, accidentally presented with an egg-sized abdominal mass. Symptoms of fever, abdominal pain, and weight loss were not present, and she had previously undergone myomectomy. Physical examination revealed a rigid mass, with moderate motion and no tenderness.

Ultrasound examination showed multiple hypoechoic masses in the subcutaneous fascia layer. The two larger ones are approximately 41 x 25mm and 20 x 16mm with clear

boundaries that were connected (Figure 1A). Color Doppler flow imaging (CDFI) showed a punctate blood flow signal within the mass (Figure 1B), and resistance index of 0.74. Contrast-enhanced ultrasound (CEUS) was performed using the contrast agent SonoVue. Simultaneously, an ultrasound-guided abdominal wall mass core needle biopsy was performed on the two masses. The larger mass showed relatively high enhancement in both arterial and venous phases. The smaller mass showed relatively no enhancement in the arterial phase and low enhancement around in venous phase (Figure 1C). An MRI was performed, which showed similar circular abnormal signal shadows on the anterior abdominal wall and abdominal cavity, with sizes of 29 x 16mm and 31 x 21mm, a slightly longer T1 and slightly longer T2, limited diffusion, and progressive enhancement after enhancement (Figures 2A–F). Chest Computed Tomography (CT) examination showed no abnormality. CEA, AFP, CA724, CA199 and CA125 markers were all normal.

Pathology of the biopsy suggested a spindle cell tumor, and combined with the patient's surgical history, a fibromatosis in the abdominal wall was considered. The patient underwent the elective resection of the abdominal wall and abdominal cavity tumors. Two masses of 4 x 3cm and 2 x 2cm were observed during the operation, the larger one protruding into the abdominal cavity and the smaller one located in the anterior sheath of the rectus muscle. Two masses, about 2/3 of the rectus abdominis muscle and part of the posterior sheath, were removed completely. The surgeon performed tension-free repair of an abdominal wall hernia, inserting the patch into the abdominal cavity under the incision, fixing it on the abdominal wall, and suturing the rectus abdominis muscle and anterior sheath of the rectus abdominis muscle.

The histopathological examination showed spindle cells. Immunohistochemical staining showed that smooth muscle actin (SMA), desmin, estrogen receptor (ER) and progesterone receptor (PR) were positive, and cell proliferation antigen Ki-67 was less than

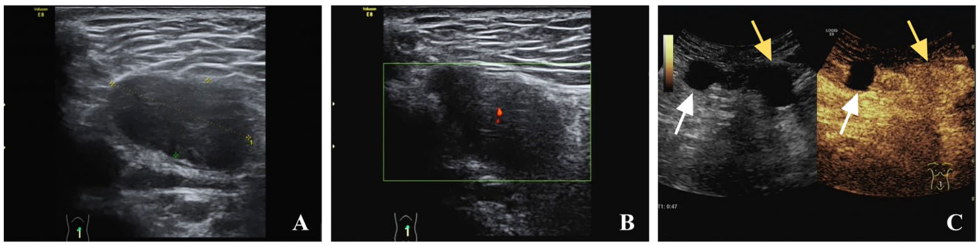

FIGURE 1
Abdominal ultrasonography, contrast-enhanced ultrasound (CEUS) of case. **(A)** Gray scale ultrasound showed a hypoechoic mass in the abdominal wall; **(B)** color Doppler flow imaging (CDFI) showed the mass with little blood flow signal; **(C)** CEUS showed hyper-enhancement of the large mass (yellow arrow) and no enhancement of the small mass (white arrow) in the arterial stage.

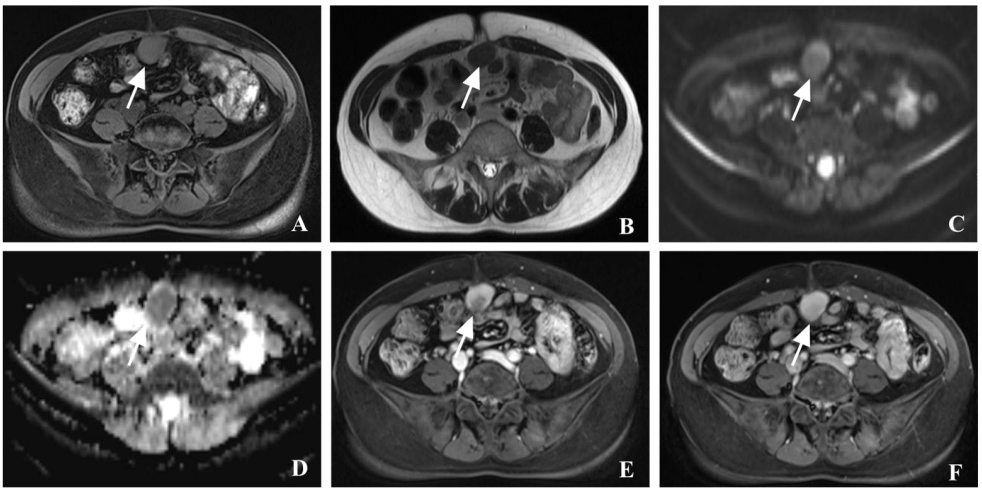

FIGURE 2
Contrast-enhanced magnetic resonance imaging (CE-MRI) of case. **(A–D)** MRI showed a slightly high signal in T1-weighted imaging, and a slightly high signal in T2-weighted imaging, diffusion-weighted imaging (DWI) and apparent diffusion coefficient (ADC); **(E, F)** CE-MRI showed that the mass progressive enhancement in the arterial phase and the delayed phase (see arrows).

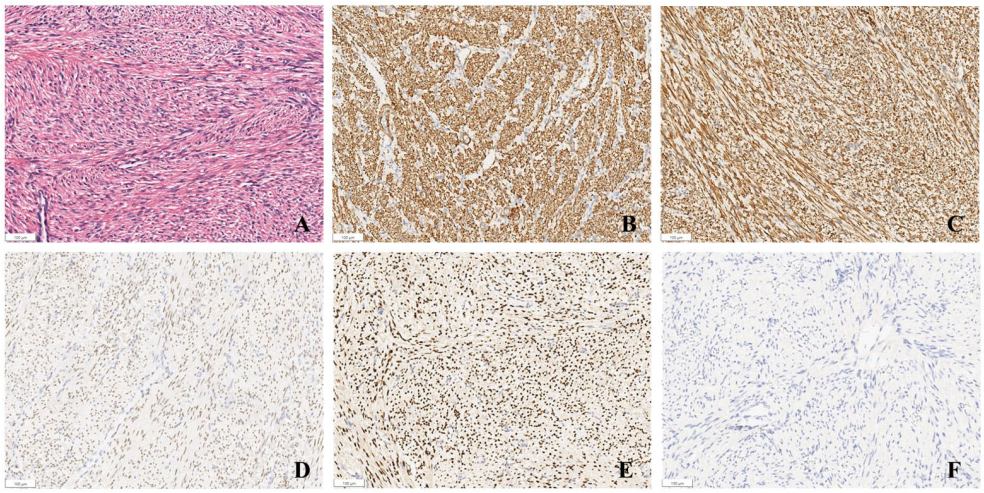

FIGURE 3
Pathology of case. **(A)** mass stained with hematoxylin and eosin (original magnification x 10); **(B–F)** SMA (+), DES (+), PR (+), ER (+), Ki-67 (<1%) was detected by immunohistochemical staining (original magnification x 10).

1% (Figures 3A–F). Based on these findings, the tumor was diagnosed as BML.

Discussion

The mechanism of BML has been reported in various reports and remains controversial. Most instances of BML occur after uterine myomectomy or hysterectomy. The mechanism may be that surgery increases surgically induced hematogenous spread. In this case, iatrogenic peritoneal seeding theory seems to be a more reasonable explanation for the occurrence of BML (6, 7). Immunohistochemistry showed that ER and PR of tumor cells were positive, suggesting that BML may also be induced by hormone stimulation. Chromosomal abnormalities such as 19q, 22q, 1p, 13q deletion and 6p21 rearrangement can be found in these tumors (8). Other possible mechanisms include mesothelial metaplasia and misdiagnosed low-grade uterine leiomyosarcoma metastasis (9).

The clinical symptoms of BML are related to the affected sites. The most common site of metastasis is the lung, and the patients have no obvious clinical manifestations in the early stage, with a few having cough, chest pain, dyspnea and other symptoms (10, 11). In patients with BML involving the spine, leg pain and paresthesia have been reported (5). Patients with metastasis to the femur and muscles may have difficulty walking (12). BML involving the uterus, heart, and lymph nodes may be asymptomatic. Multiple abdominal wall metastases are rare, as reported in this case. BML with abdominal wall metastases has been reported in the literature (Table 1). Although most cases of BML occur following myomectomy or hysterectomy, some cases of BML are not related to prior surgical history (22). Studies have shown that BML can occur in premenopausal or postmenopausal women, and up to 30% of cases may have respiratory symptoms (23).

BML is radiographically characterized as a benign mass. On ultrasound, BML can be manifested as multiple hypoechoic masses in the abdominal wall or pelvic cavity, and blood flow signals can be seen inside. It can be shown as multiple nodules with clear boundaries on CT, with no significant enhancement on enhanced CT (24). Notably, fluorodeoxyglucose (FDG) -positron emission tomography (PET)/CT showed that FDG uptake by tumors was all within the physiological range (12). According to the review of the FDG-PET/CT examination results of BML, the FDG uptake level of more than 90% of BML patients is lower than the medium level (25), which can be used as one of the crucial bases for the differentiation of benign and malignant tumors. Therefore, physicians must maintain heightened awareness and index of suspicion when approaching a woman with a mass in any region of the abdomen or pelvis. Further investigation with abdominal and pelvic ultrasonography and magnetic resonance imaging or computed tomography is necessary. Benign lesions can be found even in patients presenting with giant masses and higher CA125 than normal levels (26). CA125 and CA199 are considered to be important gynecological tumor indicators, which are commonly seen in malignant tumor diseases, and their elevated levels do not represent absolute malignancy (27, 28).

Regarding pathological diagnostic criteria for BML, BML presents as an extra-uterine smooth muscle cell proliferation with histological features similar to those of primary benign uterine fibroids. Uterine leiomyoblastoma can also exhibit some malignant features, making it difficult for physicians to distinguish (29). Immunohistochemistry is also very helpful in differentiating leiomyoma from leiomyosarcoma. Studies have shown that the positive rate of ER/PR in MBL patients is over 90%, and only 4.4% are negative at the same time (30). ER/PR positivity is specific for uterine leiomyomas and may be helpful in diagnosing BML. In the present case, the abdominal mass was excised, and immunohistochemistry confirmed that the patient's ER/PR was positive.

10.3389/fonc.2024.1391850

TABLE 1 Summary of BML cases with abdominal wall metastasis.

Metastasis	Age	History of gynecologic surgery	Surgical treatment
abdominal wall and pelvic cavity	37 (13)	myomectomy 10 years earlier	extirpation of the abdominal and pelvic tumors and partial greater omentum
abdominal wall and pelvic cavity	46 (14)	hysterectomy 8 years earlier	extirpation of the abdominal and pelvic tumors and bilateral oophorectomy
abdominal wall and pulmonary	33 (15)	myomectomy 13 years earlier	extirpation partial tumors
abdominal wall	42 (16)	mysterectomy 8 years earlier	extirpation of the tumors
abdominal wall	44 (17)	hysterectomy	extirpation of the tumors
abdominal wall and pulmonary	44 (18)	myomectomy	N/A
abdominal wall and pelvic cavity	49 (18)	myomectomy 12 years earlier	N/A
abdominal wall, pelvic cavity and pulmonary	47 (19)	twice myomectomy and hysterectomy	N/A
abdominal wall and pulmonary	44 (20)	myomectomy and abdominal hysterectomy	extirpation of the tumors in pulmonary
multiple metastasis (abdominal wall, ventricle wall, lungs, liver, muscles, and pelvic cavity)	37 (21)	twice myomectomy	hysterectomy and resection of the nodules in the mesosalpinx, mesenterium, and abdominal wall
abdominal wall, abdominal and pelvic cavity	54 (9)	abdominal hysterectomy and bilateral salpingo-oophorectomy 6 years earlier	extirpation of the tumors

There is currently no standardized treatment for BML. Due to the behavioral characteristics of the slow growth of BML, most lesions do not change in size after long-term follow-up, and regular follow-up and periodic imaging examinations can be chosen. Since BML can be hormone-dependent (ER and PR-positive), hormone therapy such as GnRH-a, progesterone antagonists (Mifepristone), selective estrogen receptor modulators (SERMs, tamoxifen) and aromatase inhibitors may be considered, or even surgery to remove the ovaries, particularly for patients with symptomatic lung involvement (24, 30, 31). Although bilateral oophorectomy is commonly used, unilateral oophorectomy is sufficient to promote the reduction of lung BML mass (2). In addition, surgical removal of the tumor is an effective treatment.

Conclusion

The characteristics of low specificity and incidence rate of BML can lead physicians to be unfamiliar with the disease, enabling it to be misdiagnosed as a malignant tumor. Asking operation history of myomectomy or hysterectomy can help us diagnose BML. Pathological diagnosis plays an essential role in determining the follow-up treatment. Obtaining part of the specimens through ultrasound-guided tissue core needle biopsy is effective and safe and can be used as one of the recommended methods.

Data availability statement

The original contributions presented in the study are included in the article/supplementary material. Further inquiries can be directed to the corresponding author.

Ethics statement

Written informed consent was obtained from the individual(s) for the publication of any potentially identifiable images or data included in this article.

Author contributions

JH: Writing – original draft. ST: Writing – review & editing. QP: Writing – review & editing. YY: Writing – review & editing.

Funding

The author(s) declare that no financial support was received for the research, authorship, and/or publication of this article.

Conflict of interest

The authors declare that the research was conducted in the absence of any commercial or financial relationships that could be construed as a potential conflict of interest.

Publisher's note

References

1. Steiner PE. Metastasizing fibroleiomyoma of the uterus: report of a case and review of the literature. *Am J Pathol*. (1939) 15:89–110.

2. Pacheco-Rodriguez G, Taveira-DaSilva AM, Moss J. Benign metastasizing leiomyoma. *Clin Chest Med*. (2016) 37:589–95. doi: 10.1016/j.ccm.2016.04.019

3. Liu Y, Li D, Li X, Wang J, Wang J. Benign metastasizing leiomyoma: is "Wait and watch" Strategy feasible? *Reprod Sci*. (2023) 30:3568–77. doi: 10.1007/s43032-023-01314-9

4. Karnib M, Rhea I, Elliott R, Chakravarty S, Al-Kindi SG. Benign metastasizing leiomyoma in the heart of a 45-year-old woman. *Tex Heart Inst J*. (2021) 48:e197066. doi: 10.14503/THIJ-19-7066

5. Hur JW, Lee S, Lee JB, Cho TH, Park JY. What are MRI findings of spine benign metastasizing leiomyoma? Case report with literature review. *Eur Spine J*. (2015) 24 Suppl 4:S600–5. doi: 10.1007/s00586-015-3774-8

6. Beck MM, Biswas B, D'Souza A, Kumar R. Benign metastasising leiomyoma after hysterectomy and bilateral salpingo-oophorectomy. *Hong Kong Med J*. (2012) 18:153–5

7. Cucinella G, Granese R, Calagna G, Somigliana E, Perino A. Parasitic Myomas after Laparoscopic Surgery: An Emerging Complication in the use of Morcellator? Description of Four Cases. *Fertil Steril*. (2011) 96:e90–6. doi: 10.1016/j.fertnstert.2011.05.095

8. Bowen JM, Cates JM, Kash S, Itani D, Gonzalez A, Huang D, et al. Genomic imbalances in benign metastasizing leiomyoma: characterization by conventional karyotypic, fluorescence in *situ* hybridization, and whole genome SNP array analysis. *Cancer Genet*. (2012) 205:249–54. doi: 10.1016/j.cancergen.2012.04.005

9. Awonuga AO, Rotas M, Imudia AN, Choi C, Khulpateea N. Recurrent benign metastasizing leiomyoma after hysterectomy and bilateral salpingo-oophorectomy. *Arch Gynecol Obstet*. (2008) 278:373–6. doi: 10.1007/s00404-008-0581-z

10. Panagiotou E, Vamvakaris I, Syrigos NK, Kotteas E. Pulmonary benign metastasizing leiomyoma: A case report. *Monaldi Arch Chest Dis*. (2023) 94:A6925. doi: 10.4081/monaldi.2023.2411

11. AlQudah MA, Hamouri S, Haddad HK, Tawalbeh R, Haddad HK. Pulmonary benign metastasizing leiomyoma: A report of two cases. *Future Sci OA*. (2022) 8: FSO814. doi: 10.2144/fsoa-2022-0021

12. Aoki K, Yamamoto T, Terauchi R, Mori T, Shirai T, Kitawaki J. Benign metastasizing leiomyoma in femur and thigh with A history of uterine leiomyoma: A case report and literature review. *J Obstet Gynaecol Res*. (2021) 47:812–7. doi: 10.1111/jog.14545

13. Li Y, Xu T, Wang M, Jiang L, Liu Q, Liu K. Concurrent benign metastasizing leiomyoma in the abdominal wall and pelvic cavity: A case report and review of the literature. *Front Surg*. (2022) 9:842707. doi: 10.3389/fsurg.2022.842707

14. Xiao H, Li B, Li W, Feng X, Wu L. A rare case of benign abdominal wall and pelvic metastasizing leiomyomas following hysterectomy. *J Obstet Gynaecol*. (2012) 32:198–9. doi: 10.3109/01443615.2011.622059

15. Zhao L, Jiang R, Li S, Gui Q, Wang Z, Yang Y. Clinicopathological study of 6 cases of benign metastasizing leiomyoma. *Chin J Clin Exp Pathol*. (2017) 33:529–33. doi: 10.13315/j.cnki.cjcep.2017.05.013

16. Kapila K, Mallik MK, Amanguno HG, Ahmed A. Fine needle aspiration diagnosis of a benign metastasizing leiomyoma of the abdominal wall. *J Cytology*. (2008) 25:105–7. doi: 10.4103/0970-9371.44047

17. Schwarz EI, Ramach C, Mende KA, Strobel K. Physiologic FDG uptake in the ovary together with an abdominal wall leiomyoma mimicking metastasizing ovarian cancer on PET/CT imaging. *Clin Nucl Med*. (2009) 34:249–50. doi: 10.1097/RLU.0b013e31819a208f

18. Liang Q, Ling M, Yu H. The imaging findings and literature of 4 cases with pulmonary benign metastasizing leiomyoma. *J Clin Radiol*. (2019) 38:746–50. doi: 10.13437/j.cnki.jcr.2019.04.042

19. Gosavi A, Shah S, Purandare NC, Puranik A, Agrawal A, Rangarajan V. Benign metastasizing leiomyoma and findings on fluorodeoxyglucose positron emission tomography/contrast-enhanced computed tomography. *Indian J Nucl Med*. (2022) 37:68–70. doi: 10.4103/ijnm.ijnm_118_21

20. Ağaçkiran Y, Findik G, Ustün LN, Aydoğdu K, Kaya S. Pulmonary benign metastasizing leiomyoma: an extremely rare case. *Turk Patoloji Derg*. (2014) 32:193–5. doi: 10.5146/tjpath.2013.01217

21. Cai A, Li L, Tan H, Mo Y, Zhou Y. Benign metastasizing leiomyoma. Case report and review of the literature. *Herz*. (2014) 39:867–70. doi: 10.1007/s00059-013-3904-1

22. Pitts S, Oberstein EM, Glassberg MK. Benign metastasizing leiomyoma and lymphangioleiomyomatosis: sex-specific diseases? *Clin Chest Med*. (2004) 25:343–60. doi: 10.1016/j.ccm.2004.01.014

23. Miller J, Shoni M, Siegert C, Lebenthal A, Godleski J, McNamee C. Benign metastasizing leiomyomas to the lungs: an institutional case series and a review of the recent literature. *Ann Thorac Surg*. (2016) 101:253–8. doi: 10.1016/j.athoracsur.2015.05.107

24. Yuan X, Sun Y, Jin Y, Xu L, Dai H, Wang J, et al. Multiple organ benign metastasizing leiomyoma: A case report and literature review. *J Obstet Gynaecol Res*. (2019) 45:2132–6. doi: 10.1111/jog.14066

25. Sawai Y, Shimizu T, Yamanaka Y, Niki M, Nomura S. Benign metastasizing leiomyoma and 18-FDG-PET/CT: A case report and literature review. *Oncol Lett*. (2017) 14:3641–6. doi: 10.3892/ol.2017.6609

26. Mulita F, Tavlas P, Maroulis I. A giant ovarian mass in a 68-year-old female with persistent abdominal pain and elevated serum CA-125 level. *Prz Menopauzalny*. (2020) 19:108–10. doi: 10.5114/pm.2020.97870

27. Mulita F, Oikonomou N, Tchabashvili L, Liolis E, Kehagias I. A giant ovarian mucinous tumor in a 58-year-old postmenopausal patient with persistent abdominal pain and high serum levels of CA 19-9. *Pan Afr Med J*. (2020) 37:76. doi: 10.11604/pamj.2020.37.76.25932

28. Mulita F, Liolis E, Kehagias D, Tchabashvili L, Kaplanis C, Iliopoulos F, et al. An Enormous Pelvic Tumor in a 46-year-old Woman with an Elevated Serum CA 125 level, What Lies Beneath it? Investigation of Uterine Tumors in Postmenopausal Women. *Prz Menopauzalny*. (2021) 20:154–7. doi: 10.5114/pm.2021.109773

29. Mulita F, Iliopoulos F, Plachouri KM, Kehagias I. Uterine leiomyoblastoma. *BMJ Case Rep*. (2021) 14:e241533. doi: 10.1136/bcr-2020-241533

30. Lewis EI, Chason RJ, DeCherney AH, Armstrong A, Elkas J, Venkatesan AM. Novel hormone treatment of benign metastasizing leiomyoma: an analysis of five cases and literature review. *Fertil Steril*. (2013) 99:2017–24. doi: 10.1016/j.fertnstert.2013.01.147

31. Zong D, He W, Li J, Peng H, Chen P, Ouyang R. Concurrent benign metastasizing leiomyoma in the lung and lumbar spine with elevated standardized uptake value level in positron-emission tomography computed tomography: A case report and literature review. *Med (Baltimore)*. (2018) 97:e11334. doi: 10.1097/MD.0000000000011334

frontiers | Frontiers in Oncology

TYPE Case Report
PUBLISHED 24 May 2024
DOI 10.3389/fonc.2024.1415928

OPEN ACCESS

EDITED BY
Andrea Tinelli,
Veris delli Ponti Hospital, Italy

REVIEWED BY
Omer Iqbal,
Loyola University Chicago, United States
Xin Tang,
Hangzhou Wuyunshan Hospital, China

*CORRESPONDENCE
Yankui Wang
qdwangyk@163.com
Xiao Yu
qdu_yuxiao@163.com

†These authors have contributed equally to this work

RECEIVED 11 April 2024
ACCEPTED 13 May 2024
PUBLISHED 24 May 2024

CITATION
Dong S, Sun X, Yu F, Wang W, Zhang L, Wang Y and Yu X (2024) Case report: A case of perineal prolapse of giant uterine fibroids complicated by multiple pulmonary embolisms and deep venous thrombosis. *Front. Oncol.* 14:1415928.
doi: 10.3389/fonc.2024.1415928

Case report: A case of perineal prolapse of giant uterine fibroids complicated by multiple pulmonary embolisms and deep venous thrombosis

Shixiang Dong[1,2], Xin Sun[1], Fengsheng Yu[1], Wenjie Wang[1], Li Zhang[3], Yankui Wang[1*†] and Xiao Yu[1*†]

[1]Department of Gynecology, The Affiliated Hospital of Qingdao University, Qingdao, China, [2]Medical College, Qingdao University, Qingdao, China, [3]Department of Pathology, The Affiliated Hospital of Qingdao University, Qingdao, China

A 43-year-old woman with a history of uterine fibroids, anemia, and deep vein thrombosis presented with a chief symptom of prolapse of tumor from the perineum, complicated by infection. The case was further complicated by bilateral pulmonary multiple embolism, deep vein thrombosis, acute cardiac insufficiency, acute renal insufficiency, and shock. The patient was treated with preoperative placement of an inferior vena cava filter, open hysterectomy, and perioperative anticoagulation with low-molecular-weight heparin. She smoothly navigated the perioperative period and recovered completely.

KEYWORDS

giant uterine fibroids prolapse from vagina complicated infection, intravascular leiomyomatosis, pulmonary embolism, deep vein thrombosis, inferior vena cava filter

Case presentation

In December 2022, a 43-year-old woman was hospitalized with a chief complaint of having had uterine fibroids for four years and experiencing irregular menstruation for the past three months. She had a history of uterine fibroids for four years and had a history of blood transfusion because of anemia. The patient had a menstrual cycle of 30 days, menstrual period of 4 days, moderate menstrual flow, and no dysmenorrhea. She had an obstetric history of G3P1 and had never used oral short-acting contraceptives. Pelvic examination showed a smooth cervix and a 3-cm tumor protruding from the cervical canal, which was polypoid and irregular in shape. Pelvic and abdominal examination suggested a tumor comparable in size to a 5-month gestational uterus, with a clear boundary and no obvious tenderness. Pathological examination of cervical neoplasia showed endometrial polyps. Transvaginal ultrasound did not show a normal uterine structure but identified a 20.6 cm × 17.7 cm × 10.7 cm hypoechoic mass with an irregular shape and uneven echo in

the pelvic and abdominal cavities, which protruded downward out of the cervical canal over an area of 2.6 cm × 2.0 cm. Around this mass, another hypoechoic mass measuring 18.3 cm × 14.3 cm × 8.3 cm was detected. Lower limb vascular ultrasound showed a left lower limb intermuscular venous thrombosis measuring approximately 4.1 cm in length, with a D-dimer level of 1340 ng/mL, suggesting a new thrombosis. The patient had not got the COVID-19 immunization. She was infected with COVID-19, got a fever, and a chest CT revealed lung inflammation; therefore, her operation was postponed. After discharge, the patient stopped oral anticoagulant therapy with rivaroxaban and did not seek further medical consultation.

On December 14, 2023, the patient returned to the outpatient clinic complaining of a vaginal prolapse tumor appearing two days prior. She explained that the tumor had prolapsed from her vagina after coughing and could not be repositioned, accompanied by slight vaginal bleeding. The patient described feeling weak, experiencing slight chest tightness and suffocation, considerable abdominal and lumbosacral pain. She had difficulty urinating but had no chest pain, or swelling and pain in her lower limbs. Physical examination showed that the abdomen was distended, with a palpable hard mass in the lower abdomen ranging about 25 cm. The upper edge of the mass reached 4 cm above the navel. Mild edema was observed in the left lower limb. Pelvic examination showed that the vaginal prolapse tumor measured approximately 8 cm in length; it was columnar in shape and obstructed the vaginal opening. The tumor was purple-red in color, extending upward along the vagina, and was associated with a significant amount of pale yellow vaginal fluid with an unpleasant odor. The cervix was not palpable. In the pelvic and abdominal cavity, tumors comparable in size to more than six months' gestational uterus were palpable, but these had no tenderness.

The patient was admitted to the hospital for emergency treatment. The admission diagnosis included possible uterine fibroids, vaginal prolapse tumor complicated with infection, and a history of deep vein thrombosis. Transvaginal ultrasound revealed a solid hypoechoic mass in the pelvis and abdominal cavity, measuring at least 27 cm × 24 cm × 14 cm. The internal echo was uneven, showing multiple irregular cystic cavities, with a ring-shaped strong echo observed at the edge of the mass. The upper part of the mass reached under the xiphoid process, and the lower part protruded outside the vaginal opening. After admission, the vaginal prolapse tumor continued to grow, although its color became ruddy. The patient was treated with indwelling catheterization, and vaginal secretions were collected for bacterial culture. Empirical anti-infection treatment was initiated with an intravenous drip of cefoperazone sodium and sulbactam sodium at a dose of 3.0 g every 8 hours.

Subsequent diagnostic tests revealed the following. D-dimer levels were considerably elevated at 14620 (reference range 0–500) ng/mL; prothrombin time and activated partial thromboplastin time of hemagglutination were normal; the white blood cell count was elevated at 15.25 × 10^9/L (reference range 3.5–9.5 × 10^9/L); hemoglobin levels were low at 84 (reference range 115–150) g/L; C-reactive protein levels were significantly increased at 61.55 (reference range 0–5) mg/L; procalcitonin levels were slightly elevated at 0.068 (reference range 0–0.05) ng/mL, and CA125 levels were elevated at 106 (reference range 0–47) U/mL. A lower-extremity vascular ultrasound revealed solid hypoechoic fillings in the left common femoral vein, popliteal vein, posterior tibial vein, peroneal vein, calf intermuscular vein, great saphenous vein, and small saphenous vein, leading to a diagnosis of deep venous thrombosis of the left lower extremity. Cardiac ultrasound showed a pulmonary artery pressure of 66 mmHg, indicating severe pulmonary hypertension, along with enlargement of the right atrium and right ventricle, reduced right heart function, and severe tricuspid regurgitation. CT angiography of the pulmonary artery showed multiple filling defects in various segments of both the left and right pulmonary arteries, including the left pulmonary artery, left upper pulmonary artery, left lower pulmonary artery, right pulmonary artery, right upper pulmonary artery, and right lower pulmonary artery, suggesting the presence of multiple thromboembolism in both pulmonary arteries, as shown in Figure 1. Fortunately, CT angiography of the inferior vena cava showed no thrombosis. During the examination, the patient experienced slight chest tightness, slight breath-holding symptoms, slight shortness of breath, and considerable abdominal pain. Measures were taken to manage her symptoms and potential complications; the patient was advised to elevate her left lower limb and lie in bed while restricting activities. Continuous ECG monitoring and oxygen inhalation were also initiated.

A myocardial enzyme test showed elevated levels of high-sensitivity troponin T at 0.333 (reference range 0–0.014) μg/L, suggesting acute myocardial injury. The patient had symptoms of oliguria, including decreased food intake, vaginal discharge, sweating, and only 50 mL of urine in 12 hours. Acute renal insufficiency was considered due to the patient's inadequate intake, the urine volume not increasing substantially even after rehydration, and an increase in creatinine levels from 45.9 μmol/L to 89.6 (reference range 41.0–73.0) μmol/L. The patient's left leg was obviously swollen, and she showed a progressive drop in blood pressure, with values between 85–90/45–60 mmHg. Blood oxygen saturation levels were maintained at 95%–99% with nasal tube oxygen inhalation at 3 L/min and dropped to 90%–95% in a non-oxygen inhalation state. The patient's body temperature ranged from 36.0°C to 36.5°C, and her heart rate fluctuated between 85 and 95 beats/min. Blood gas analysis in an oxygen inhalation state revealed a pH of 7.39 (reference range 7.35–7.45) increased partial pressure of oxygen of 139 (reference range 83–106) mmHg, decreased partial pressure of carbon dioxide at 26 (reference range 35–45) mmHg, and elevated lactic acid levels at 4.6 (reference range 0.5–1.6) mmol/L. The patient had persistent hypotension and hyperlactatemia, indicating shock and circulatory failure. Consequently, she was transferred to the ICU for further treatment.

The patient was administered norepinephrine and other vasoactive drugs via an intravenous pump, and imipenem–cilastatin sodium at a dosage of 1 g every 8 hours for anti-inflammatory purposes. To improve oxygenation, red blood cell infusions were administered, and efforts were made to correct hypoproteinemia. The medical team carefully controlled the rate and volume of fluid infusion and provided appropriate diuretic

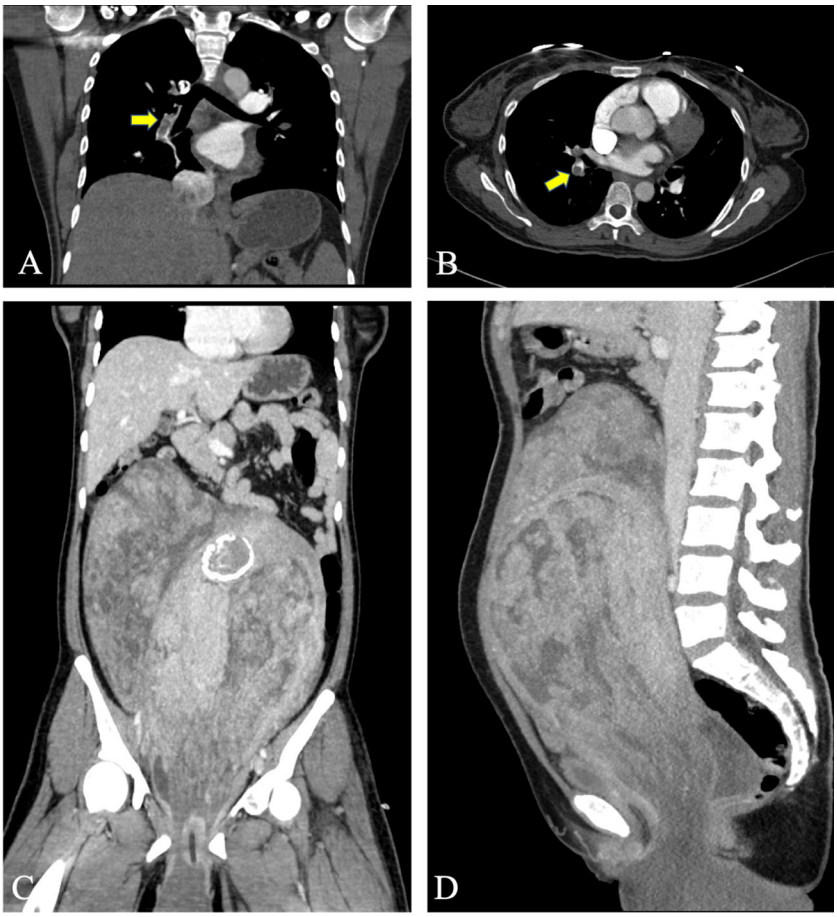

FIGURE 1
Preoperative CT evaluation of the patient. **(A, B)** CT angiography of the pulmonary artery shows multiple pulmonary emboli, and the arrow indicates the thrombus in the right pulmonary vessel. **(C, D)** A huge tumor can be seen in the pelvis and abdomen, with uneven density. Calcium density shadow can be seen, and the tumor protrudes downward out of the perineum.

treatment. During the treatment, a multidisciplinary team (MDT) consultation (imaging doctors, vascular surgeons, ICU doctors, anesthesiologists, cardiologists, respiratory doctors, and gynecologists) was arranged. The consensus from the consultation was that the pelvic and abdominal cavity tumors with infection were likely uterine tumors. Given the severity of the pain and indications for emergency surgery, the consultation highlighted the patient's critical state, including the challenges posed by bilateral pulmonary multiple embolism; extensive deep venous thrombosis in the left lower limb; rapid disease progression; and severe comorbidities such as acute cardiac insufficiency, acute renal insufficiency, shock, circulatory failure, and hyperlactatemia. The risk of circulatory instability and respiratory and cardiac arrest during surgery was noted, considering the patient's right ventricular dysfunction, which significantly increases the risk of mortality. Considering that the patient had symptoms of vaginal bleeding and a need for emergency surgery owing to the prolapsed huge tumor, low-molecular-weight heparin was selected for anticoagulation treatment. It was recommended that an inferior vena cava filter be placed before the operation to prevent the dislodgement of lower-extremity thrombi that could aggravate the pulmonary embolism. Therefore, the patient was administered low-molecular-weight heparin therapy, with instructions to stop the drug 12 hours before surgery, and efforts were intensified to improve the circulatory state of the patient.

After 12 hours of ICU support and treatment, the overall condition of the patient improved. Preoperative evaluation revealed that her body temperature had returned to normal, heart rate had stabilized at 80–90 beats/min, blood pressure had improved to 100–105/60–65 mmHg, with low-dose norepinephrine being administered intravenously, oxygen saturation was 100% with high-flow humidified oxygen therapy (FiO_2 at 40%, flow rate 20 L/min), and the 12-hour urine volume had significantly increased to 1200 mL. Although the vaginal prolapse tumor had further increased in size, measuring about 25 cm × 20 cm × 20 cm, symptoms of abdominal compression had improved. However, the left lower limb remained obviously edematous. Laboratory examination showed that the D-dimer levels had decreased to 3960 ng/mL, white blood cell count had increased to 21.71×10^9/L, hemoglobin level had dropped to 72 g/L, CRP level had decreased to 17.64 mg/L, PCT had increased to 0.170 ng/mL, N-terminal pro-B-type natriuretic peptide had increased significantly from 43.04 to 1733 (reference range 0–125) pg/mL, high-sensitivity troponin T had decreased to 0.075 μg/L, creatinine

had decreased to 50 μmol/L, blood gas had returned to almost normal levels, and lactate had decreased to 1.4 nmol/L.

The patient underwent emergency surgery on December 18, 2023, while minimizing traction on the tumor to avoid causing vagus nerve reflex that could aggravate the burden of circulation. The inferior vena cava filter was initially placed through the right femoral vein, positioning the filter at the L2–3 vertebral body level, and the blood flow to the inferior vena cava was unobstructed after the operation. The gynecological surgery was performed as an open procedure. During the operation, the uterine body was found to be comparable in size to a 5-month gestational uterus. A lobulated mass was palpable on the right side of the uterine body, measuring approximately 20 cm × 15 cm × 10 cm, protruding to the right broad ligament with a surface rich in blood vessels. The right accessory was pushed to the right rear of the uterine body by the right parametrial mass. There were abundant vascular bundles under the right infundibular ligament. The right ovary was deformed and elongated, and could not be retained. A decision to perform a hysterectomy, right adnexectomy, and left salpingectomy was made. The dissected uterus showed prolapsed tumor like submucosal fibroids, with edema and degenerative tissue changes, irregular boundaries in cotton-wool shape, and abundant blood vessels in the tumor, as shown in Figure 2. White, worm-like tissue growths were observed along the blood vessels, which could be pulled out, suggestive of endovascular leiomyomatosis. No tumor involvement was observed in the parametrial or mesosalpinx vessels of the resected uterine specimens. Intraoperative exploration of the parauterine and bilateral internal iliac vessels showed no obvious thickening or stiffening, and no intraluminal strip tumor bodies were palpated. Despite the surgical challenges, the operation proceeded smoothly with precise hemostasis. The intraoperative bleeding amounted to 100 mL, with an infusion volume of 3060 mL. The patient received four units of red blood cells and 290 mL of plasma. The excised uterine specimen weighed 5620 g. Initial rapid frozen section analysis suggested a diagnosis of leiomyoma. The intraoperative diagnosis included prolapsed uterine leiomyoma with infection, endovascular leiomyomatosis, bilateral pulmonary embolism, deep vein thrombosis, circulatory failure, acute cardiac dysfunction, acute renal dysfunction, severe pulmonary hypertension, severe tricuspid regurgitation, anemia, hypoproteinemia, and hyperlactatemia. Postoperative pathological examination revealed a smooth muscle-derived tumor with hemorrhage and infarction, with a huge tumor volume but without obvious atypia of tumor cells. Some areas showed degeneration and edema, and the specimen was rich in blood vessels. Tumor thrombus structures were observed in the focal large blood vessels of the uterine muscle wall, as shown in Figure 3.

The patient was treated in the ICU after the operation, where she continued to receive anti-infection and anticoagulation treatments. Anticoagulation therapy was resumed 12 hours after the operation with low-molecular-weight heparin, administered at a dose of 5000 IU subcutaneously every 12 hours. Efforts were also made to improve her anemia and provide nutritional support. After releasing the brake of the right lower extremity, the patient was treated with an intermittent pneumatic pressure device and antithrombotic pressure bandages. On postoperative day 1, ventilator support was discontinued, and vasoactive drugs were gradually reduced. On postoperative day 3, the patient was transferred back to the gynecological ward. Her symptoms of chest tightness and suffocation had resolved, and the swelling in her left lower limb had gradually improved. A CT angiography of the pulmonary arteries conducted seven days postoperatively showed that the pulmonary embolism was only seen in some branches of the bilateral lower pulmonary arteries but had significantly reduced. On postoperative day 10, the patient was successfully discharged from the hospital. She was prescribed oral rivaroxaban anticoagulant therapy (15 mg bid).

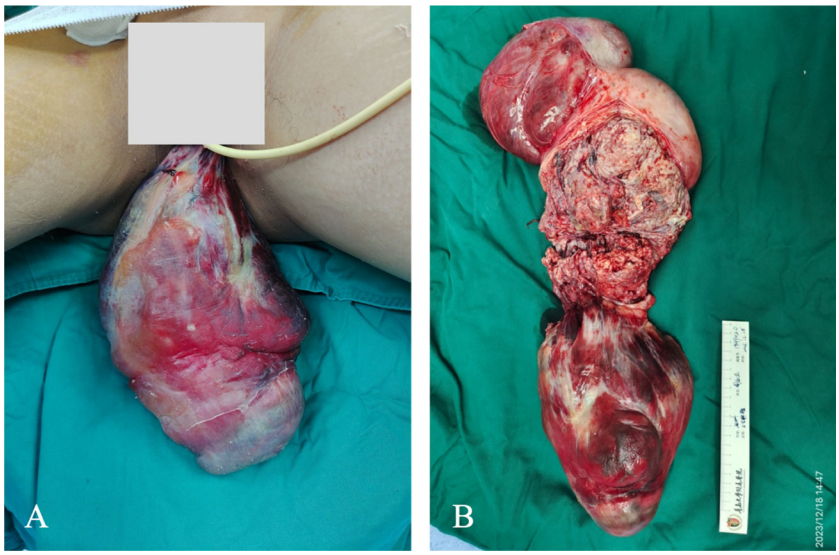

FIGURE 2
Intraoperative investigation of the patient. **(A)** The tumor prolapsed from the perineum measured about 25 cm × 20 cm × 20 cm. Parts of the tumor showed necrosis, while the majority was ruddy and had an unpleasant odor. **(B)** Dissection of the uterus.

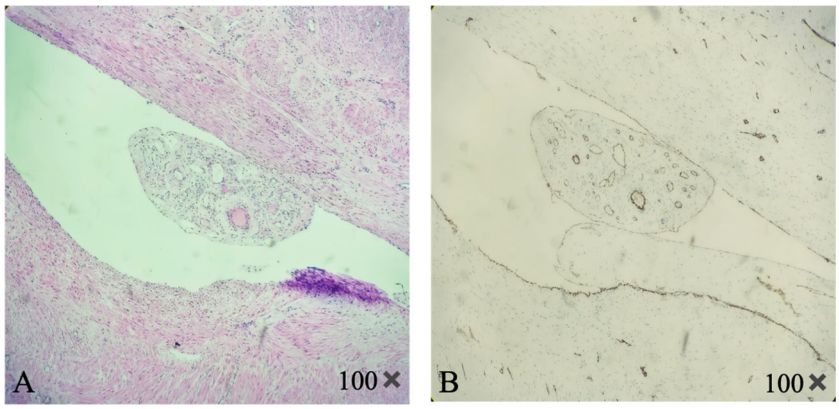

FIGURE 3
Pathology of the uterine tumor. The figure shows the lumen of the uterine vein, which contains tumor tissue derived from smooth muscle. Abundant blood vessels can be seen inside. **(A)** H&E staining **(B)** CD31 immunohistochemical staining shows tumor blood vessels.

One month after the operation, CT angiography of the pulmonary artery revealed no thrombus. Vascular ultrasound identified a strip-like hyperechoic area at the beginning of the left deep femoral vein, measuring approximately 0.19 cm in width, which was interpreted as an old thrombus. The patient's D-dimer levels decreased to 200 ng/mL, and other test results were normal. The patient had no symptoms such as chest tightness, suffocation, or lower-limb edema. In light of her recovery and stabilization, the anticoagulation therapy with rivaroxaban was adjusted to a maintenance dose of 20 mg once daily. Pulmonary artery CT angiography and lower limb vascular ultrasonography were reexamined three months following the initial surgery, and the findings were in concordance. The patient had no bleeding events and a D-dimer reading of 280 ng/mL. After successfully removing the inferior vena cava filter on March 29th, she resumed taking 20 mg of rivaroxaban once per day. After a month, she was planned to lower the dosage and discontinue taking rivaroxaban. We will follow up with the patient closely.

Discussion

Intravenous leiomyomatosis (IVL) is a rare smooth muscle tumor that arises from the growth of uterine fibroids into blood vessels or from the proliferation of leiomyoma tissue in blood vessel walls. It initially develops in the uterine blood vessels; however, the lesion can grow beyond the uterus, along the pelvic veins to the inferior vena cava, and even invade the heart to cause pulmonary embolism, which can be life-threatening in severe cases (1). Venous thromboembolism (VTE) includes deep venous thrombosis (DVT) and pulmonary embolism (PE). Perioperative venous thrombosis is one of the causes of serious complications and death in patients (2). For DVT, the 30-day mortality rate ranges from 2% to 5.5%, while for PE, it ranges from 3.9% to 33%. The mortality rate of surgical patients has increased by over six times due to the development of VTE (3). The dense network of female pelvic veins, combined with venous plexus traffic between organs, exacerbated by factors such as anesthesia, immobility due to surgery, estrogen, and preoperative fasting, creates a hypercoagulable state. In addition, the specific position required for pelvic surgery (head low and feet high) increases the risk of DVT formation and detachment. If the thrombus falls off, it could pass through the inferior vena cava and the right heart into the pulmonary arteries, causing pulmonary embolism, which could be fatal in severe cases. Studies have reported that the probability of VTE is fourfold higher in cases of uterine fibroids weighing more than 1000 g compared to small fibroids (4). Another research reported that the median uterine volume of women who developed VTE was 2715 mL (5).

The patient had been diagnosed with venous thrombosis in the left lower extremity in 2022. The absence of formal anticoagulant treatment aggravated her condition. The huge tumor in the pelvic and abdominal cavity compressed the pelvic vein and inferior vena cava, leading to reduced blood flow. The tumor, combined with the patient's anemia, caused a hypercoagulable state. The left common iliac vein was located between the right common iliac vein and the lumbosacral vertebra, making it susceptible to compression, resulting in slow blood flow in the veins of the left lower extremity. Furthermore, the infection of the vaginal prolapse tumor and the release of inflammatory factors worsened the situation. The above factors accounted for the filling of the deep and superficial veins of the patient's left lower extremity with thrombi. The dislodgement of these venous thrombi led to multiple pulmonary embolisms in both pulmonary arteries. In this case, the intravascular leiomyoma was confined to the uterus, and the DVT and PE were not considered to be caused by intravascular leiomyomatosis.

The patient had multiple emboli in both pulmonary arteries, but the symptoms were not obvious. There were no typical pulmonary embolism manifestations such as chest pain, hemoptysis, or dyspnea. This discrepancy between clinical symptoms and diagnostic findings made pulmonary embolism difficult to identify without specific examinations such as cardiac ultrasound and

pulmonary artery CT angiography. The patient's symptoms were not consistent with the results of the auxiliary examination. Considering that the patient's pulmonary embolism could be a combination of chronic and acute episodes, her cardiopulmonary function was in the compensatory stage at the time of admission. As her condition progressed, the mechanical obstruction caused by the thrombus and the pulmonary artery contraction caused by hypoxia led to severe pulmonary hypertension. This increased the afterload on the right ventricle, causing it to enlarge and leading to acute right heart dysfunction. Due to the limitation of pericardial volume, the left ventricular diastolic volume further reduced, and combined with pulmonary circulation disorder, reduced left cardiac output, causing acute renal dysfunction (prerenal). A large amount of fluid was retained in the tissue space, leading to significant edema in the lower limbs, decreasing venous return and aggravating circulatory and shock symptoms.

The expert recommends that surgical management of large uterine fibroids is contraindicated for a minimum of 4 weeks following diagnosis of acute DVT, and ideally delayed for 3 months to allow for thrombus stabilization (6). However, our patient's situation was complex and was changing rapidly. The treatment of giant uterine fibroids prolapse complicated with DVT and PE was challenging and conflicting. There were two main goals of treatment, one was to stabilize and treat DVT and PE, and the other was to eliminate the predisposing factors, the tumor (7). According to the literature, there have been cases of giant uterine fibroids complicated by DVT and PE treated successfully; however, the majority of these patients received gynecologic surgery once the pulmonary embolism situation had stabilized (8–15), as shown in Table 1. None of these cases guided the emergency treatment of vaginal prolapse with a large tumor and infection. In order to assess the potential risks of various forms of therapy and the anticipated benefits for the patient, we arranged multidisciplinary discussions. We then discussed the treatment plan with the patient and ultimately made treatment decisions. The patient experienced a massive prolapse of uterine fibroid that was deteriorated by bleeding and infection, bilateral numerous emboli, and widespread thrombosis of the left lower extremity's deep and superficial veins. Therefore, thrombolytic therapy, interventional therapy, or pulmonary thrombectomy were all restricted. Performing pelvic surgery in the state of acute pulmonary embolism was associated with a high risk and mortality rate. From the perspective of medical treatment of pulmonary embolism, low molecular weight heparin anticoagulation for at least 2 weeks was recommended before gynecological surgery, the patient has already developed circulatory failure, so timely surgical treatment was implemented. Relieving strain on pelvic and lower leg blood vessels, improving circulation significantly, and removing the restrictions of medication-assisted anticoagulant therapy could only be achieved by surgical intervention (16). Surgery should be performed after a short-term of preoperative anticoagulation, but anticoagulant therapy brings challenges to surgical treatment and increases the risk of bleeding before, during and after surgery. Furthermore, when pulmonary embolism was combined with circulatory insufficiency, the risk of anesthesia increased significantly. During patient transportation and surgery, the movement and compression

TABLE 1 The summary of literature review.

Author	No. of cases	age	Diagnosis	Etiology	Implemented therapies	Weight of resected uterus (g)	Size of uterus (cm)
Satti MA et al.2016 (8)	3	47 60 41	DVT(L)+PE DVT(L+R)+PE PE	pelvic vein compression pelvic vein compression pelvic vein compression +blood transfusion	heparin+warfarin; IVC heparin+warfarin; IVC; hysterectomy massive PE; expired before surgery	—— 3010 ——	22×8.8×14 23.5×14×21.2 18×13×14.9
Cărbunaru A et al.2016 (9)	1	40	DVT(L)+inferior vena cava thrombus	pelvic vein compression	low-weight heparin; IVC; hysterectomy(2 weeks after IVC)	4500	25×21×20
Fernandes FL et al.2014 (10)	1	29	DVT(R)+PE	pelvic vein compression	low-weight heparin+warfarin; hysterectomy (4 months after thrombolytic therapy)	——	largest myoma 10×8×7
Khademvatani K et al.2014 (11)	1	42	DVT(L)+PE	pelvic vein compression + medroxyprogesterone acetate	streptokinase+warfarin; myomectomy (3 months after thrombolytic therapy)	——	20-week size uterus

(Continued)

TABLE 1 Continued

Author	No. of cases	age	Diagnosis	Etiology	Implemented therapies	Weight of resected uterus (g)	Size of uterus (cm)
Kurakazu M et al.2012 (12)	1	40	PE	pelvic vein compression	heparin and tissue plasminogen activator under PCPS treatment; hysterectomy (12 days after thrombolytic therapy)	2700	22×12×11
Nishikawa H et al.2000 (13)	1	51	DVT(L+R)+PE	pelvic vein compression	heparin+warfarin; IVC; hysterectomy (7 days after IVC)	——	——
Bonito M et al.2007 (14)	1	49	DVT(L)+PE	pelvic vein compression	heparin; IVC; hysterectomy	5000	——
Unosawa S et al.2009 (15)	1	53	DVT+PE	pelvic vein compression +extreme obesity+ myomatous erythrocytosis syndrome	pulmonary thrombectomy; IVC; hysterectomy	2714	——

DVT, deep venous thrombosis; PE, pulmonary embolism; L, left; R, right; PCPS, percutaneous cardiopulmonary support; IVC, inferior vena cava filter.

of tumors protruding from the external genitalia and large tumors in the pelvic cavity may increase the risk of thrombosis and thrombus detachment, exacerbating pulmonary embolism. The key issue during the perioperative period was how to avoid new pulmonary embolism. Fortunately, the patient had no thrombus in the inferior vena cava. It was very necessary to place an inferior vena cava filter through interventional surgery before gynecological surgery to prevent further shedding of lower limb thrombus. Given that the patient is 43 years old and had no fertility requirements, open hysterectomy was chosen over uterine fibroid resection to minimize intraoperative bleeding, shorten the surgical time, and prevent recurrence of fibroids. After intraoperative wound hemostasis was verified, an abdominal drainage tube with a large diameter was inserted to get prepared to receive postoperative anticoagulant therapy. Under the guidance of an MDT consultation, a strategy was adopted that involved short-term active anticoagulation before surgery, rapid improvement of the circulation state of the patient, and placement of an inferior vena cava filter before the operation to prevent further dislodgement of the lower limb thrombus. An open hysterectomy was performed, along with careful bleeding management, and postoperative care in the ICU centered on stabilizing circulation, maintaining low-molecular-weight heparin anticoagulation, and administering anti-infection treatments. The patient smoothly navigated the perioperative period. One month following the procedure, a pulmonary artery CT angiography showed no thrombus and just a small amount of residual thrombus in the lower leg veins. The patient's D-dimer levels went back to normal, and she denied any discomfort, which suggests a full recovery. Three months following surgery, the inferior vena cava filter was successfully removed.

This patient was a middle-aged woman with a huge uterine fibroid prolapsed from the vagina and complicated with infection, along with the presence of multiple pulmonary emboli and lower limb venous thrombosis. This case highlights the urgent need for early surgical intervention in patients with uterine fibroids when there are clear indications for such treatment. Moreover, it brings to light the importance of distinguishing IVL from more typical presentations of uterine fibroids. Gynecologists should pay attention to the early detection and management of potential complications associated with giant uterine fibroids, such as lower-extremity venous thrombosis, to reduce the incidence of pulmonary embolism and consequent mortality.

Data availability statement

The original contributions presented in the study are included in the article/supplementary material. Further inquiries can be directed to the corresponding authors.

Ethics statement

The studies involving humans were approved by the Ethics Committee of the Qingdao University Affiliated Hospital. The

studies were conducted in accordance with the local legislation and institutional requirements. The participants provided their written informed consent to participate in this study. Written informed consent was obtained from the individual(s) for the publication of any potentially identifiable images or data included in this article.

Author contributions

SD: Writing – original draft, Methodology, Data curation. XS: Writing – original draft, Data curation. FY: Writing – original draft. WW: Writing – original draft, Data curation. LZ: Writing – original draft, Data curation. YW: Writing – review & editing, Supervision. XY: Writing – review & editing, Supervision, Data curation.

Funding

The author(s) declare that no financial support was received for the research, authorship, and/or publication of this article.

Acknowledgments

We would like to thank Bullet Edits Limited for the linguistic editing and proofreading of the manuscript.

Conflict of interest

The authors declare that the research was conducted in the absence of any commercial or financial relationships that could be construed as a potential conflict of interest.

Publisher's note

References

1. Tang L, Lu B. Intravenous leiomyomatosis of the uterus: A clinicopathologic analysis of 13 cases with an emphasis on histogenesis. *Pathol Res Pract*. (2018) 214:871–5. doi: 10.1016/j.prp.2018.04.011

2. Kotaska A. Venous thromboembolism prophylaxis may cause more harm than benefit: an evidence-based analysis of Canadian and international guidelines. *Thromb J*. (2018) 16:25. doi: 10.1186/s12959–018-0180–6

3. Tafler K, Kuriya A, Gervais N, Leyland N. Guideline no. 417: prevention of venous thromboembolic disease in gynaecological surgery. *J Obstet Gynaecol Can*. (2022) 44:82–96.e1. doi: 10.1016/j.jogc.2021.04.003

4. Shiota M, Kotani Y, Umemoto M, Tobiume T, Tsuritani M, Shimaoka M, et al. Deep-vein thrombosis is associated with large uterine fibroids. *Tohoku J Exp Med*. (2011) 224:87–9. doi: 10.1620/tjem.224.87

5. Cai E, Shao YH, Suarthana E, Bergeron A, Mansour FW, Krishnamurthy S. A case series of patients with large uterine fibroids and venous thromboembolisms. *J Obstet Gynaecol Can*. (2021) 43:352–60. doi: 10.1016/j.jogc.2020.10.009

6. Moulder JK, Siedhoff MT, Till SR, Moll S. Management considerations for patients with uterine fibroids and concurrent venous thromboembolism. *Curr Opin Obstet Gynecol*. (2016) 28:329–35. doi: 10.1097/GCO.0000000000000286

7. Gupta S, Manyonda IT. Acute complications of fibroids. *Best Pract Res Clin Obstet Gynaecol*. (2009) 23:609–17. doi: 10.1016/j.bpobgyn.2009.01.012

8. Satti MA, Paredes Saenz C, Raju R, Cuthpert S, Kanzy A, Abhari S, et al. Should prophylactic anticoagulation be considered with large uterine leiomyoma? A case series and literature review. *Case Rep Obstet Gynecol*. (2016) 2016:9803250. doi: 10.1155/2016/9803250

9. Cărbunaru A, Herlea, Ionescu M, Dumitraşcu T. Extensive left iliac veins and inferior vena cava thrombosis revealing a giant uterine myoma. *Rom J Intern Med*. (2016) 54:70–3. doi: 10.1515/rjim-2016–0009

10. Fernandes FL, Dinardo CL, Terra-Filho M. Uterine myoma as a cause of iliac vein thrombosis and pulmonary embolism: common disease, rare complication. *Respirol Case Rep*. (2014) 2:132–4. doi: 10.1002/rcr2.79

11. Khademvatani K, Rezaei Y, Kerachian A, Seyyed-Mohammadzad MH, Eskandari R, Rostamzadeh A. Acute pulmonary embolism caused by enlarged uterine leiomyoma: a rare presentation. *Am J Case Rep*. (2014) 15:300–3. doi: 10.12659/AJCR.890607

12. Kurakazu M, Ueda T, Matsuo K, Ishikura H, Kumagai N, Yoshizato T. Percutaneous cardiopulmonary support for pulmonary thromboembolism caused by large uterine leiomyomata. *Taiwan J Obstet Gynecol*. (2012) 51:639–42. doi: 10.1016/j.tjog.2012.09.023

13. Nishikawa H, Ideishi M, Nishimura T, Kawamura A, Kamochi H, Tahara H, et al. Deep venous thrombosis and pulmonary thromboembolism associated with a huge uterine myoma–a case report. *Angiology*. (2000) 51:161–6. doi: 10.1177/000331970005100210

14. Bonito M, Gulemì L, Basili R, Brunetti G, Roselli D. Thrombosis associated with a large uterine myoma: case report. *Clin Exp Obstet Gynecol*. (2007) 34:188–9.

15. Unosawa S, Hata M, Sezai A, Niino T, Yoshitake I, Minami K. Pulmonary embolism with myomatous erythrocytosis syndrome and extreme obesity. *Thorac Cardiovasc Surg*. (2009) 57:313–4. doi: 10.1055/s-2008–1038880

16. Srettabunjong S. Systemic thromboembolism after deep vein thrombosis caused by uterine myomas. *Am J Forensic Med Pathol*. (2013) 34:207–9. doi: 10.1097/PAF.0b013e318298a456

frontiers | Frontiers in Medicine

TYPE Case Report
PUBLISHED 31 May 2024
DOI 10.3389/fmed.2024.1407546

OPEN ACCESS

EDITED BY
Radmila Sparic,
University of Belgrade, Serbia

REVIEWED BY
Mladen Anđić,
University of Belgrade, Serbia
Andrea Tinelli,
Veris delli Ponti Hospital, Italy
Safak Hatirnaz,
Medicana Hospital, Türkiye

*CORRESPONDENCE
Igor Ilic
✉ ilicigor2909@gmail.com

RECEIVED 26 March 2024
ACCEPTED 13 May 2024
PUBLISHED 31 May 2024

CITATION
Bicanin-Ilic M, Ilic I, Dimitrijevic A, Mujkovic S, Jovic N, Rakic D, Arsenijevic N, Nikolic-Turnic T, Balovic G, Peric A, Mitrovic A and Nikolov A (2024) Case report: Spontaneous rupture of leiomyosarcoma uteri 8 months after primary laparoscopic surgery of STUMP.
Front. Med. 11:1407546.
doi: 10.3389/fmed.2024.1407546

Case report: Spontaneous rupture of leiomyosarcoma uteri 8 months after primary laparoscopic surgery of STUMP

Marija Bicanin-Ilic[1,2], Igor Ilic[3]*, Aleksandra Dimitrijevic[1,2], Srdjan Mujkovic[1,2], Nikola Jovic[1,2], Dejana Rakic[1,2], Neda Arsenijevic[1,2], Tamara Nikolic-Turnic[4,5], Goran Balovic[6,7], Andjela Peric[1,2], Aleksandra Mitrovic[1,2] and Aleksandar Nikolov[1,2]

[1]Department of Gynecology and Obstetrics, Faculty of Medical Sciences, University of Kragujevac, Kragujevac, Serbia, [2]Clinic of Gynecology and Obstetrics, University Clinical Center Kragujevac, Kragujevac, Serbia, [3]Department of Radiology, University Clinical Center Kragujevac, Kragujevac, Serbia, [4]Department of Pharmacy, Faculty of Medical Sciences, University of Kragujevac, Kragujevac, Serbia, [5]N.A. Semashko Public Health and Healthcare Department, F.F. Erismann Institute of Public Health, I.M. Sechenov First Moscow State Medical University (Sechenov University), Moscow, Russia, [6]Department of Surgery, Faculty of Medical Sciences, University of Kragujevac, Kragujevac, Serbia, [7]Center of Pediatric Surgery, University Clinical Center Kragujevac, Kragujevac, Serbia

Introduction: Leiomyosarcoma (LMS), together with smooth muscle tumors of uncertain malignant potential (STUMP) and benign leiomyomas, belongs to a heterogeneous group of uterine neoplasms. According to the World Health Organization, tumors originating from uterine smooth muscle fibers are the second most frequent tumors. It is challenging to distinguish between STUMP and LMS because of an overlap of symptoms, lack of a precise definition, and unequivocal information obtained using imaging diagnostic methods. Following myomectomy or hysterectomy with laparoscopic or laparotomy surgery and a definitive histological diagnosis of STUMP, the course of treatment is determined by the need to preserve fertility. In 2014, the U.S. Food and Drug Administration published an alert that unprotected laparoscopic morcellation is correlated with a 3-fold higher likelihood of dissemination of malignant cells and disease progression. Unprotected morcellation was independently associated with a higher risk of disease recurrence after demolition or conservative surgery, with a relative risk of 2.94.

Conclusion: Hematoperitoneum resulting from the spontaneous rupture of a uterine tumor is a rare gynecological emergency, with very few cases reported in the last decade.

KEYWORDS

STUMP, leiomyosarcoma, leiomyosarcoma rupture, STUMP progression, STUMP recurrence, laparoscopy, uterus

1 Introduction

Leiomyosarcoma (LMS), together with smooth muscle tumors of uncertain malignant potential (STUMP) and benign leiomyoma, belongs to a group of heterogeneous mesenchymal uterine neoplasms (1). This group of tumors originating from uterine smooth muscle fibers is the second most frequent tumor category, affecting 70% of women in their lifetime and causing

significant quality of life and economic problems (2, 3). The common symptoms caused by this group of tumors include dysmenorrhea, abnormal uterine bleeding, back pain, pelvic pressure, urinary urgency, anemia, and infertility (1, 3, 4). These tumors are classified into three groups according to mitotic activity, proliferative capacity, cytological atypia, and tumor necrosis or coagulation. The Stanford criteria, proposed by Bell et al., are an attempt to objectivize the pathohistological diagnosis of malignant smooth muscle tumors. By these criteria, LMS must satisfy at least two of the three diagnostic indicators: diffuse moderate-to-severe atypia, a mitotic count of at least 10 mitotic figures (MFs)/10 high power fields (HPFs), and tumor cell necrosis (5). In contrast, STUMP usually only exhibits one indicator (2, 6, 7). Diagnosis should be obtained by a dedicated pathologist with a high level of experience in gynecological oncology. It is challenging to distinguish between STUMP and LMS because of an overlap of symptoms, lack of a precise definition, complexity of pathophysiological findings, and unequivocal information obtained using imaging diagnostic methods. According to the World Health Organization definition, any uterine smooth muscle tumor with features indicating a potential malignancy that does not fulfill the criteria for LMS or leiomyoma may be diagnosed as a STUMP (8). LMSs are rare malignant tumors, representing 1–3% of all malignant uterine tumors, with an unfavorable prognosis, early metastases, and high rates of recurrence (9, 10). Total en bloc hysterectomy is the treatment of choice for LMS (without morcellation), while adjuvant radiotherapy is not recommended. There is no consensus on the use of adjuvant chemotherapy (10). The clinical symptoms and morphological characteristics of malignant and benign uterine tumors widely overlap, making preoperative diagnosis difficult (11). There is also a significant overlap in terminologies, such as STUMP, atypical leiomyoma, atypical leiomyoma with a low risk of recurrence, and atypical leiomyoma with low malignant potential, which contributes to confusion and unequivocal diagnosis (11). Usually, patients with symptom onset require surgical intervention that depends on the patient's age, fertility requirements, tumor type, and surgical skill. Although imaging studies can provide useful information, they are not sufficient to distinguish between the malignant and benign nature of the tumor. Therefore, histopathological STUMP or LMS diagnosis is most often determined by a pathologist postoperatively (3, 8, 9). Diagnoses are usually made incidentally after patients have undergone fibroid surgery (12). There are no specific postoperative management protocols for STUMP, as they are extremely rare tumors. Data regarding recurrence and metastasis are obtained from case studies, and there is a lack of data regarding their biological behavior and long-term outcomes. Additionally, there is heterogeneity in histopathological and imaging features (4, 13).

After patients undergo laparoscopy or laparotomy (myomectomy or hysterectomy) and a definitive histopathological STUMP diagnosis is made, further medical treatment depends on the requirements for fertility preservation (4). Myomectomy is an acceptable choice for patients who want to preserve fertility, but surgical radicalization should be proposed when childbearing is completed (3, 11). The reported recurrence rate after primary surgical resection varies from 7 to 36.4%, and recurrence can present as STUMP or LMS (14). A literature review reported that 5 of 76 (6.6%) patients who underwent myomectomy experienced a relapse, with a follow-up interval ranging from 0.1 to 18 years. Regular follow-ups and monitoring are required if patients decide to undergo conservative treatments. Ultrasonography of the minor pelvis and abdomen, chest radiography, and a gynecologic examination should be performed to rule out new masses and signs of hemorrhage (14). Annual whole abdominal computed tomography should be performed together with magnetic resonance imaging (MRI), especially in patients who undergo unprotected laparoscopic morcellation. In 2014, the U.S. Food and Drug Administration published an alert that this specific procedure is correlated with a 3-fold higher likelihood of dissemination of malignant cells and disease progression (4, 14). Unprotected morcellation was independently associated with a higher risk of disease recurrence after demolition or conservative surgery, with a relative risk of 2.94 (4).

Hematoperitoneum resulting from the spontaneous rupture of a uterine tumor is a rare gynecological emergency, with very few cases reported in the last decade (1). Gynecological hematoperitoneum is usually caused by an ectopic pregnancy, ruptured ovarian cysts, torsion, or trauma (15, 16).

2 Case report

A 49-year-old Caucasian woman was admitted to the Clinical Center Kragujevac, Department of Gynecology and Obstetrics. She was referred by a private practice gynecologist and presented with symptoms of prolonged metrorrhagia and severe anemia. The patient denied taking any medications, food allergies, or previous surgical interventions. She was diagnosed with multiple sclerosis. She had been prescribed corticosteroid therapy but avoided taking medications and follow-up visits; she was symptom-free at the time. Family history: Her mother had a malignant ovarian tumor. Personal history: Our patient had menarche at the age of 13 years, with regular periods every 30 days lasting 7 days. The last period started 1 month prior and was still ongoing. The patient had two vaginal deliveries and no miscarriages.

Clinical findings on the first day of hospitalization: The patient had abnormal uterine bleeding.

Abdominal probe ultrasound findings: The entire minor pelvis was filled with an isoechogenic non-uniform myometrial lesion $133 \times 119 \times 120$ mm in diameter that involved more than 50% of the myometrium, with moderate acoustic shadowing and a circumferential vascular pattern of the lesion.

Laboratory findings on admission day: leukocytes, 8.8×10^9/L; erythrocytes, 2.12×10^9/L; hemoglobin, 50 g/L; hematocrit, 0.162 L/L; mean corpuscular volume, 76.6 fL; mean corpuscular hemoglobin, 23.7 pg.; mean corpuscular hemoglobin concentration, 309 g/L; red cell distribution width, 18.6%; and platelets, 716×10^9/L.

The patient was treated at the hospital with three doses of red blood cells and resuspended erythrocytes for moderate anemia.

Laboratory findings after therapy/hematology: leukocytes, 8.61×10^9/L; erythrocytes, 3.36×10^{12}/L; hemoglobin, 89 g/L; and hematocrit, 0.297 L/L; mean corpuscular volume, 88.4 fL.

Considering the patient's age (49 years) and size and ultrasound image characteristics of the tumor, together with no desire for fertility, our surgeon proposed open hysterectomy as surgical treatment.

Abbreviations: LMS, leiomyosarcoma; MDCT, multidetector computed tomography; MRI, magnetic resonance imaging; MUSA, Morphologic Uterine Sonographic Assessment; STUMP, smooth muscle tumors of uncertain malignant potential.

The patient agreed to the proposed abdominal hysterectomy; however, she reconsidered her decision and sought a second opinion. The patient was discharged from the hospital for personal reasons. Our patient underwent laparoscopic myomectomy (unprotected) in a private surgical clinic performed by an expert gynecological surgeon. Histopathological findings showed that the tumor removed laparoscopically was a STUMP. The patient was advised by her surgeon to undergo another surgery—a hysterectomy; however, she did not accept the treatment proposal.

During the first and second postoperative follow-up visits, ultrasonography revealed an isoechoic lesion at the postoperative scarring site on the uterus, which was described by the radiologist as a hematoma. The patient received conservative treatment with antibiotics and anti-anemia therapy.

Eight months after the laparoscopic surgery, the patient was admitted to the hospital by a gynecologist because of severe abdominal pain, nausea, and vomiting.

Gynecological examination revealed that the entire minor pelvis and lower and middle abdomen were filled with a painful solid tumor mass with limited mobility.

Abdominal ultrasonography revealed a large hyperechogenic tumor with an unclear anterior surface and free fluid in the abdominal cavity.

Urgent multidetector computed tomography (MDCT) of the abdomen and pelvis showed an enlarged uterus with a tumor mass of 110 × 100 mm in diameter, a lobulated contour, and disruption of the anterior wall of the uterine contour (consistent with uterine rupture), which caused hematoperitoneum. A cystic lesion in the liver with small solid parts and a septum 38 mm in diameter were also found. A few cyst-like focal lesions up to 20 mm in size were found in the lungs (Figure 1).

The patient was informed about the urgency of the medical condition and the need for surgical intervention. After the patient provided signed informed consent and adequate preoperative preparation, an open laparotomy was performed.

Intraoperative findings revealed an enlarged uterus with a tumor mass, anterior wall rupture with focal necrosis, and hemorrhage with multiple urinary bladder peritoneal adhesions. Both the adnexa were morphologically unremarkable. A total abdominal hysterectomy with bilateral adnexectomy and omentectomy was performed (Figure 2).

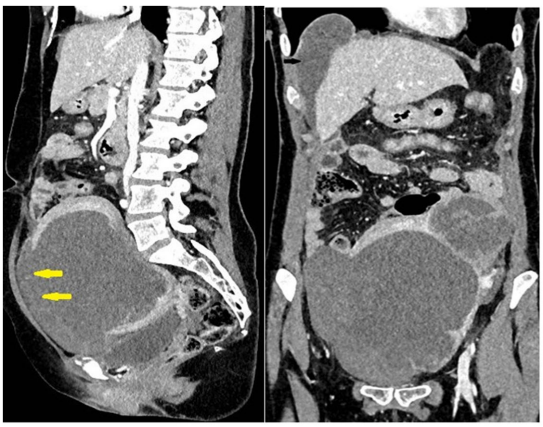

FIGURE 1
Large uterine tumor rupture (yellow arrows) with hemoperitoneum. Metastases in the lung and liver.

Histopathological macroscopic findings showed both adnexa with a deformed uterus, 200 × 110 × 120 mm in diameter, weighing 1,200 g. On the right lateral anterior uterine wall, a 30 mm long defect of uterine tissue with rough edges was yellowish-red in color, distinctly softened, and 102 mm in diameter. On the uterine surface, there was a subserosal nodule, 83 mm in diameter, soft in consistency, with a ring-shaped field on the cross-section. The cavum was dislocated, and the endometrium was up to 3 mm thick in the uterine body section. The adnexa and cervix appeared normal. Processing methods: hematoxylin and eosin staining and immunohistochemistry (IHC).

The front uterine wall was infiltrated by a necrotic tumor mass with extensive fields of hemorrhage, mostly a swirling appearance, a very thin stroma, and markedly proliferated blood vessels. The tumor showed a fascicular-solid morphology, composed of strikingly polymorphic cells, mostly spindle-shaped and eosinophilic cytoplasm, with hypertrophic-hyperchromatic, partly bizarre nuclei, including visible multinucleated giant cell elements, with clearly visible increased mitotic activity. Tumor tissue with the same characteristics was seen in separately delivered tissue fragments and in tissue fragments labeled as "small intestine changes biopsy." The blood vessel invasion was multifocal. Remnants of a benign mesenchymal smooth cell tumor were observed in the surrounding tissue. Immunohistochemically, tumor cells were diffusely positive for smooth muscle actin, desmin, caldesmon, calponin, p16, and cytokeratin AE1/AE3; approximately 30% of cells expressed p53 (measured twice), approximately 10% of cells expressed estrogen receptors (10%++, score 4), and were negative for CD10 and progesterone receptors. The proliferation index was remarkably high, and Ki-67 was expressed in approximately 75% of the cells (Figure 3).

Pathologist's conclusion: The pathohistological picture of the tumor, along with the obtained immunophenotype, corresponded to malignant mesenchymal proliferation, which is a classical variant of uterine LMS with a high degree of malignancy.

Radiologists performed multiple diagnostic imaging studies that revealed lung, liver, colon, and peritoneal metastases. There was a right-sided neck colliquative mass (most likely metastasis), 75 × 40 × 35 mm in diameter, with C5 and C6 vertebral destruction and propagation to the spinal canal (Figure 4).

The patient was then referred to a multidisciplinary oncology advisory board. The patient had distant metastases; hence, the disease was classified as an IVB stage as per the International Federation of Gynecology and Obstetrics classification. The Oncology Advisory Board proposed chemotherapy, including adriamycin monotherapy.

3 Discussion

The strength of our study is the report of the unwanted outcome of the STUMP misdiagnosis and surgery outcome. This study has potential limitations: the effect estimates in the model are based on a retrospective observational study. There is also a lack of available data (from private clinic surgery and pathophysiological examination). Considering that the study is a case report, there is a lack of data that can lead to a conclusion that could be generalized. Therefore, future studies on this delicate topic are necessary.

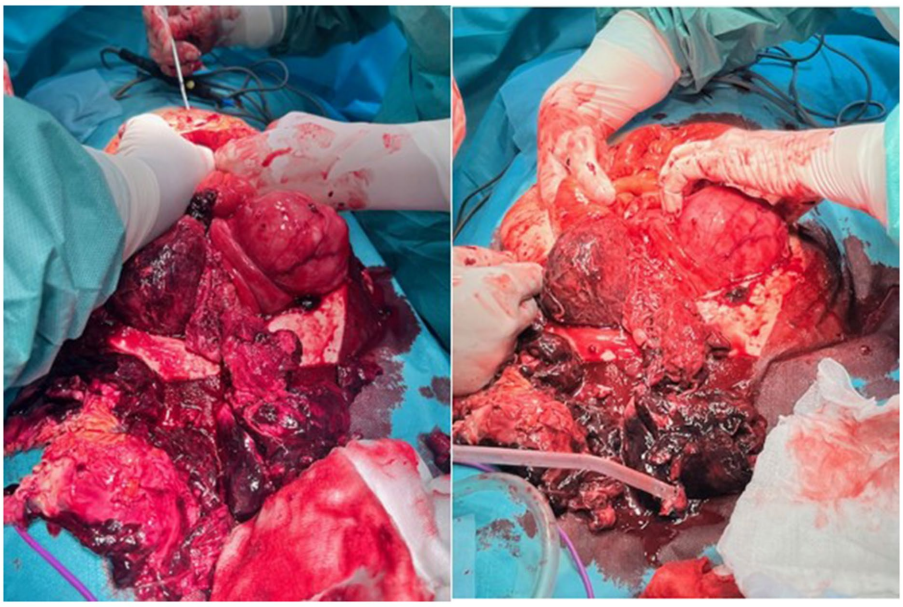

FIGURE 2
Infraumbilical laparotomy and exploration of the abdominal cavity, discontinuity of the anterior uterine wall with a large hematoma on the rupture spot.

FIGURE 3
Uterus with both salpinges and tumor on the anterior wall, with a hematoma on the rupture spot with parts of the tumor.

This paper presents a 49-year-old woman with STUMP with non-specific symptoms, such as abdominal pain, pelvic pressure, abnormal uterine bleeding, and anemia (17). She had non-specific symptoms and belonged to an age group in which STUMP and LMS mostly occur (18). Our Clinical Center's diagnostic imaging protocol for uterine tumors includes ultrasonography, MDCT, and MRI.

Ultrasound examination is the first step in the evaluation of uterine tumors; however, a limited field of view is a problem with large tumors. Some sonographic features, such as gross tumor size (>5 cm), highly vascularized mass, irregular outline, and necrotic areas, are more often linked to LMS and STUMP (11). Morphological uterine sonographic assessment (MUSA) has been proposed by consensus to describe the ultrasonographic features of the myometrium and uterine mass. According to the MUSA, STUMP shows higher color Doppler enhancement than that in benign masses due to higher intralesional and perilesional vascularization (11).

MDCT of the abdomen and pelvis is the first choice for urgent diagnostic imaging. It provides information on tumor size, extension, margins, structure (necrosis and hemorrhage), potential ascites, lymphadenopathy, and metastasis.

The absence of ionizing radiation, visualization of the uterine zonal anatomy, and multiparametric protocols make MRI the most useful imaging modality for evaluating uterine tumors (19).

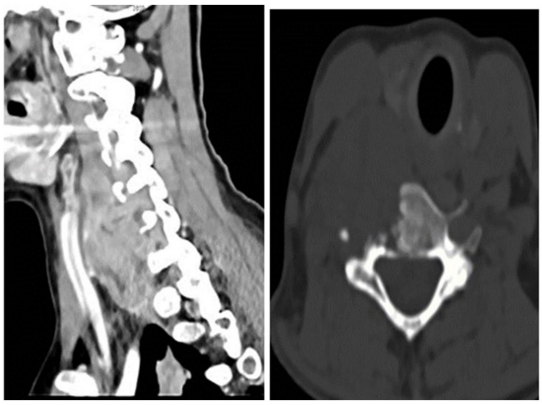

FIGURE 4
Right-sided neck mass.

There should be no difficulty for experienced radiologists to differentiate between typical leiomyoma (sharp, smooth margins, diffuse transverse relaxation time-weighted image hypointensity, no diffusion restriction–low diffusion-weighted imaging/apparent diffusion coefficient of water "blackout phenomenon," and mild postcontrast enhancement) and LMS (irregular ill-defined margins, areas of necrosis and hemorrhage, diffusion restriction, and heterogeneous postcontrast enhancement) (19–21).

However, there is a large overlap between variant leiomyomas (atypical and degenerative), STUMP, and LMSs.

There are a few examples of malignancy scoring systems and MRI models for uterine tumor evaluation that assess tumor margins, transverse relaxation time, diffusion-weighted imaging/apparent diffusion coefficient of water (apparent diffusion coefficient of water value below a threshold), and contrast enhancement (22–25).

Thus far, there has been an average predictive value in the difference between these two groups, and a larger series of cases is necessary to confirm the reliability of the MRI models and scoring systems (21).

After the first laparoscopic surgery, the diagnosis of STUMP was made on the specimen after morcellation. Morcellated tumors can often be overdiagnosed or underdiagnosed by the pathologist because of the limitations of histological evaluation (26). Because of those limitations and the lack of exact pathological criteria, the combination of IHC and clinicopathological findings can be more helpful in determining the final diagnosis and risk of recurrence in STUMP (18).

In a previous study, IHC played a significant role in the differentiation between smooth muscle tumors and endometrial stromal tumors based on positive h-Caldesmon expression and CD10 negative expression; p16 and p53 were diffusely positive, indicating a poor prognosis (7).

Late molecular studies have focused on finding solutions for the preoperative diagnosis of LMS and STUMP and their differential diagnosis of benign uterine fibroids, seeking possible biomarkers based on molecular variations (3, 9). Analyses of gene mutations and chromosomal abnormalities revealed 21 upregulated genes and 74 downregulated genes with possible roles in LMS development (3, 27). These findings are not yet clinically applicable. However, in the era of omics, they are promising starting points, together with technical improvements in imaging diagnostics. Investigating the involvement of the PD1/PD-L1 axis checkpoint in the pathogenesis of mesenchymal tumors is another promising research field. Some studies have shown tumor PD-L1 expression in 70% of LMSs and 14% of atypical leiomyomas; however, no cases of STUMP or benign leiomyomas have shown PD-L1 expression (28).

All of these efforts to achieve a preoperative diagnosis of STUMP and LMS are very important in individualizing therapeutic approaches for each patient. The treatment of choice for STUMP is surgery, myomectomy, or hysterectomy with or without bilateral salpingo-oophorectomy (3, 6, 29). The surgical approach should be tailored based on the patient's age, fertility-sparing wishes, and the size and location of the tumor. The laparoscopic approach is an acceptable choice if performed with "in bag" morcellation because of the peritoneum dissemination of malignant cells (3, 11, 30). It results in shorter hospitalization, less postoperative pain, less morbidity, and less adhesion formation (3, 30, 31). Total hysterectomy is the golden standard treatment, and preservation of ovaries could be considered in perimenopausal women, especially in stages I and II of the disease (2, 32).

4 Conclusion

STUMP are extremely rare and are mostly diagnosed in perimenopausal women, at an average age of 44 years (29, 33). Hematoperitoneum due to spontaneous rupture of a uterine tumor is even rarer (16). Our patient had no desire for fertility preservation but refused open surgery during her first hospitalization. There was no convincing preoperative evidence obtained by imaging studies, laboratory investigations, or clinical examination of the malignant potential of her uterine tumor. Therefore, the patient was unable to obtain adequate information about the potential risk of not accepting the proposed surgical treatment. Even after surgery, when a histopathological diagnosis of STUMP is obtained, a detailed explanation of the unpredictable course of the disease should be provided to the patient. For patients who have achieved fertility or have no desire to become pregnant, total hysterectomy with or without bilateral salpingo-oophorectomy should be the treatment of choice to avoid possible recurrence (4, 34–36). In our case, recurrence and malignant progression occurred within a short period. This could be linked to cellular diffusion in the peritoneal cavity owing to unprotected electrical morcellation (4). Although there is no established follow-up protocol for patients with STUMP, follow-up may include a physical examination and blood tests every 6–12 months with additional imaging tests on an as-needed basis (37).

5 Patient perspective

My first doctor told me that I most likely had leiomyoma, and when I came to the Clinical Center for the first time, there was no convincing evidence of the malignant nature of the tumor; therefore, I decided to undergo minimally invasive surgery instead of open hysterectomy. Even after the first surgery, there was no strong evidence to convince me to undergo another radical surgery. I was worried about the long hospital stay, pain after surgery, and scarring.

Data availability statement

The raw data supporting the conclusions of this article will be made available by the authors, without undue reservation.

Ethics statement

Written informed consent was obtained from the participant for the publication of any potentially identifiable images or data included in this article.

Author contributions

MB-I: Writing – original draft, Writing – review & editing, Conceptualization, Validation, Visualization. II: Writing – original draft, Conceptualization, Data curation, Formal analysis, Funding acquisition, Investigation, Methodology, Project administration, Resources, Software, Supervision, Validation, Visualization. AD: Project administration, Resources, Supervision, Writing – review & editing. SM: Data curation, Methodology, Validation, Software, Writing – review & editing. NJ: Investigation, Methodology, Validation, Writing – review & editing. DR: Data curation, Software, Visualization, Writing – original draft. NA: Conceptualization, Data curation, Methodology, Writing – review & editing. TN-T: Conceptualization, Data curation, Formal analysis, Funding acquisition, Investigation, Methodology, Project administration, Resources, Software, Supervision, Validation, Visualization, Writing – review & editing. GB: Conceptualization, Methodology, Validation, Writing – review & editing. AP: Data curation, Investigation, Writing – original draft. AM: Investigation, Project administration, Validation, Writing – original draft. AN: Conceptualization, Data curation, Formal analysis, Funding acquisition, Investigation, Methodology, Project administration, Resources, Software, Supervision, Validation, Visualization, Writing – review & editing.

Funding

The author(s) declare that no financial support was received for the research, authorship, and/or publication of this article.

Conflict of interest

The authors declare that the research was conducted in the absence of any commercial or financial relationships that could be construed as a potential conflict of interest.

Publisher's note

All claims expressed in this article are solely those of the authors and do not necessarily represent those of their affiliated organizations, or those of the publisher, the editors and the reviewers. Any product that may be evaluated in this article, or claim that may be made by its manufacturer, is not guaranteed or endorsed by the publisher.

References

1. Oda H, Hirakawa H. Spontaneous rupture of uterine smooth muscle tumour presenting acute abdominal pain and haemoperitoneum. *BMJ Case Rep*. (2018) 2018:bcr2017222806. doi: 10.1136/bcr-2017-222806

2. Bosoteanu M, Deacu M, Voda RI, Orasanu CI, Aschie M, Vlad SE, et al. Five-year retrospective study of uterine STUMP and Leiomyosarcoma. *Clin Pract*. (2022) 12:897–907. doi: 10.3390/clinpract12060094

3. Sparić R, Andjić M, Babović I, Nejković L, Mitrović M, Štulić J, et al. Molecular insights in uterine Leiomyosarcoma: a systematic review. *Int J Mol Sci*. (2022) 23:9728. doi: 10.3390/ijms23179728

4. Di Giuseppe J, Grelloni C, Giuliani L, Delli Carpini G, Giannella L, Ciavattini A. Recurrence of uterine smooth muscle tumor of uncertain malignant potential: a systematic review of the literature. *Cancers*. (2022) 14:2323. doi: 10.3390/cancers14092323

5. Dall'Asta A, Gizzo S, Musarò A, Quaranta M, Noventa M, Migliavacca C, et al. Uterine smooth muscle tumors of uncertain malignant potential (STUMP): pathology, follow-up and recurrence. *Int J Clin Exp Pathol*. (2014) 7:8136–42.

6. Olga T, Stavroula Lila K, Kounidas G, Maria P, Nikolaos V. Uterine smooth muscle tumour of uncertain malignant potential and in vitro fertilization treatment in an infertile patient. *SAGE Open Med Case Rep*. (2021) 9:2050313X2110125. doi: 10.1177/2050313X211012516

7. Zheng YY, Liu XB, Mao YY, Lin MH. Smooth muscle tumor of uncertain malignant potential (STUMP): a clinicopathologic analysis of 26 cases. *Int J Clin Exp Pathol*. (2020) 13:818–26.

8. Carcangiu MLCSH, Kurman RJ, Carcangiu ML, Herrington S. *WHO classification of Tumours of female reproductive organs. 4th* ed. Lyon: International Agency for Research on Cancer (2014).

9. Mas A, Simón C. Molecular differential diagnosis of uterine leiomyomas and leiomyosarcomas. *Biol Reprod*. (2019) 101:1115–23. doi: 10.1093/biolre/ioy195

10. Kyriazoglou A, Liontos M, Ntanasis-Stathopoulos I, Gavriatopoulou M. The systemic treatment of uterine leiomyosarcomas. *Medicine*. (2021) 100:e25309. doi: 10.1097/MD.0000000000025309

11. Tinelli A, D'Oria O, Civino E, Morciano A, Hashmi AA, Baldini GM, et al. Smooth muscle tumor of uncertain malignant potential (STUMP): a comprehensive multidisciplinary update. *Medicina*. (2023) 59:1371. doi: 10.3390/medicina59081371

12. Shim JI, Han AKW, Jeon HJ, Kim ML, Jung YW, Yun BS, et al. Clinical experience of uterine smooth muscle tumor of uncertain malignant potential in two gynecological centers: oncological and obstetrical aspects. *Eur J Obstet Gynecol Reprod Biol*. (2020) 246:7–13. doi: 10.1016/j.ejogrb.2020.01.002

13. Richtarova A, Boudova B, Dundr P, Lisa Z, Hlinecka K, Zizka Z, et al. Uterine smooth muscle tumors with uncertain malignant potential: analysis following fertility-saving procedures. *Int J Gynecol Cancer*. (2023) 33:701–6. doi: 10.1136/ijgc-2022-004038

14. Liu HT, Wong CN, Wong CN, Liu FS. Uterine smooth muscle tumor of uncertain malignant potential: a review of current knowledge. *Taiwan J Obstet Gynecol*. (2022) 61:935–40. doi: 10.1016/j.tjog.2022.08.003

15. Sandal K, Yetimoglu I, Saragin M, Tug N. Ruptured myometrial tumors as a cause of spontaneous hemoperitoneum. *Clin Exp Obstet Gynecol*. (2020) 47:303. doi: 10.31083/j.ceog.2020.02.5005

16. Danikas D, Theodorou SJ, Kotrotsios J, Sills C, Cordero PE. Hemoperitoneum from spontaneous bleeding of a uterine leiomyoma: a case report. *Am Surg*. (1999) 65:1180–2. doi: 10.1177/000313489906501219

17. Ip PPC, Tse KY, Tam KF. Uterine smooth muscle tumors other than the ordinary leiomyomas and Leiomyosarcomas: a review of selected variants with emphasis on recent advances and unusual morphology that may cause concern for malignancy. *Adv Anat Pathol*. (2010) 17:91–112. doi: 10.1097/PAP.0b013e3181cfb901

18. Akbarzadeh-Jahromi M, Todarbary N, Aslani FS, Najib F, Zare M, Amirmoezi F. Uterine smooth muscle tumors of uncertain malignant potential: a retrospective evaluation of clinical pathology and immunohistochemistry features. *Surg Exp Pathol*. (2024) 7:2. doi: 10.1186/s42047-024-00145-5

19. DeMulder D, Ascher SM. Uterine Leiomyosarcoma: can MRI differentiate Leiomyosarcoma from benign leiomyoma before treatment? *AJR Am J Roentgenol*. (2018) 211:1405–15. doi: 10.2214/AJR.17.19234

20. Aminzadeh P, Alibrahim E, Dobrotwir A, Paul E, Goergen S. Multiparametric MR evaluation of uterine leiomyosarcoma and STUMP versus leiomyoma in symptomatic women planned for high frequency focussed ultrasound: accuracy of imaging parameters and interobserver agreement for identification of malignancy. *Br J Radiol*. (2021) 94:20200483. doi: 10.1259/bjr.20200483

21. Sun S, Bonaffini PA, Nougaret S, Fournier L, Dohan A, Chong J, et al. How to differentiate uterine leiomyosarcoma from leiomyoma with imaging. *Diagn Interv Imaging*. (2019) 100:619–34. doi: 10.1016/j.diii.2019.07.007

22. Sato K, Yuasa N, Fujita M, Fukushima Y. Clinical application of diffusion-weighted imaging for preoperative differentiation between uterine leiomyoma and leiomyosarcoma. *Am J Obstet Gynecol*. (2014) 210:368.e1–8. doi: 10.1016/j.ajog.2013.12.028

23. Suzuki Y, Wada S, Nakajima A, Fukushi Y, Hayashi M, Matsuda T, et al. Magnetic resonance imaging grading system for preoperative diagnosis of leiomyomas and uterine smooth muscle tumors. *J Minim Invasive Gynecol*. (2018) 25:507–13. doi: 10.1016/j.jmig.2017.08.660

24. Thomassin-Naggara I, Dechoux S, Bonneau C, Morel A, Rouzier R, Carette MF, et al. How to differentiate benign from malignant myometrial tumours using MR imaging. *Eur Radiol*. (2013) 23:2306–14. doi: 10.1007/s00330-013-2819-9

25. Lakhman Y, Veeraraghavan H, Chaim J, Feier D, Goldman DA, Moskowitz CS, et al. Differentiation of uterine Leiomyosarcoma from atypical leiomyoma: diagnostic accuracy of qualitative MR imaging features and feasibility of texture analysis. *Eur Radiol*. (2017) 27:2903–15. doi: 10.1007/s00330-016-4623-9

26. Pavlakis K, Messini I, Yiannou P, Gavresea T, Chrysanthakis D, Hilaris G, et al. Morcellating uterine mesenchymal tumors: the pathologist's view. *J Obstet Gynaecol Res*. (2017) 43:580–6. doi: 10.1111/jog.13240

27. Zang Y, Gu L, Zhang Y, Wang Y, Xue F. Identification of key genes and pathways in uterine leiomyosarcoma through bioinformatics analysis. *Oncol Lett*. (2018) 15:9361–8. doi: 10.3892/ol.2018.8503

28. Shanes ED, Friedman LA, Mills AM. PD-L1 expression and tumor-infiltrating lymphocytes in uterine smooth muscle tumors. *Am J Surg Pathol*. (2019) 43:792–801. doi: 10.1097/PAS.0000000000001254

29. Arcieri M, Cianci S, Martinelli C, Parisi S, Pergolizzi S, Capozzi VA, et al. Uterine smooth muscle tumor of uncertain malignant potential (STUMP) treated with conservative surgery: systematic review of reproductive outcomes. *Clin Exp Obstet Gynecol*. (2022) 49:267. doi: 10.31083/j.ceog4912267

30. Glaser LM, Friedman J, Tsai S, Chaudhari A, Milad M. Laparoscopic myomectomy and morcellation: a review of techniques, outcomes, and practice guidelines. *Best Pract Res Clin Obstet Gynaecol*. (2018) 46:99–112. doi: 10.1016/j.bpobgyn.2017.09.012

31. Buckley VA, Nesbitt-Hawes EM, Atkinson P, Won HR, Deans R, Burton A, et al. Laparoscopic myomectomy: clinical outcomes and comparative evidence. *J Minim Invasive Gynecol*. (2015) 22:11–25. doi: 10.1016/j.jmig.2014.08.007

32. Lim D, Alvarez T, Nucci MR, Gilks B, Longacre T, Soslow RA, et al. Interobserver variability in the interpretation of tumor cell necrosis in uterine Leiomyosarcoma. *Am J Surg Pathol*. (2013) 37:650–8. doi: 10.1097/PAS.0b013e3182851162

33. Oliva E, Zaloudek CJ, Soslow RA. Mesenchymal tumors of the uterus In: RJ Kurman, LH Ellenson and BM Ronnett, editors. *Blaustein's pathology of the female genital tract*. Cham: Springer International Publishing (2019). 535–647.

34. Guntupalli SR, Ramirez PT, Anderson ML, Milam MR, Bodurka DC, Malpica A. Uterine smooth muscle tumor of uncertain malignant potential: a retrospective analysis. *Gynecol Oncol*. (2009) 113:324–6. doi: 10.1016/j.ygyno.2009.02.020

35. Gupta M, Laury AL, Nucci MR, Quade BJ. Predictors of adverse outcome in uterine smooth muscle tumours of uncertain malignant potential (<scp>STUMP</scp>): a clinicopathological analysis of 22 cases with a proposal for the inclusion of additional histological parameters. *Histopathology*. (2018) 73:284–98. doi: 10.1111/his.13515

36. Huo L, Wang D, Wang W, Cao D, Yang J, Wu M, et al. Oncologic and reproductive outcomes of uterine smooth muscle tumor of uncertain malignant potential: a single center retrospective study of 67 cases. *Front Oncol*. (2020) 10:10. doi: 10.3389/fonc.2020.00647

37. Bastu E, Akhan SE, Ozsurmeli M, Galandarov R, Sozen H, Gungor-Ugurlucan F, et al. Acute hemorrhage related to spontaneous rupture of an uterine fibroid: a rare case report. *Eur J Gynaecol Oncol*. (2013) 34:271–2.

frontiers | Frontiers in Surgery

TYPE Original Research
PUBLISHED 01 August 2024
DOI 10.3389/fsurg.2024.1430439

OPEN ACCESS

EDITED BY
Luigi Della Corte,
University of Naples Federico II, Italy

REVIEWED BY
Diana Buzinskiene,
Vilnius University, Lithuania
Clarissa Lim Velayo,
University of the Philippines Manila, Philippines

*CORRESPONDENCE
Oğuz Güler
✉ oguz_gulerss@yahoo.com

RECEIVED 09 May 2024
ACCEPTED 16 July 2024
PUBLISHED 01 August 2024

CITATION
Güler O, Hatırnaz Ş, Sparic R, Basbug A, Erol O, Kalkan Ü, Ulubaşoğlu H, Trojano G, Ürkmez SS and Tinelli A (2024) Long-term obstetric, perinatal, and surgical complications in singleton pregnancies following previous cesarean myomectomy: a retrospective multicentric study.
Front. Surg. 11:1430439.
doi: 10.3389/fsurg.2024.1430439

Long-term obstetric, perinatal, and surgical complications in singleton pregnancies following previous cesarean myomectomy: a retrospective multicentric study

Oğuz Güler[1]*, Şafak Hatırnaz[2], Radmila Sparic[3,4], Alper Basbug[5], Onur Erol[6], Üzeyir Kalkan[7], Hasan Ulubaşoğlu[8], Giuseppe Trojano[9], Sebati Sinan Ürkmez[10] and Andrea Tinelli[11]

[1]Department of Obstetrics and Gynecology, Private Asya Hospital, Istanbul, Turkey, [2]Department of Obstetrics and Gynecology, Mediliv Medical Center, Samsun, Turkey, [3]Clinic for Obstetrics and Gynecology, University Clinical Center of Serbia, Belgrade, Serbia, [4]Faculty of Medicine, University of Belgrade, Belgrade, Serbia, [5]Department of Obstetrics and Gynecology, School of Medicine, Duzce University, Duzce, Turkey, [6]Department of Obstetrics and Gynecology, Memorial Antalya Hospital, Antalya, Turkey, [7]Department of Obstetrics and Gynecology, Koç University Hospital, Istanbul, Turkey, [8]Department of Obstetrics and Gynecology, Ankara Bilkent City Hospital, Ankara, Turkey, [9]Department of Obstetrics and Gynecology, Madonna Delle Grazie Hospital, Matera, Italy, [10]Department of Medical Biochemistry, Faculty of Medicine, Ondokuz Mayıs University, Samsun, Turkiye, [11]Department of Obstetrics and Gynecology, and CERICSAL (CEntro di RIcerca Clinico SALentino), "Veris delli Ponti Hospital", Scorrano, Italy

Objectives: The safety of cesarean myomectomy has been proven by previous studies. Our study aimed to reveal the long-term perinatal, obstetric, and surgical outcomes of cesarean myomectomy (CM) by comparing different CM techniques.

Material and methods: This retrospective multicentric case–control study involved 7 hospitals and included 226 singleton pregnancies that underwent repeated cesarean section (CS) between 2015 and 2020. Among these pregnancies, 113 of 226 cases had CM (Group A), and 113 had only CS (Group B). Of the 113 cases in which CM was performed, 58 underwent endometrial myomectomy (EM) (Subgroup A1) and 55 underwent serosal myomectomy (SM) (Subgroup A2). The groups were compared in terms of obstetric, perinatal, and surgical outcomes, and fibroid recurrence, myomectomy scar healing rate, and adhesion formation were noted.

Results: There was no significant difference between the groups in terms of maternal age, body mass index, gravidity, parity, and fibroid diameter in previous CS ($p > 0.05$). In the perinatal and obstetric evaluation of the groups, there was no significant difference between the groups in terms of neonatal weight, Apgar score, fetal growth restriction, preterm premature rupture of membranes, preterm delivery, hypertension in pregnancy, and diabetes mellitus ($p > 0.05$). The fibroid recurrence rate was 28.3%, and the myomectomy scar good healing rate was 99.1%. There was no difference between the groups in terms of CS duration, preoperative and postoperative hemoglobin levels, perioperative blood transfusion rates, febrile morbidity, and prolonged hospitalization ($p > 0.05$). In terms of adhesion formation, although the adhesion rate of the SM group was higher than that of the EM group, no statistically significant difference was detected between the groups.

Conclusion: This study showed that in pregnancies following CM, obstetrical, perinatal, and surgical outcomes were unaffected. Obstetricians can safely use CM, either the trans-endometrial or serosal technique, as it is a safe and effective method with long-term results.

KEYWORDS

cesarean myomectomy, endometrial myomectomy, serosal myomectomy, uterine fibroids, myoma recurrence, pregnancy, adhesions, complications

Introduction

The most common benign tumors in the female reproductive system are fibroids or myomas, which can pose a significant health risk, especially to expectant mothers (1). Since childbearing is becoming more and more of a worldwide trend, this load has grown in importance in recent decades (2). Although estimates of the prevalence of fibroids in pregnant women vary, a conservative estimate for those found during regular second-trimester ultrasounds is 2.7%. When a woman is having *in vitro* fertilization (IVF), this incidence rises to 12.6%, and it may even reach 25% in older women who are doing IVF with an ovum donor (3).

Most fibroids do not cause any major problems during pregnancy, delivery, or puerperium; however, they are linked to several perinatal issues, including miscarriage, early pregnancy bleeding, premature labor and rupture of membranes, placental abruption, malpresentation, labor dystocia, postpartum hemorrhage, and retained placenta (4).

Cesarean myomectomy (CM), a procedure involving myomectomy performed during cesarean delivery, was first reported in 1913. For an extended period, it was considered a hazardous operation due to the pronounced risk of massive perioperative hemorrhage, which often necessitated a hysterectomy to achieve hemostasis (5). However, since the last decades of the previous century, CM has gained increasing support, attributed to its numerous advantages over interval myomectomy (6). Despite initial reservations, five meta-analyses published in the past decade have not demonstrated significant complications associated with myomectomy during cesarean section (CS), compared to CS alone (7–10). Traditionally, CM is performed using a serosal uterine incision hysterotomy. Yet, recent reports have indicated that CM can be effectively conducted via an endometrial incision in suitable cases, yielding favorable outcomes (11).

There is a lack of data on the long-term outcomes of CM, with only a limited number of reports available in the existing literature (12, 13). Additionally, none of the meta-analyses published to date have included data on this aspect (7–10). The primary aim of this study was to investigate the perinatal and perioperative complications during pregnancy and delivery in women subjected to CM during previous delivery. The secondary aim was to determine if there is a difference in the frequency of these complications according to the CM technique used.

Material and methods

This study was designed as a retrospective, multicentric case–control investigation conducted across seven hospitals, comprising four tertiary-level and three secondary-level facilities. The study population consisted of women who underwent repeated CS in singleton pregnancies over a 5-year period from 2015 to 2020. Ethics committee approval was obtained for all the participating hospitals, and the study was registered at clinicaltrials.gov, with No. NCT04766567. Informed consent was obtained and signed by all the patients included in the study. The enrolled women were categorized into two groups: (1) Group A comprised patients who have had CM during previous CS. The inclusion criteria for CM included patients expressing a desire for the procedure after being informed about its risks and benefits before delivery. The exclusion criteria for CM included patient refusal, uterine hypotony, and/or atony, cervical myomas that cannot be reached from the abdomen, and women with bleeding disorders due to medical or obstetric causes. (2) Group B comprised patients who have had CS only. Due to the large number of potential participants in Group B, patients who matched Group A in terms of age and BMI were identified. Subsequently, an equal number of patients to Group A were selected from this pool, using an online random picker tool. Then, further subdivision of Group A was conducted into the following: (3) Subgroup A1, all patients who underwent endometrial myomectomy (EM), and (4) Subgroup A2, all women who underwent serosal myomectomy (SM). We excluded women who have had any other intra-abdominal surgery except CS (with or without CM), those having more than one previous CS, those having any coagulopathy, and cases of repeated CM. Patients with a history of malignancy, pelvic inflammatory disease, and endometriosis were also excluded from the study. No anti-adhesion materials were used during previous CS and CM of the cases. All CSs were performed according to the technique previously described by Stark (14). SMs were performed in all the cases according to the technique previously described by Tinelli et al. (15). EMs were performed in all the cases according to the technique previously described by Hatirnaz et al. (11). The medical charts were reviewed, and the following sociodemographic and clinical data were extracted: age at repeated CS, gravidity and parity, gestational age at delivery, time interval since previous CS, type of previous laparotomy, neonatal weight, and Apgar score at 1 and 5 min. The following pregnancy complications were registered for all the participants: fetal growth restriction (FGR), intrauterine fetal demise, diabetes mellitus (DM), hypertensive

disorder in pregnancy, preterm premature rupture of membranes (PPROM), preterm delivery, placenta previa, placental abruption, abnormally invasive placenta (AIP), uterine rupture, and venous thromboembolism. Perioperative characteristics were also recorded for all the patients, including the kind of relaparotomy used for the repeated CS, duration of the CS (from skin incision to skin closure in minutes), preoperative and postoperative serum hemoglobin levels, transfusion frequency, postoperative intestinal sub-occlusion/occlusion, febrile morbidity, and prolonged hospitalization (≥2 days longer than the institutional average). Postoperative serum hemoglobin levels were measured 12 h after the CS. Febrile morbidity was defined as temperature ≥38 °C measured at least twice at an interval of at least 6 h between the two measurements, except within the first postoperative 24 h. Healing of the previous CM scar in Group A was evaluated by intraoperative inspection and with palpation, and the findings were classified into three categories, namely, good healing (scar thicker than 50% of the surrounding uterine wall), poor healing (scar thinner than 50% of the surrounding uterine wall), and scar dehiscence. The recurrence rate of fibroids in Group A was determined from the presence of fibroids during the repeated CS. In cases of fibroid presence, the diameter of fibroids was registered from the operative records. Surgical complications associated with the repeated CS were evaluated according to Clavien–Dindo classification (16), in all cases, as absent, Grade I (any deviation from the normal postoperative course: drugs as antiemetics, antipyretics, analgesics, diuretics, electrolytes, physiotherapy, and wound infections opened at the bedside), Grade II (drugs other than such allowed for Grade I complications, blood transfusions, and total parenteral nutrition), and Grade III and above.

The presence of postoperative adhesions registered during repeated CS was evaluated according to the peritoneal adhesion index (PAI) (17). In the PAI system, the human abdomen is divided into nine equal anatomical regions. The grade score of peritoneal adhesions in these regions is defined as 0, no adhesions; 1, filmy adhesions; 2, strong adhesions; and 3, very strong vascularized adhesions. The sum of the adhesion grade scores of nine regions results in PAI.

The data in the study were analyzed using IBM SPSS Statistics for Windows v 21.0 (IBM Corp, Armonk, NY, USA). The quantitative data are presented as the median (minimum–maximum) values. The categorical data are presented as frequencies (n) and percentages (%). Kruskal–Wallis's test and Mann–Whitney U test were used to compare the independent groups, and Pearson's chi-square test, Fisher's exact test, and Fisher–Freeman–Halton test were used to compare the categorical variables. Logistic regression analyses were conducted to calculate the odds ratios to explore the relationship between surgical techniques and both long-term postoperative complications and the incidence of intraoperative adhesions. The regression models were constructed in two phases for the entire study population. Initially, univariate models were developed. Subsequently, multivariate models were adjusted for age, BMI, gravidity, parity, and the time interval between operations. These analyses were replicated exclusively within the CS myomectomy group to assess the impact of myoma diameters in the initial CS/myomectomy operations. Initially, univariate models were established. This was followed by the development of multivariate models, which were adjusted for age, BMI, gravidity, parity, time interval between operations, and myoma diameter at the initial operations. Data were determined at the 95% confidence level, and a p-value of <0.05 was accepted as statistically significant.

Results

A total of 226 women submitted for repeated CS were included in the study. Participants were divided into two main groups: Group A comprising 113 patients who have had either serosal myomectomy (SM) or endometrial myomectomy (EM) and Group B comprising 113 patients who have had CS only. Group A was further subdivided into two subgroups: Subgroup A1 consisting of 58 patients who have had EM and Subgroup A2 consisting of 55 patients who have had SM. Myomas enucleated in Subgroup A1 were G1, G2, G3, G4, G5, and G6 [by the International Federation of Gynecology and Obstetrics (FIGO) leiomyoma subclassification system] myomas. The myomas enucleated in Subgroup A2 were G4, G5, G6, and G7 myomas. The clinical characteristics of patients within the two primary groups (Group A and Group B), as well as the two subgroups (Subgroup A1 and Subgroup A2), are shown in Table 1.

All participants had a history of transverse laparotomy in their previous CS. The analysis revealed no statistically significant differences across the groups in terms of median age, BMI, gravidity, parity, and time interval since the previous CS. The median diameter of the fibroid enucleated during previous CS was 20 mm (range, 20–110) in Subgroup A1 and 55 mm (range, 20–110) in Subgroup A2, without statistically significant difference between the subgroups. There was no statistically significant difference between the groups in terms of newborn weight, Apgar scores, premature birth frequency, PPROM, diabetes, and hypertension.

There was an isolated case of complete uterine rupture in Subgroup A1. It occurred in a 34-year-old woman (gravida 3, para 1) who had EM of a 45 mm FIGO type 2 fibroid localized at the posterior wall of the uterus. Her previous CS was 17 months prior to the presentation. She was admitted to the hospital with the chief complaint of abdominal pain at 37 weeks of a previously uneventful pregnancy. The patient was delivered by emergency CS, due to non-reassuring fetal heart rate. On laparotomy, complete uterine rupture at the site of previous LUS incision. A live 3,050 g neonate with an Apgar score of 5/7 was delivered. The patient's preoperative and postoperative hemoglobin levels were 12.6 g/L and 6.5 g/L, respectively, after receiving 1,000 ml of packed red blood cells. The postoperative recovery was unremarkable, and the patient was discharged from the hospital on the second postoperative day.

One patient in Subgroup A1 underwent a repeated CS through a median laparotomy due to complete placenta previa. The patient

TABLE 1 The comparisons of the clinical characteristics of the study cohorts.

Characteristic		Total $n = 226$	Group A $n = 113$	Group B $n = 113$	p (Group A vs. Group B)	Subgroup A1 $n = 58$	Subgroup A2 $n = 55$	Group B $n = 113$	p (Subgroup A1 vs. Subgroup A2 vs. Group B)
Age, years [median (Min.–Max.)]		34 (24–44)	35 (24–44)	33 (22–44)	0.256[a]	34 (25–42)[†]	35 (24–44)[†]	33 (22–44)[†]	0.242[d]
BMI, kg/m^2 [median (Min.–Max.)]		28 (20–38)	28 (20–37)	28 (22–38)	0.102[a]	28.2 (20–37.7)[†]	28 (23.7–35)[†]	28 (22–38)[†]	0.183[d]
Gravidity [median (Min.–Max.)]		2 (1–5)	2 (1–5)	2 (2–5)	0.462[a]	2 (2–5)[†]	2 (1–5)[†]	2 (2–5)[†]	0.387[d]
Parity [median (Min.–Max.)]		1 (1–4)	1 (1–4)	1 (1–4)	0.084[a]	1 (1–4)[†]	1 (1–3)[†]	1 (1–4)[†]	0.206[d]
Time interval since previous CS, months [median (Min.–Max.)]		45.5 (13–132)	46 (13–132)	44 (15–108)	0.978[a]	45 (17–106)[†]	47 (13–132)[†]	44 (15–108)[†]	0.998[d]
Myoma diameter in previous CS, mm [median (Min.–Max.)]		N.A.	50 (20–110)	N.A.	N.A.	20 (20–110)	55 (20–110)	N.A.	0.782
Apgar score [median (Min.–Max.)]	first min	8 (5–9)	8 (5–9)	8 (5–9)	0.551[a]	8 (5–9)[†]	8 (5–9)[†]	8 (5–9)[†]	0.243[d]
	fifth min	9 (7–10)	9 (7–10)	9 (7–10)	0.517[a]	9 (7–10)[†]	9 (7–10)[†]	9 (7–10)[†]	0.798[d]
Neonatal weight, g [median (Min.–Max.)]		3,210 (2,050–4,800)	3,200 (2,050–4,620)	3,260 (2,080–4,800)	0.477[a]	3,205 (2,050–4,520)[†]	3,200 (2,480–4,620)[†]	3,260 (2,080–4,800)[†]	0.584[d]
FGR [n (%)]		9 (4.0%)	5 (4.4%)	4 (3.5%)	1.000[b]	2 (3.4%)[†]	3 (5.5%)[†]	4 (3.5%)[†]	0.823[e]
Diabetes mellitus [n (%)]		17 (7.5%)	10 (8.8%)	7 (6.2%)	0.449[c]	4 (6.9%)[†]	6 (10.9%)[†]	7 (6.2%)[†]	0.571[e]
Hypertension in pregnancy [n (%)]		20 (8.8%)	11 (9.7%)	9 (8.0%)	0.639[c]	6 (10.3%)[†]	5 (9.1%)[†]	9 (8.0%)[†]	0.872[c]
PPROM [n (%)]		9 (4.0%)	5 (4.4%)	4 (3.5%)	1.000[b]	2 (3.4%)[†]	3 (5.5%)[†]	4 (3.5%)[†]	0.823[e]
Preterm delivery [n (%)]		14 (62%)	7 (6.1%)	7 (6.1%)	1.000[c]	5 (8.6%)[†]	2 (3.6%)[†]	7 (6.1%)[†]	0.554[e]

BMI, body mass index; CS, cesarean; FGR, fetal growth restriction; PPROM, preterm premature rupture of membranes.
Gravidity and parity were calculated before repeated CS.
[a]Mann–Whitney U test.
[b]Fisher's exact test.
[c]Pearson χ^2 test.
[d]Kruskal–Wallis test.
[e]Fisher–Freeman–Halton test.
[†,‡,§]The different symbol above the upper character on the "data" indicates that this group is statistically different from the other groups with $p < 0.05$.

was a 37-year-old woman (gravida 4, para 1) who had EM of a 100 mm FIGO type 4 fibroid localized at the fundal anterior wall of the uterus. The previous CS was 26 months prior to presentation. The patient was delivered by emergency CS due to excessive vaginal bleeding at the 35th week of pregnancy, the newborn was 2,600 g with an Apgar score of 7/9. Hysterectomy was not required, and 1,000 ml of blood was transfused. No intensive care unit was required for both the mother and baby. The patient was discharged on the third postoperative day. All other patients throughout the study had a transverse relaparotomy.

There was no discernible difference in the length of repeated CS across the groups. The preoperative hemoglobin (Hb) levels in the two main groups were examined, and the results showed no significant differences. In a similar vein, these group's postoperative hemoglobin levels were similar. Subgroup analysis showed that preoperative hemoglobin levels did not differ across the groups. Median postoperative Hb levels also did not reveal significant differences between Subgroups A1 and A2 and Group B [102 (range, 64–127); 104 (range, 79–126); 99 (range, 63–126), respectively] ($p = 0.051$). However, there was an observable trend suggesting a disparity, attributable to the relatively lower Hb levels in Group B. The underlying cause of this trend can be primarily attributed to the disproportionate influence of patients with hemorrhage in Group B. In terms of perioperative transfusion, 6.9% of patients in Subgroup A1, 5.5% of patients in Subgroup A2, and 1.8% of patients in Group B received transfusions, without significant differences between the groups.

The preoperative, intraoperative, and postoperative characteristics of the patients are shown in Table 2.

The myomectomy scars of all patients in Group A were mostly evaluated as good healing (99.1%), while poor healing was determined in only one patient (0.9%). This poor healing case was a 34-year-old woman with two gravida and one parity (CM). Elective CS was performed at the 39th week of pregnancy, the fetal weight was 3,100 g, and the Apgar score was 8/9. The previous CM was performed 15 months ago. It was determined from the patient records that, in the previous CM, a FIGO type 6 fibroid of 65 mm diameter located in the anterior wall of the uterine corpus had been excised using the serosal myomectomy technique. Preoperative and postoperative Hb levels were 11.9 g/L and 11.1 g/L, respectively. There were no intraoperative or postoperative complications. If we evaluate myomectomy scar

TABLE 2 The preoperative, intraoperative, and postoperative characteristics of the study cohorts.

Characteristic		Total $n = 226$	Group A $n = 113$	Group B $n = 113$	p (Group A vs. Group B)	Subgroup A1 $n = 58$	Subgroup A2 $n = 55$	Group B $n = 113$	p (Subgroup A1 vs. Subgroup A2 vs. Group B)
Duration of the repeated CS, min [median (Min.–Max.)]		35 (12–135)	35 (12–135)	36 (17–106)	0.382[b]	35 (18–120)[†]	33 (12–135)[†]	36 (17–106)[†]	0.188[f]
Preoperative Hb, g/L [median (Min.–Max.)]		118 (93–144)	119 (95–144)	117 (93–144)	0.124[b]	118.5 (95–139)[†]	119 (119–144)[†]	117 (93–144)[†]	0.305[f]
Postoperative Hb, g/L [median (Min.–Max.)]		102 (63–127)	102 (64–127)	99 (63–126)	0.080[b]	102 (64–127)[†]	104 (79–126)[†]	99 (63–126)[†]	0.051[f]
Perioperative transfusion [n (%)]		9 (4.0%)	7 (6.2%)	2 (1.8%)	0.171[a]	4 (6.9%)[†]	3 (5.5%)[†]	2 (1.8%)[†]	0.233[d]
Myomectomy scar healing [n (%)]	good	N.A.	112 (99.1%)	N.A.	N.A.	58 (100%)	54 (98.2%)	N.A.	0.487[e,!]
	poor	N.A.	1 (0.9%)	N.A.		0	1 (1.8%)	N.A.	
	dehiscence	N.A.	0	N.A.		0	0	N.A.	
Myoma recurrence [n (%)]		N.A.	32 (28.3%)	N.A.	N.A.	21 (36%)	11 (20%)	N.A.	0.560[c,!]
Recurrent myoma diameter[g], mm [median (Min.–max.)]		N.A.	55 (20–80)	N.A.	N.A.	30 (20–60)	60 (30–80)	N.A.	**<0.001**[b,!]
Febrile morbidity [n (%)]		11 (4.9%)	7 (6.2%)	4 (3.5%)	0.354[c]	4 (6.9%)[†]	3 (5.5%)[†]	4 (3.5%)[†]	0.609[d]
Prolonged hospitalization [n (%)]		11 (4.9%)	6 (5.3%)	5 (4.4%)	0.757[c]	2 (3.4%)[†]	4 (7.3%)[†]	5 (4.4%)[†]	0.660[d]

CS, cesarean; Hb, hemoglobin.
[a]Fisher's exact test.
[b]Mann–Whitney U test.
[c]Pearson χ^2 test.
[d]Fisher–Freeman–Halton test.
[e]Fisher's exact Test.
[f]Kruskal–Wallis Test.
[g]The subgroup is formed by cases of recurrent myoma.
[†,‡,§]The different symbol above the upper character on the "data" indicates that this group is statistically different from the other groups with $p < 0.05$.
[!]Pairwise p-values (Group A1 vs. Group A2).
The value expressed in bold font indicates statistical significance.

healing between subgroups, all cases in Subgroup A1 exhibited good healing outcomes. In Subgroup A2, most of the cases exhibited good healing outcomes (98.2%), while poor healing was determined in only one patient (1.2%). These differences between the subgroups were not statistically significant.

Regarding fibroid recurrence, recurrent myoma locations were different from the previous myomectomy site. The myoma recurrence rate was 28.3% ($n = 32$) in Group A. Within the subgroups, the recurrence rates were 36% ($n = 21$ cases) in Subgroup A1% and 20% ($n = 11$ cases) in Subgroup A2; however, this difference was not statistically significant. Notably, the median diameter of recurrent fibroids in Subgroup A1 was significantly smaller at 30 mm (range, 20–60 mm), compared to Subgroup A2, where the median diameter was 60 mm (range, 30–80 mm) ($p > 0.001$). Febrile morbidity was mostly detected in cases of membrane rupture lasting longer than 12 h or in cases of emergency CS. All patients with febrile morbidity received broad-spectrum antibiotics, and their fever decreased. Regarding febrile morbidity, no discernible variations were seen between the groups. A minimum of 1,000 ml of blood transfusion, severe headaches following a spinal puncture, uterine rupture, midline laparotomy, and extended febrile morbidity were among the patients who required a protracted hospital stay. There were no discernible differences between the groups in terms of extended hospital stays. None of the individuals had any symptoms of ileus or venous thromboembolism.

Surgical complications associated with repeated CS were evaluated according to the Clavien–Dindo classification (16) (Table 3). Most of the patients in the study did not have any of the complications ($n = 134$, 59.3%). Grade I complications were determined in 83 (36.7%) patients. All of these include the additional use of analgesics and antiemetics. No other therapeutic agent was used, and no case of wound infections opened at the bedside was detected. Grade II complications were determined in 9 patients (4.0%), all of whom required blood transfusion. No higher-grade complications were observed. When subgroup analysis was performed, no complications were observed in 32 patients in Subgroup A1 (55.2%), 30 patients in Subgroup A2 (54.5%), and 72 patients in Group B (63.7%). Similarly, Grade I complications were observed in 22 patients in Subgroup A1 (37.9%), 22 patients in Subgroup A2 (40.0%), and 39 patients in Group B (34.5%). Finally, Grade II complications were observed in four patients in Subgroup A1 (6.9%), three patients in Subgroup A2 (5.5%), and two patients in Group B (1.8%). Statistical analysis indicated no significant differences among the groups.

Upon evaluating the intraoperative adhesion values of the patients according to PAI 2013 (17) (Table 4), no adhesions were detected in 70 patients in Group A (61.9%) and 80 patients in

TABLE 3 Evaluation of the long-term postoperative complications (Clavien–Dindo classification) (16).

Grade	Total $n = 226$	Group A $n = 113$	Group B $n = 113$	p (Group A vs. Group B)	Subgroup A1 $n = 58$	Subgroup A2 $n = 55$	Group B $n = 113$	p (Subgroup A1 vs. Subgroup A2 vs. Group B)
No complication	134 (59.3%)	62 (54.9%)[†]	72 (63.7%)[†]	0.156[a]	32 (55.2%)[†]	30 (54.5%)[†]	72 (63.7%)[†]	0.360[a]
Grade I [n (%)]	83 (36.7%)	44 (38.9%)[†]	39 (34.5%)[†]		22 (37.9%)[†]	22 (40.0%)[†]	39 (34.5%)[†]	
Grade II [n (%)]	9 (4.0%)	7 (6.2%)[†]	2 (1.8%)[†]		4 (6.9%)[†]	3 (5.5%)[†]	2 (1.8%)[†]	

[a]Fisher–Freeman–Halton test.
[†,‡,§]The different symbol above the upper character on the "data" indicates that this group is statistically different from the other groups with $p < 0.05$.

TABLE 4 Evaluation of intraoperative adhesions (PAI 2013) (17).

PAI	Total $n = 226$	Group A $n = 113$	Group B $n = 113$	p (Group A vs. Group B)	Subgroup A1 $n = 58$	Subgroup A2 $n = 55$	Group B $n = 113$	p (Subgroup A1 vs. Subgroup A2 vs. Group B)
Cases without adhesion [n (%)]	150 (66.4%)	70 (61.9%)[†]	80 (70.8%)[†]	0.159[a]	40 (69.0%)[†]	30 (54.5%)[†]	80 (70.8%)[†]	0.100[a]
Cases with adhesion [n (%)]	76 (33.6%)	43 (38.1%)[†]	33 (29.2%)[†]		18 (31.0%)[†]	25 (45.5%)[†]	33 (29.2%)[†]	
Sum of scores per patient [median (Min.–Max.)]	0 (0–6)	0 (0–6)	0 (0–4)	0.119[b]	0 (0–6)[†]	0 (0–6)[†]	0 (0–4)[†]	0.074[c]

PAI, peritoneal adhesion index.
[a]Pearson chi-square test.
[b]Mann–Whitney U test.
[c]Kruskal–Wallis Test.
[†,‡,§]The different symbol above the upper character on the "data" indicates that this group is statistically different from the other groups with $p < 0.05$.

Group B (70.8%). Subgroup analysis revealed that 40 patients (69.0%) in Subgroup A1 and 30 patients (54.5%) in Subgroup A2 had no adhesions. Adhesions were determined in 45% of Subgroup A2 and 31.1% of Subgroup A1. The comparison between Group A and Group B revealed no statistically significant difference in the sum of scores per patient ($p = 0.119$). Additionally, within Group A, Subgroups A1 ($n = 58$) and A2 ($n = 55$) showed no significant difference compared to each other as well as Group B in terms of the sum of scores per patient ($p = 0.074$).

Logistic regression analysis investigated the relationship between different surgical techniques and long-term postoperative complications, categorized according to the Clavien–Dindo classification (complications were considered based on their presence or absence, without accounting for grades).

Univariate analysis for whole study groups ($n = 226$)

In the univariate model, comparing Group B (used as the reference group) to Subgroup A2 (OR = 1.463; $p > 0.05$) and Subgroup A1 (OR = 1.427; $p > 0.05$), the results suggest that neither serosal nor endometrial myomectomy significantly increased the risk of long-term complications when added to cesarean section.

Multivariate analysis for whole study groups ($n = 226$)

Adjusting for age, body mass index, gravidity, parity, and the time interval between the operations, the multivariate model yielded similar odds ratios (1.494 and 1.382 respectively). However, these adjusted odds ratios were not statistically significant ($p > 0.05$), indicating that the additional risk factors adjusted for did not substantially alter the relationship between surgical techniques and postoperative complications.

Univariate analysis for the myomectomy groups ($n = 113$)

When focusing solely on the myomectomy groups, using Subgroup A2 as the reference, the odds ratio for Subgroup A1 was 0.975 ($p > 0.05$), indicating no significant difference in the risk of postoperative complications between the two myomectomy techniques.

Multivariate analysis for the myomectomy groups ($n = 113$)

Further adjusting for age, body mass index, gravidity, parity, the time interval between the operations, and the myoma

diameter at the first operation, the multivariate model for the myomectomy groups showed an OR of 0.835 ($p = 0.664$) for Subgroup A1 compared to Subgroup A2. This result also did not reach statistical significance, suggesting that the type of myomectomy performed does not significantly impact the likelihood of long-term postoperative complications. These findings underscore that neither serosal nor endometrial myomectomy significantly alters the risk of long-term complications when performed alongside cesarean section, regardless of the patient's age, body mass index, gravidity, parity, or time interval between operations (detailed in Table 5).

Logistic regression analysis also assessed the relationship between surgical techniques and the incidence of intraoperative adhesions, as classified by PAI 2013 (adhesions were considered based on their presence or absence).

Univariate analysis for the whole study groups ($n = 226$)

The univariate model indicated that cesarean section combined with serosal myomectomy was associated with significantly higher odds of intraoperative adhesions compared to cesarean section alone (OR = 2.020; 95% CI: 1.036–3.940; $p = 0.039$). In contrast, cesarean section combined with endometrial myomectomy did not show a significant increase in the odds of adhesions (OR = 1.091; 95% CI: 0.548–2.171; $p > 0.05$).

Multivariate analysis for the whole study groups ($n = 226$)

After adjusting for age, body mass index, gravidity, parity, and the time interval between operations, the odds ratio in Subgroup A2 increased (OR = 2.327; 95% CI: 1.157–4.680; $p = 0.018$), further supporting a significant association with higher adhesion rates. However, the association in Subgroup A1 remained non-significant (OR = 1.062; 95% CI: 0.522–2.158; $p > 0.05$).

TABLE 5 Relationship between surgical techniques and long-term postoperative complications (according to the Clavien–Dindo classification)[a].

Variable		OR (95% CI)	p
Univariate model for whole study groups	Group B (reference)	–	–
	Subgroup A2	1.463 (0.760–2.817)	0.254
	Subgroup A1	1.427 (0.749–2.717)	0.279
Multivariate model for whole study groups[b]	Group B (reference)	–	–
	Subgroup A2	1.494 (0.761–2.932)	0.243
	Subgroup A1	1.382 (0.712–2.683)	0.339
Univariate model for the myomectomy groups	Subgroup A2 (reference)	–	–
	Subgroup A1	0.975 (0.465–2.046)	0.947
Multivariate model for the myomectomy groups[c]	Subgroup A2 (reference)	–	–
	Subgroup A1	0.835 (0.370–1.885)	0.664

OR, odds ratio; CI, confidence interval.
[a]Logistic regression analysis.
[b]Adjusted for age, body mass index, gravidity, parity, and time interval between the operations.
[c]Adjusted for age, body mass index, gravidity, parity, time interval between the operations, and myoma diameter at first operation.

Univariate model for the myomectomy groups

Within the groups undergoing myomectomy, using Subgroup A2 as the reference, Subgroup A1 showed reduced, though not statistically significant, odds of adhesions (OR = 0.540; $p > 0.05$).

Multivariate model for the myomectomy groups

When further adjustments were made for age, body mass index, gravidity, parity, the time interval between the operations, and the myoma diameter at the first operation, the results for Subgroup A1 indicated lower but not significant odds of adhesions (OR = 0.457; $p = 0.062$). These analyses suggest that serosal myomectomy in conjunction with cesarean section significantly increases the likelihood of intraoperative adhesions, whereas endometrial myomectomy does not significantly alter this risk (detailed in Table 6).

Discussion

Since its initial introduction into obstetrics practice, CM is a surgical treatment that is being performed by an increasing number of surgeons. Because of the significant risk of perioperative complications, such as severe bleeding, the need for blood transfusions, the potential for cesarean hysterectomy, and extended hospital stays, CM was avoided in the past (18). Although rare, massive hemorrhage can lead to maternal death (19). It has been stated in many articles that even fibroids <8 cm can be safely removed during cesarean delivery (20), longer recovery times and lower hemoglobin levels are unavoidable (7, 8).

TABLE 6 Relationship between surgical techniques and the existence of intraoperative adhesions (according to PAI 2013)[a].

Variable		OR (95% CI)	p
Univariate model for whole study groups	Group B (reference)	–	–
	Subgroup A2	2.020 (1.036–3.940)	0.039
	Subgroup A1	1.091 (0.548–2.171)	0.804
Multivariate model for whole study groups[b]	Group B (reference)	–	–
	Subgroup A2	2.327 (1.157–4.680)	0.018
	Subgroup A1	1.062 (0.522–2.158)	0.869
Univariate model for the myomectomy groups	Subgroup A2 (reference)	–	–
	Subgroup A1	0.540 (0.250–1.165)	0.116
Multivariate model for the myomectomy groups[c]	Subgroup A2 (reference)	–	–
	Subgroup A1	0.457 (0.201–1.039)	0.062

PAI, peritoneal adhesion index; OR, odds ratio; CI, confidence interval.
[a]Logistic regression analysis.
[b]Adjusted for age, body mass index, gravidity, parity, time interval between the operations.
[c]Adjusted for age, body mass index, gravidity, parity, time interval between the operations, and myoma diameter at first operation.

Complications may also arise if fibroids are not removed after a CS because of surgical inexperience or the fibroid's placement. If fibroids are not removed during CS, certain issues could arise. It was formerly believed that fibroids prevented the uterus from involution, which resulted in heavy bleeding during the early puerperal phase (21) or prolapsed from the cervix to the vagina, which led to an infection and myomectomy during this time. Fibroids were suspected of causing infertility, miscarriage or preterm birth of the fetus, excessive monthly flow, and symptoms connected to surrounding organ pressure, late after the delivery. Pregnant women who experience severe pain that is unresponsive to medical intervention may be more inclined to choose CM (22).

During CS, eliminating fibroids has several benefits. Due to increased myometrial elasticity during pregnancy, it will be easier to distinguish healthy and fibroid myometrial tissue, and myoma removal becomes easier. During pregnancy, uterine expansion is more noticeable than fibroid growth. This reduces tissue damage when surgeons remove fibroids from smaller incisions. Significant contractions following CS and uterine involution reduce the quantity of bleeding from the fibroid bed. It saves the patient from myoma symptoms and possible subsequent myomectomy. The serosal technique has been used for a very long time to accomplish myomectomy during CS. SM can remove easily accessible fibroids that are near the serosal surface (G7, G6, G5, G4, G3, G2-5 fibroids). By using an endometrial approach, fibroids that are deeply ingrained (G4, G5, G6 fibroids) in the myometrium and near the endometrium (G1, G2, G3, G2-5, fibroids) can be removed. The application of hysteroscopic myomectomy served as the model for EM. The EM can also be performed for fibroids located in the posterior uterine wall or fibroids located in isthmic or cornual regions that cannot be removed by SM (23). Moreover, the EM can be combined with SM for the removal of all fibroids present during CS, and those fibroids located on the incision line can be removed by the trans-incisional route.

There are no internationally established guidelines for my myoma management during the CS. Most of the classical textbooks and internationally established opinions advise against performing myomectomy during CS except in very few situations (24). On the other hand, literature data provide a lot of publications promoting CM (6, 11, 12, 20, 23, 25). Moreover, five available meta-analyses failed to document any major complications of CM and documented its safety and feasibility in properly selected cases (8, 9, 10, 22, 26).

Although short-term outcomes were reported in many publications, studies and meta-analyses of long-term outcomes of CM are lacking (9, 10, 26). In their recent review, Sparic et al. evaluated six studies comparing the short-term results of CM according to the myomectomy technique. This study, which once again demonstrates the reliability of CM, states that none of the techniques is superior to the other and well-designed studies are needed for long-term outcomes (27). Akkurt et al. (12) evaluated 32 out of 91 women who had CM for their pregnancies after CM for preterm delivery, uterine rupture, and placental adhesion abnormalities, detecting a very low maternal morbidity rate for those factors (9.3%). Adesiyun et al. (28) reported that CM has no negative impact on the obstetrical outcomes of 29 women who had previous CM. Yıldırım Karaca et al. (29) compared obstetrical and neonatal outcomes (Apgar score, neonatal birthweights, birth weeks) after EM and SM in two groups, reporting no statistically significant difference in both groups.

In our study, we evaluated long-term obstetrical outcomes of women who had previous CM and for neonatal Apgar scores, birthweights of babies, fetal growth restrictions, diabetes mellitus, PPROM, and preterm delivery, and our results showed no significant difference in both methods.

We found a uterine rupture in one of the cases assigned to Subgroup A1; however, the ruptured site was from the lower uterine segment (LUS) and not the prior CM site, demonstrating that the rupture and CM are unrelated. The incidence of placenta previa in the general population ranges from 0.28% to 1.5% (30). In our 113 cases, we only recorded one case with placenta previa. However, Akkurt et al. and Adesiyun et al. reported higher rates of placenta previa, understandably due to a very low number of studied populations (12, 28). Contrary to their report, Huang et al. performed EM to 63 cases and then performed CS to the same 63 cases, and the rate of placenta previa was determined to be the same in both groups. The author concluded that EM does not cause an increase in the risk of placenta previa (31).

The length of CS, preoperative and postoperative hemoglobin levels, the need for blood transfusions, febrile morbidity, and extended hospital stays were among the perioperative data that we did not observe to differ significantly from one another during our analysis. It is possible to identify no discernible change because both groups had CS.

According to the study of Fauconnier et al. (32), the rate of fibroid recurrence following abdominal myomectomy ranges from 15.4% to 62% if transvaginal ultrasound examination is the recommended approach to assess it. Kotani et al. followed women with previous open myomectomy for fibroid recurrence and found 5.3%, 34.2%, 46.9%, and 63.4% in their 1, 3, 5, and 8 years of follow-up, respectively (33). From the publication, the mean recurrence rate was expected 40% during follow-up. Our study revealed a 28% recurrence rate, and the mean time for second CS was 3.9 years. The low recurrence rate in our study may be explained by the removal of palpable and visualized fibroids during CS instead of transvaginal ultrasound examination. The disadvantage of EM is that we cannot determine small fibroids. Literature is lacking about the long-term outcomes of healing of CM scar. Cobellis et al. published two consecutive articles in the same year. In their first article, they compared ultrasonographic findings of myomectomy scars in both the CM and myomectomy groups, while in the second publication, they compared myomectomy scar healing of previously evaluated patients during CS (34, 35). Both studies showed that scar healing is much better in the CM group. Moreover, Adesiyun et al. (28) evaluated 29 women with previous CM, with 13 women who delivered by vaginal route and 16 women who had CS. In both groups, none of the cases had uterine dehiscence or uterine rupture. In our investigation, we detected a good healing rate in 99.1% of patients, where we

evaluated the scar healing by palpation during CS. Our findings are matched with the limited data present in the literature.

Myomectomy scar pregnancy is one of the rarest myomectomy side effects. Zhu et al. (36) published their case along with a review study that featured seven myomectomy scar pregnancies. Out of the eight myomectomy scar pregnancies, three cases were noted following laparoscopic myomectomy, and five were the consequence of abdominal myomectomies. Although it is theoretically feasible, none of the few documented cases of myomectomy scar pregnancy were caused by CM (37, 38).

An inevitable complication after all abdominal surgeries is adhesion formation. The adhesion rates after abdominal myomectomy range from 28.1% to 81% (39, 40). Adhesion formation after CS was 24%–46%, 43%–75%, and 83% in second, third, and fourth CS, respectively (41, 42).

Turgal et al. (13) stated the adhesion rate in CS after serosal myolysis and SM performed during previous CS as 19% and 41%, respectively. When these rates were compared with the CS after CS group (21.1% adhesions), no statistically significant difference was detected. This finding was further supported by Akkurt et al., where they reported a 25% adhesion rate during CS in 32 women who had previous SM (12).

In our investigation, Group B had a rate of adhesion development of 29.2% compared to Group A's 38.1%; nevertheless, this difference was not statistically significant. Mercorio et al. (43) in their recent review evaluated adhesion formations after myomectomy and stated that the size of the uterine serosal incision is related to adhesion. Based on this result, since the uterine serosa is not damaged in the EM technique, less adhesion is expected compared to the SM technique. Moreover, women with prior SM during CS were observed to have higher adhesion development in their second CS as opposed to women with EM during CS, according to Yıldırım Karaca et al. (29). We realized that Subgroup A1 had a 31% adhesion rate and Subgroup A2 had a 45.5% adhesion rate in the multiple group comparisons. Although Subgroup A2 had a higher rate, this difference was not statistically significant. However, further evaluation through logistic regression analysis to assess the risk of adhesions across different surgical groups revealed a different pattern. The analysis showed that the likelihood of intraoperative adhesions was significantly higher between Subgroup A2 and Group B (OR = 2.020; 95% CI: 1.036–3.940; $p = 0.039$). This association was found to strengthen further when adjusted for demographic and preoperative variables (OR = 2.327; 95% CI: 1.157–4.680; $p = 0.018$). Conversely, there was no significant increase in the risk of adhesions between Subgroup A1 and Group B (Table 5). The results obtained in this evaluation seem to be consistent with the literature. To draw any conclusions on adhesion formation following myomectomy, a more extensive series should be examined in future research.

The growing incidence of CS globally raises awareness of the risks associated with the procedure, with heavy bleeding during CS being the most common consequence (7%) (44). The range of intestinal blockage is 0.05%–0.2% (45). There were incredibly few other organ injuries. Delporte et al. (46) examined 882 women who had CS, 17% of whom had repeated CS, and assessed the problems associated with the procedure using the Clavien–Dindo classification. In accordance with this classification scheme, problems were noted in Grades I, II, and III at 89.2%, 8.7%, and 2.0%, respectively. We added severe postoperative pain, analgesic use, and antiemetic use due to severe nausea and vomiting to Grade I and reported a 36.7% Grade I complication rate using the same classification approach. In 4% of the instances, we found bleeding and the need for blood transfusions because of the bleeding, classifying them as Grade II.

We did not uncover any Grade III complications in our investigation. While the Grade I complication rate was lower than the literature, the Grade II complication rate was comparable. Regarding surgical complications, there does not appear to be a statistically significant difference between the groups and subgroups. Further investigation into the relationship between surgical techniques and long-term postoperative complications across different groups showed no significant differences. The results from both univariate and multivariate analyses indicated non-significant odds ratios among Group A1, Group A2, and Group B, demonstrating that different myomectomy procedures together with CS do not substantially alter the risk of long-term complications comparing CS alone. Adjustments for factors such as age, body mass index, and time intervals between operations did not change these findings (Table 6).

This study's first strength was its ability to consistently disclose both short- and long-term obstetric and surgical outcomes through comparative analysis of groups similar in terms of case numbers and fundamental features. The sample size was adequate for a thorough analysis of the primary and secondary outcomes, which is the study's second strength. There are various restrictions on this study. We conducted a multicentric, retrospective investigation. Furthermore, standardizing and avoiding bias in the gathering of data on adhesion and scar healing is a challenging task. The standardization of the data is limited by the various follow-up periods (1–10 years) when evaluating the long-term outcomes of our investigation. Data comparing the long-term effects of SM and CM are scarce. There are not many reports and few cases in the literature yet that can be compared to the findings of our investigation.

Conclusion

This study demonstrated that obstetrical and perinatal outcomes were unaltered in pregnancies that followed CM. Surgical problems from CS after CM are similar to those from multiple cesarean sections. This applies to both categories of CM techniques. Repetitive CS and CM are comparable in terms of how long-term adhesions are created. However, because there is no serosal incision in EM, there is less adhesion formation than in SM. Both the trans-endometrial and serosal techniques of CM are safe, effective, and produce long-lasting outcomes, thus obstetricians can safely utilize them.

Data availability statement

The raw data supporting the conclusions of this article will be made available by the authors, without undue reservation.

Ethics statement

The studies involving humans were approved by the IRB of Medicana International Samsun Hospital with a grant number of 7100/07-01/10.06.2020. The studies were conducted in accordance with the local legislation and institutional requirements. The participants provided their written informed consent to participate in this study.

Author contributions

OG: Writing – original draft, Visualization, Investigation, Writing – review & editing, Project administration. ŞH: Data curation, Conceptualization, Writing – review & editing, Writing – original draft, Investigation. RS: Writing – original draft, Visualization, Writing – review & editing, Investigation, Data curation. AB: Validation, Supervision, Software, Writing – review & editing, Writing – original draft. OE: Writing – review & editing, Methodology, Formal Analysis, Writing – original draft. ÜK: Writing – review & editing, Writing – original draft, Methodology, Formal Analysis. HU: Writing – review & editing, Resources, Writing – original draft, Methodology. GT: Writing – review & editing, Validation, Writing – original draft, Resources. SÜ: Writing – review & editing, Project administration, Writing – original draft, Validation. AT: Writing – review & editing, Supervision, Conceptualization, Writing – original draft, Project administration.

Funding

The authors declare that no financial support was received for the research, authorship, and/or publication of this article.

Conflict of interest

The authors declare that the research was conducted in the absence of any commercial or financial relationships that could be construed as a potential conflict of interest.

The authors declared that they were an editorial board member of Frontiers, at the time of submission. This had no impact on the peer review process and the final decision.

Publisher's note

All claims expressed in this article are solely those of the authors and do not necessarily represent those of their affiliated organizations, or those of the publisher, the editors and the reviewers. Any product that may be evaluated in this article, or claim that may be made by its manufacturer, is not guaranteed or endorsed by the publisher.

References

1. Sparic R, Mirkovic L, Malvasi A, Tinelli A. Epidemiology of uterine fibroids: a review. *Int J Fertil Steril*. (2016) 9(4):424–35. doi: 10.22074/ijfs.2015.4599

2. Human Fertility Database. Max Planck Institute for Demographic Research (Germany) and Vienna Institute of Demography (Austria). Available online at: www.humanfertility.org (data downloaded on 2021).

3. Klatsky PC, Tran ND, Caughey AB, Fujimoto VY. Fibroids and reproductive outcomes: a systematic literature review from conception to delivery. *Am J Obstet Gynecol*. (2008) 198:357–66. doi: 10.1016/j.ajog.2007.12.039

4. Lee HJ, Norwitz ER, Shaw J. Contemporary management of fibroids in pregnancy. *Rev Obstet Gynecol*. (2010) 3:20–7. doi: 10.3909/riog0101

5. Sparic R, Malvasi A, Kadija S, Babovic I, Nejkovic L, Tinelli A. Cesarean myomectomy trends and controversies: an appraisal. *J Matern Fetal Neonatal Med*. (2017) 30(9):1114–23. doi: 10.1080/14767058.2016.1205024

6. Sparić R, Kadija S, Stefanović A, Spremović Radjenović S, Likić Ladjević I, Popović J, et al. Cesarean myomectomy in modern obstetrics: more light and fewer shadows. *J Obstet Gynaecol Res*. (2017) 43(5):798–804. doi: 10.1111/jog.13294

7. Song D, Zhang W, Chames MC, Guo J. Myomectomy during cesarean delivery. *Int J Gynaecol Obstet*. (2013) 121(3):208–13. doi: 10.1016/j.ijgo.2013.01.021

8. Pergialiotis V, Sinanidis I, Louloudis IE, Vichos T, Perrea DN, Doumouchtsis SK. Perioperative complications of cesarean delivery myomectomy: a meta-analysis. *Obstet Gynecol*. (2017) 130(6):1295–303. doi: 10.1097/AOG.0000000000002342

9. Huang Y, Ming X, Li Z. Feasibility and safety of performing cesarean myomectomy: a systematic review and meta-analysis. *J Matern Fetal Neonatal Med*. (2022) 35(13):2619–27. doi: 10.1080/14767058.2020.1791816

10. Goyal M, Dawood AS, Elbohoty SB, Abbas AM, Singh P, Melana N, et al. Cesarean myomectomy in the last ten years; A true shift from contraindication to indication: a systematic review and meta-analysis. *Eur J Obstet Gynecol Reprod Biol*. (2021) 256:145–57. doi: 10.1016/j.ejogrb.2020.11.008

11. Hatırnaz Ş, Güler O, Başaranoğlu S, Tokgöz C, Kılıç GS. Endometrial myomectomy: a novel surgical method during cesarean section. *J Matern Fetal Neonatal Med*. (2018) 31(4):433–8. doi: 10.1080/14767058.2017.1286320

12. Akkurt MO, Yavuz A, Eris Yalcin S, Akkurt I, Turan OT, Yalcin Y, et al. Can we consider cesarean myomectomy as a safe procedure without long-term outcome? *J Matern Fetal Neonatal Med*. (2017) 30(15):1855–60. doi: 10.1080/14767058.2016.1228057

13. Turgal M, Ozgu-Erdinc AS, Beksac K, Ozyuncu O, Karaagaoglu E, Beksac MS. Myomectomy during cesarean section and adhesion formation as a long-term postoperative complication. *Ginekol Pol*. (2015) 86(6):457–60. doi: 10.17772/gp/2404

14. Stark M. Evidence-Bbased cesarean section for universal use in China: the "stark (Misgav Ladach) method". *Matern Fetal Med*. (2019) 1(1):48–52. doi: 10.1097/FM9.0000000000000003

15. Tinelli A, Malvasi A, Mynbaev OA, Barbera A, Perrone E, Guido M, et al. The surgical outcome of intracapsular cesarean myomectomy. A match control study. *J Matern Fetal Neonatal Med*. (2014) 27(1):66–71. doi: 10.3109/14767058.2013.804052

16. Dindo D, Demartines N, Clavien PA. Classification of surgical complications: a new proposal with evaluation in a cohort of 6336 patients and results of a survey. *Ann Surg*. (2004) 240(2):205–13. doi: 10.1097/01.sla.0000133083.54934.ae

17. Coccolini F, Ansaloni L, Manfredi R, Campanati L, Poiasina E, Bertoli P, et al. Peritoneal adhesion index (PAI): proposal of a score for the "ignored iceberg" of medicine and surgery. *World J Emerg Surg*. (2013) 8(1):6. doi: 10.1186/1749-7922-8-6

18. Tabakova N, Sparić R, Tinelli A. Reflections on postpartum hysterectomy as a possible complication of cesarean myomectomy: a long debate. *Medicina (B Aires)*. (2024) 60:594. doi: 10.3390/medicina60040594

19. Seffah JD. Re-laparotomy after cesarean section. *Int J Gynecol Obstet*. (2005) 88:253–7. doi: 10.1016/j.ijgo.2004.12.014

20. Shi C, Chen J, Chen A. Clinical outcome analysis of intramural fibroid greater than 8 cm in diameter removed during caesarean section: a retrospective study. *BMC Womens Health*. (2023) 23(1):60. doi: 10.1186/s12905-023-02210-9

21. Zhao R, Wang X, Zou L, Li G, Chen Y, Li C, et al. Adverse obstetric outcomes in pregnant women with uterine fibroids in China: a multicenter survey involving 112,403 deliveries. *PLoS One*. (2017) 12(11):e0187821. doi: 10.1371/journal.pone.0187821

22. Spyropoulou K, Kosmas I, Tsakiridis I, Mamopoulos A, Kalogian nidis I, Athanasiadis A, et al. Myomectomy during pregnancy: a systematic review. *Eur J Obstetr Gynecol Reprod Biol*. (2020) 254:15–24. doi: 10.1016/j.ejogrb.2020.08.018

23. Wang Q, Lin J, Dai Y. Outcomes of cesarean myomectomy via trans-endometrial approach in women with single intramural fibroid in the posterior uterine wall. *J Matern Fetal Neonatal Med*. (2023) 36(2):2232655. doi: 10.1080/14767058.2023.2232655

24. Ouyang DW, Norwitz ER. Uterine fibroids (leiomyomas): issues in pregnancy. In: Barss VA, editor. *UpToDate*. Waltham, Massachusetts. (2024). Topic 6801 Version 65.0. Available online at: https://www.uptodate.com/contents/uterine-fibroids-leiomyomas-issues-in-pregnancy?search=myoma%20pregnancy&source=search_result&selectedTitle=1%7E150&usage_type=default&display_rank=1#topicContent (Accessed June 13, 2024).

25. Dai QH, Zhang L, Chen AE. Prognostic and reproductive outcomes in women who had uterine myomas removed during cesarean section and sutured using different techniques. *BMC Women's Health*. (2024) 24(1):7. doi: 10.1186/s12905-023-02852-9

26. Youshanloie MM, Vaezi M, Pashazadeh F. Consequences of concurrent myomectomy and caesarean section versus caesarean section alone in the last two decades: systematic review and meta-analysis. *Curr Women's Health Rev*. (2023) 19 (4):133–46. doi: 10.2174/1573404819666221115113516

27. Sparić R, Andrić L, Guler O, Malvasi A, Babović I, Hatirnaz S, et al. Cesarean myomectomy: reflections on clinical and surgical controversies between a new trans-decidual technique vs. traditional method. *Medicina (B Aires)*. (2024) 60:609. doi: 10.3390/medicina60040609

28. Adesiyun AG, Ojabo A, Durosinlorun-Mohammed A. Fertility and obstetric outcome after caesarean myomectomy. *J Obstet Gynaecol*. (2008) 28(7):710–2. doi: 10.1080/01443610802462712

29. Yıldırım Karaca S, Kantarcı S, Adıyeke M, Bulut S, Özcan A, Rabia Şenkaya A, et al. Comparison of transendometrial myomectomy versus conventional myomectomy in cesarean section. *Eur J Obstet Gynecol Reprod Biol*. (2021) 267:68–72. doi: 10.1016/j.ejogrb.2021.10.019

30. Rosenberg T, Pariente G, Sergienko R, Wiznitzer A, Sheiner E. Critical analysis of risk factors and outcome of placenta previa. *Arch Gynecol Obstet*. (2011) 284 (1):47–51. doi: 10.1007/s00404-010-1598-7

31. Huang SY, Shaw SW, Su SY, Li WF, Peng HH, Cheng PJ. The impact of a novel transendometrial approach for caesarean myomectomy on obstetric outcomes of subsequent pregnancy: a longitudinal panel study. *BJOG*. (2018) 125(4):495–500. doi: 10.1111/1471-0528.14798

32. Fauconnier A, Chapron C, Babaki-Fard K, Dubuisson JB. Recurrence of leiofibroidta after myomectomy. *Hum Reprod Update*. (2000) 6(6):595–602. doi: 10.1093/humupd/6.6.595

33. Kotani Y, Tobiume T, Fujishima R, Shigeta M, Takaya H, Nakai H, et al. Recurrence of uterine fibroid after myomectomy: open myomectomy versus laparoscopic myomectomy. *J Obstet Gynaecol Res*. (2018) 44(2):298–302. doi: 10.1111/jog.13519

34. Cobellis G, Messalli EM, Stradella L, Pecori E, Cobellis L. Restitutio ad integrum of myometrium after myomectomy. Different results in pregnant and non-pregnant patients. *Minerva Ginecol*. (2002) 54(5):393–5.

35. Cobellis L, Messali EM, Stradella L, Pecori E, Gioino E, De Lucia E, et al. Miomectomia in corso di taglio cesareo e al di fuori della gravidanza. Differenti esiti della cicatriche [myomectomy during cesarean section and outside pregnancy. Different outcomes of scars]. *Minerva Ginecol*. (2002) 54(6):483–6.

36. Zhu L, Yang X, Sun W, Qian L, Li S, Li D. Myomectomy scar pregnancy: a case report and review of the literature. *J Int Med Res*. (2020) 48(7): 300060520924542. doi: 10.1177/0300060520924542

37. Kandaswami D, Jayapal K, Sudhakar P, Usman S. Myomectomy scar ectopic pregnancy: diagnostic challenges and management conundrum: a case report. *Int J Reprod Contracept Obstet Gynecol*. (2022) 11(3):954–6. doi: 10.18203/2320-1770.ijrcog20220586

38. Zhang H, Pan H. Laparoscopic management of myomectomy scar pregnancy after a cryopreserved embryo transfer. *J Minim Invasive Gynecol*. (2021) 28 (11):1806–7. doi: 10.1016/j.jmig.2021.06.019

39. Tinelli A, Malvasi A, Guido M, Tsin DA, Hudelist G, Hurst B, et al. Adhesion formation after intracapsular myomectomy with or without adhesion barrier. *Fertil Steril*. (2011) 95(5):1780–5. doi: 10.1016/j.fertnstert.2010.12.049

40. Abu-Elhasan AM, Abdellah MS, Hamed HO. Safety and efficacy of postoperative continuous intra-peritoneal wash with lactated Ringer's for minimizing post-myomectomy pelvic adhesions: a pilot clinical trial. *Eur J Obstet Gynecol Reprod Biol*. (2014) 183:78–82. doi: 10.1016/j.ejogrb.2014.09.002

41. Morales KJ, Gordon MC, Bates GW Jr. Postcesarean delivery adhesions associated with delayed delivery of infant. *Am J Obstet Gynecol*. (2007) 196 (5):461.e461–e466. doi: 10.1016/j.ajog.2006.12.017

42. Tulandi T, Agdi M, Zarei A, Miner L, Sikirica V. Adhesion development and morbidity after repeat cesarean delivery. *Am J Obstet Gynecol*. (2009) 201 (1):56.e51–e56. doi: 10.1016/j.ajog.2009.04.039

43. Mercorio A, Della Corte L, Boccia D, Palumbo M, Reppuccia S, Buonfantino C, et al. Myomectomy in infertile women: more harm than good? *Front Surg*. (2023) 10:1151901. doi: 10.3389/fsurg.2023.1151901

44. Holm C, Langhoff-Roos J, Petersen KB, Norgaard A, Diness BR. Severe postpartum haemorrhage and mode of delivery: a retrospective cohort study. *BJOG*. (2012) 119(5):596–604. doi: 10.1111/j.1471-0528.2011.03267.x

45. Andolf E, Thorsell M, Kallen K. Cesarean delivery and risk for postoperative adhesions and intestinal obstruction: a nested case-control study of the Swedish medical birth registry. *Am J Obstet Gynecol*. (2010) 203(4):406.e1–6. doi: 10.1016/j.ajog.2010.07.013

46. Delporte V, Grabarz A, Ramdane N, Bodart S, Debarge V, Subtil D, et al. Cesarean during labor: is induction a risk factor for complications? *J Gynecol Obstet Hum Reprod*. (2019) 48(9):757–61. doi: 10.1016/j.jogoh.2019.08.008

frontiers | Frontiers in Medicine

TYPE Study Protocol
PUBLISHED 06 August 2024
DOI 10.3389/fmed.2024.1382822

OPEN ACCESS

EDITED BY
Andrea Tinelli,
Veris Delli Ponti Hospital, Italy

REVIEWED BY
Mihai Dumitrascu,
Carol Davila University of Medicine and Pharmacy, Romania
Timothy Abiola Olusesan Oluwasola,
University of Ibadan, Nigeria

*CORRESPONDENCE
Gulzhanat Aimagambetova
gulzhanat.aimagambetova@nu.edu.kz

RECEIVED 06 February 2024
ACCEPTED 12 June 2024
PUBLISHED 06 August 2024

CITATION
Aimagambetova G, Bapayeva G, Ukybassova T, Zemlyanskiy V, Gusmanov A and Terzic M (2024) The role of VEGF and TGF-β blood levels for fibroid shrinkage, menorrhagia score, and quality of life improvement after uterine artery embolization for uterine fibroids: a study protocol.
Front. Med. 11:1382822.
doi: 10.3389/fmed.2024.1382822

The role of VEGF and TGF-β blood levels for fibroid shrinkage, menorrhagia score, and quality of life improvement after uterine artery embolization for uterine fibroids: a study protocol

Gulzhanat Aimagambetova[1]*, Gauri Bapayeva[2], Talshyn Ukybassova[2], Viktor Zemlyanskiy[3], Arnur Gusmanov[4] and Milan Terzic[1,2]

[1]Department of Surgery, School of Medicine, Nazarbayev University, Astana, Kazakhstan, [2]Clinical Academic Department of Women's Health, CF "University Medical Center", Astana, Kazakhstan, [3]Clinical Academic Department of Radiology and Nuclear Medicine, CF "University Medical Center", Astana, Kazakhstan, [4]Department of Biomedical Sciences, School of Medicine, Nazarbayev University, Astana, Kazakhstan

Uterine leiomyoma is a common condition affecting women that occurs in more than 70% of females. Women with leiomyomas overall have lower quality of life and deficiency in many specific spheres of life including work-related productivity, sexuality, relationships, social–emotional health, and physical well-being that might be present even in pre-and extended throughout early postmenopausal life. Choices for symptomatic fibroid management include medical, interventional radiology procedures, surgical, and expectant management. The uterine artery embolization (UAE) procedure has gained justified popularity for myoma management. Growth factors, vascular endothelial growth factor (VEGF) and tumor growth factor β (TGF-β), hold an important role in leiomyoma progression. However, blood levels of VEGF and TGF-β in patients before and after UAE are not fully investigated and the possible relationship with myoma shrinkage has not been evaluated. Therefore, this study aims to assess menorrhagia score and quality of life improvement after UAE for uterine fibroids and compare blood levels of VEGF and TGF-β in patients with uterine leiomyoma before and after UAE. This cross-sectional study will be performed at the University Medical Center, Astana, Kazakhstan. Women undergoing the UAE procedure for uterine leiomyoma will be involved in the study following the precisely defined inclusion/exclusion criteria. Uterine leiomyoma nodules' structural changes after UAE will be assessed along with the blood levels of growth factors (VEGF and TGF-β), menorrhagia score, and quality of life. An important outcome of this project will be an investigation of the blood levels of growth factors (VEGF and TGF-β) before and after the procedure and their association with leiomyoma shrinkage in correlation with the menorrhagia score and quality of life alterations among patients undergoing UAE.

KEYWORDS

menorrhagia, quality of life, uterine artery embolization (UAE), uterine fibroids, fibroid shrinkage, VEGF, TGF-β

1 Introduction

Uterine leiomyoma (myoma or fibroid), is the most continual benign mass of the uterus, which occurs in more than 70% of women (1). Hysterectomy is still the most frequently offered and performed intervention to treat uterine leiomyoma (2). However, surgical management may lead to complications and negatively affects the patients' quality of life (3, 4). Over the past three decades, a minimally invasive approach has been acquiring popularity. Uterine fibroids embolization became a typical option for many patients who are looking for an organ-sparing procedure (5–7). Since the implementation, strong evidence has been constructed presenting safety and efficacy of this approach and low rates of complication and side effects (5, 8).

Uterine artery embolization (UAE) was initially defined as a therapeutic option for symptomatic uterine fibroids in 1995 and became very popular in the last two decades (9). The advantages of UAE over surgery are a short hospital admission period, a quick return to normal life activities (usually 1–2 weeks), a low rate of major complications, the opportunity for uterine/fertility-sparing procedure, and the overall better quality of life in most of the cases (5, 10). The goal of UAE is to decrease blood flow to fibroid nodules that will cause ischemia/infarction and shrinkage of the uterine leiomyoma nodes (fibroids). It is an efficient and effective method as it reduces uterine bleeding in up to 85% of the cases and decreases pain in up to 80% of the patients treated with this method.

The latest Royal College of Obstetrics and Gynecology (RCOG) and American College of Obstetricians and Gynecologists (ACOG) guidelines recognized UAE as effective as surgery for control of symptoms and recommended the procedure for patients with symptomatic uterine leiomyoma (11, 12). The Cardiovascular and Interventional Radiological Society of Europe (CIRSE) standards of practice also recognized UAE as a "true alternative to hysterectomy in women who wanted to preserve their uterus" (13). However, previous studies confirmed that within the following 5 years after UAE due to the uterine leiomyoma relapse, 10% of patients may require a hysterectomy, 3% - myomectomy, and 2% will require repeating the UAE procedure (14–17).

Uterine leiomyoma development is associated with the involvement of a variety of growth factors. Those are proteins or polypeptides, which are produced by several cell types (18). They have a variety of biological functions/effects and generally act via an autocrine and/or paracrine pathway. Growth factors effects on target cells by targeting specific receptors on a cell surface. The subsequent signaling transmits the effects of growth factors in the cell (14). The most important markers for uterine fibroid growth are vascular endothelial growth factor (VEGF) and transforming growth factor β (TGF-β) (14, 19, 20).

VEGF is a cytokine, which possesses multiple effects: increases microvascular permeability, and stimulates endothelial cells' growth and angiogenesis. VEGF is synthesized and secreted by various tumor cells and tumors in humans. It is an essential growth factor that supports the vascular endothelial cells proliferation, promotes cell migration and proliferation, and regulate angiogenesis (14, 21). Thus, VEGF plays a significant role in the growth of uterine fibroids (22). Although uterine leiomyoma is a benign mass, angiogenesis is also critical for its existence and development. UAE procedure could induce uterine fibroids' tissue ischemia and hypoxia via the blood supply obstruction. In the next step, hypoxia can prompt VEGF gene transcription, thus, elevating the expression level of VEGF and invigorating leiomyoma-related angiogenesis (14, 21, 23). According to the literature data, it is not clear and has to be elucidated further whether VEGF blood levels could be used as a prognostic factor for patients with uterine leiomyoma following UAE treatment (23).

TGF-β is known as a versatile cytokine with a dimeric polypeptide structure. TGF-β has three different isoforms and belongs to a large family of proteins entitled TGF-β superfamily (24). TGF-β regulates multiple inflammation mediators, cell division, and extracellular matrix production (24). Moreover, it plays a major part in cellular migration within a tumor, stimulates tumor growth, and enhances metabolism. Therefore, the synthesis and release of TGF-β in a fibroid nodule are increased, and results in excessive extracellular matrix production and deposition. According to available data, TGF-β substantially contributes to the growth and development of uterine leiomyoma by at least two mechanisms: (1) acts as an intermediary for sex steroid hormones, and (2) involvement in the processes of cell proliferation and migration, progression of fibrosis, and angiogenesis. TGF-β has meaningfully higher expression in uterine fibroid tissue than in normal myometrium (17). Furthermore, it has been specified that elevated levels of serum TGF-β are complemented by an elevated likelihood of uterine leiomyoma incidence (25). Recent investigation confirmed that inhibitors of VEGF and TGF-β can be used as therapeutic agents for uterine leiomyoma (19).

Currently, there is no data about the levels of VEGF and TGF-β in the peripheral blood of patients undergoing UAE, and their relationship with the uterine fibroid shrinkage. Moreover, blood levels of these growth factors in patients before and after UAE are not systematically investigated and eventual relationship with myoma shrinkage has not been evaluated. Therefore, this project aims to (1) assess menorrhagia score and quality of life improvement after uterine artery embolization for uterine fibroids and (2) compare blood levels of VEGF, and TGF-β in patients with uterine fibroids before and after UAE and to investigate their association with myoma shrinkage.

2 Methods

2.1 Study design and study setting

This study will utilize a three-year prospective cross-sectional study, including an 18-month recruitment period, data collection, laboratory processing, and post-study analysis. The study population will be drawn from women between the ages of 18–45 years with a history of uterine leiomyoma seeking UAE treatment, strictly following the inclusion and exclusion criteria. The patients will be recruited for the study from the gynecology and outpatient departments of the Clinical Academic Department (CAD) of Women's Health, University Medical Center (UMC), Astana, Kazakhstan.

2.2 Study subjects

2.2.1 Sample size justification

UMC outpatient department has an average of 2,000 outpatient visits per month and the Interventional Radiology Department performs 20–25 UAE per month (overall more than 250 procedures

per year). To assess whether changes in blood levels of growth factors after UAE are correlated with alterations in the uterine fibroid's volume, the required sample size is 120 patients. Using this desired sample size and formula indicated below, we computed achieved statistical power by setting Cohen's d at 0.5, and significance level at 0.05. Calculations resulted in a statistical power of 99.97% for a two-tailed paired t-test. Null hypothesis: no statistical significance will exist in a set of given observations in blood levels of growth factors (VEGF, TGF beta) in patients before and after uterine artery embolization.

$$n = \left(\frac{2 * \left(Z_{\alpha/2} + Z_{\beta} \right)^2}{d^2} \right)^2$$

$Z_{\alpha/2}$ – Z score that corresponds to significance level (α) for a two-tailed test.

Z_{β} – Z score that corresponds to the desired statistical power $(1-\beta)$ for the test.

d – denotes the desired effect size (Cohen's d), for which a moderate standardized difference (0.5) was taken.

2.2.2 Patients evaluation

All patients scheduled for UAE will be evaluated by a gynecologist, an interventional radiologist, and an anesthesiologist. A detailed general and menstrual history and a thorough clinical evaluation will be performed to exclude other causes of menorrhagia. Magnetic resonance imaging (MRI) is proven to be the best imaging modality for evaluation of patients before and after UAE. MRI allows an accurate pre-procedure delineation of the vascular anatomy. Ultrasound (US) is an available and fast imaging modality to evaluate uterine fibroids. Both transvaginal and abdominal US scans will be required for a complex evaluation of the patient before the procedure. Although US imaging is a less sensitive modality for complete fibroid designation and delineation of possible concurrent pathologies within the uterus and adnexal regions, it allows a rapid evaluation, is less expensive, and is more feasible for patients' selection.

2.2.3 Inclusion and exclusion criteria

This project will strictly follow the inclusion and exclusion criteria.

2.2.3.1 Inclusion criteria

Patients of 18–45 years old; history of symptomatic uterine intramural fibroids, or multiple symptomatic fibroids confirmed by visualization methods (ultrasound, magnetic resonance imaging) with severe menstrual bleeding and/or mechanical complaints/symptoms (pain, abdominal pressure, urinary urgency/frequency, dyspareunia); patient agrees with the method of treatment of uterine myoma – UAE.

2.2.3.2 Exclusion criteria

Patients not fulfilling the inclusion criteria; asymptomatic women with uterine fibroids; women with isolated adenomyosis, cervical leiomyoma, pedunculated subserous and/or submucous leiomyoma, intraligamentous leiomyoma; leiomyoma larger than 10 cm in diameter; endometrial polyps and/or hyperplasia or presence of any malignancy; pregnant or breastfeeding women; the presence of any disease or medical condition that could worsen the patient's safety and compliance in the study [chronic hypertension, cardiac insufficiency, renal insufficiency, diabetes mellitus (Type I or Type II), untreated hyper/hypothyroidism, hyperprolactinemia, chronic kidney disease, non-treated congenital of acquired cardiac pathology, multiple sclerosis, active vasculitis, uncontrolled coagulopathies]; pelvic irradiation history; contrast material allergy; concomitant use of GnRH analogs.

2.3 Basic angiographic and embolization techniques

Transcatheter embolization will be performed in an operating room with angiographic equipment in the Department of Interventional Radiology, UMC. Moderate sedation will be administered intravenously by an anesthesiologist to prevent pain and anxiety. The procedure for uterine artery embolization will be as follows: under local infiltration of anesthetic (Sol. Novocain 0.5% −20.0 mL/Sol. Lidocaine 1.0% −20.0 mL) puncture and catheterization of the right/left common femoral/radial artery by Seldinger will be performed. A 4- or 5-F selective angiographic catheter will be utilized for evaluation of the internal iliac artery, and a 2- or 3-F microcatheter will be used for super-selective catheterization of the uterine artery. The uterine artery originates from the internal iliac artery (anterior division), and it is well seen on the contralateral oblique projection. Robert's Uterine Catheter (RUC) will be used to hook both uterine arteries. For embolization, microspheres and/or microparticles with a diameter of 500–1,100 μm will be used.

2.4 Growth factors analysis

The blood samples from the cubital vein will be centrifuged (15,000 r/m) and subject to deep freezing at −80°C (25). Storage of samples will be carried out in conditions of deep freezing. Transportation of blood samples to the laboratory of the Republican Diagnostic Center (part of UMC) will be carried out in a special container with refrigerants. The test values (TGF-β and VEGF) will be determined via the enzyme-linked immunosorbent assay (ELISA) using standard sets Multiplex MAP Human Cytokine/Chemokine Magnetic Bead Panel, Merck according to the manufacturer's protocol on a Bio-Plex 3D flow cytometer. The expected values are given in the instructions attached to the kits. For the cohort of recruited patients (120), 480 blood samples will be analyzed (4 samples for each patient, overall 960 results for 2 growth factors) (Table 1).

2.5 Data collection procedures' sequence

Before embolization of the uterine arteries, patients will be asked to fill out the questionnaire on quality of life and menorrhagia score. Also, before embolization coagulation analysis will be done and prophylactic antibiotics given. Prophylactic antibiotics will be given via intravenous access 30 min before the UAE procedure. A Foley catheter will be installed for patients before the UAE procedure to keep the bladder empty and prevent obscuration of the uterus by a contrast-filled bladder.

TABLE 1 Timeline of procedures and investigations in the project.

Item/factor/procedure	Before UAE	1 week after UAE	1 month after UAE	3 months after UAE	1 year after UAE
UFS-QOL questionnaire	+	–	–	+	+
Menorrhagia score questionnaire	+	–	–	+	+
VEGF	+	+	+	+	–
TGF-β	+	+	+	+	–
US scan	+	+	+	+	–
MRI	+	–	–	–	+

After embolization of uterine arteries, patients will be provided with painkillers, prophylaxis of thromboembolic complications, and encouraged for early activation. Blood sampling for investigation of growth factors will be performed according to the protocol of the study: before the procedure (1), at 1 week (2), 1 month (3), 3 months (4) after the procedure of UAE in the CAD of Women's Health, UMC. After discharge from the hospital, the members of the study group will observe all patients for the entire study period on an outpatient basis. Ultrasound and/or magnetic resonance imaging will be performed at the Interventional Radiology Department of UMC on the same equipment, by the same physician. MRI will be performed before the procedure in UAE and one year after it, while US scans will be done 1 week after the procedure, and repeated 1 month and 3 months after the UAE procedure on the same US device, by the same physician (Table 1).

2.5.1 Study instruments (questionnaires)

Uterine Fibroid Symptom Health-related Quality of Life Questionnaire (UFS-QOL) and Menstrual Assessment Chart (Menorrhagia score questionnaire) will be utilized for the study.

The UFS-QOL is a tool specifically created to assess the symptoms associated with uterine leiomyoma (26, 27). It was developed by the SIR Foundation and validated in many languages (28). The UFS-QOL tool is currently in use by many researchers . The UFS-QOL contact information and permission to use: Mapi Research Trust, Lyon, France, https://eprovide.mapi-trust.org, No 98290.

The UFS-QOL is a self-reported questionnaire utilized to measure a patient's objective "pre-treatment and post-treatment symptoms" (e.g., bleeding, cramping) and subjective experience (e.g., a patient feeling "blue" or "less productive"). Information reported in the questionnaire might indicate a patient's condition without more invasive measures.

Menstrual Assessment Chart (Menorrhagia score questionnaire) is a pictorial method to assess heavy menstrual bleeding (Supplementary material) (29), which was used by many studies assessing blood loss (30).

Both questionnaires will filled by patients before the UAE procedure and repeated 3 and 12 months after the procedure (Table 1).

2.5.2 Blood sampling for growth factors investigation

The blood sampling procedure will be performed for identification of growth factors of interest according to the protocol of the study: before the procedure (1st sample), at 1 week (2nd sample), 1 month (3rd sample), 3 months (4th sample) after the UAE procedure.

2.5.3 Magnetic resonance imaging

The MRI procedures will be performed before the procedure of UAE – initially and one year after UAE (10).

2.5.4 Ultrasound scans

US examination will be done 1 week after the procedure (first control), and repeated 1 month (second control) and 3 months (third control) after the UAE procedure.

2.6 Statistical analysis

Descriptive statistics will be used to analyze the study variables (e.g., proportion, mean and standard error, median and interquartile ranges). Statistical methods will include checking assumptions and selecting appropriate tests to compare point estimates and frequencies. Bivariate associations between exposure factors and outcome will be determined by statistical tests (repeated measures ANOVA or Friedman's test, Pearson's or Spearman's correlation coefficients). A linear regression analysis will be used to analyze the associations further to determine which factor best explains the resulting outcome. To adjust for confounders, we will examine associations of all covariates with primary exposure factors and the outcome variable and apply potential confounders to a regression model. Statistical processing of data will be carried out in the software Stata 16.1 (31).

2.7 Ethical considerations

The study will follow the standards of the Helsinki Declaration and was approved by the Institutional Ethical Committee of the UMC, protocol#2, date of approval – November 14, 2022.

Participants of the study will be informed about the study's aims, benefits, possible outcomes, and eventual complications. After the detailed explanation, patients will be asked to sign an informed consent. Support and counseling will be provided throughout the study period. Participation in the study is voluntary, and the study participant will be allowed to leave the study at any stage. If the patient refuses to participate in the study, she will be treated according to the clinical guidelines approved by the Ministry of Health and the UMC clinic. Each patient has the right to refuse to participate in the study without explaining the reasons.

3 Anticipated results

3.1 Study outcomes

The study hypothesizes that a statistically significant association between blood levels of growth factors (VEGF, TGF-β) in patients before and after UAE will be found.

3.1.1 Primary outcome measures

1 Identify changes in menorrhagia score and Quality of life after uterine artery embolization for uterine fibroids;
2 Define the role of blood levels of growth factors (VEGF, TGF-β) in patients with fibroids before and after uterine artery embolization.

3.1.2 Secondary outcome measures

1 Define the correlation between menorrhagia score and quality of life and blood levels of growth factors (VEGF, TGF-β) before and after the procedure;
2 Outline the correlation between blood levels of growth factors (VEGF, TGF-β) before UAE and fibroid volume;
3 Shape the correlation between fibroid volume after UAE and blood levels of growth factors (VEGF, TGF-β) during follow-up.

3.2 Variables to be measured

3.2.1 Study subjects socio-demographic and clinical characteristics

Based on patients' socio-demographic and clinical data collected during the study subjects' recruitment, descriptive statistics will be calculated and presented (Table 2). Specific details of Uterine leiomyoma type, nodules count and size (volume), as well as the indication(s) for the UAE procedure, will be analyzed.

TABLE 2 Study subjects' socio-demographic and clinical characteristics.

Variables	Absolute numbers and percentages
Age	
Ethnicity	
Place of residence	
Education	
Marital status	
BMI	
Menarche	
Gynecological condition(s)	
Gynecological surgeries	
Infection(s)	
Pelvic Inflammatory Disease	
Cervical cytology	
Uterine leiomyoma type	
Uterine leiomyoma nodule(s) size	
Uterine leiomyoma nodules count	
Indications for UAE	
Total	

3.2.2 Analysis of data on patients' follow-up after the UAE procedure

A specific schedule for study subjects' follow-up is created to measure anticipated study results (Table 1). UFS-QOL results and menorrhagia scores will be analyzed before, 3 months after, and 1 year after the UAE procedure. Moreover, the structural changes of uterine leiomyoma nodules after UAE will be monitored via a series of US and MRI procedures as presented in Table 3.

Along with the uterine leiomyoma measurements, blood levels of VEGF and TGF-β will be measured. Possible correlations and associations between (1) changes in UFS-QOL results and menorrhagia scores, (2) structural changes in the uterine leiomyoma nodules, and (3) blood levels of growth (VEGF, TGF-β) factors will be defined and analyzed (Table 4).

4 Discussion

Considering that uterine leiomyomas present a significant healthcare problem for women and society; the treatment of uterine fibroids is the subject of close attention to both world and national gynecology societies. The pragmatism of radical surgical intervention in situations with an acute clinical picture or gigantic dimensions of fibroids is beyond doubt (32). At the same time, justification for its high frequency in current practice is sometimes questionable. According to experts, even in the US, the number of organ-preserving myomectomies does not exceed 10% among all hysterectomies, and the vaginal approach was identified as the most appropriate whenever feasible (3, 33–36). On the other side, a recently published review evaluated myomectomy done in infertile patients and found that, due to its extremely high adhesiogenic potential, this procedure has been confirmed more harmful than good. Therefore, when myomectomy is performed as an infertility treatment, attention should be drawn to whether the benefits offset the risks (37). Therefore, minimally invasive procedures are of paramount interest.

Furthermore, after the organ-saving operations, the risk of relapse remains high. A recently published retrospective cross-sectional study compared the rates of reappearance and the effect on the quality of life between myomectomy and uterine fibroid embolization in patients diagnosed with uterine leiomyoma (38). The authors reported that there was no notable statistical difference between the two groups, which indicates that both UAE and myomectomy were reasonably successful in preventing uterine fibroid recurrence. These results in line with prior studies that reported similar outcomes for both treatment modalities (39, 40).

Nowadays, it would seem that most practitioners should strive to keep the female reproductive organs. One of the hopes of modern gynecology is the embolization of uterine arteries, which has been widely practiced in modern gynecology since the mid-1990s of the 20th century (41–43). This high-tech surgical procedure is certainly preferable to hysterectomy since it preserves both the organ and its function.

TABLE 3 Patients' follow-up after UAE procedure to register uterine leiomyoma structural changes.

Variables	Follow-up measurements					T-test
	MRI procedure		US procedure			
	Initial	After 1 year	Day 7 after UAE	1 month after UAE	3 months after UAE	
Overall number of myomas						
localization vs. numbers of myomas						
Leading myoma nodule's localization						
Leading myoma nodule's size (diameter and volume)						
Leading myoma nodule's vascularization						
Volume of the uterus						
Uterine artery Doppler flow						

TABLE 4 VEGF and TGF-β measurements.

Variables	Follow-up measurements				T-test
	Before UAE	Day 7 after UAE	1 month after UAE	3 months after UAE	
VEGF					
TGF-β					

Although UAE was confirmed to be preferable to surgical treatment in patients with symptomatic uterine fibroids (11, 44, 45), it might be accompanied by specific side effects (5) and extremely rare, but life-threatening complications (6).

Embolization of uterine arteries for management of uterine leiomyomas was introduced into Kazakhstani gynecological practice in 2008 at the National Research Center for Maternal and Child Health, Astana. During this period, significant clinical experience was accumulated, and the UAE procedure was proven to be successful. Thus, it can be considered an effective and reliable procedure for leiomyoma treatment (7).

Uterine leiomyoma development is a complex process that involves variety of cytokines and different growth factors; among them, the most important are VEGF and TGF-β (14). Molecular mechanisms of their action are not completely understood and the relationship between their blood levels and fibroid volume is not defined. Currently, many studies on the UAE in women with uterine leiomyomas have been performed worldwide (39, 42, 46). However, blood levels of VEGF and TGF-β in patients before and after UAE are not systematically investigated and the eventual relationship with myoma shrinkage has not been evaluated.

The results of this project will assess menorrhagia score and quality of life improvement after the UAE procedure, and define the association of VEGF and TGF-β blood levels with fibroid shrinkage in patients undergoing UAE, thus, improving knowledge of biochemical markers' role and approach to clinical management of women with uterine fibroids. The results of this project may become a serious scientific argument for justifying the patient's choice of UAE as a preferable treatment for uterine fibroids.

4.1 Study strengths and limitations

This is the first study comparing blood levels of growth factors (VEGF, TGF-β) with the fibroid volume before and after UAE. Moreover, this study is the first one that links blood levels of VEGF and TGF-β before and after UAE with menorrhagia score and the QoL. This study will assess the value of UAE for myoma shrinkage, menorrhagia score, and QoL of patients undergoing UAE in the local clinical setting. Moreover, this study logistics will allow us to have full insight into patients' past medical history and clinical data that will facilitate the research outcomes. However, this study has some limitations. Although justified, it has a relatively small sample size. Moreover, the study has a follow-up period of 1 year, which increases the risk of incomplete data collection or missing data in some cases. The third limitation is a relatively short follow-up period of one year, which might limit insight into some parameters/factors that could appear 3 or 5 years after the procedure.

Ethics statement

The studies involving humans were approved by University Medical Center Institutional Research Ethics Committee. The study will be conducted in accordance with the local legislation and institutional requirements. The participants will provide their written informed consent to participate in this study.

Author contributions

GA: Conceptualization, Investigation, Methodology, Writing – original draft, Writing – review & editing. GB: Conceptualization, Project administration, Writing – original draft. TU: Conceptualization, Supervision, Writing – original draft. VZ: Conceptualization, Methodology, Writing – original draft. AG: Methodology, Software, Writing – original draft, Writing – review & editing. MT: Conceptualization, Methodology, Project administration, Resources, Writing – original draft, Writing – review & editing.

Funding

The author(s) declare that no financial support was received for the research, authorship, and/or publication of this article.

Acknowledgments

The authors would like to thank the Nazarbayev University School of Medicine for the continuous support.

Conflict of interest

The authors declare that the research was conducted in the absence of any commercial or financial relationships that could be construed as a potential conflict of interest.

Publisher's note

All claims expressed in this article are solely those of the authors and do not necessarily represent those of their affiliated organizations, or those of the publisher, the editors and the reviewers. Any product that may be evaluated in this article, or claim that may be made by its manufacturer, is not guaranteed or endorsed by the publisher.

Supplementary material

The Supplementary material for this article can be found online at: https://www.frontiersin.org/articles/10.3389/fmed.2024.1382822/full#supplementary-material

References

1. Lou Z, Huang Y, Li S, Luo Z, Li C, Chu K, et al. Global, regional, and national time trends in incidence, prevalence, years lived with disability for uterine fibroids, 1990-2019: an age-period-cohort analysis for the global burden of disease 2019 study. *BMC Public Health*. (2023) 23:916. doi: 10.1186/s12889-023-15765-x

2. Aggarwal H, Aggarwal H, Wanjari A. Unnecessary hysterectomies among premenopausal women in developed and developing countries: a critical review of steps taken to improve Women's health. *Cureus*. (2023) 15:e49943. doi: 10.7759/cureus.49943

3. Don EE, Mijatovic V, van Eekelen R, Hehenkamp WJK, Huirne JAF. The effect of a myomectomy on Myoma-related symptoms and quality of life: a retrospective cohort study. *J Minim Invasive Gynecol*. (2023) 30:897–904. doi: 10.1016/j.jmig.2023.07.001

4. Anchan RM, Spies JB, Zhang S, Wojdyla D, Bortoletto P, Terry K, et al. Long-term health-related quality of life and symptom severity following hysterectomy, myomectomy, or uterine artery embolization for the treatment of symptomatic uterine fibroids. *Am J Obstet Gynecol*. (2023) 229:275.e1–275.e17. doi: 10.1016/j.ajog.2023.05.020

5. Yerezhepbayeva M, Terzic M, Aimagambetova A. Comparison of two invasive non-surgical treatment options for uterine myomas: uterine artery embolization and magnetic resonance guided high intensity focused ultrasound— systematic review. *BMC Womens Health*. (2022) 22:55. doi: 10.1186/s12905-022-01627-y

6. Imankulova B, Terzic M, Ukybassova T, Bapayeva G, Lesbekov T, Mustafinova G, et al. Repeated pulmonary embolism with cardiac arrest after uterine artery embolization for uterine arteriovenous malformation: a case report and literature review. *Taiwan J Obstet Gynecol*. (2018) 57:890–3. doi: 10.1016/j.tjog.2018.10.021

7. Ukybassova T, Terzic M, Dotlic J, Imankulova B, Terzic S, Shauyen F, et al. Evaluation of uterine artery embolization on Myoma shrinkage: results from a large cohort analysis. *Gynecol Minim Invasive Ther*. (2019) 8:165–71. doi: 10.4103/GMIT.GMIT_50_19

8. Middelkoop MA, Harmsen MJ, Manyonda I, Mara M, Ruuskanen A, Daniels J, et al. Uterine artery embolization versus surgical treatment in patients with symptomatic uterine fibroids: protocol for a systematic review and meta-analysis of individual participant data. *Eur J Obstet Gynecol Reprod Biol*. (2021) 256:179–83. doi: 10.1016/j.ejogrb.2020.11.027

9. Ravina JH, Herbreteau D, Ciraru-Vigneron N, Bouret JM, Houdart E, Aymard A, et al. Arterial embolisation to treat uterine myomata. *Lancet*. (1995) 346:671–2. doi: 10.1016/S0140-6736(95)92282-2

10. Psilopatis I, Fleckenstein FN, Collettini F, Can E, Frisch A, Gebauer B, et al. Short- and long-term evaluation of disease-specific symptoms and quality of life following uterine artery embolization of fibroids. *Insights Imaging*. (2022) 13:106. doi: 10.1186/s13244-022-01244-1

11. American College of Obstetricians and Gynecologists' Committee on Practice Bulletins–Gynecology. Management of Symptomatic Uterine Leiomyomas: ACOG practice bulletin, number 228. *Obstet Gynecol*. (2021) 137:e100–15. doi: 10.1097/AOG.0000000000004401

12. Royal College of Obstetricians and Gynaecologists. (2013). Uterine artery embolization in the management of fibroids. Available at: www.rcog.org.uk/en/guidelinesresearch-services/guidelines/uterine-artery-embolization-inthe-management-of-fibroids (Accessed January 22, 2024)

13. Memarian S, Krokidis M, O'Sullivan G, Peynircioglu B, Rossi M, Kashef E. CIRSE standards of practice on arterial access for interventions. *Cardiovasc Intervent Radiol*. (2023) 46:302–9. doi: 10.1007/s00270-022-03349-y

14. Ciarmela P, Islam MS, Reis FM, Gray PC, Bloise E, Petraglia F, et al. Growth factors and myometrium: biological effects in uterine fibroid and possible clinical implications. *Hum Reprod Update*. (2011) 17:772–90. doi: 10.1093/humupd/dmr031

15. Islam MS, Greco S, Janjusevic M, Ciavattini A, Giannubilo SR, D'Adderio A, et al. Growth factors and pathogenesis. *Best Pract Res Clin Obstet Gynaecol*. (2016) 34:25–36. doi: 10.1016/j.bpobgyn.2015.08.018

16. Dixon D, He H, Haseman JK. Immunohistochemical localization of growth factors and their receptors in uterine leiomyomas and matched myometrium. *Environ Health Perspect*. (2000) 108:795–802. doi: 10.1289/ehp.00108s5795

17. Ciebiera M, Włodarczyk M, Wrzosek M, Męczekalski B, Nowicka G, Łukaszuk K, et al. Role of transforming growth factor β in uterine fibroid biology. *Int J Mol Sci*. (2017) 18:2435. doi: 10.3390/ijms18112435

18. Stone WL, Leavitt L, Varacallo M. Physiology, growth factor. Stat pearls. Treasure Island, FL: StatPearls Publishing (2024)

19. Park JY, Chae B, Kim MR. The potential of transforming growth factor-beta inhibitor and vascular endothelial growth factor inhibitor as therapeutic agents for uterine leiomyoma. *Int J Med Sci*. (2022) 19:1779–86. doi: 10.7150/ijms.75203

20. Tal R, Segars JH. The role of angiogenic factors in fibroid pathogenesis: potential implications for future therapy. *Hum Reprod Update*. (2014) 20:194–216. doi: 10.1093/humupd/dmt042

21. Pourgholami MH, Morris DL. Inhibitors of vascular endothelial growth factor in cancer. *Cardiovasc Hematol Agents Med Chem*. (2008) 6:343–7. doi: 10.2174/187152508785909528

22. Plewka D, Morek M, Bogunia E, Waloszek J, Plewka A. Expression of VEGF isoforms and their receptors in uterine myomas. *Ginekol Pol*. (2016) 87:166–77. doi: 10.17772/gp/60979

23. Mu Y, He J, Yan R, Hu X, Liu H, Hao Z. IGF-1 and VEGF can be used as prognostic indicators for patients with uterine fibroids treated with uterine artery embolization. *Exp Ther Med*. (2016) 11:645–9. doi: 10.3892/etm.2015.2924

24. Yang Q, Al-Hendy A. Update on the role and regulatory mechanism of extracellular matrix in the pathogenesis of uterine fibroids. *Int J Mol Sci*. (2023) 24:5778. doi: 10.3390/ijms24065778

25. Kamalipooya S, Zarezadeh R, Latifi Z, Nouri M, Fattahi A, Salemi Z. Serum transforming growth factor β and leucine-rich α-2-glycoprotein 1 as potential biomarkers for diagnosis of uterine leiomyomas. *J Gynecol Obstet Hum Reprod*. (2021) 50:102037. doi: 10.1016/j.jogoh.2020.102037

26. Spies JB, Coyne K, Guaou Guaou N, Boyle D, Skyrnarz-Murphy K, Gonzalves SM. The UFS-QOL, a new disease-specific symptom and health-related quality of life questionnaire for leiomyomata. *Obstet Gynecol*. (2002) 99:290–300. doi: 10.1016/s0029-7844(01)01702-1

27. Spies JB, Coyne K, Guaou Guaou N, Boyle K, Gonzalves SM. The UFS-QOL, a new diseasespecific symptom and health-related quality of life questionnaire for leiomyomata. *Qual Life Res*. (2002) 99:290–300.

28. SIR Foundation. (n.d.) Uterine Fibroid Symptom Health-Related Quality of Life Questionnaire (UFS-QOL). Available at: https://www.sirfoundation.org/research-and-registries/clinical-research/ufs-qol/#:~:text=The%20UFS%2DQOL%20is%20a,severity%20of%20the%20patient's%20condition (Accessed January 29, 2024)

29. Higham JM, O'Brien PM, Shaw RW. Assessment of menstrual blood loss using a pictorial chart. *Br J Obstet Gynaecol*. (1990) 97:734–9. doi: 10.1111/j.1471-0528.1990.tb16249.x

30. Magnay JL, O'Brien S, Gerlinger C, Seitz C. Pictorial methods to assess heavy menstrual bleeding in research and clinical practice: a systematic literature review. *BMC Womens Health*. (2020) 20:24. doi: 10.1186/s12905-020-0887-y

31. StataCorp. Stata statistical software: Release 16. College Station, TX: StataCorp LLC (2019).

32. Donnez J, Dolmans MM. Uterine fibroid management: from the present to the future. *Hum Reprod Update*. (2016) 22:665–86. doi: 10.1093/humupd/dmw023

33. Terzic M, Dotlic J, Maricic S, Babovic I. Hydatiform mole mimicking enlarged uterine Fibromyoma four months after ART. *Cent Eur J Med*. (2011) 6:201–4. doi: 10.2478/s11536-010-0077-7

34. Terzic M, Likic Ladjevic I, Ladjevic N, Terzic S, Dotlic J, Cekerevac M, et al. Anaplastic T-cell lymphoma of the urinary bladder with unspecific clinical and radiological characteristics – a unique case report. *Eur J Gynecol Oncol*. (2019) 40:136–9. doi: 10.12892/ejgo4630.2019

35. Akhatova A, Aimagambetova G, Bapayeva G, Laganà AS, Chiantera V, Oppelt P, et al. Reproductive and obstetric outcomes after UAE, HIFU, and TFA of uterine fibroids: systematic review and Meta-analysis. *Int J Environ Res Public Health*. (2023) 20:4480. doi: 10.3390/ijerph20054480

36. Terzic M, Maricic S, Dotlic J. Vaginal removal of very large nascent uterine Myoma–case report and literature review. *Geburtsh Frauenheilk*. (2013) 73:724–6. doi: 10.1055/s-0032-1328724

37. Mercorio A, Della Corte L, Boccia D, Palumbo M, Reppuccia S, Buonfantino C, et al. Myomectomy in infertile women: more harm than good? *Front Surg*. (2023) 10:1151901. doi: 10.3389/fsurg.2023.1151901

38. Aktürk H, Dura MC, Gürsoy B, Ikizoğlu F, Göl E, Alsalamin WOI, et al. Comparison of recurrence and quality of life between Myoma embolization and myomectomy. *Cureus*. (2023) 15:e40372. doi: 10.7759/cureus.40372

39. Daniels J, Middleton LJ, Cheed V, McKinnon W, Rana D, Sirkeci F, et al. Uterine artery embolisation versus myomectomy for premenopausal women with uterine fibroids wishing to avoid hysterectomy: the FEMME RCT. *Health Technol Assess*. (2022) 22:6110. doi: 10.3310/ZDEG6110

40. Goodwin SC, Bradley LD, Lipman JC, Stewart EA, Nosher JL, Sterling KM, et al. Uterine artery embolization versus myomectomy: a multicenter comparative study. *Fertil Steril*. (2006) 85:14–21. doi: 10.1016/j.fertnstert.2005.05.074

41. Kröncke T. An update on uterine artery embolization for uterine leiomyomata and adenomyosis of the uterus. *Br J Radiol*. (2023) 96:20220121. doi: 10.1259/bjr.20220121

42. Ito H, Nakai M, Yunaiyama D, Shirota N, Kobayashi T, Yasutomi M, et al. Efficacy of uterine artery embolization (UAE) for uterine fibroids according to FIGO classification: a single-center experience. *Jpn J Radiol*. (2024) 42:174–81. doi: 10.1007/s11604-023-01492-1

43. Cappelli A, Mosconi C, Cocozza MA, Brandi N, Bartalena L, Modestino F, et al. Uterine artery embolization for the treatment of symptomatic uterine fibroids of different sizes: a single Center experience. *J Pers Med*. (2023) 13:906. doi: 10.3390/jpm13060906

44. Otify M, Critchley HOD. Pathophysiology of uterine fibroids In: M Mostafa Metwally and TC Li, editors. Modern Management of Uterine Fibroids. Cambridge: Cambridge University Press (2020). 1–13.

45. Zhang J, Go VA, Blanck JF, Singh B. A systematic review of minimally invasive treatments for uterine fibroid-related bleeding. *Reprod Sci*. (2022) 29:2786–809. doi: 10.1007/s43032-021-00722-z

46. Sirkeci F, Moss J, Belli AM, McPherson K, Daniels J, Manyonda I, et al. Effects on heavy menstrual bleeding and pregnancy of uterine artery embolization (UAE) or myomectomy for women with uterine fibroids wishing to avoid hysterectomy: the FEMME randomized controlled trial. *Int J Gynaecol Obstet*. (2023) 160:492–501. doi: 10.1002/ijgo.14626

frontiers | Frontiers in Oncology

TYPE Original Research
PUBLISHED 16 August 2024
DOI 10.3389/fonc.2024.1451626

OPEN ACCESS

EDITED BY
Andrea Tinelli,
Veris delli Ponti Hospital, Italy

REVIEWED BY
Mladen Anđić,
University of Belgrade, Serbia
Omer Iqbal,
Loyola University Chicago, United States

*CORRESPONDENCE
Sheng Chen
chenyuansen246@163.com

RECEIVED 19 June 2024
ACCEPTED 30 July 2024
PUBLISHED 16 August 2024

CITATION
Xue H, Wu S, Xiao K, Ding G and Chen S (2024) Sonographic features of uterine fibroids that predict the ablation rate and efficacy of high-intensity focused ultrasound. *Front. Oncol.* 14:1451626.
doi: 10.3389/fonc.2024.1451626

Sonographic features of uterine fibroids that predict the ablation rate and efficacy of high-intensity focused ultrasound

Hailan Xue[1,2], Songsong Wu[2], Kunhong Xiao[3], Guisheng Ding[2] and Sheng Chen[2,4]*

[1]Fujian Maternity and Child Health Hospital College of Clinical Medicine for Obstetrics and Gynecology and Pediatrics, Fujian Medical University, Fuzhou, China, [2]Shengli Clinical Medical College of Fujian Medical University, Fuzhou, China, [3]Department of Ophthalmology and Optometry, Fujian Medical University, Fuzhou, China, [4]Ultrosound Department, Fujian Medical University Union Hospital, Fuzhou, China

Objective: This study aimed to identify the sonographic indicators that predict the ablation rate and efficiency of uterine fibroids during high-intensity focused ultrasound (HIFU) treatment.

Methods: In this retrospective study, we analyzed the clinical data of patients with uterine fibroids who underwent HIFU treatment at Fujian Provincial Hospital between April 2019 and April 2022. Routine abdominal ultrasound examinations were performed to observe potential indicators before the HIFU treatment. After the treatment, enhanced magnetic resonance imaging (MRI) examination was performed within 2 weeks. The fibroid and non-perfused volumes (NPV) were determined, and the ablation rate and energy efficiency factor (EEF) were calculated.

Results: A total of 75 patients (124 uterine fibroids) were included in this study. Uterine fibroids with a larger volume, high echogenicity, elliptical/diffuse leaf shape, and a posterior attenuation band had a higher HIFU ablation rate ($p<0.05$). Uterine fibroids with a larger volume and high echogenicity and without necrotic areas had a lower EEF ($p<0.05$). Multiple comparisons between fibroid types revealed statistically significant differences in EEF between subserosal and submucosal fibroids ($p < 0.05$) and between subserosal and mixed-type fibroids ($p < 0.05$). However, no statistically significant difference was observed between mixed-type and submucosal fibroids. The HIFU ablation rate and EEF showed no significant differences based on location within the wall and blood flow within the fibroids.

Abbreviations: HIFU, High-Intensity Focused Ultrasound; NPV, Non-Perfused Volume; EEF, Energy Efficiency Factor; MRI, Magnetic Resonance Imaging; FIGO, Federation of Gynecology and Obstetrics; SE, Spin Echo; T1WI, T1-Weighted Imaging; TSE, Turbo Spin Echo; T2WI, T2-Weighted Imaging; NPVR, Non-Perfused Volume Ratio.

Conclusion: Sonographic features of uterine fibroids can predict the rate and efficiency of HIFU ablation, providing useful guidance in selecting appropriate treatment for patients.

KEYWORDS

uterine fibroids, sonographic features, high-intensity focused ultrasound, ablation rate, energy efficiency factor

1 Introduction

Uterine fibroids, the most common benign tumors of the female reproductive system (1), affect 25-40% of women of childbearing age (2). While many patients are asymptomatic, others experience severe symptoms, such as heavy menstrual bleeding, prolonged menstruation, and pelvic pain. Other symptoms may be related to the compression caused by the mass, including frequent urination, urgency, constipation, and a sensation of pelvic pressure. Larger fibroids may also negatively affect fertility. Treatment is necessary for clinically symptomatic uterine fibroids. However, fibroids often regrow to their pre-treatment size even after intervention (3).

The definitive treatment for uterine fibroids is hysterectomy; however, it is unsuitable for patients who desire pregnancy. Myomectomy is an alternative treatment for those aiming to retain uterine function and fertility, but it is invasive and increases the risk of uterine rupture in subsequent pregnancies. High-intensity focused ultrasound (HIFU) ablation offers a non-invasive alternative with proven safety and efficacy for treating uterine fibroids (4–7). Nevertheless, some fibroids exhibit a suboptimal response to HIFU, emphasizing the need for an improved preoperative assessment to select suitable candidates. Magnetic resonance imaging (MRI) is an option for preoperative fibroid evaluation for response to HIFU (8–10). However, the preoperative use of MRI has limitations, including limited availability, prolonged examination time, high cost, and exclusion of specific patients. Therefore, a more economical, straightforward, and widely applicable preoperative test is crucial to guide the selection of uterine fibroids for HIFU treatment.

With advances in technology and the rapid development of medical devices, ultrasound has become increasingly sophisticated, offering excellent tissue contrast and image reproducibility. Ultrasound examinations are convenient, fast, accurate, safe, non-invasive, and highly reproducible. Consequently, ultrasound imaging is promising as a preoperative assessment of uterine fibroids for HIFU treatment. However, research investigating whether the sonographic features of fibroids can predict effective HIFU treatment is lacking. This study aimed to explore sonographic characteristics of uterine fibroids to identify parameters that can predict the ablation rate and efficiency of HIFU treatment.

2 Materials and methods

2.1 Study population

A retrospective analysis was conducted on the clinical data of 361 patients with uterine fibroids who underwent HIFU ablation at the ultrasound department of Fujian Provincial Hospital between April 2019 and April 2022.

2.2 Inclusion and exclusion criteria

The inclusion criteria were as follows: 1) patients who underwent ultrasound examination the day before or on the day of HIFU treatment and 2) patients who underwent follow-up enhanced MRI within 2 weeks of HIFU treatment. The exclusion criteria were as follows: 1) patients who underwent special interventions before or during HIFU treatment (e.g., local ethanol injection or transcatheter arterial embolization), 2) patients with pedunculated subserosal fibroids and fibroids in specific locations such as the cervix or broad ligament, and 3) patients with incomplete data.

This study was approved by the Ethics Committee of Fujian Provincial Hospital (Approval No: K2021-04-038). All participants signed standard informed consent forms during their medical treatment, agreeing that their data could be used for research purposes.

2.3 Instruments and equipment

The treatment utilized a JC200-focused ultrasound tumor therapy system (Chongqing Haifu Technology Co., Ltd.). This system performs real-time ultrasound positioning, HIFU three-dimensional scanning, and treatment. Controlled by a computer, it automatically locates the predetermined tumor target area, determines the treatment range, conducts three-dimensional conformal scanning, monitors, and analyzes the treatment effects in real-time, and provides feedback control for the treatment dosage. The main treatment parameters were as follows: 1)

treatment frequency of 0.97 MHz; 2) focal width of 3 mm; 3) focal length of 8 mm; 4) focal distance of 162 mm; and 5) maximum power of 400 W for a single-point treatment.

For ultrasound examinations, the SIEMENS S3000 Color Doppler Ultrasound Diagnostic Instrument with a 6C1 convex array probe (frequency: 2.0–5.0 MHz) was employed. MRI examinations were conducted using Philips Achieva 1.5T and 3.0T MRI systems.

2.4 Examination methods, procedures, and treatment

2.4.1 Ultrasound examination

On the day before or the day of the HIFU treatment, two-dimensional grayscale and color Doppler flow ultrasound imaging of the uterine fibroids were performed, and the images were stored. All patients underwent an ultrasound examination with an empty bladder. The examinations were conducted transabdominally with the patients in a supine position. The ultrasound was adjusted to achieve optimal resolution by scanning the pelvic cavity, uterus, and bilateral adnexal areas in longitudinal, transverse, and oblique sections. Fibroid location, size, morphology, number, internal echo characteristics, presence of necrotic areas, boundaries, attenuation zones, blood flow, and their relationship with the endometrium and surrounding organs was noted. Measurements of the three axes of the uterine fibroids were obtained from the maximum cross-sectional and vertical-sectional images. Subsequently, SonoVue ultrasound contrast was injected intravenously for contrast-enhanced ultrasound evaluation of fibroid perfusion.

2.4.2 Observational parameters in ultrasound examination

(1) Uterine fibroid location was classified into three types: anterior wall, lateral and fundal wall, or posterior wall.

(2) Uterine fibroids were classified into nine types using the International Federation of Gynecology and Obstetrics (FIGO) (11) classification system. Types 7 and 8 were excluded according to the exclusion criteria. The remaining seven types were grouped based on the location of the fibroids in the uterine wall. Types 0, 1, and 2 were classified as submucosal, types 3 and 4 as intramural, and types 5 and 6 as subserosal. Fibroids exhibiting characteristics of both types 2 and 5, protruding into the submucosa by ≤50% and the serosa by ≤50%, were classified as mixed-type fibroids.

(3) Uterine fibroid size was measured using three axes on maximum cross-sectional and vertical-sectional images. The volume of each fibroid was calculated using the formula $V=0.5233\times D1\times D2\times D3$ (12).

(4) Uterine fibroids were categorized into two shapes, round or irregular (elliptical/diffuse or leaf-shaped).

(5) To assess the internal uterine fibroid echo, a comparison was made with the normal uterine muscular layer in the same horizontal plane, with consideration for abdominal wall thickness and interference from the intestines. Fibroids with internal echoes that were predominantly higher than the muscle layer were classified as hyperechoic, whereas those with lower internal echoes were classified as hypoechoic, and those with equal internal echoes were classified as isoechoic (Figures 1A, B). Fibroids with similar proportions of hypoechoic and isoechoic areas were grouped as hypo/isoechoic fibroids and the others as hyperechoic fibroids.

(6) The presence or absence of necrotic areas within the fibroids was determined based on the presence or absence of hypoechoic regions, thereby categorizing the fibroids into groups with or without necrotic areas, respectively.

(7) The number of posterior attenuation bands of the fibroid on the maximum cross-sectional image excluding lateral shadowing was counted (Figures 1C, D).

(8) Using the Adler grading system (13), blood flow was categorized into four levels: grade 0, grade 1, grade 2, and grade 3.

2.4.3 Treatment method

Patients were placed in a prone position, and their vital signs and mental status were monitored. The patients underwent preoperative catheterization, bladder filling, and injection of midazolam (1 mg), sufentanil (10-40 μg), flurbiprofen ester (50 mg), and tropisetron (5 mg). During treatment, flurbiprofen ester (100 mg) and oxytocin (80U + 500 ml saline) were intravenously infused.

A preoperative scan was performed to formulate the HIFU ablation plan and adjust the focal point position. A layer-by-layer scanning approach was implemented throughout the ablation, sequentially progressing from point to line, line to plane, and plane to volume. This was done using a water cushion to displace the intestines. Ablation was conducted at a single point with a power of 400 W, applying continuous irradiation for 1 s, followed by a 1-s pause. Node spacing, pitch, irradiation time, and pause time ratios were adjusted based on real-time changes in the ultrasound images and patient responses. An immediate assessment using contrast-enhanced ultrasound was performed, and the absence of contrast agent perfusion indicated effective ablation.

After treatment, the patient's conditions were observed, and the treated area of the skin and sensory-motor function in both lower limbs were examined. The patients were discharged after a 2-h rest period.

2.4.4 MRI examination and observation parameters

The HIFU ablation rate was defined as the ratio of the volume of the ablated portion after HIFU treatment to the initial volume of the fibroid. It served as the primary indicator for evaluating the efficacy of HIFU, with a higher ablation rate indicating better effectiveness.

The energy efficiency factor (EEF) is the ultrasound energy required for HIFU ablation of 1 mm^3 of tumor tissue. It acts as an index for measuring HIFU ablation efficiency and ease of ablation, with lower EEF values indicating higher ablation efficiency and easier ablation.

Contrast-enhanced MRI was conducted within 2 weeks before and after HIFU treatment. Routine spin echo (SE) sequence T1-weighted imaging (T1WI) and turbo spin echo (TSE) sequence T2-

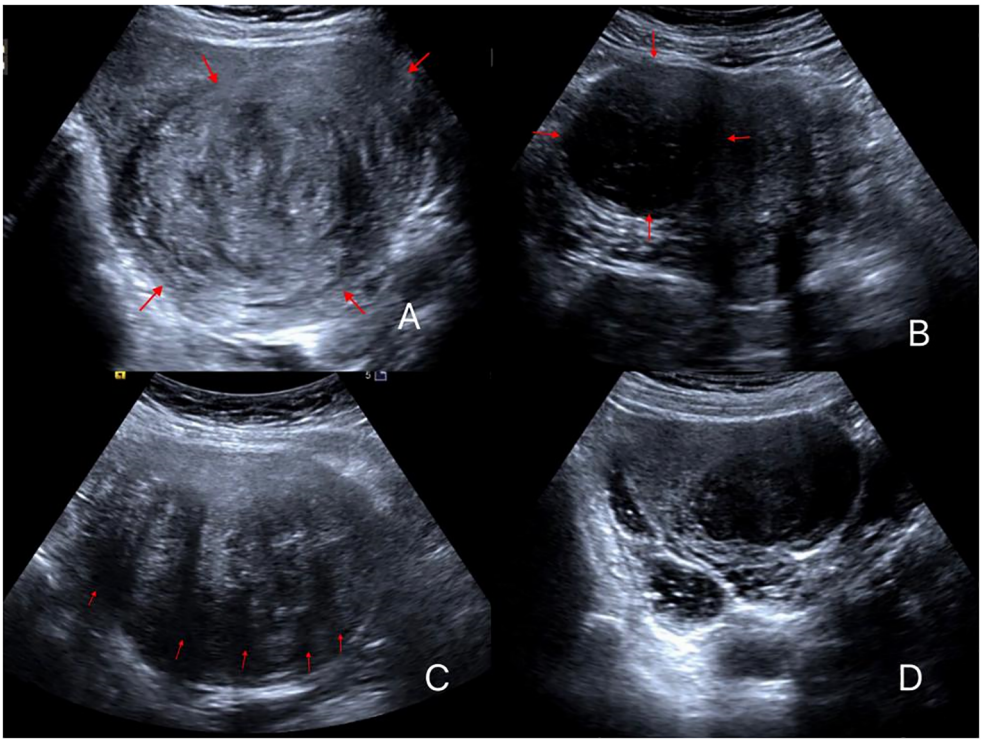

FIGURE 1
Different ultrasonic image features of uterine fibroids. **(A)** Fibroid is elliptical with high echogenicity; **(B)** Fibroid has a round shape with low echogenicity; **(C)** Fibroid with five attenuation bands; **(D)** Fibroids with no attenuation band and low echogenicity.

weighted imaging (T2WI) were performed in the cross-sectional, coronal, and sagittal planes, along with fat-suppressed sequences. The maximum cross-sectional images of the fibroids in the sagittal and transverse planes were analyzed postoperatively to measure the size of the targeted fibroids and non-perfused area. The volumes of the nonperfused area and fibroid were calculated in three dimensions (Figure 2): longitudinal (D1), anteroposterior (D2), and transverse (D3), using the formula V=0.5233×D1×D2×D3 (12). The ablation rate was computed as follows:

$$nonperfused\ \ volume\ \ ratio\ \ (NPVR)$$
$$= \frac{nonperfused\ \ area\ \ volume}{targeted\ \ fibroid\ \ volume} \times\ \ 100\,\%$$

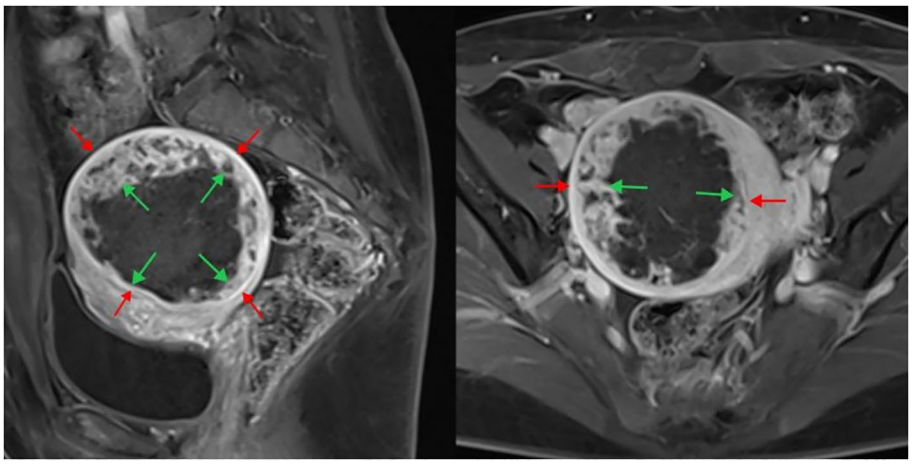

FIGURE 2
Enhanced MRI image after HIFU treatment of uterine fibroids. The sagittal plane is shown on the left, and the cross-section is shown on the right. The inner arrow indicates the size of the non-perfused area, and the outer arrow indicates the fibroid size. HIFU, high-intensity focused ultrasound; MRI, magnetic resonance imaging.

Finally, the time taken for ablation was recorded to calculate the EEF using the following formula:

$$EEF = \frac{\eta \times P \times t}{V} \ (J/mm^3)$$

Where η is the focusing factor (=0.7), P is ultrasound power (W), t is the duration of ultrasound exposure, and V is the non-perfused volume (mm^3) (14).

HIFU ablation is often performed in patients with multiple uterine fibroids; thus, non-target fibroids may partially absorb energy. To obtain accurate EEF data, we only calculated the EEF for single fibroids.

The sonographic features of the uterine fibroids, including position, classification, size, morphology, echogenicity, presence of internal necrotic areas, attenuation bands, and blood flow were recorded. The correlation between these features and the ablation rate, as well as the EEF of HIFU were analyzed.

2.5 Statistical analysis

All data were analyzed using IBM SPSS Statistics for Windows, version 26 (IBM Corp., Armonk, NY, USA). Categorical data are presented as frequencies, whereas continuous data are expressed as means ± standard deviations. Pearson's correlation coefficient was used to assess the correlation between two continuous variables. The values ranged from -1 to +1, with higher values indicating a stronger relationship. Negative values denoted a negative correlation; positive values indicated a positive correlation, and zero values indicated no correlation. The significance level was set at $p < 0.01$.

Homogeneity of variance analysis was conducted to assess the overall distribution consistency for variables with count data and dependent variables with continuous data. If the homogeneity of variance was met, a one-way ANOVA (F-test) was performed to analyze whether the differences were statistically significant, assessing whether different levels of the same influencing factor impacted the dependent variable. If the homogeneity of variance was not met, Tamhane's T2 test was used for multiple comparisons. Differences were considered statistically significant at $p < 0.05$. The results were illustrated through bar graphs and scatter plots with fitted curves for a more intuitive representation.

3 Results

A total of 75 patients with 124 uterine fibroids met the inclusion criteria and were included in the study. Among them, 41 patients had solitary fibroids, and 34 patients (83 fibroids) had multiple fibroids. Their ages ranged from 27 to 52 years, with a mean age of 43.5 ± 4.29 years. The maximum diameter of the fibroids ranged from 20 to 119 mm, with an average of 47.90 ± 19.54 mm.

3.1 Correlation between the sonographic features of uterine fibroids and the HIFU ablation rate

The analysis revealed a significant positive correlation between uterine fibroid volume and ablation rate ($p < 0.01$) (Table 1). Figure 3 illustrates a positive correlation between uterine fibroid volumes and ablation rates.

The ablation rate in hyperechoic fibroids was higher than that in hypoechoic or isoechoic fibroids, and the difference between the two groups was statistically significant ($p < 0.05$) (Table 2, Figure 4). A comparison of HIFU ablation rates between the two groups based on morphology revealed that the elliptical/diffuse leaf-shaped fibroid group had a significantly higher HIFU ablation rate than the round fibroid group ($p < 0.05$) (Table 2, Figure 5).

A comparison of the HIFU ablation rates based on the presence or absence of attenuation bands revealed that the group with attenuation bands had a significantly higher HIFU ablation rate than the group without attenuation bands ($p < 0.05$) (Table 2, Figure 6).

No statistically significant differences were seen in the ablation rates among anterior, lateral and fundal, and posterior wall fibroids ($p > 0.05$) (Table 2). The anterior wall fibroid group had the highest average ablation rate, slightly higher than the average ablation rates of the posterior, lateral, and fundal wall fibroid groups (Figure 7).

No statistically significant differences were seen in the ablation rates among the four different types of fibroids based on the FIGO classification (Table 2, Figure 8). Furthermore, no statistically significant differences were seen in the ablation rates between uterine fibroids without internal necrotic areas and those with necrotic areas ($p > 0.05$) (Table 2, Figure 9).

Analysis of the ablation rates among the four groups with different blood flow signal levels showed no statistically significant differences ($p > 0.05$). However, fibroids with a blood flow grade of 3 exhibited the lowest average ablation rate, significantly lower than those of the other groups (Table 2).

3.2 Correlation between sonographic features of uterine fibroids and the EEF

A significant negative correlation was observed between uterine fibroid volume and the EEF ($p < 0.01$) (Table 3). The scatter plot with a fitted curve also demonstrated an overall negative correlation, indicating that larger uterine fibroid volumes required lower ultrasound energy per unit volume for ablation (Figure 10), indicating a higher ablation efficiency.

Analysis of the EEF between low or equivalent echogenic uterine fibroids and high-echogenicity uterine fibroids revealed a statistically significant difference ($p < 0.05$). Fibroids in the low or equivalent-echogenicity group exhibited a higher EEF than those in the high-echogenicity group (Table 4, Figure 11).

TABLE 1 Results of correlation between fibroid volume and HIFU NPV ratio.

Variable/Ablation rates (%)	Pearson Correlation (r)	P value
Fibroid Volume(mm^3)	0.287	0.001

$p < 0.01$ indicates a significant linear relationship. HIFU, high-intensity focused ultrasound; NPV, non-perfused volume.

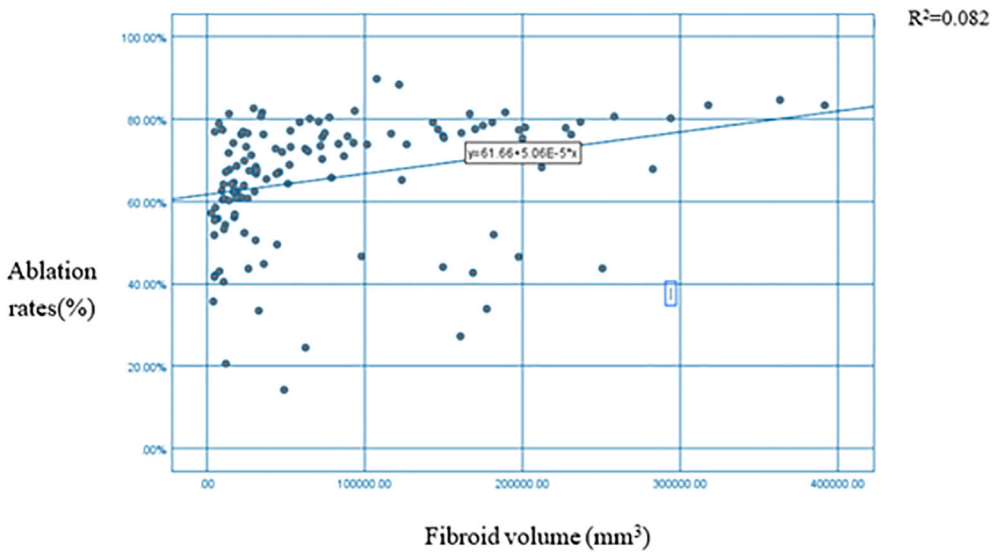

FIGURE 3
Scatter plot + fitting curve of myoma volume and HIFU NPV ratio. HIFU, high-intensity focused ultrasound; NPV, non-perfused volume.

TABLE 2 Correlation analysis between ultrasound features of fibroids and NPV ratio.

Ultrasound features of fibroids		Examples	Mean ablation rate(%)	F value	P value
Echo				4.145	0.044
	Hyperechoic fibroids	65	68.30 ± 14.07		
	Hypo-/isoechoic fibroids	59	62.87 ± 15.63		
Morphology				5.621	0.019
	Round-shaped	93	63.91 ± 15.04		
	Elliptical/diffuse leaf-shaped	31	71.15 ± 13.81		
Attenuation bands				6.296	0.013
	Absence of attenuation bands	63	62.46 ± 15.08		
	Presence of attenuation bands	61	69.09 ± 14.31		
Location				1.128	0.327
	Anterior wall	61	67.78 ± 12.16		
	Lateral and fundal wall	25	63.76 ± 17.76		
	Posterior wall	38	63.71 ± 17.08		
Type				2.379	0.073
	Submucosal	29	66.84 ± 13.90		
	Intramural	9	54.24 ± 16.39		
	Subserosal	41	68.42 ± 12.81		
	Mixed	45	64.83 ± 16.56		
Necrosis internally				0.139	0.710
	Absence of necrosis	118	65.83 ± 14.64		
	Presence of necrosis	6	63.49 ± 23.01		

(Continued)

TABLE 2 Continued

Ultrasound features of fibroids		Examples	Mean ablation rate(%)	F value	P value
Blood flow signal levels				2.510	0.086
	0	14	68.58 ± 15.53		
	1	45	61.78 ± 14.67		
	2	55	69.69 ± 10.97		
	3	10	57.64 ± 26.47		

Differences are statistically significant at p < 0.05. NPV: non-perfused volume.

Multiple comparisons between fibroid types revealed statistically significant differences in EEF between subserosal and submucosal fibroids ($p < 0.05$) and between subserosal and mixed-type fibroids ($p < 0.05$). However, no statistically significant difference was observed between mixed-type and submucosal fibroids (Table 5). Subserosal fibroids exhibited a significantly lower EEF than submucosal and mixed-type fibroids (Figure 12). The EEF for fibroids without internal necrotic areas was lower than in those with internal necrotic areas (Figure 13), and this difference was statistically significant ($p < 0.05$) (Table 4).

No statistically significant difference ($p > 0.05$) was observed in the EEF among the three groups based on fibroid location (Table 4). The average EEF value was lower in the anterior wall fibroid group, followed by the lateral and fundal wall fibroid groups. In contrast, the posterior wall fibroid group showed a relatively higher EEF (Figure 14).

The EEF comparison between the two groups based on the presence or absence of attenuation bands revealed no statistically significant differences ($p > 0.05$). However, the group with attenuation bands exhibited a lower average EEF than those

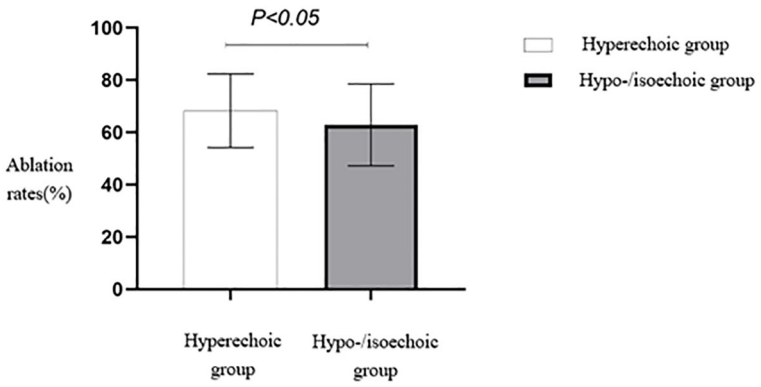

FIGURE 4
Statistical comparison of HIFU ablation rates of fibroids with different echo characteristics. HIFU, high-intensity focused ultrasound.

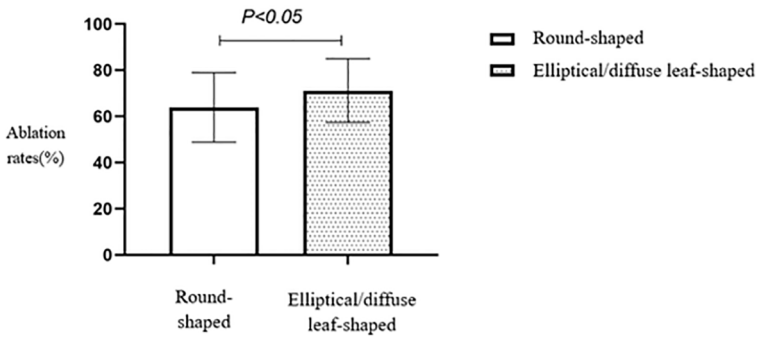

FIGURE 5
Statistical comparison of HIFU ablation rates for fibroids of different shapes. HIFU, high-intensity focused ultrasound.

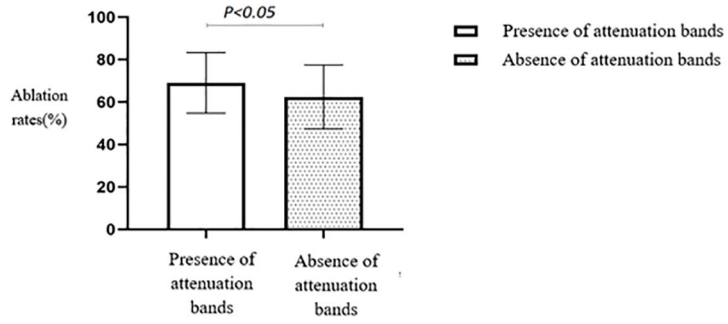

FIGURE 6
Statistical comparison of HIFU ablation rate with or without attenuated fibroids. HIFU, high-intensity focused ultrasound.

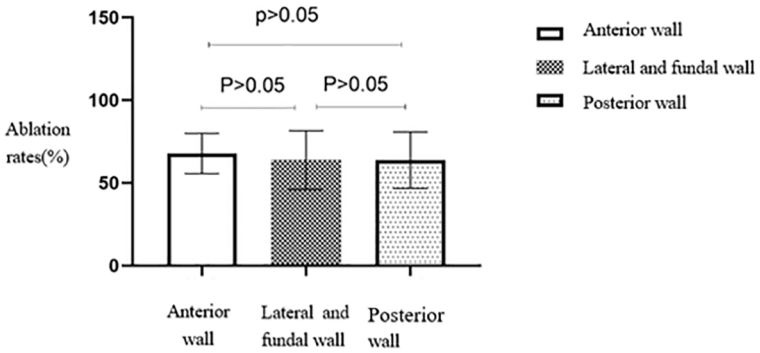

FIGURE 7
Statistical comparison of HIFU ablation rate of uterine fibroids at different locations. HIFU, high-intensity focused ultrasound.

without attenuation bands (Table 4). The EEF comparison between the groups with round and elliptical/diffuse leaf-shaped fibroids showed no statistically significant differences ($p > 0.05$) (Table 4).

The EEF differences among the four groups with different blood flow signal levels were not statistically significant ($p > 0.05$). However, the mean EEF in the group with a blood flow signal level of 3 was notably higher than that in the group with a blood flow signal level of 0 (Table 4).

4 Discussion

The study found a positive correlation between the volume of uterine fibroids and ablation rate and a negative correlation with EEF. This shows that larger fibroids were easier to ablate. *In vitro* experiments indicated that the EEF for ablating a segment of tissue was less than that for ablating linear tissue but more than the EEF for ablating a cubic tissue (15). This may be because larger fibroids

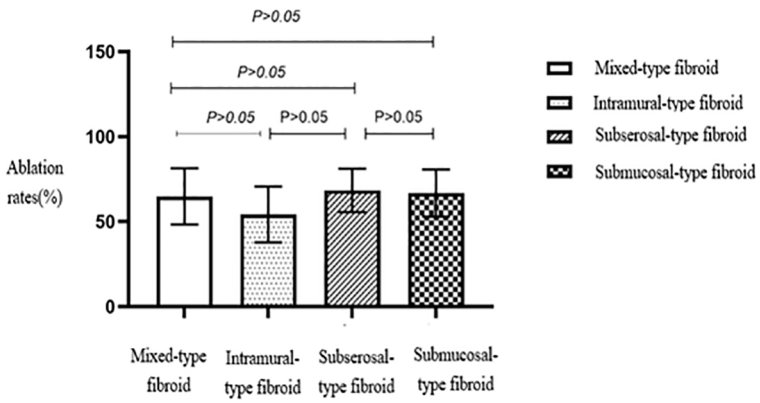

FIGURE 8
Statistical comparison of HIFU ablation rates for different types of uterine fibroids. HIFU, high-intensity focused ultrasound.

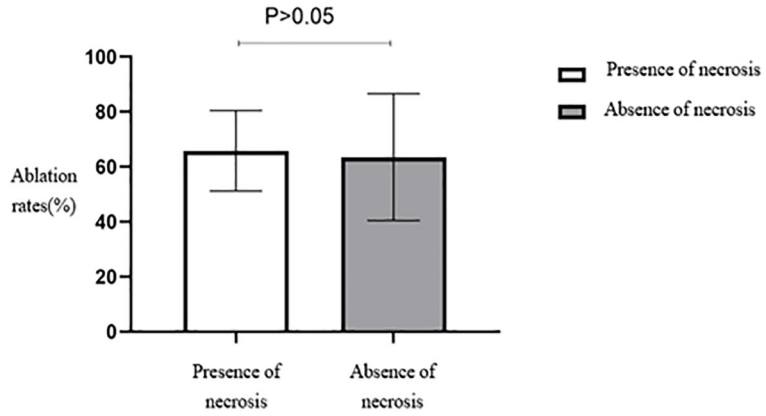

FIGURE 9
Statistical comparison of HIFU ablation rate of uterine fibroids with or without necrotic areas. HIFU, high-intensity focused ultrasound.

occupy a larger acoustic pathway area, allowing more ultrasound energy to be delivered in the same amount of time while preventing cooling of the treatment area. The "damage-damage" interference effect may also explain this phenomenon. The dynamically changing area of necrotic tissue during ablation in the fibroid alters the "acoustic environment." The high temperature reached during ablation changes the tissue properties (16), the destruction of blood vessels in the ablated tissue leads to a poor blood supply, indirectly preventing heat dissipation and thereby enhancing the ablation effect (17).

TABLE 3 Results of correlation analysis between fibroid volume and EEF.

Variable/EEF	Pearson Correlation (p)	P value
Fibroid volume (mm^3)	-0.464	0.002

EEF, energy efficiency factor.

Our study observed higher ablation success in fibroids with greater echogenicity compared to those with lower echogenicity. This echogenicity disparity stems from variations in fibroid composition, such as the smooth muscle cells to fibrous tissue ratio, cellular attributes, and degenerative traits (18). Compared to fibroids with low or moderate echogenicity, those with high echogenicity present a significant difference in acoustic impedance between the components owing to their higher fibrous scaffold content and woven arrangement of smooth muscle cells (19). This results in increased ultrasound interfaces, making it more challenging for the ultrasound beam to penetrate, thus facilitating the deposition of ultrasound energy and consequently achieving better ablation outcomes.

We observed a difference in EEF values between fibroids with and without internal necrotic areas. Fibroids with necrotic areas exhibited

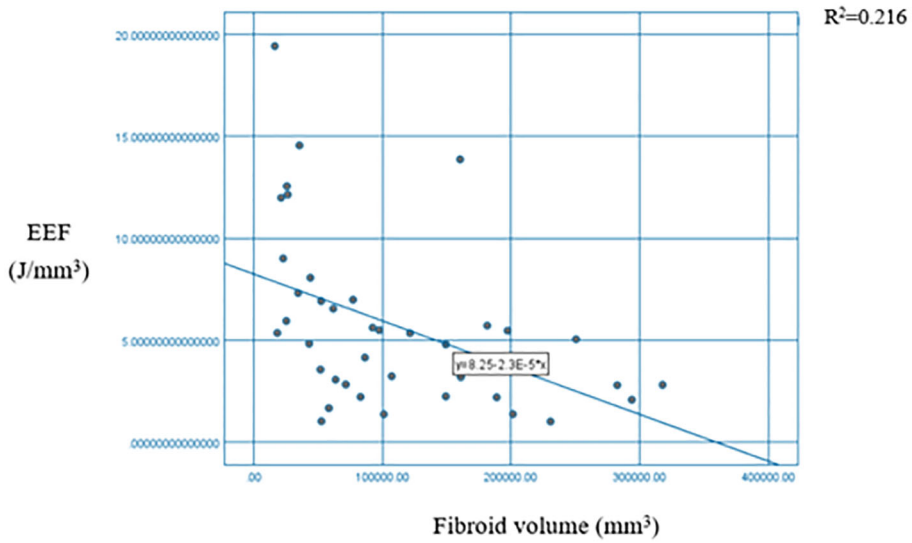

FIGURE 10
Scatter plot + fitting curve of fibroid volume and EEF. EEF, energy efficiency factor.

TABLE 4 Correlation analysis results between different ultrasonic characteristics of uterine fibroids and EEF.

Ultrasound features of fibroids		EEF value (J/mm3)	F value	P value
Echo			5.535	0.024
	Hyperechoic fibroids	7.32 ± 4.11		
	Hypo/isoechoic fibroids	4.58 ± 2.97		
Necrosis internally			5.545	0.024
	Absence of necrosis	5.25 ± 3.80		
	Presence of necrosis	10.81 ± 5.90		
Location			0.350	0.705
	Anterior wall	4.02 ± 3.31		
	Lateral and fundal wall	4.26 ± 3.04		
	Posterior wall	4.60 ± 3.53		
Attenuation bands			0.769	0.386
	Absence of attenuation bands	6.45 ± 3.75		
	Presence of attenuation bands	5.25 ± 4.36		
Morphology			0.000	0.987
	Round-shaped	5.66 ± 3.99		
	Elliptical/diffuse leaf-shaped	5.64 ± 4.71		
Blood flow signal levels			0.463	0.711
	0	3.99 ± 0.80		
	1	5.83 ± 4.07		
	2	5.50 ± 4.34		
	3	7.64 ± 5.00		

Differences are statistically significant at $p < 0.05$. EEF, energy efficiency factor.

higher EEF, suggesting that they may be more resistant to ablation. Increased free water content in fibroids undergoing degenerative necrosis facilitates ultrasound penetration but impedes energy disposition, affecting ablation outcomes. Additionally, a study revealed that tissues with a higher water content exhibited better thermal conductivity (20). Consequently, ultrasound energy deposition becomes more challenging, making ablation more difficult. Although no significant difference in ablation rates was found, prolonged procedure time and increased ultrasound dose may compensate for the resistance in fibroids without necrotic areas.

We noted a significant difference in ablation rates between fibroid groups exhibiting elliptical/diffuse leaf-shaped morphology

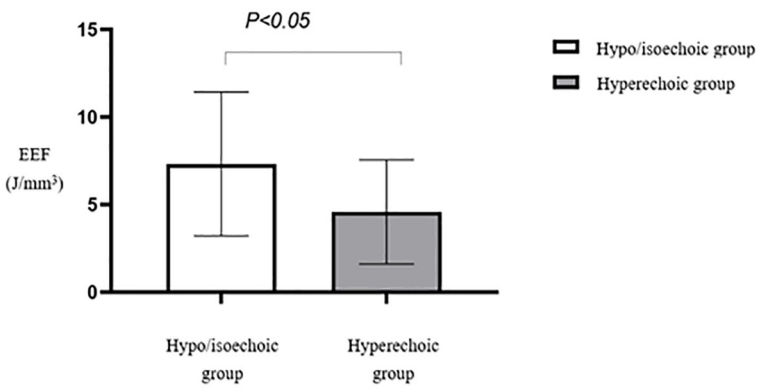

FIGURE 11
Statistical comparison of EEF of uterine fibroids with different echoes. EEF, energy efficiency factor.

TABLE 5 Multiple comparisons of EEF of different types of uterine fibroids.

Types of uterine fibroids/EEF	Subserosal fibroid	Mixed-type fibroid	Submucosal fibroid
EEF	3.93 ± 2.27	8.06 ± 5.68*	7.83 ± 5.04*

*Indicates a statistically significant difference compared to subserosal fibroids ($p < 0.05$).
EEF, energy efficiency factor.

and those with round morphology. The irregular elliptical/diffuse leaf-shaped fibroids displayed a higher ablation rate, possibly due to their larger size and intricate fibrous structure hindering ultrasound penetration. Consequently, ultrasound energy deposition was more effective, enhancing ablation efficacy. While the EEF did not significantly vary between different morphologies, the elliptical/diffuse leaf-shaped group exhibited a lower average EEF compared to the circular fibroid group, implying a higher susceptibility to ablation for fibroids with irregular shapes.

The presence of an attenuation band positively impacted ablation rates, attributed to the vortex-like structures, increased fibrous content, and denser smooth muscle cell arrangement associated with such fibroids. This led to enhanced ultrasound interface echo, facilitating energy deposition and subsequently higher ablation rates. Despite no statistically significant difference in EEF between groups with and without an attenuation band, the correlation between fibroid size, morphology, and ablation efficacy suggests that larger fibroids with irregular shapes or more attenuation bands are more amenable to HIFU treatment. Increasing sample size and employing controlled variable methods can provide more accurate insights into these relationships.

We observed no significant variation in HIFU ablation rates across different types of uterine fibroids, including submucosal, intramural, subserosal, and mixed-type fibroids. Clinicians tend to prolong the procedure time for a more thorough treatment of relatively resistant fibroids, thereby minimizing ablation rate differences. However, we noted a statistically significant difference in EEF between the subserosal fibroid group and the submucosal/mixed-type fibroid group. The subserosal fibroid group exhibited a notably lower average EEF, possibly due to their farther location from the endometrium and reduced amount of surrounding uterine tissue. This finding corresponds with Cheng Hailing's observations

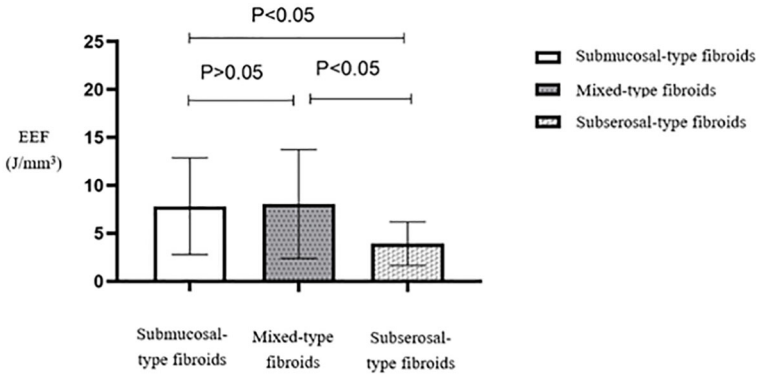

FIGURE 12
Statistical comparison of EEF of different types of uterine fibroids. EEF, energy efficiency factor.

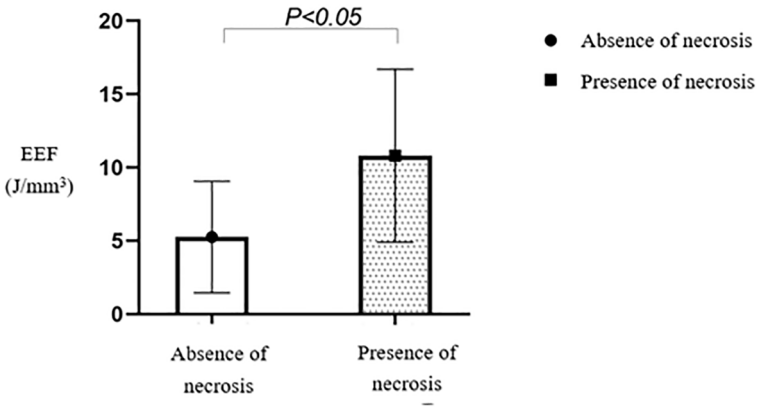

FIGURE 13
Statistical comparison of EEF in fibroids with or without necrotic areas. EEF, energy efficiency factor.

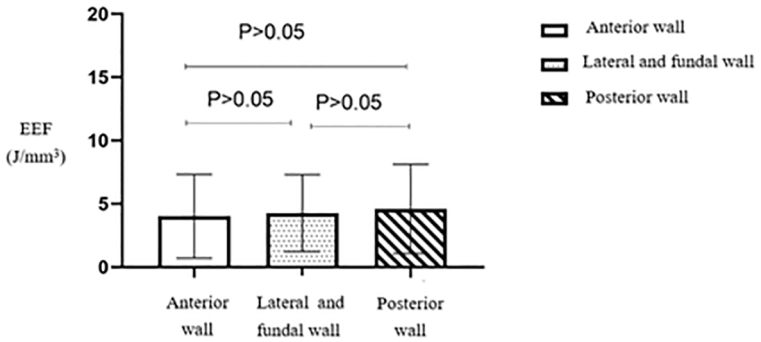

FIGURE 14
Statistical comparison of EEF of uterine fibroids at different locations. EEF, energy efficiency factor.

(21) regarding the relationship between various MRI characteristics of uterine fibroids and HIFU efficacy.

In our study, anterior wall fibroids exhibited the highest ablation rates compared to posterior and lateral/fundal wall fibroids. This may be explained by minimal ultrasound attenuation as anterior wall fibroids are situated farther from the intestines and sacrum. Conversely, posterior wall fibroids are located near the sacrum and surrounded by abundant nerves and connective tissue, with severe ultrasound attenuation, making ablation more challenging (22, 23). However, this finding lacked statistical significance. It's worth noting that certain studies have reported significantly higher ablation rates for anterior wall fibroids compared to lateral and posterior wall fibroids. These differences could stem from factors not accounted for, such as patient body mass index, subcutaneous fat thickness, body shape, and position, or limited sample size.

We found no significant correlation between ablation rates and the EEF in fibroids with different levels of blood flow. Some researchers suggest that fibroids with abundant blood flow may respond less to HIFU due to energy dispersion (22). Moreover, fibroids with more blood vessels are easier for ultrasound to penetrate, making energy deposition challenging. However, in our study, ablation efficacy did not notably vary based on blood flow conditions, likely due to the consistent use of oxytocin in all HIFU treatments. Oxytocin induces sensitive fibroid contraction, reduces perfusion, and mitigates blood flow's impact during treatment (24). Nonetheless, our study's limited sample size may have influenced these results, emphasizing the need for a larger sample size and controlled variables for more accurate future research.

This study has limitations as a retrospective analysis, where confounding factors like patient weight, subcutaneous fat thickness, and body shape may have impacted outcomes differently. Furthermore, variations in treatment efficacy could arise from HIFU procedures being performed by different physicians.

5 Conclusion

A higher HIFU ablation rate is associated with fibroids with larger volume, hyperechoic appearance, elliptical/diffuse leaf-shaped, and the presence of a posterior attenuation zone. A higher HIFU ablation efficiency is associated with fibroids with larger volume, hyperechoic appearance, subserosal location, and absence of internal necrotic areas. This study confirms that ultrasound imaging characteristics associated with uterine fibroids can predict the ablation rate and efficiency of HIFU treatment. It provides essential guidance for clinically assessing and selecting suitable cases for HIFU therapy, further assisting in the judicious selection of energy levels for treatment. Future research should explore the correlation between the ablation efficacy among different fibroid types and their origin from distinct clone cells. Furthermore, a large-scale multicenter prospective study with a standardized protocol and a larger sample size is warranted to confirm these findings.

Data availability statement

The original contributions presented in the study are included in the article/supplementary material. Further inquiries can be directed to the corresponding author.

Ethics statement

The studies involving humans were approved by Ethics Committee of Fujian Provincial Hospital (Approval No: K2021-04-038). The studies were conducted in accordance with the local legislation and institutional requirements. The participants provided their written informed consent to participate in this study. Written informed consent was obtained from the individual(s) for the publication of any potentially identifiable images or data included in this article.

Author contributions

HX: Conceptualization, Data curation, Writing – original draft. SW: Data curation, Writing – review & editing. KX: Visualization, Writing – review & editing. GD: Supervision, Writing – review &

editing. SC: Conceptualization, Funding acquisition, Project administration, Supervision, Writing – review & editing.

Funding

The author(s) declare financial support was received for the research, authorship, and/or publication of this article. This research was funded by the Fujian Provincial Natural Science Foundation (Grant No: 2021J01370).

Acknowledgments

Thanks to Li Li for his contributions to edit this article's format.

Conflict of interest

The authors declare that the research was conducted in the absence of any commercial or financial relationships that could be construed as a potential conflict of interest.

Publisher's note

All claims expressed in this article are solely those of the authors and do not necessarily represent those of their affiliated organizations, or those of the publisher, the editors and the reviewers. Any product that may be evaluated in this article, or claim that may be made by its manufacturer, is not guaranteed or endorsed by the publisher.

References

1. Yang Q, Ciebiera M, Bariani MV, Ali M, Elkafas H, Boyer TG, et al. Comprehensive review of uterine fibroids: developmental origin, pathogenesis, and treatment. *Endocrine Rev*. (2022) 43:678–719. doi: 10.1210/endrev/bnab039

2. Kwas K, Nowakowska A, Fornalczyk A, Krzycka M, Nowak A, Wilczyński J, et al. Impact of contraception on uterine fibroids. *Medicina*. (2021) 57:717. doi: 10.3390/medicina57070717

3. Talaulikar VS. Medical therapy for fibroids: an overview. *Best Pract Res Clin Obstet Gynaecol*. (2018) 46:48–56. doi: 10.1016/j.bpobgyn.2017.09.007

4. Cabras P, Auloge P, Bing F, Rao PP, Hoarau S, Dumont E, et al. A new versatile MR-guided high-intensity focused ultrasound (HIFU) device for the treatment of musculoskeletal tumors. *Sci Rep*. (2022) 12:9095. doi: 10.1038/s41598-022-13213-1

5. Lee JY, Chung HH, Kang SY, Park EJ, Park DH, Son K, et al. Portable ultrasound-guided high-intensity focused ultrasound with functions for safe and rapid ablation: prospective clinical trial for uterine fibroids-short-term and long-term results. *Eur Radiol*. (2020) 30:1554–63. doi: 10.1007/s00330-019-06468-2

6. Jeng CJ, Ou KY, Long CY, Chuang L, Ker CR. 500 cases of high-intensity focused ultrasound (HIFU) ablated uterine fibroids and adenomyosis. *Taiwan J Obstet Gynecol*. (2020) 59:865–71. doi: 10.1016/j.tjog.2020.09.013

7. Liu L, Wang T, Lei B. High-intensity focused ultrasound (HIFU) ablation versus surgical interventions for the treatment of symptomatic uterine fibroids: a meta-analysis. *Eur Radiol*. (2022) 32:1195–204. doi: 10.1007/s00330-021-08156-6

8. Liao D, Xiao Z, Lv F, Chen J, Qiu L. Non-contrast enhanced MRI for assessment of uterine fibroids' early response to ultrasound-guided high-intensity focused ultrasound thermal ablation. *Eur J Radiol*. (2020) 122:108670. doi: 10.1016/j.ejrad.2019.108670

9. Wenjing Y, Yunqing B. The advantages of focused ultrasound ablation for uterine fibroids and the use of MRI in management. *Int J Front Med*. (2023) 5(9):122–8. doi: 10.25236/IJFM.2023.050920

10. Sainio T, Saunavaara J, Komar G, Mattila S, Otonkoski S, Joronen K, et al. Feasibility of apparent diffusion coefficient in predicting the technical outcome of MR-guided high-intensity focused ultrasound treatment of uterine fibroids - a comparison with the Funaki classification. *Int J HYPERTHERmia*. (2021) 38:85–94. doi: 10.1080/02656736.2021.1874545

11. Figo Committee on Gynecologic Oncology. FIGO staging for uterine sarcomas. *Int J Gynecol Obstet*. (2009) 104:179. doi: 10.1016/j.ijgo.2008.12.009

12. Orsini LF, Salardi S, Pilu G, Bovicelli L, Cacciari E. Pelvic organs in premenarcheal girls: real-time ultrasonography. *Radiology*. (1984) 153:113–6. doi: 10.1148/radiology.153.1.6473771

13. Adler DD, Carson PL, Rubin JM, Quinn-Reid D. Doppler ultrasound color flow imaging in the study of breast cancer: preliminary findings. *Ultrasound Med Biol*. (1990) 16:553–9. doi: 10.1016/0301-5629(90)90020-D

14. Li F, Wang Z, Du Y, Ma P, Bai J, Wu F, et al. Study on therapeutic dosimetry of HIFU ablation tissue. *Sheng Wu Yi Xue Gong Cheng Xue Za Zhi*. (2006) 23:839–43.

15. Wang Y, Geng J, Bao H, Dong J, Shi J, Xi Q, et al. Comparative effectiveness and safety of high-intensity focused ultrasound for uterine fibroids: A systematic review and meta-analysis. *Front Oncol*. (2021) 11:600800. doi: 10.3389/fonc.2021.600800

16. Liu X, Mohamed A. Temperature control of the focal point of focused ultrasound excitation using neural network approach. In: *2021 IEEE UFFC Latin America Ultrasonics Symposium (LAUS)*. IEEE (2021). p. 1–4.

17. deSouza NM, Gedroyc W, Rivens I, Haar GT. Tissue specific considerations in implementing high intensity focussed ultrasound under magnetic resonance imaging guidance. *Front Oncol*. (2022) 12:1037959. doi: 10.3389/fonc.2022.1037959

18. Cabezas N, López-Picazo A, Diaz P, Valero B, Rodriguez MJ, Redondo A, et al. How frequently benign uterine myomas appear suspicious for sarcoma as assessed by transvaginal ultrasound? *Diagnostics (Basel)*. (2023) 13:501. doi: 10.3390/diagnostics13030501

19. Wong CM, Chan SF, Wu WC, Suen CH, Yau HM, Wang DY, et al. Tunable high acoustic impedance alumina epoxy composite matching for high frequency ultrasound transducer. *Ultrasonics*. (2021) 116:106506. doi: 10.1016/j.ultras.2021.106506

20. Huang H, Ran J, Xiao Z, Ou L, Li X, Xu J, et al. Reasons for different therapeutic effects of high-intensity focused ultrasound ablation on excised uterine fibroids with different signal intensities on T2-weighted MRI: a study of histopathological characteristics. *Int J Hyperthermia*. (2019) 36:477–84. doi: 10.1080/02656736.2019.1592242

21. Cheng H, Wang C, Tian J. Correlation between uterine fibroids with various magnetic resonance imaging features and therapeutic effects of high-intensity focused ultrasound ablation. *Pak J Med Sci*. (2015) 31:869–73. doi: 10.12669/pjms.314.7294

22. Gong C, Lin Z, Lv F, Zhang L, Wang Z. Magnetic resonance imaging parameters in predicting the ablative efficiency of high-intensity focused ultrasound for uterine fibroids. *Int J Hyperthermia*. (2021) 38:523–31. doi: 10.1080/02656736.2021.1904152

23. Liu Y, Liu Y, Lv F, Zhong Y, Xiao Z, Furong Lv. Factors influencing magnetic resonance imaging finding of endopelvic fascial edema after ultrasound-guided high-intensity focused ultrasound ablation of uterine fibroids. *Int J Hyperthermia*. (2022) 39:1088–96. doi: 10.1080/02656736.2022.2112306

24. Otonkoski S, Sainio T, Komar G, Suomi V, Saunavaara J, Sequeiros RB, et al. Oxytocin selectively reduces blood flow in uterine fibroids without an effect on myometrial blood flow: a dynamic contrast enhanced MRI evaluation. *Int J Hyperthermia*. (2020) 37:1293–300. doi: 10.1080/02656736.2020.1846792

frontiers | Frontiers in Medicine

TYPE Case Report
PUBLISHED 26 September 2024
DOI 10.3389/fmed.2024.1457611

OPEN ACCESS

EDITED BY
Andrea Tinelli,
Veris Delli Ponti Hospital, Italy

REVIEWED BY
Diana Buzinskiene,
Vilnius University, Lithuania
Yosuke Ono,
Teine Keijinkai Hospital, Japan
Silvia Vannuccini,
University of Florence, Italy

*CORRESPONDENCE
Toshifumi Takahashi
✉ totakaha@fmu.ac.jp

RECEIVED 01 July 2024
ACCEPTED 11 September 2024
PUBLISHED 26 September 2024

CITATION
Ota Y, Ota K, Takahashi T, Horikawa N, Kuroda R, Okamoto H, Tanaka Y, Kusumoto T, Oda T, Matsuyama T, Miyake T, Honda T and Shimoya K (2024) Case Report: The first case of successful pregnancy and live birth following laparoscopic resection of adenomyosis under real-time intraoperative ultrasound elastography guidance. *Front. Med.* 11:1457611.
doi: 10.3389/fmed.2024.1457611

Case Report: The first case of successful pregnancy and live birth following laparoscopic resection of adenomyosis under real-time intraoperative ultrasound elastography guidance

Yoshiaki Ota[1], Kuniaki Ota[1,2], Toshifumi Takahashi[2]*, Naoki Horikawa[3], Ryosuke Kuroda[3], Hana Okamoto[1], Yu Tanaka[3], Tomoyuki Kusumoto[3], Takashi Oda[4], Takehiko Matsuyama[5], Takahito Miyake[4], Tetsuro Honda[3] and Koichiro Shimoya[1]

[1]Department of Gynecologic Oncology, Kawasaki Medical School, Okayama, Japan, [2]Fukushima Medical Center for Children and Women, Fukushima Medical University, Fukushima, Japan, [3]Department of Obstetrics and Gynecology, Kurashiki Chuo Hospital, Okayama, Japan, [4]Department of Obstetrics and Gynecology, Miyake Clinic, Okayama, Japan, [5]Department of Obstetrics and Gynecology, Koujin Hospital, Kagawa, Japan

Objective: Adenomyosis-related infertility is increasingly being diagnosed, and surgical intervention has been suggested to improve fertility. Elastography, a noninvasive ultrasound technique, is promising for diagnosing and guiding the resection of adenomyosis. This report presents the first case of successful delivery after twin pregnancies achieved with IVF following intraoperative elastography-guided laparoscopic adenomyomectomy.

Case report: A 35-year-old Japanese woman with uterine adenomyosis received a gonadotropin analog before surgery. Preoperative MRI revealed a 5.0 × 7.0 cm adenomyoma, leading to scheduled laparoscopic adenomyomectomy with intraoperative elastography. During surgery, elastography ensured the complete resection of the adenomyotic tissue while preserving the endometrium. Postoperative MRI confirmed the absence of residual adenomyosis. The patient underwent *in vitro* fertilization and embryo transfer, leading to a successful twin pregnancy after double blastocyst transfer. Despite a stable perinatal course, she required hospitalization to prevent preterm labor. At 32 weeks, an elective cesarean section delivered healthy twins. The intra- and post-operation was uncomplicated, and the patient and infants had an optimal health.

Conclusion: This is the first reported case of a twin pregnancy resulting from vitrified-warmed embryo transfer after elastography-guided laparoscopic adenomyomectomy, culminating in a successful delivery via cesarean section. This technique allows precise resection and mitigates the risks of uterine rupture and placenta accreta spectrum disorders. Although promising, further studies are required to validate the safety and efficacy of this innovative surgical approach.

KEYWORDS
adenomyosis, infertility, laparoscopic adenomyomectomy, intraoperative elastography, uterine rupture, embryo transfer, placenta accreta spectrum, twin pregnancy

1 Introduction

Patients with infertility are increasingly diagnosed with adenomyosis (1, 2). The mechanisms of infertility in patients with adenomyosis include intrauterine abnormalities such as adenomyomas, which May obstruct the tubes and distort the uterine cavity (2, 3). However, emerging evidence suggests that surgical intervention improves fertility (4–8). Focal adenomyosis refers to localized adenomyotic lesions or nodules, while diffuse adenomyosis involves more widespread involvement of the myometrium (8, 9). Hysterosalpingography studies have shown uterine cavity distortion in 78% of patients with diffuse adenomyosis compared to 54% with focal adenomyosis (10). Therefore, diffuse adenomyosis uteri requires aggressive infertility treatment such as the surgical intervention because the impact on fertility May differ, with diffuse adenomyosis potentially having more widespread effects on uterine function. Concretely, diffuse adenomyosis uteri tends to be treated with laparotomy or laparoscopy because the adenomyotic lesion cannot be directly palpated (11, 12). Laparoscopic adenomyomectomy is associated with the risk of too little or extensive resection since the boundary between the adenomyoma and myometrium was ill-defined, resulting in upregulating recurrence rates of adenomyosis or the rate of uterine rupture depending on the extent of excision (13, 14).

Elastography, a medical imaging procedure that is capable of measuring tissue mechanical properties and elasticity, is expected to be a noninvasive diagnostic ultrasound for uterine adenomyosis (15). A recent meta-analysis found that elastography had high sensitivity and specificity for adenomyosis diagnosis, and its findings correlated with histopathological results (16). In 2020, we developed a surgical technique that allows complete resection of adenomyotic lesions using intraoperative elastography (17). To date, only a few have reported that laparoscopic excision of an adenomyotic lesion using intraoperative ultrasound elastography is a feasible technique to completely resect adenomyotic lesions (17–19).

We report the first case of successful twin delivery after two vitrified-warmed embryo transfers and intraoperative elastography-guided laparoscopic adenomyomectomy. Two neonates were delivered by elective cesarean section at 32 weeks following perinatal management.

2 Case presentation

A 35-year-old nulliparous Japanese woman had no past medical history or family history, had suffered from dysmenorrhea for several years, and was diagnosed with transvaginal ultrasound as having uterine adenomyosis at the previous gynecology outpatient clinic. She received gonadotropin analog agonist (leuprorelin acetate®, 1.88 mg, ASUKA Pharmaceutical Co., Ltd) for 6 months and following continuously taking dienogest (Dinagest tab®, 2 mg/day Mochida Pharmaceutical Co., Ltd.) with the same protocol (20). The medications were discontinued after the patient decided to conceive. After that, she underwent the program for *in vitro* fertilization (IVF) and intracytoplasmic sperm injection (ICSI) because she did not conceive after three ovulation induction cycles combined with intrauterine insemination. After adequate hormonal stimulation of ovarian follicles, she had transvaginal oocyte retrieval of 6 mature oocytes and underwent conventional IVF or ICSI resulting in preserving 4 high-quality frozen blastocysts as evaluated using Gardner's classification (21). She underwent three times of vitrified-warmed blastocyst transfers using hormone replacement therapy as previously described (22), and all transfers failed unfortunately. Therefore, the reproductive medicine specialist advised her to treat adenomyosis as the causal factor of implantation failure, she visited our department for uterine adenomyosis surgery. Thereafter, the reproductive medicine specialist and we discussed the therapeutic strategy, and she decided to undergo laparoscopic adenomyomectomy with intraoperative elastography initially, and subsequently retrieve oocytes in the IVF program to transfer embryos following completely healing the myometrial wounded after the enucleation.

Preoperative T2-weighted magnetic resonance imaging (MRI) mainly showed diffuse thickening of the junctional zone in the posterior wall, leading to the diagnosis of a 5.0 × 7.0 cm intramural solid adenomyoma (Figures 1A,B). Therefore, we scheduled a laparoscopic adenomyomectomy with intraoperative elastography for a more accurate resection. This technique has been previously described (17, 18). Briefly, the intraoperative course of this case combined with this surgical technique was described below. Laparoscopy revealed a 12-week gestation-sized enlarged uterus with obliteration of the pouch of Douglas due to endometriosis; adhesions were promptly dissected. Vasopressin (1 IU/70 mL normal saline) was injected into the uterine wall to minimize bleeding (Figure 2A). A no. Eleven scalpel was introduced into the abdomen after removing the trocar, and a longitudinal incision was made over the uterine fundus (Figure 2B). Adenomyotic lesions in the posterior uterine wall were meticulously excised. After initial enucleation, a laparoscopic ultrasound probe was used to detect any remaining tissue. A posterior 1–2 cm transverse colpotomy was performed in the midline of the posterior fornix, marked with a Vagi-Pipe® (Hakko Medical, Nagano, Japan). An ultrasound probe (ARIETTA 850, Hitachi, Ltd., Tokyo, Japan) inserted through the colpotomy identified the residual adenomyosis as bright blue areas (Figure 2C). Tissues were resected using scissor forceps (Figure 2D). Subsequent real-time elastography confirmed the complete removal of the adenomyosis, preserving the endometrium (Figure 2E). The resected specimens were extracted via colpotomy. The uterine incisions were repaired in multiple layers using barbed sutures (0 Stratafix® Symmetric PDS® Plus, Ethicon Endo-Surgery, Tokyo, Japan) (Figure 2F). After myometrium reapproximation and hemostasis, an adhesion barrier (Interseed®, Ethicon Endo-Surgery, Tokyo, Japan) was placed. The surgery was completed without complications and lasted 188 min, with an estimated blood loss of 100 mL (Supplementary Video S1). The

FIGURE 1
The preoperative T2-weighted magnetic resonance imaging (MRI). **(A)** Sagittal T2-weighted preoperative pelvic MRI showed diffuse adenomyosis with thickening of the junctional zone in the posterior wall and severe adhesion on the pouch of Douglas. **(B)** Axial T2-weighted postoperative pelvic MRI showed intramural solid adenomyosis.

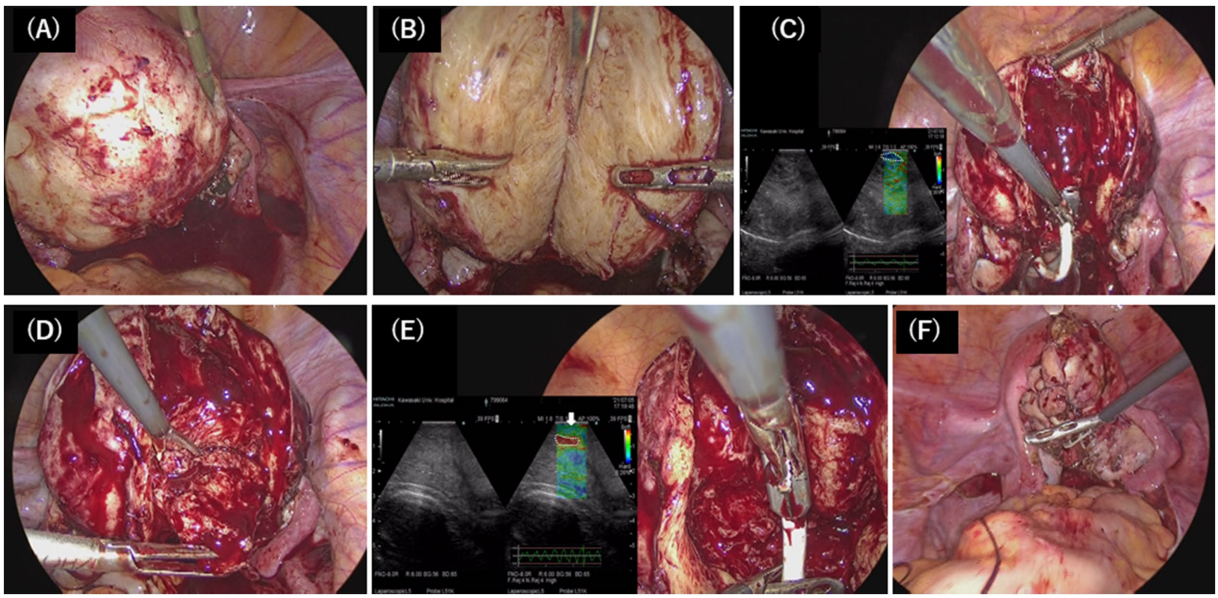

FIGURE 2
Surgical technique of laparoscopic adenomyomectomy. **(A)** Vasopressin was injected into the uterine wall. **(B)** The uterus was longitudinally incised with the scalpel to directly access the adenomyotic tissue, and the nucleation was resected in a wide wedge shape. **(C)** The probe of the elastography was applied on the dissected uterine wall to detect the residual adenomyotic tissue, indicated by the bright blue areas (white-dotted circle). **(D)** The residual adenomyotic tissues were resected by scissors forceps. **(E)** After complete resection, the bright blue areas were changed to bright green areas, which indicated the normal layer of the myometrium (white arrow), and the endometrium was indicated by the bright red areas (white dotted circle). **(F)** The uterine incisions were repaired in multiple layers using barbed sutures.

resected lesion weighed 102.5 grams. The patient's postoperative recovery was uneventful. A 12-week postoperative MRI showed sufficient myometrial thickness and no residual adenomyotic lesions in the resected area (Figures 3A,B).

Five months after surgery, she began an *in vitro* fertilization and embryo transfer (IVF-ET) program and successfully preserved multiple high-quality frozen blastocysts as evaluated using Gardner's classification (21). She underwent vitrified-warmed blastocyst transfer using hormone replacement therapy with same protocol of hormone replacement therapy (22). After three failed attempts with single blastocyst transfers, she consented to a double blastocyst transfer due to recurrent implantation failures, was informed of the risks, such as placenta accreta spectrum (PAS) and uterine rupture, and obtained permission for maternal–fetal invasive care unit (MFICU) monitoring. At 5 weeks, transvaginal ultrasonography revealed a dichorionic diamniotic twin pregnancy, with gestational

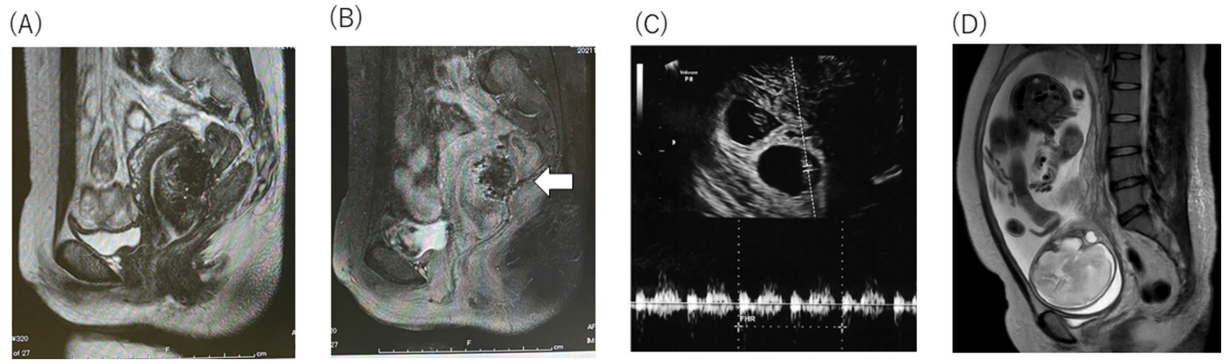

FIGURE 3
The preoperative T2-weighted magnetic resonance imaging (MRI). **(A)** Sagittal T2-weighted postoperative pelvic MRI showed o adenomyotic lesion and the complete resection macro-imagingly. **(B)** Sagittal T2-weighted postoperative contrast-enhanced pelvic MRI showed incomplete blood flow in the posterior wall of the uterine (white arrow), and the normal repair process of the myometrium. **(C)** Two embryos with heartbeats at 8 weeks 0 day were observed with M-mode (white dotted line) **(D)** T2-weighted MRI revealed that the uterine wall remained circumferentially thick.

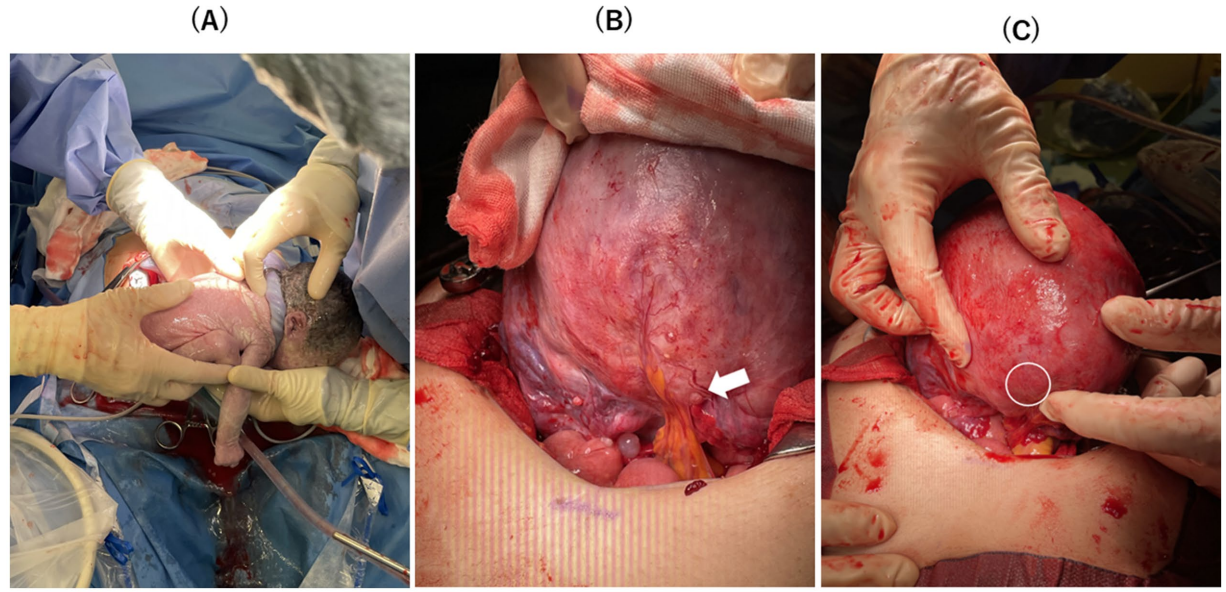

FIGURE 4
(A) Healthy neonates were delivered. **(B)** There was one adhesion between the lower margin of the posterior uterine wall wound and mesenteric fat at the pouch of Douglas (white arrow). **(C)** The thumb-sized thin myometrium on the posterior wall was slightly confirmed (white circle), although there was no sign of uterine rupture.

sacs measuring 9.4 and 8.3 mm. By 8 weeks, the crown-rump lengths were 15.7 mm and 13.8 mm, with detectable fetal heartbeats (Figure 3C). Despite a stable perinatal course at 26 weeks, she was admitted for magnesium sulfate infusion to prevent preterm labor due to a short cervical canal (5 mm) with funneling membranes and uterine contractions. This treatment was effective and no further preterm labor was observed. At 27 weeks, MRI showed no placenta accreta or significant thinning of the muscle layer because the placenta was on the anterior wall (Figure 3D). An elective cesarean section was scheduled at 32 weeks to prevent uterine rupture, and betamethasone (12 mg every 24 h, 2 doses) was preoperatively treated to promote the maturity of the fetal lung. The procedure at 32 weeks and 0 days resulted in the delivery of healthy twins: one weighing 1,650 g with Apgar scores of 8 (1 min)/ 9 (5 min) and 7.346 of umbilical artery pH, and the other weighing 1,466 g with Apgar scores of 4 (1 min)/ 7 (5 min) and 7.244 of umbilical artery pH (Figure 4A). There were postnatal abnormalities such as respiratory distress syndrome or intraventricular hemorrhage in both neonates. The placenta was removed manually without complications. Upon exteriorizing the uterus for myometrial suturing, adhesions to the posterior uterine wall and a thin myometrium were confirmed (Figures 4B,C). The operation lasted 87 min, with an estimated blood loss of 2,164 mL. The patient recovered without complications and was discharged on postoperative day five. The infants were discharged on day 28 in excellent condition, requiring no oxygen or feeding tubes.

3 Discussion

Here, we reported the first case of a twin pregnancy conceived through vitrified-warmed embryo transfer after intraoperative elastography-guided laparoscopic adenomyomectomy, resulting in the delivery of two neonates by elective cesarean section at 32 weeks with careful perinatal management. Despite the high risk of uterine rupture and PAS after adenomyomectomy, this novel fertility-sparing technique using intraoperative elastography enabled successful live births.

The prevalence of uterine rupture during pregnancy following adenomyomectomy is reported to be 2.8–12.5% (23–25). The risk of uterine rupture in twin pregnancies after laparoscopic adenomyomectomy is unknown, with only three reported cases (26–28). The first case reported that spontaneous uterine rupture at 30 weeks of gestation occurred after a monochorionic twin pregnancy following IVF-ET 12 months post-surgery (26). The second case reported successful delivery at 31 weeks of gestation with an elective cesarean section for a monochorionic twin pregnancy 30 months after IVF-ET (27). The third case reported that the uterine was already ruptured and two babies expired before the patient was emergently transferred to the hospital at 30 weeks of gestation (28). In particular, Kweon et al. reported a case–control study of five cases of twins after adenomyomectomy, all of which resulted in emergency cesarean section due to preterm delivery, but the most successful pregnancy course was at 33 weeks of gestation, and the earliest stage was at 28 weeks of gestation (28). To our best knowledge, there have been no cases of successful planned delivery after 34 weeks of gestation in twins after adenomyomectomy. Hence, we consulted with pediatricians in MFICU to decide on plan delivery at least at 32 weeks of gestation, with mature fetal lungs by predelivery betamethasone, thus avoiding prematurity and related complications of perinatal morbidity and mortality. Consequently, live birth was achieved at 32 weeks without uterine rupture, despite a slight myometrial defect undetected by perinatal ultrasound.

Several reports have been published regarding the prevention and prediction of uterine rupture after adenomyosis enucleation. Some studies recommend using a cold scalpel instead of electrocautery during uterine incision to prevent rupture (29–31). Additionally, electrosurgery and multilayered myometrial closures should be avoided because they May predispose the wound to rupture owing to poor healing characteristics (30, 32). Otsubo et al. examined uterine wall thickness in patients undergoing abdominal adenomyomectomy for diffuse adenomyosis and found that a uterine wall thickness of less than 7 mm increased the risk of uterine rupture (33). Kwak et al. recommended regular monitoring of uterine contractions and wall thickness to prevent rupture (27). In this case, postoperative and prenatal MRIs confirmed myometrial preservation, and the patient successfully delivered at 32 weeks without rupture; however, we attributed our success to our adherence to previously reported methods of preventing uterine rupture.

Patients with a history of uterine surgery, including adenomyomectomy, have a higher likelihood of preterm delivery. After undergoing adenomyomectomy, patients have shorter cervical lengths upon admission and a significantly higher rate of cervical length shortening (34). Extensive myometrial removal, particularly from the caudal uterus, May have contributed to this issue. Kwak et al. performed an elective cesarean section at 31 weeks in a twin pregnancy after laparoscopic adenomyomectomy for cervical shortening (27). Given these risks, we recommend scheduling an elective cesarean section at an appropriate time in consultation with a pediatrician and the MFICU rather than waiting until term, although the exact mechanism of uterine contraction and cervical shortening post-adenomyomectomy remains unclear.

Another serious pregnancy complication after adenomyomectomy is PAS, which can lead to uterine rupture. Recently, Sayama et al. conducted a retrospective study to evaluate the impact of adenomyomectomy on pregnancy outcomes in women with adenomyosis. The results revealed that while adenomyomectomy reduced the incidence of complications such as preterm prelabor rupture of membranes, preeclampsia, and small-for-gestational-age infants, it also increased the risk of PAS (35). Embryo implants at the myometrial incision site can cause PAS and rupture during pregnancy. Sumigawa et al. noted that the incidence of PAS after uterine surgery May depend on the suture method used for myometrial closure (36). In this case, we speculate that the placement outside the adenomyomectomy site and the use of barbed sutures for closure May have prevented PAS. Further studies are required to evaluate whether surgical techniques using barbed sutures reduce the incidence of PAS. However, it is also possible that our technique is uniquely superior because elastography can easily depict the hardness and softness of the tissue and detect the endometrium indicated by the bright red areas. Areas (Figure 2E), although Wada et al. concluded that one of the risks of PAS is intraoperative uterine cavity breach (37). Therefore, perforation of the uterine cavity May be avoided with elastography.

Adenomyotic lesions May disturb the process of spiral artery remodeling in the myometrial junctional zone from the onset of decidualization, causing defective placentation (38, 39), and consequently, the risk of fetal growth restriction (FGR) May increase due to placental blood flow during pregnancy (40).In retrospective cohort study, Ono et al. concluded that the laparoscopic adenomyomectomy had a significantly lower prevalence of FGR compared to the no surgery group (41). In this case, we did not diagnose FGR, albeit at the lower end of the normal range of fetal weight due to twin, and we speculated that elastography ensured resection of the adenomyosis foci, which promoted normal placentation.

In conclusion, to the best of our knowledge, this is the first report of dichorionic twin delivery without uterine rupture after laparoscopic adenomyomectomy under elastography guidance. Adenomyomectomy is a uterus-preserving surgical treatment for adenomyosis that offers symptom relief and potential fertility preservation but comes with risks of recurrence, surgical complications, and potential uterine rupture in future pregnancies (42). Hence, the success of adenomyomectomy heavily depends on surgical expertise, with experienced surgeons better equipped to handle the procedure's complexity, select appropriate cases, manage complications, and implement evolving techniques (43). While adenomyomectomy can be effective if the selection of case was correct, its use requires careful consideration of individual patient factors, and ongoing research is needed to optimize long-term outcomes and refine patient selection criteria. On the other hand, Elastography, particularly shear wave elastography, has emerged as a valuable tool for improving diagnosis, surgical planning, and treatment monitoring. This technique May have the possibility to allow precise resection and mitigate the risks of

uterine rupture and PAS, although adenomyomectomy is not strongly recommended, and meticulous surgical techniques are important to minimize uterine defects. The use of elastography in this context lacks robust evidence and is currently evolving through clinical research. Further studies involving larger cohorts are required to establish the safety and efficacy of laparoscopic elastography-guided adenomyomectomies.

Data availability statement

The original contributions presented in the study are included in the article/Supplementary material, further inquiries can be directed to the corresponding author.

Ethics statement

The studies involving humans were approved by this study was reviewed and approved by the Human Research Ethics Committee of Kawasaki Medical School (trial registration no.: 5075-01). The studies were conducted in accordance with the local legislation and institutional requirements. The participants provided their written informed consent to participate in this study.

Written informed consent was obtained from the individual(s) for the publication of any potentially identifiable images or data included in this article.

Author contributions

YO: Conceptualization, Writing – original draft. KO: Conceptualization, Writing – original draft, Writing – review & editing. TT: Conceptualization, Writing – review & editing, Writing – original draft. NH: Data curation, Writing – review & editing. RK: Data curation, Writing – review & editing. HO: Data curation, Writing – review & editing. YT: Data curation, Writing – review & editing. TK: Data curation, Writing – review & editing. TO: Data curation, Writing – review & editing. TMa: Supervision, Writing – review & editing. TMi: Supervision, Writing – review & editing. TH: Supervision, Writing – review & editing. KS: Supervision, Writing – review & editing.

Funding

The author(s) declare financial support was received for the research, authorship, and/or publication of this article. This work was supported by JSPS KAKENHI Grant Number: JP21K09498.

Acknowledgments

This work would not have been possible without the great effort made by Yoshimi Harada.

Conflict of interest

The authors declare that the research was conducted in the absence of any commercial or financial relationships that could be construed as a potential conflict of interest.

Publisher's note

All claims expressed in this article are solely those of the authors and do not necessarily represent those of their affiliated organizations, or those of the publisher, the editors and the reviewers. Any product that may be evaluated in this article, or claim that may be made by its manufacturer, is not guaranteed or endorsed by the publisher.

Supplementary material

The Supplementary material for this article can be found online at: https://www.frontiersin.org/articles/10.3389/fmed.2024.1457611/full#supplementary-material

References

1. Maheshwari A, Gurunath S, Fatima F, Bhattacharya S. Adenomyosis and subfertility: a systematic review of prevalence, diagnosis, treatment and fertility outcomes. *Hum Reprod Update*. (2012) 18:374–92. doi: 10.1093/humupd/dms006

2. Vercellini P, Viganò P, Bandini V, Buggio L, Berlanda N, Somigliana E. Association of endometriosis and adenomyosis with pregnancy and infertility. *Fertil Steril*. (2023) 119:727–40. doi: 10.1016/j.fertnstert.2023.03.018

3. Dueholm M, Lundorf E. Transvaginal ultrasound or MRI for diagnosis of adenomyosis. *Curr Opin Obstet Gynecol*. (2007) 19:505–12. doi: 10.1097/GCO.0b013e3282f1bf00

4. Sharara FI, Kheil MH, Feki A, Rahman S, Klebanoff JS, Ayoubi JM, et al. Current and prospective treatment of adenomyosis. *J Clin Med*. (2021) 10:3410. doi: 10.3390/jcm10153410

5. Tsui K-H, Lee F-K, Seow K-M, Chang W-C, Wang J-W, Chen S-U, et al. Conservative surgical treatment of adenomyosis to improve fertility: controversial values, indications, complications, and pregnancy outcomes. *Taiwanese J Obstet Gynecol*. (2015) 54:635–40. doi: 10.1016/j.tjog.2015.05.003

6. Oliveira MAP, Crispi CP, Brollo LC, Crispi CP, De Wilde RL. Surgery in adenomyosis. *Arch Gynecol Obstet*. (2018) 297:581–9. doi: 10.1007/s00404-017-4603-6

7. Jiang L, Han Y, Song Z, Li Y. Pregnancy outcomes after uterus-sparing operative treatment for Adenomyosis: a systematic review and Meta-analysis. *J Minim Invasive Gynecol*. (2023) 30:543–54. doi: 10.1016/j.jmig.2023.03.015

8. Moawad G, Youssef Y, Fruscalzo A, Faysal H, Merida M, Pirtea P, et al. The impact of conservative surgical treatment of Adenomyosis on fertility and perinatal outcomes. *J Clin Med*. (2024) 13:2531. doi: 10.3390/jcm13092531

9. Chapron C, Vannuccini S, Santulli P, Abrão MS, Carmona F, Fraser IS, et al. Diagnosing adenomyosis: an integrated clinical and imaging approach. *Hum Reprod Update*. (2020) 26:392–411. doi: 10.1093/humupd/dmz049

10. Szubert M, Koziróg E, Olszak O, Krygier-Kurz K, Kazmierczak J, Wilczynski J. Adenomyosis and infertility-review of medical and surgical approaches. *Int J Environ Res Public Health*. (2021) 18:1235. doi: 10.3390/ijerph18031235

11. Ahn JW, You S-G, Go EB, Lee SH, Kim JS, Cho HJ, et al. Minimally invasive adenomyomectomy via a laparoscopic-assisted approach compared to a laparoscopic or laparotomic approach. *Taiwanese J Obstet Gynecol*. (2021) 60:1005–10. doi: 10.1016/j.tjog.2021.09.010

12. Kwack JY, Im KS, Kwon Y-S. Conservative surgery of uterine adenomyosis via laparoscopic versus laparotomic approach in a single institution. *J Obstet Gynaecol Res*. (2018) 44:1268–73. doi: 10.1111/jog.13658

13. Wood C. Surgical and medical treatment of adenomyosis. *Hum Reprod Update*. (1998) 4:323–36. doi: 10.1093/humupd/4.4.323

14. Younes G, Tulandi T. Conservative surgery for adenomyosis and results: a systematic review. *J Minim Invasive Gynecol*. (2018) 25:265–76. doi: 10.1016/j.jmig.2017.07.014

15. Ren Q, Dong X, Yuan M, Jiao X, Sun H, Pan Z, et al. Application of elastography to diagnose adenomyosis and evaluate the degree of dysmenorrhea: a prospective observational study. *Reprod Biol Endocrinol*. (2023) 21:98. doi: 10.1186/s12958-023-01145-y

16. Brunelli AC, Brito LGO, Moro FAS, Jales RM, Yela DA, Benetti-Pinto CL. Ultrasound Elastography for the diagnosis of endometriosis and Adenomyosis: a systematic review with Meta-analysis. *Ultrasound Med Biol*. (2023) 49:699–709. doi: 10.1016/j.ultrasmedbio.2022.11.006

17. Ota Y, Ota K, Takahashi T, Suzuki S, Sano R, Shiota M. New surgical technique of laparoscopic resection of adenomyosis under real-time intraoperative ultrasound elastography guidance: a case report. *Heliyon*. (2020) 6:e04628. doi: 10.1016/j.heliyon.2020.e04628

18. Ota Y, Ota K, Takahashi T, Morimoto Y, Suzuki S, Sano R, et al. Laparoscopic Adenomyomectomy under real-time intraoperative ultrasound Elastography guidance: a case series and feasibility study. *J Clin Med*. (2022) 11:707. doi: 10.3390/jcm11226707

19. Ota Y, Ota K, Takahashi T, Morimoto Y, Suzuki S-I, Sano R, et al. A case of elastography-assisted laparoscopic fertility preservation for severe deep endometriosis causing ureteral stenosis and subtype II adenomyosis. *Endocrine*. (2021) 2:348–55. doi: 10.3390/endocrines2030032

20. Chan I-S, Hsu T-F, Shih Y-C, Chang Y-H, Wang P-H, Chen Y-J. Maintenance dienogest therapy following adjuvant gonadotropin-releasing hormone agonist treatment after uterus-sparing surgery in adenomyosis: a retrospective cohort study. *Int J Gynecol Obstet*. (2023) 161:751–9. doi: 10.1002/ijgo.14635

21. Gardner DK, Schoolcraft WB. Culture and transfer of human blastocysts. *Curr Opin Obstet Gynecol*. (1999) 11:307–11. doi: 10.1097/00001703-199906000-00013

22. Ota K, Takahashi T, Mitsui J, Kuroda K, Hiraoka K, Kawai K. A case of discrepancy between three ERA tests in a woman with repeated implantation failure complicated by chronic endometritis. *BMC Pregnancy Childbirth*. (2022) 22:891. doi: 10.1186/s12884-022-05241-6

23. Kishi Y, Yabuta M, Taniguchi F. Who will benefit from uterus-sparing surgery in adenomyosis-associated subfertility? *Fertil Steril*. (2014) 102:802–7. doi: 10.1016/j.fertnstert.2014.05.028

24. Saremi A, Bahrami H, Salehian P, Hakak N, Pooladi A. Treatment of adenomyomectomy in women with severe uterine adenomyosis using a novel technique. *Reprod Biomed Online*. (2014) 28:753–60. doi: 10.1016/j.rbmo.2014.02.008

25. Nishida M, Otsubo Y, Ichikawa R, Arai Y, Sakanaka S. Shikyusenkinshokakushutsujutsu-go ninshin-ji no shikyuharetsu-yobo ni tsuite (prevention of uterine rupture during pregnancy after adenomyomectomy). *Obstet Gynecol Surg (Tokyo Medical View)*. (2016) 27:69–76.

26. S-i W. Kudo M, Minakami H. Spontaneous uterine rupture of a twin pregnancy after a laparoscopic adenomyomectomy: a case report. *J Minim Invasive Gynecol*. (2006) 13:166–8. doi: 10.1016/j.jmig.2005.12.002

27. Kwack JY, Jeon SB, Kim K, Lee SJ, Kwon YS. Monochorionic twin delivery after conservative surgical treatment of a patient with severe diffuse uterine adenomyosis without uterine rupture. *Obstet Gynecol Sci*. (2016) 59:311–5. doi: 10.5468/ogs.2016.59.4.311

28. Kweon S, Lee JS, Kim S, Kwack JY, Kwon Y-S. Antenatal and delivery outcomes in twin pregnant women after uterine Adenomyomectomy: summary of 5 cases. *Perinatology*. (2023) 34:175–9. doi: 10.14734/PN.2023.34.4.175

29. Hadisaputra W, Anggraeni TD. Laparoscopic resection versus myolysis in the management of symptomatic uterine adenomyosis: alternatives to conventional treatment. *Med J Indones*. (2006) 15:9–17. doi: 10.13181/mji.v15i1.208

30. Parker WH, Einarsson J, Istre O, Dubuisson J-B. Risk factors for uterine rupture after laparoscopic myomectomy. *J Minim Invasive Gynecol*. (2010) 17:551–4. doi: 10.1016/j.jmig.2010.04.015

31. Prapas Y, Kalogiannidis I, Prapas N. Laparoscopy vs laparoscopically assisted myomectomy in the management of uterine myomas: a prospective study. *Am J Obstet Gynecol*. (2009) 200:144. doi: 10.1016/j.ajog.2008.08.063

32. Pistofidis G, Makrakis E, Balinakos P, Dimitriou E, Bardis N, Anaf V. Report of 7 uterine rupture cases after laparoscopic myomectomy: update of the literature. *J Minim Invasive Gynecol*. (2012) 19:762–7. doi: 10.1016/j.jmig.2012.07.003

33. Otsubo Y, Nishida M, Arai Y, Ichikawa R, Taneichi A, Sakanaka M. Association of uterine wall thickness with pregnancy outcome following uterine-sparing surgery for diffuse uterine adenomyosis. *Aust N Z J Obstet Gynaecol*. (2016) 56:88–91. doi: 10.1111/ajo.12419

34. Sugiyama M, Takahashi H, Baba Y, Taneichi A, Suzuki H, Usui R, et al. Perinatal outcome of pregnancy after adenomyomectomy: summary of 10 cases with a brief literature review. *J Matern Fetal Neonatal Med*. (2020) 33:4145–9. doi: 10.1080/14767058.2019.1597845

35. Sayama S, Iriyama T, Hashimoto A, Suzuki K, Ariyoshi Y, Yano E, et al. Possible risks and benefits of adenomyomectomy on pregnancy outcomes: a retrospective analysis. *AJOG Glob Rep*. (2023) 3:100265. doi: 10.1016/j.xagr.2023.100265

36. Sumigama S, Sugiyama C, Kotani T, Hayakawa H, Inoue A, Mano Y, et al. Uterine sutures at prior caesarean section and placenta accreta in subsequent pregnancy: a case-control study. *BJOG*. (2014) 121:866–75. doi: 10.1111/1471-0528.12717

37. Wada S, Fukushi Y, Ono Y, Ota H, Tsuzuki Y, Yamada H. Influence of uterine cavity breach in laparoscopic myomectomy on the risk of obstetric complications. *Gynecol Minim Invasive Ther*. (2022) 11:221–3. doi: 10.4103/gmit.gmit_146_21

38. Yen C-F, Huang SJ, Lee C-L, Wang H-S, Liao S-K. Molecular characteristics of the endometrium in uterine Adenomyosis and its biochemical microenvironment. *Reprod Sci*. (2017) 24:1346–61. doi: 10.1177/1933719117691141

39. Brosens I, Pijnenborg R, Benagiano G. Defective myometrial spiral artery remodelling as a cause of major obstetrical syndromes in endometriosis and adenomyosis. *Placenta*. (2013) 34:100–5. doi: 10.1016/j.placenta.2012.11.017

40. Yorifuji T, Makino S, Yamamoto Y, Sugimura M, Kuwatsuru R, Takeda S. Time spatial labeling inversion pulse magnetic resonance angiography in pregnancy with adenomyosis. *J Obstet Gynaecol Res*. (2013) 39:1480–3. doi: 10.1111/jog.12088

41. Ono Y, Ota H, Fukushi Y, Tagaya H, Okuda Y, Yoshino O, et al. Effectiveness of laparoscopic Adenomyomectomy on perinatal outcomes. *Gynecol Minim Invasive Ther*. (2023) 12:211–7. doi: 10.4103/gmit.gmit_45_22

42. Vannuccini S, Petraglia F. Recent advances in understanding and managing adenomyosis. *F1000Res*. (2019):8. doi: 10.12688/f1000research.17242.1

43. Capezzuoli T, Toscano F, Ceccaroni M, Roviglione G, Stepniewska A, Fambrini M, et al. Conservative surgical treatment for adenomyosis: new options for looking beyond uterus removal. *Best Pract Res Clin Obstet Gynaecol*. (2024) 95:102507. doi: 10.1016/j.bpobgyn.2024.102507

frontiers | Frontiers in Medicine

TYPE Clinical Trial
PUBLISHED 19 November 2024
DOI 10.3389/fmed.2024.1485211

OPEN ACCESS

EDITED BY
Andrea Tinelli,
Veris delli Ponti Hospital, Italy

REVIEWED BY
Song Zhang,
Shanghai Jiao Tong University, China
Jieying Zhang,
First Teaching Hospital of Tianjin University of Traditional Chinese Medicine, China

*CORRESPONDENCE
Huadi Yang
88mummy@163.com

†These authors share first authorship

RECEIVED 23 August 2024
ACCEPTED 25 October 2024
PUBLISHED 19 November 2024

CITATION
Mao P, Meng W, Mao T, Li H, Xu X, Jiang X and Yang H (2024) Efficacy of thumbtack needle acupuncture combined with PCIA on patients after laparoscopic myomectomy: a randomized controlled trial.
Front. Med. 11:1485211.
doi: 10.3389/fmed.2024.1485211

Efficacy of thumbtack needle acupuncture combined with PCIA on patients after laparoscopic myomectomy: a randomized controlled trial

Peiyu Mao[1†], Weijie Meng[2†], Tongxin Mao[3], Hui Li[1], Xuqun Xu[1], Xuelu Jiang[1] and Huadi Yang[1*]

[1]Department of Gynecology and Obstetrics, The First Affiliated Hospital of Zhejiang Chinese Medical University, Zhejiang Provincial Hospital of Chinese Medicine, Hangzhou, China, [2]Department of 16# Wards, The First Affiliated Hospital of Zhejiang Chinese Medical University, Zhejiang Provincial Hospital of Chinese Medicine, Hangzhou, China, [3]First Clinical Medical College, Zhejiang Chinese Medical University, Hangzhou, China

Background: Pain and gastrointestinal dysfunction after laparoscopic myomectomy (LM) are significant issues that prevent this procedure from being classified as a "Day Surgery." This study aims to assess the effectiveness and safety of thumbtack needle acupuncture (TNA) combined with patient-controlled intravenous analgesia (PCIA) for promoting enhanced recovery after LM.

Methods: A total of 52 patients were enrolled in the study, divided into a treatment group receiving TNA and a control group. Both groups were administered PCIA without background sufentanil. For rescue analgesia or antiemetic needs, a bolus infusion of flurbiprofen axetil (50 mg) or intravenous metoclopramide (10 mg) was provided. The primary outcomes measured were the Visual Analog Scale (VAS) scores at awakening, as well as at 36 h, 48 h, and 60 h after LM. Secondary outcomes included VAS scores at 6 h, 12 h, 24 h, and 72 h after LM, total sufentanil consumption, the number of PCIA analgesic requests (attempts), the number of doses of rescue flurbiprofen axel analgesia required, preoperative anxiety scores, gastrointestinal function recovery assessment, first ambulation time, length of hospital stay, and patient satisfaction. Adverse events were also recorded.

Results: Compared to the control group, the treatment group showed significantly lower VAS scores, fewer analgesia attempts, reduced total sufentanil consumption, and a smaller number of rescue analgesia doses after LM, along with lower preoperative anxiety scores and higher satisfaction with pain management ($p < 0.05$). Gastrointestinal function recovery was enhanced in the treatment group, as indicated by earlier flatus and defecation, a lower incidence of postoperative nausea and vomiting (PONV), and a smaller number of metoclopramide doses required ($p < 0.05$). Additionally, ambulation occurred earlier, and the length of hospital stay was shorter in the treatment group ($p < 0.05$). No adverse events were observed in patients receiving TNA.

Conclusion: TNA is a safe intervention that effectively alleviates postoperative pain, decreases the total consumption of sufentanil, reduces preoperative anxiety, enhances the recovery of gastrointestinal function, and shortens the duration of hospitalization, making it an ideal adjunct treatment for postoperative

recovery after LM. Further research is required to understand the mechanisms underlying this intervention.

Clinical trial registration: www.chictr.org.cn, ChiCTR2300069015.

KEYWORDS

thumbtack needle acupuncture, PCIA, laparoscopic myomectomy, pain control, postoperative recovery, randomized controlled clinical trial

Introduction

China, with the largest population in the world, has been facing a shortage of medical resources. Therefore, the concept of enhanced recovery after surgery (ERAS) (1) has gained widespread acceptance among the majority of medical professionals in the country.

Laparoscopic myomectomy (LM) has replaced conventional laparotomy for decades due to its advantages, including less influence on ovarian function, lower oxidative damage, and a higher successful pregnancy rate after operation (2, 3). This procedure is now proficiently performed by many gynecologists and is expected to transition into daytime surgery. However, postoperative pain and gastrointestinal dysfunction prolong hospital stays and escalate medical costs, which prevent it from becoming a "Day Surgery."

Despite advancements in the prevention and control of postoperative pain over the past 20 years, insufficient analgesia remains a common issue in China. Comprehensive, goal-directed perioperative analgesia (4) is essential to mitigate patients' traumatic stress responses, especially during often-overlooked phases of preoperative prophylactic analgesia, early postoperative analgesia, and pain management after the withdrawal of patient-controlled intravenous analgesia (PCIA). It is worth noting that preoperative anxiety (5, 6) can also influence the intensity of postoperative pain, anesthesia, and analgesia requirements. Additionally, gastrointestinal dysfunction, including postoperative nausea and vomiting (PONV) and intestinal paralysis caused by anesthesia and analgesics, plays a significant role in affecting postoperative recovery (7, 8).

Thumbtack needle acupuncture (TNA) is a specialized acupuncture therapy that has been used to promote rehabilitation after LM in China. It has attracted clinical attention due to its ease of application, minimal invasiveness, and positive therapeutic effects, although existing evidence supporting its effectiveness remains limited. This study aims to evaluate the effects of TNA during the perioperative period of LM, with the aim of establishing a safe ERAS pathway for this procedure.

Methods

Aim

This study aims to assess the efficacy and safety of TNA combined with PCIA without background sufentanil infusion in supporting patient rehabilitation after LM.

Abbreviations: TNA, Thumbtack needle acupuncture; LM, Laparoscopic myomectomy; ERAS, Enhanced recovery after surgery; VAS, Visual Analog Scale; PCIA, Patient-controlled intravenous analgesia; HADS, Hospital Anxiety and Depression Scale; PONV, Postoperative nausea and vomiting.

Study design

This prospective, single-center, randomized, participant-blinded, controlled clinical trial was conducted at *The First Affiliated Hospital of Zhejiang Chinese Medical University (Zhejiang Provincial Hospital of Chinese Medicine)* from 1 October 2023, to 30 May 2024, in accordance with the Declaration of Helsinki and the Medical Research Involving Human Subjects Act.

Setting

All eligible patients scheduled for LM were considered for participation in this study, unless they met the exclusion. The exclusion criteria were as follows: pedunculated subserosal myomas, broad ligament, cervical, or submucosal myomas identified through preoperative ultrasound examination, malignant lesions, use of analgesics within 48 h before surgery, preoperative administration of agents affecting gut motility (e.g., tricyclic antidepressants, opioids, or butylscopolamine), history of preoperative chronic pain, history of gastrointestinal diseases or surgery, previous severe cardiopulmonary disease, liver or kidney dysfunction, history of mental illness, pregnancy or lactation, language and self-expression disorders, limb disability, or smoking habits. The postoperative exclusion criteria were as follows: re-operation exploration, hemodynamic instability, including systolic blood pressure (SBP) <90 mmHg, complications of intervention procedure (fainting when exposed to needles, pain, bleeding, or infection at the needle location), pedunculated subserosal myomas or broad ligament myoma identified through surgery, malignant lesions identified through pathological confirmation, and postoperative complications (severe arrhythmia, hemorrhage, postoperative confusion, urinary tract infection, or reproductive system infection).

Sample size calculation

In a preliminary trial that evaluated pain scores evaluated using the Visual Analog Scale (VAS) at awakening, as well as at 36 h, 48 h and 60 h, as the main index, it was found that VAS scores at awakening was significantly lower in the treatment group. The treatment group recorded a score of 2.57 ± 0.81, compared to 3.61 ± 1.5 in the control group. This difference achieved the minimal clinically important difference (MCID). Therefore, the sample size calculation was based on VAS scores at awakening. At a two-sided significance level of 0.05 and 90% power, a sample of 104 women was needed (52 per group), accounting for a 15% increase.

Randomization and masking

Eligible participants were randomly assigned to receive either TNA or control measures using an interactive web response system (IWRS) for clinical research in a 1:1 ratio. Group assignment was conducted exclusively by the acupuncturist (*Nurse Weijie Meng*), who performed the intervention procedure. Clinicians, ward nurses, participants, outcome assessors, and statisticians were all blinded to the treatment allocation.

Perioperative management and surgery

To minimize bias, we defined standard patient management protocols for all participants in the perioperative periods.

Preoperatively, the patients fasted for 6–8 h before surgery and received an enema in the morning of the surgery.

All LM procedures were performed by our surgical team (consisting of Doctor *Huadi Yang, Peiyu Mao, Xuelu Jiang,* and *Xuqun Xu*), according to standard operating procedures. These surgeries involved the use of a 12-mm, a 10-mm, and two 5-mm laparoscopic trocars and maintenance of intra-abdominal pressure of 11–12 mmHg during the procedure to remove uterine fibroids. A single-shot antibiotic prophylaxis was administered. Sufentanil (0.4 μg/kg), propofol (2–3 mg/kg), and rocuronium (0.6–0.8 mg/kg) were administered intravenously to induce anesthesia. Propofol (3 mg/kg/h), remifentanil (0.1–0.3 μg/kg/min), and sevoflurane (1.0–2.5%) were administered to maintain the depth of anesthesia after tracheal intubation. The bispectral index value was maintained between 40 and 60.

Intervention procedure

Once the vital signs were stable, the PCIA pumps were connected in the post-anesthesia care unit. Each pump was prepared with 2 μg/kg sufentanil (*Yichang Humanwell Pharmaceutical Jiangxi Province, China*) diluted in 100 mL of physiological saline, set for no background infusion and locked for 6 min. After the setup was complete, the patients were sent back to their wards. The PCIA pumps were discontinued after 36 h for all participants, with sufentanil replenished if depleted within that timeframe. The participants were instructed to use the PCIA pump and were told to press the button (delivering 0.5 mL) whenever they felt pain. For rescue analgesia, a bolus infusion of 50 mg flurbiprofen axel was available if patients reported intolerable pain, which could be repeated as necessary to ensure that analgesia failure was ruled out. Additionally, intravenous metoclopramide 10 mg was administered as a rescue antiemetic upon patients' request. If severe nausea persisted after two consecutive doses of rescue antiemetics, the PCIA was paused for 2 h and restarted after the symptoms subsided.

TNA (*Huatuo*) used in this study is produced by Suzhou Medical Supplies Factory Co., Ltd., China. Its packing box and the packing of TNA itself are showed in (Figure 1a–c). Figure 1d showed the operation steps through images and Figure 1e showed that TNA consists of a tiny needle (measuring 2 × 9 mm) and a circular adhesive tape with a radius of 5 mm. The night before surgery, *Nurse Meng* performed the intervention for both groups. The acupoints Hegu (LI 4) (9), Sanyinjiao (SP 6), Zusanli (ST 36) (10), and Zhongji (RN 3) were pressed for 10 s, and the superficial skin at these points was disinfected with 75% alcohol. Then, the thumbtack needle was inserted vertically into each acupoint according to the instructions for the treatment group (Figures 1d, 2). In contrast, the control group received only a single acupuncture shot, and an adhesive tape without the tiny needle was placed at the same acupoints for the control group. The intervention procedure was maintained for 48 h. In both groups, *Nurse Meng* reminded the participants to move their limbs normally and to avoid washing or tearing the adhesive tape. To ensure safety, we removed the TNA and immediately reinserted it after the surgery. Postoperative mobilization was standardized in both groups.

Patients with successful defecation, good tolerance to solid meals, no fever in the last 24 h, VAS ≤ 3, full mobilization, no evidence of complications, and who completed the trial were discharged from the hospital.

Outcome measures

Patient characteristics

We collected data on baseline demographics (including marital status, gravidity, parity, previous abdominal operations, age, and body mass index) and surgical characteristics (including the number and size of myomas, pelvic adhesions, operation duration, blood loss, and infusion volume).

Primary observation items

VAS scores at awakening, 36 h, 48 h, and 60 h after LM for different types of pain, including visceral pain, incision pain, lower back pain, and shoulder pain, were recorded at awakening, 36 h, 48 h, and 60 h after LM as primary observation items. The intensity of pain was recorded using a 10-point VAS, which ranged from 0 (no pain) to 10 (the worst pain imaginable).

Secondary observation items

VAS scores at 6 h, 12 h, 24 h, and 72 h for different types of pain, the total amount of sufentanil consumed, the number of PCIA analgesic requests (attempts), and the number of doses of rescue flurbiprofen axel analgesia required were recorded as secondary pain assessment.

Preoperative anxiety scores assessed using the Hospital Anxiety and Depression Scale (HADS) were recorded.

The first flatus time, the first defecation time, and the incidence of PONV during 48 h after surgery (i.e., nausea refers to an uneasy feeling in the stomach, while vomiting refers to the forceful expulsion of gastric contents (11)), and the number of metoclopramide doses required were recorded to assess gastrointestinal function recovery. PONV is assessed using a four-point verbal scale (none = no nausea, mild = nausea but no vomiting, moderate = vomiting one attack, severe = vomiting > one attack).

First, the ambulation time and the length of hospital stay were recorded as part of the postoperative recovery assessment. Upon discharge, we evaluated patient satisfaction based on four aspects: health education provided by health workers, nursing care, availability of drugs and supplies, and pain management.

Adverse events

Adverse events were recorded by *Nurse Meng* and forwarded the information to *Doctor Mao*, who then sent a report to the medical ethics committee to evaluate the case.

FIGURE 1
A comprehensive introduction of TNA. (a) Front of packing box of TNA; (b) back of packing box of TNA; (c) packing of TNA in the packing box; (d) the introduction of procedure of TNA on the back of packing box; (e) the TNA consists of a tiny needle and an adhesive tape.

Statistical analyses

Statistical analysis was performed using SPSS® (v. 22.0; IBM Corp., New York, NY) and GraphPad Prism (version 8.0; San Diego, CA, USA) for Windows. Continuous variables are presented as $\bar{x} \pm S$. Comparisons between pre-treatment and post-treatment were performed using Student's *t*-test. Proportions between groups were compared using chi-squared tests, with Fisher's exact test used as appropriate because of the small sample sizes.

Results

Patient characteristics

A total of 111 patients were assessed for eligibility, of which 7 were excluded due to non-compliance with the study protocol. Thus, 104 patients were randomized and completed the trial, with 52 patients in each of the treatment and control groups (Figure 3).

As shown in Table 1, there was no significant difference in baseline demographics and surgical characteristics between the two groups. The postoperative pathology of all participants was confirmed to be benign.

Primary outcome measures

Table 2 shows that compared with the control group, the treatment group had significantly lower VAS scores for incision and shoulder pain at awakening, shoulder pain at 36 h, and all pain types at 48 h and 60 h ($p < 0.05$). In both groups, incision pain was the highest at awakening, visceral pain was the highest at 36 h and 48 h, and shoulder pain was the highest at 60 h.

Secondary pain assessment

As shown in Tables 3, 4, the treatment group exhibited significantly lower VAS scores for shoulder pain at 6 h, 12 h, and 24 h, as well as for all pain types at 72 h, compared to the control group.

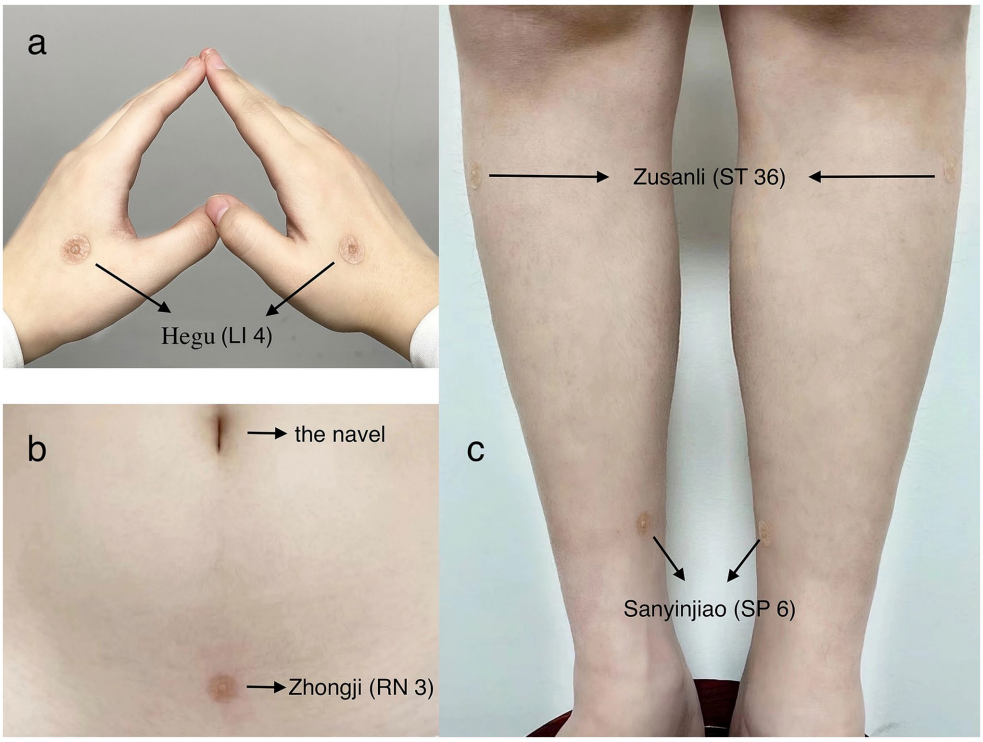

FIGURE 2
TNA of the marked acupoints. (a) TNA on Hegu (LI 4) of both sides; (b) TNA on the Zhongji (RN 3); (c) TNA on Zusanli (ST 36) and Sanyinjiao (SP 6) of both sides.

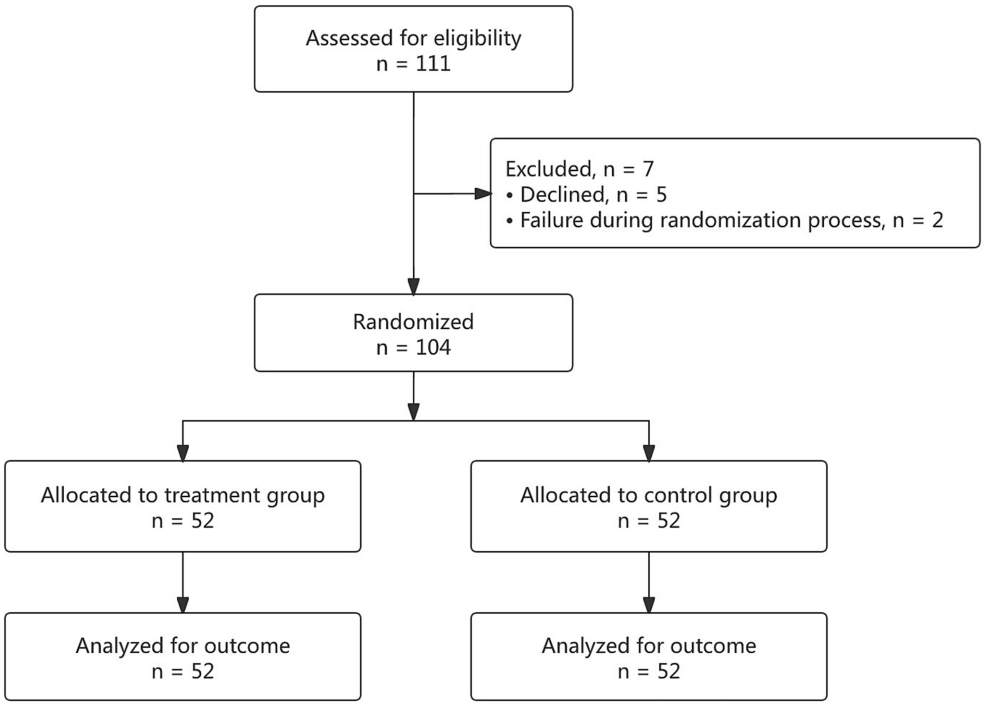

FIGURE 3
CONSORT flow diagram of the randomized trial.

TABLE 1 Preoperative and clinical/surgical characteristics of patients.

Variables	Dimensions	Treatment group	Control group	*p* value
Marital status	Married	48 (92.3%)	50 (96.1%)	0.163[a]
	Single and divorced	4 (7.7%)	2 (3.9%)	
Gravidity	Means ± SD	2.37 ± 1.47	2.98 ± 1.86	0.092[b]
Parity	Means ± SD	1.16 ± 0.64	1.29 ± 0.76	0.327[b]
Previous abdominal operation(s)	0	24 (46.1%)	24 (46.1%)	0.551[c]
	1	25 (48.0%)	22 (42.3%)	
	≥2	3 (5.9%)	6 (11.6%)	
Age	Means ± SD	44 ± 5.90	45 ± 7.43	0.601[b]
Body mass index (kg/m^2)	Means ± SD	24.60 ± 3.41	23.83 ± 3.67	0.212[b]
Number of myomas removed	1–3	32 (61.5%)	33 (63.5%)	0.883[c]
	4–5	15 (28.9%)	13 (25%)	
	>5	5 (9.6%)	6 (11.5%)	
Diameter of myomas, cm	Means ± SD	7.25 ± 1.72	7.41 ± 1.51	0.626[b]
Pelvic adhesion	YES	29 (55.8%)	28 (53.8%)	>0.999[c]
	NO	23 (44.2%)	24 (46.2%)	
Operation duration, h	Means ± SD	2.33 ± 0.73	2.44 ± 0.92	0.583[b]
Blood loss (range), mL	Means ± SD	53.14 ± 12.57	53.14 ± 12.57	0.940[b]
Infusion volume intraoperatively (range), mL	Means ± SD	1064.71 ± 154.69	1064.71 ± 154.69	>0.999[b]

[a]Fisher's exact test, [b]Student's *t*-test, [c]Chi-Squared test.

TABLE 2 VAS scores at awakening time, 36 h, 48 h, and 60 h after surgery for two groups.

Time	Pain types	VAS scores		*P* value
		Treatment group (*n* = 52)	Control group (*n* = 52)	
Awakening time	Visceral pain	2.81 ± 0.56	2.94 ± 0.64	0.257[a]
	Incision pain	3.88 ± 0.78	4.21 ± 0.72	0.029[a]
	Lower back pain	2.69 ± 0.54	2.88 ± 0.47	0.057[a]
	Shoulder pain	2.77 ± 0.58	3.00 ± 0.56	0.042[a]
36 h	Visceral pain	2.60 ± 0.98	2.90 ± 0.80	0.081[a]
	Incision pain	2.56 ± 0.83	2.85 ± 0.78	0.070[a]
	Lower back pain	2.50 ± 0.73	2.71 ± 0.64	0.118[a]
	Shoulder pain	2.37 ± 0.60	2.62 ± 0.57	0.030[a]
48 h	Visceral pain	2.54 ± 1.18	2.98 ± 0.90	0.034[a]
	Incision pain	2.29 ± 2.00	2.62 ± 0.63	0.020[a]
	Lower back pain	2.27 ± 0.60	2.56 ± 0.75	0.033[a]
	Shoulder pain	2.27 ± 0.93	2.62 ± 0.69	0.034[a]
60 h	Visceral pain	1.83 ± 0.68	2.15 ± 0.70	0.017[a]
	Incision pain	1.75 ± 0.62	2.02 ± 0.64	0.032[a]
	Lower back pain	1.67 ± 0.58	1.94 ± 0.61	0.010[a]
	Shoulder pain	2.04 ± 0.82	2.35 ± 0.62	0.033[a]

[a]Student's *t*-test. Values are given as means ± SD.

TABLE 3 VAS scores at 6 h, 12 h, 24 h, and 72 h after surgery for two groups.

Time	Pain types	VAS scores		*P* value
		Treatment group (*n* = 52)	Control group (*n* = 52)	
6 h	Visceral pain	2.75 ± 0.76	3.00 ± 0.66	0.077[a]
	Incision pain	2.46 ± 0.61	2.65 ± 0.59	0.105[a]
	Lower back pain	2.67 ± 0.68	2.87 ± 0.56	0.118[a]
	Shoulder pain	2.56 ± 0.64	2.87 ± 0.69	0.020[a]
12 h	Visceral pain	2.38 ± 0.69	2.62 ± 0.66	0.085[a]
	Incision pain	2.35 ± 0.68	2.58 ± 0.67	0.084[a]
	Lower back pain	2.17 ± 0.76	2.38 ± 0.69	0.140[a]
	Shoulder pain	2.12 ± 0.68	2.38 ± 0.63	0.038[a]
24 h	Visceral pain	2.23 ± 0.73	2.48 ± 0.61	0.061[a]
	Incision pain	2.13 ± 0.71	2.35 ± 0.59	0.103[a]
	Lower back pain	2.00 ± 0.69	2.23 ± 0.61	0.074[a]
	Shoulder pain	2.52 ± 0.78	2.88 ± 0.88	0.027[a]
72 h	Visceral pain	1.65 ± 0.68	1.98 ± 0.75	0.022[a]
	Incision pain	1.77 ± 0.73	2.10 ± 0.87	0.040[a]
	Lower back pain	1.56 ± 0.61	1.83 ± 0.68	0.035[a]
	Shoulder pain	1.48 ± 0.58	1.75 ± 0.65	0.028[a]

[a]Student's *t*-test. Values are given as means ± SD.

Additionally, the treatment group had fewer attempts, reduced total sufentanil consumption, and a fewer doses of rescue analgesia ($p < 0.05$).

Preoperative anxiety assessment

As shown in Table 4, the HADS scores for anxiety were significantly lower in the treatment group ($p < 0.05$).

Gastrointestinal function recovery assessment

As shown in Table 4, gastrointestinal function recovery was enhanced in the treatment group with earlier flatus and defecation ($p < 0.05$), a lower incidence of PONV, and a fewer doses of metoclopramide required ($p < 0.05$).

First ambulation time and hospital stay assessment

As shown in Table 4, the time of ambulation was earlier and the length of hospital stay was shorter in the treatment group ($p < 0.05$).

Patient satisfaction assessment

As shown in Table 5, there was no significant difference in satisfaction with the health education provided by health workers, nursing care, and availability of drugs and supplies. However, the satisfaction score for pain management in the treatment group was significantly higher than that in the control group ($p < 0.01$).

Adverse events

No significant intraoperative or postoperative complications were observed in both groups. TNA therapy was well tolerated. No complications such as skin allergies, fainting when exposed to needles, pain, bleeding, or infection at the needle location were noted.

Discussion

This study aims to investigate the benefits and safety of TNA combined with PCIA for patients after LM. According to the American Pain Society postoperative guidelines (12), the use of background infusion is not required due to the potential aggravation of PONV. Therefore, PCIA was administered without a background infusion of sufentanil in this trial.

Although PCIA pumps are commonly used to manage postoperative pain, pain during the awakening period and after PCIA discontinuation is frequently overlooked due to healthcare providers' busy schedules. Even if a ward nurse or surgeon provides rescue analgesic treatment at the patient's request, the effect is often unsatisfactory, followed by constant complaints. Inadequate pain management has emerged as a primary cause of dissatisfaction among postoperative patients and their families. It is also an important cause of postoperative acute pain evolving into chronic pain and an important blind spot that has not yet been taken seriously by surgeons

and anesthesiologists. Besides, although opioids can control incision and visceral pain, they cannot effectively control post-laparoscopic shoulder pain (13). A previous study (14) reported that TNA combined with PCIA obtained better analgesic effects on incision dynamic pain and uterine contraction pain in patients after cesarean section. In this trial, we confirmed that TNA not only significantly alleviates postoperative incision and visceral pain but also alleviates shoulder pain. The application of TNA can cover the analgesic blind spots: preoperative prophylactic analgesia, early awakening analgesia, and pain after withdrawal of PCIA. Milder pain levels result in lower sufentanil use, reducing opioid-related adverse events (15), especially respiratory depression and postoperative ileus.

Preoperative anxiety is another factor that influences the intensity of postoperative pain and analgesia requirements. Our findings indicate that patients receiving TNA reported lower HADS anxiety scores. It is reported (6) that patients with preoperative anxiety could benefit from multimodal analgesia, including non-pharmacological methods. Therefore, relieving anxiety may be another analgesic mechanism of TNA.

PONV and constipation are classical side effects of opioids (7, 16), which are other difficulties that need to be solved in the ERAS context. With the return of patients' water intake and upcoming PONV pathophysiological climax (24 h postoperatively), PONV occurs more frequently and intensively (17). In this trial, we also found that the first flatus time and first defecation time were shorter, and the incidence of PONV during postoperative 48 h was lower in patients with TNA, showing enhanced recovery of gastrointestinal function, which is related to the less consumption of sufentanil and may relate to the mechanism of TNA itself. A pragmatic randomized controlled trial study (18) of TNA on functional constipation has shown that compared with mosapride citrate, TNA produced a greater improvement in complete and spontaneous bowel movement scores, consistent with this study's results.

Earlier ambulation was also observed in the treatment group, which is related to better pain control. It is reported (19) that early ambulation can reduce stress response and pain and accelerate patients' recovery, creating a good mutually reinforcing cycle.

TABLE 4 Attempts, total sufentanil consumption, and number of rescue analgesia/antemetic, preoperative anxiety, time of flatus, defecation and ambulation, and hospital stay for two groups.

Variable		Treatment group (n = 52)	Control group (n = 52)	P value
Attempts		13.85 ± 4.43	16.27 ± 5.41	0.014[a]
Total sufentanil consumption (μg.)		0.12 ± 0.04	0.15 ± 0.07	0.013[a]
Number of rescue analgesia	1	4 (6.7%)	1 (9.1%)	0.035[b]
	2	2 (33.3%)	7 (63.6%)	
	≥3	0 (0.0%)	3 (27.3%)	
HADS scores of anxiety		3.40 ± 1.0	3.79 ± 0.80	0.032[a]
Time to first flatus (h)		13.67 ± 3.92	15.18 ± 3.06	0.022[a]
Time to first defecation (h)		23.08 ± 3.75	24.86 ± 3.24	0.014[a]
The incidence of PONV		6 (11.5%)	15 (28.8%)	0.049[a]
Number of metoclopramides required	1	4 (80.0%)	2 (6.7%)	0.044[b]
	2	1 (20.0%)	9 (75%)	
	≥3	0 (0.0%)	1 (8.3%)	
Time to ambulation (h)		15.76 ± 2.29	17.27 ± 3.62	0.014[a]
Length of hospital stay (d) after LM		4.00 ± 0.89	5.00 ± 0.99	0.030[a]

[a]Student's t-test. Continuous data are shown as mean ± SD, enumeration data are shown as number (percentage).

TABLE 5 Participants' satisfaction outcomes.

Variables	Groups	Very satisfied (5)	Satisfied (4)	Neutral (3)	Dissatisfied (2)	Very dissatisfied (1)	Means ± SD	P value
Health education provided by the health workers	Treatment group	3 (5.8%)	36 (69.2%)	10 (19.2%)	2 (3.8%)	1 (2.0%)	3.73 ± 0.72	0.826[a]
	Control group	3 (5.8%)	36 (69.2%)	10 (19.2%)	2 (3.8%)	1 (2.0%)	3.65 ± 0.79	
Nursing care	Treatment group	4 (7.7%)	35 (67.3%)	12 (23.1%)	1 (1.9%)	0 (0.0%)	3.78 ± 0.58	>0.999[a]
	Control group	3 (5.7%)	37 (71.2%)	11 (21.2%)	1 (1.9%)	0 (0.0%)	3.80 ± 0.57	
Availability of drug and supply	Treatment group	6 (11.5%)	34 (65.4%)	11 (21.2%)	1 (1.9%)	0 (0.0%)	3.86 ± 0.63	0.515[a]
	Control group	3 (5.7%)	36 (69.2%)	12 (23.1%)	1 (2.0%)	0 (0.0%)	3.78 ± 0.58	
Pain management	Treatment group	10 (19.2%)	20 (38.5%)	21 (40.4%)	1 (1.9%)	0 (0.0%)	3.75 ± 0.80	<0.0001[a]
	Control group	2 (3.8%)	10 (19.2%)	35 (67.3%)	3 (5.7%)	2 (4.0%)	3.14 ± 0.75	

[a]Student's t-test.

Notably, the outcomes of TNA therapy largely depend on the patient's cooperation. In this study, the patients showed good tolerance to the treatment. The TNA procedure was brief, caused minimal discomfort, and showed no adverse reactions, demonstrating its safety. In addition, as a non-drug treatment, it is widely accepted by patients with liver and kidney dysfunction. Reduced pain and faster recovery led to better pain control, shorter hospital stays, and lower medical costs.

Traditional Chinese medicine views postoperative pain (20) as a result of "meridian obstruction, which can alleviated by clearing the meridian pathways (21). Stimulating acupoints serves as a method to facilitate this process, regulating the cerebral cortex and calming the nerves, thereby reducing swelling and alleviating pain (22).

TNA maintains continuous acupoint stimulation, promoting the flow of "Qi," a Chinese concept representing vitality or energy while relieving tension and alleviating associated symptoms (23). Several trials have demonstrated the effectiveness of TNA in various contexts, including pain management during obstetric delivery (24), chronic pain conditions (25), nausea and vomiting (26), and dysmenorrhoea (27). Our study confirmed its efficacy in managing pain and enhancing gastrointestinal function recovery after LM.

Multimodal analgesia is currently highly valued in the ERAS era. However, its implementation can be challenging for surgeons and anesthesiologists in China due to the demands of a busy medical environment. Therefore, TNA, performed by nurses, can serve as an integral component of multimodal analgesia to enhance recovery after LM.

Conclusion

TNA is a safe intervention that effectively alleviates postoperative pain, reduces the total consumption of sufentanil, relieves preoperative anxiety, improves the recovery of gastrointestinal function, and shortens hospitalization duration, making it an ideal adjunct treatment for the postoperative recovery of LM. Further research is required to understand the mechanisms underlying this intervention.

Data availability statement

The original contributions presented in the study are included in the article/supplementary material. Further inquiries can be directed to the corresponding author.

Ethics statement

The studies involving humans were approved by the First Affiliated Hospital of Zhejiang Chinese Medical University. The studies were conducted in accordance with the local legislation and institutional requirements. The participants provided their written informed consent to participate in this study.

Author contributions

PM: Conceptualization, Data curation, Funding acquisition, Writing – original draft. WM: Methodology, Project administration, Writing – original draft. TM: Formal analysis, Validation, Writing – review & editing. HL: Formal analysis, Methodology, Writing – original draft. XX: Methodology, Project administration, Writing – review & editing. XJ: Project administration, Supervision, Writing – review & editing. HY: Conceptualization, Funding acquisition, Methodology, Writing – review & editing, Writing – original draft.

Funding

The author(s) declare that financial support was received for the research, authorship, and/or publication of this article. This study was supported by the National Natural Science Foundation of China [No. 82104909], Zhejiang Traditional Chinese Medicine Administration [No. 2022ZB128], and the University Subject Fund of Zhejiang Chinese Medical University [No.2023JKZKTS31].

Acknowledgments

We extend our gratitude to all participants for their frank contribution.

Conflict of interest

The authors declare that the research was conducted in the absence of any commercial or financial relationships that could be construed as a potential conflict of interest.

Publisher's note

All claims expressed in this article are solely those of the authors and do not necessarily represent those of their affiliated organizations, or those of the publisher, the editors and the reviewers. Any product that may be evaluated in this article, or claim that may be made by its manufacturer, is not guaranteed or endorsed by the publisher.

References

1. Rollins KE, Lobo DN, Joshi GP. Enhanced recovery after surgery: current status and future progress. *Best Pract Res Clin Anaesthesiol*. (2021) 35:479–89. doi: 10.1016/j.bpa.2020.10.001

2. Wu X, Zheng Y. Clinicopathological features and prognostic factors for uterine myoma. *Pak J Med Sci*. (2022) 38:1580–3. doi: 10.12669/pjms.38.6.5455

3. Lee CL, Wang CJ. Laparoscopic Myomectomy. *Taiwanese J Obstetrics Gynecol*. (2009) 48:335–41. doi: 10.1016/S1028-4559(09)60321-1

4. Joshi GP. Rational multimodal analgesia for perioperative pain management. *Curr Pain Headache Rep*. (2023) 27:227–37. doi: 10.1007/s11916-023-01137-y

5. Gaulton TG, Wunsch H, Gaskins LJ, Leonard CE, Hennessy S, Ashburn M, et al. Preoperative sedative-hypnotic medication use and adverse postoperative outcomes. *Ann Surg*. (2021) 274:e108–14. doi: 10.1097/SLA.0000000000003556

6. Stamenkovic DM, Rancic NK, Latas MB, Neskovic V, Rondovic GM, Wu JD, et al. Preoperative anxiety and implications on postoperative recovery: what can we do to change our history. *Minerva Anestesiol*. (2018) 84:1307–17. doi: 10.23736/S0375-9393.18.12520-X

7. Vather R, Trivedi S, Bissett I. Defining postoperative ileus: results of a systematic review and global survey. *J Gastrointest Surg*. (2013) 17:962–72. doi: 10.1007/s11605-013-2148-y

8. Story SK, Chamberlain RS. A comprehensive review of evidence-based strategies to prevent and treat postoperative ileus. *Dig Surg*. (2009) 26:265–75. doi: 10.1159/000227765

9. Qiu RR, Zhang H, Zhao DF, Chen MY, Li D, Tan J. Acupoint selection rules of neurogenic dysphagia treated with acupuncture and moxibustion in ancient times. *Zhongguo Zhen Jiu*. (2020) 40:891–6. doi: 10.13703/j.0255-2930.20190708-k0001

10. Senna-Fernandes V, França DL, de Souza D, Santos KC, Sousa RS, Manoel CV, et al. Acupuncture at "Zusanli" (St.36) and "Sanyinjiao" (SP.6) points on the gastrointestinal tract: a study of the bioavailability of (99m)Tc-sodium Pertechnetate in rats. *Evid Based Complement Alternat Med*. (2011) 2011. doi: 10.1093/ecam/nep009

11. Lacy BE, Parkman HP, Camilleri M. Chronic nausea and vomiting: evaluation and treatment. *Am J Gastroenterol*. (2018) 113:647–59. doi: 10.1038/s41395-018-0039-2

12. Chou R, Gordon DB, de Leon-Casasola OA, Rosenberg JM, Bickler S, Brennan T, et al. Management of postoperative pain: a clinical practice guideline from the American pain society, the American Society of Regional Anesthesia and Pain Medicine, and the American Society of Anesthesiologists' committee on regional anesthesia, executive committee, and administrative council. *J Pain*. (2016) 17:131–57. doi: 10.1016/j.jpain.2015.12.008

13. Li X, Li K. Time characteristics of shoulder pain after laparoscopic surgery. *J Soc Laparoendoscopic Robotic Surgeons*. (2021) 25:e2021. doi: 10.4293/JSLS.2021.00027

14. Zhang RY, Zhang XR, Guo CF, Zeng Y, Li ZX. Clinical random trial of thumbtack needling therapy for analgesia after cesarean section. *Zhen Ci Yan Jiu*. (2022) 47:719–23. doi: 10.13702/j.1000-0607.20210959

15. Barletta JF. Clinical and economic burden of opioid use for postsurgical pain: focus on ventilatory impairment and ileus. *Pharmacotherapy*. (2012) 32:12S–8S. doi: 10.1002/j.1875-9114.2012.01178.x

16. Shaikh SI, Nagarekha D, Hegade G, Marutheesh M. Postoperative nausea and vomiting: a simple yet complex problem. *Anesth Essays Res*. (2016) 10:388–96. doi: 10.4103/0259-1162.179310

17. Weibel S, Rucker G, Eberhart LH, Pace NL, Hartl HM, Jordan OL, et al. Drugs for preventing postoperative nausea and vomiting in adults after general anaesthesia: a network meta-analysis. *Cochrane Database Syst Rev*. (2020) 2020:CD012859. doi: 10.1002/14651858.CD012859.pub2

18. Dan L, Guilin Z, Linxue Z, Yao T, Li W, Ying X, et al. Effect of thumbtack needle on functional constipation: a pragmatic randomized controlled trial. *Complement Ther Med*. (2024) 84:103069. doi: 10.1016/j.ctim.2024.103069

19. Marchand GJ, Coriell C, Taher A, King A, Ruther S, Brazil G, et al. Systematic review of the effect of implementing enhanced recovery after surgery on selected attributes of surgical recovery in gynecology. *Turk J Obstet Gynecol*. (2021) 18:245–57. doi: 10.4274/tjod.galenos.2021.47717

20. Fang JQ, Shao XM. New trains of thought about acupuncture analgesia-acupuncture analgesia feb involves multi-dimensional regulation of pain. *Zhen Ci Yan Jiu*. (2017) 42:85–9.

21. Cen L, Yi C. Therapeutic effects of auricular point acupressure on the recovery of patients after pterygium surgery: a pilot study. *Complement Ther Clin Pract*. (2021) 43:101339. doi: 10.1016/j.ctcp.2021.101339

22. Yang LH, Duan PB, Hou QM, du SZ, Sun JF, Mei SJ, et al. Efficacy of auricular acupressure for chronic low back pain: a systematic review and meta-analysis of randomized controlled trials. *Evid Based Complement Alternat Med*. (2017) 2017:6383649. doi: 10.1155/2017/6383649

23. Ni M. The yellow Emperor's classic of medicine: A new translation of the Neijing Suwen with commentary. Boston, MA: Shambhala (1995).

24. Smith CA, Collins CT, Crowther CA, Levett KM. Acupuncture or acupressure for pain management in labour. *Cochrane Database Syst Rev*. (2011) 7:CD009232. doi: 10.1002/14651858.CD009232

25. Vickers AJ, Cronin AM, Maschino AC, Lewith G, MacPherson H, Foster NE, et al. Acupuncture Trialists C: Acupuncture for chronic pain: individual patient data meta-analysis. *Arch Intern Med*. (2012) 172:1444–53. doi: 10.1001/archinternmed.2012.3654

26. Lee A, Fan LT. Stimulation of the wrist acupuncture point P6 for preventing postoperative nausea and vomiting. *Cochrane Database Syst Rev*. (2009) 2:CD003281. doi: 10.1002/14651858.CD003281.pub3

27. Smith CA, Zhu X, He L, Song J. Acupuncture for primary dysmenorrhea. *Cochrane Database Syst Rev*. (2011) 1:CD007854. doi: 10.1002/14651858.CD007854.pub2

frontiers | Frontiers in Oncology

TYPE Systematic Review
PUBLISHED 21 November 2024
DOI 10.3389/fonc.2024.1456809

OPEN ACCESS

EDITED BY
Andrea Tinelli,
Veris delli Ponti Hospital, Italy

REVIEWED BY
Robert David Hoffman,
Zhejiang Chinese Medical University, China
Jieying Zhang,
First Teaching Hospital of Tianjin University of Traditional Chinese Medicine, China

*CORRESPONDENCE
Zheng Zuo
zz120663@163.com

RECEIVED 29 June 2024
ACCEPTED 04 November 2024
PUBLISHED 21 November 2024

CITATION
Chen T, Chen X, He W, Ma X and Zuo Z (2024) Acupuncture combined with Chinese herbs versus Chinese herbs alone to improve the clinical efficacy of uterine fibroids: a systematic review and meta-analysis. *Front. Oncol.* 14:1456809.
doi: 10.3389/fonc.2024.1456809

Acupuncture combined with Chinese herbs versus Chinese herbs alone to improve the clinical efficacy of uterine fibroids: a systematic review and meta-analysis

Tianyu Chen, Xin Chen, Wei He, Xiaojing Ma and Zheng Zuo*

College of Acupuncture and Tuina, Yunnan University of Traditional Chinese Medicine, Yunnan, China

Objective: The objective of this study was to evaluate the clinical efficacy of acupuncture combined with Chinese herbs versus Chinese herbs alone in treating uterine fibroids.

Methods: A literature search of eight databases identified nine randomized controlled trials (RCTs) evaluating the clinical efficacy of acupuncture combined with Chinese herbs compared to Chinese herbs alone for treating uterine fibroids. Subsequently, data extraction and analysis were conducted to assess the methodological quality and risk of bias in the studies, followed by an analysis of the data from the randomized controlled trials.

Results: Nine randomized controlled trials involving 640 women were included. The results indicated that acupuncture combined with Chinese herbs significantly increased the overall clinical efficacy rate [Z=5.00, P=0.74, relative risk(RR)1.20, 95%CI 1.12 to 1.30, P<0.00001, I^2=0%] and reduced the size of uterine fibroids [Z=2.95, P=0.003, SMD=-0.82, 95%CI -1.36 to -0.27, P<0.00001, I^2=90%].

Conclusions: Studies have shown that acupuncture combined with Chinese herbs reduces uterine size, lowers hormone levels, and improves quality of life. According to the findings of this study, acupuncture combined with Chinese herbs has a more positive effect on the treatment of uterine fibroids than Chinese herbs alone. However, due to the limited number and quality of the included studies, these conclusions need to be validated by further high-quality research.

Systematic review registration: https://www.crd.york.ac.uk/PROSPERO/#myprospero, identifier CRD42024507248.

KEYWORDS

acupuncture, Chinese herbal medicine, uterine fibroids, clinical efficacy, systematic review, meta-analysis

Introduction

Uterine fibroids (uterine smooth muscle tumours, fibroids, or uterine fibroma) (1) are the most common type of benign tumour in the female reproductive system (2). Several factors can trigger the development of fibroids, with the primary ones being race, increasing age, family history, obesity, number of births, smoking, and lifestyle (2–5). Uterine fibroids can occur at various ages, but in China, they are most common in women between the ages of 30 and 50, with the highest incidence between 40 and 50 years old. Approximately 66% of women at the age of 50 are affected by the condition (6). Statistically, the cumulative incidence of uterine fibroids by the age of 50 is as high as 80% in African-American women and about 50% in white women (7). However, the condition is rare in women under 30, and it is extremely uncommon in women under 20. The incidence of uterine fibroids continues to rise with changes in lifestyle habits.

Most patients with uterine fibroids do not exhibit clinical symptoms (8) and require pelvic or ultrasound examinations to confirm the diagnosis, as well as to assess the location and size of the fibroids (9). However, some patients may experience symptoms such as abnormal uterine bleeding, pelvic pressure, bowel dysfunction, or genitourinary issues (10–12), which can severely affect their quality of life and daily activities. Currently, the most commonly used treatments are surgery and medication. Surgical options include myomectomy, laparoscopic dissection, uterine artery embolization, and magnetic resonance-guided focused ultrasound surgery, among others (13–15). However, these procedures often result in unavoidable side effects such as pain, fever, fertility complications, and a high likelihood of recurrence (16, 17). Pharmacological treatments include high-dose progesterone injections, oral contraceptives, and mifepristone (18), but long-term use of these medications can lead to estrogen deficiency. Both surgical and pharmacological treatments consume significant social and medical resources, placing a heavy burden on individuals and the healthcare system.

raditional Chinese Medicine (TCM) is becoming increasingly popular worldwide as a complementary and alternative treatment for uterine fibroids, with acupuncture being used to treat the condition by stimulating specific acupuncture points (19). Various methods can be used to stimulate these points, including acupuncture, electroacupuncture, warming needles, transcutaneous electrical nerve stimulation (TENS), acupoint injections, and moxibustion. Acupuncture can regulate pelvic nerves, balance female sex hormone levels, and improve blood circulation (20). Numerous clinical and animal studies have demonstrated that acupuncture can help alleviate symptoms such as heavy menstruation (21), abdominal pain, and lower back pain, as well as reduce the size of fibroids (22) in patients with uterine leiomyomas. Additionally, high-frequency TENS has been shown to reduce blood flow to the ovaries in rats (23). Other studies have indicated that using TCM or Western medicine alone has limited effectiveness in treating uterine fibroids due to the presence of numerous complications (24). Therefore, acupuncture is a reasonable alternative treatment for fibroids.

There are no detailed, high-quality, systematic methodological evaluations on the treatment of uterine fibroids using acupuncture combined with Chinese herbs. Therefore, the main objective of this study was to assess the efficacy and safety of acupuncture combined with Chinese herbs in improving the symptoms of patients with uterine fibroids. To achieve this, a systematic review and meta-analysis were conducted to compare the efficacy of acupuncture combined with Chinese herbs versus Chinese herbs alone in alleviating the symptoms of uterine fibroids, providing new evidence for the use of acupuncture combined with Chinese herbs as a treatment for uterine fibroids.

Materials and methods

This study was conducted under the Preferred Reporting Items for Systematic Evaluation and Meta-Analysis (PRISMA) (25). The study was published in the Prospective Registry for Systematic Evaluation (PROSPERO) on February 20, 2024, under the registration number CRD42024507248.

Data sources

This study searched eight databases from January 1, 2020, to January 1, 2024 [PubMed, Embase, Cochrane Central Register of Controlled Trials (CENTRAL), Web of Science (SCI), China Biomedical Database (CBM), China National Knowledge Infrastructure (CNKI), Wanfang Data Knowledge Service Platform and VIP Journal Integration Platform (VIP)], which it contains four English databases and four Chinese databases. The keywords used in the PubMed search included acupuncture, traditional Chinese medicine, leiomyomas, and randomized controlled trials. For specific search strategies, please refer to the hyperlink. PubMed retrieval type.txt.

Study selection and data extraction

Two researchers (HW and MXJ) independently screened the retrieved literature, reviewed titles and abstracts, and excluded duplicate and irrelevant studies. Based on the inclusion and exclusion criteria, eligible studies were identified, and data were extracted and cross-checked. Ambiguities were resolved through discussion. If consensus could not be reached, a third researcher (CX) was consulted to make the final decision. All excluded studies were recorded. The experimental group received acupuncture (including needling, moxibustion, electroacupuncture, and catgut implantation at acupoints) in combination with traditional Chinese medicine, while the control group received only traditional Chinese medicine. The inclusion criteria were as follows: (a) Patients definitively diagnosed with uterine fibroids through clinical and ultrasound or gynecological examinations, with no restrictions on age, gender, or source of the case; (b) the experimental group was treated with acupuncture combined with traditional Chinese medicine, and the control group was treated with traditional

Chinese medicine alone; (c) The study was a randomized controlled trial. The exclusion criteria were: (a) Subjects receiving treatments other than acupuncture and Chinese herbal medicine; (b) Duplicate publications; (c) Non-randomized controlled trials or studies with multiple control groups; (d) Reviews, systematic evaluations, animal studies, dissertations, case reports, theoretical investigations, conference abstracts, and literature not aligned with the study's purpose; (e) Studies with poorly designed trials or mismatched methodologies; (f) Studies with apparent errors or omissions; (g) Studies with incorrect or unavailable data. (Table 1).

Risk of bias assessment

The Cochrane tool was used for the risk of bias assessment (26). This tool evaluates seven key aspects: 1) Baseline comparability—whether participants in different groups are similar in key characteristics (e.g., age, sex, disease severity); 2) Random allocation method—whether participants were randomly assigned, giving each participant an equal chance of being placed in any group; 3) Concealed allocation—whether the researcher and participant were unable to predict the group assignment prior to the allocation; 4) Blinding—whether the participant, researcher, or outcome assessor was unaware of the type of intervention the participant received; 5) Completeness of outcome data—whether outcome data for all participants were fully reported; 6) Selective reporting—whether the researcher selectively reported only certain outcomes (e.g., reporting only significant results while ignoring non-significant outcomes); 7) Other sources of bias—for example, potential conflicts of interest in the study's funding, representativeness of participants, or unintended interventions or changes during the study's implementation. The results of the risk of bias assessments were entered into Review Manager 5.4 statistical software, and the risk of bias for each of the seven aspects was categorized as "low risk," "high risk," or "unclear risk."Two researchers (HW and MXJ) independently assessed these factors, and a third researcher (CX) was consulted to resolve any disagreements (Figures 1, 2).

Outcomes

Primary outcome measure: The degree of reduction in uterine fibroid size.

Statistical analysis

The I^2 test and Q test were first applied to evaluate whether there was heterogeneity among the studies, and then an appropriate effect model was selected. When $P > 0.05$ and $I^2 < 50\%$, it indicates no statistical heterogeneity among the effect sizes of the studies, and a fixed-effect model was used; When $P \leq 0.05$ and $I^2 \geq 50\%$, it indicates statistical heterogeneity among the effect sizes, and a random-effects model was selected. If statistical heterogeneity was present, the potential sources of heterogeneity were explored, and sensitivity analysis was used to assess the stability of the results if necessary. Risk Ratio (RR) was used as the effect size for categorical data and expressed as 95% confidence intervals (CI), while Mean Difference (MD) or Standardized Mean Difference (SMD) was used for continuous data in the calculation of combined statistics. Results of the meta-analysis were represented using forest plots, funnel plots, and other graphical methods.

Results

Studies retrieved

A total of 1,149 relevant papers were initially identified, and after multiple rounds of screening, nine studies (27–35) met the inclusion criteria. These nine randomized controlled trials included 640 patients who received either acupuncture or acupuncture combined with Chinese herbs for the treatment of uterine fibroids (Figure 3).

Quality of the evidence: summary of findings table

We created a "Summary of Results" table using the GRADE method to assess the quality of evidence for the outcome measures (size of uterine fibroids and overall clinical efficacy rate) in studies comparing acupuncture combined with Chinese herbs to Chinese herbs alone. The quality of evidence was evaluated using GRADE criteria, which include factors such as study limitations, inconsistency, indirectness, imprecision, and publication bias. Two investigators (HW and CTY) independently assessed the quality of the evidence (categorized as high, moderate, low, or very low) and resolved any differences through discussion. The results indicated that the quality of evidence for the reduction in uterine fibroid size was rated as "very low," while the quality of evidence for the overall clinical efficacy rate was rated as "low" (Figures 4, 5).

Results of the risk of bias assessment using the Cochrane tool

The results of the Cochrane risk of bias assessment showed the following: 1) Baseline comparability was satisfied and judged as low risk of bias. 2) The studies by Huang Qing (27) and Yang Zhen (31) used randomized allocation with random numbers, and the study by Zhou Qinglian (34) used a completely randomized allocation method. The other studies stated that they were randomized controlled trials but did not describe the specific randomization methods; these were judged as low risk of bias. 3) All studies did not explicitly report on allocation concealment, so they were judged as having unclear risk of bias. 4) All studies were non-blinded due to the limitations of the interventions and were judged as high risk of bias. 5) The outcome data were complete, so they were judged as low risk of bias. 6) None of the studies selectively reported results, so

TABLE 1 Characteristics of the studies included in this systematic review (acupuncture + Chinese herbs vs. Chinese herbs).

NO.	Study, publication year (country)	No. of patients (O/A)	Age: mean ± SD or range (years)	Duration of uterine fibroids: mean ± SD or range (years)	Intervention	Control	Period of treatment	Side effects and adverse events	Type of outcomes
1	Huang Q, 2019 (27) (China)	I:30/30 C:30/30	I:42.19 ± 3.82 (27-51) C:42.73 ± 3.94 (28-52)	I:2.43 ± 0.31 C:2.52 ± 0.34	Acupuncture + Traditional Chinese medicine	Traditional Chinese medicine	3 months	NR	total clinical efficiency, the volume of uterine fibroids
2	Fu JY, 2014 (28) (China)	I:41/41 C:40/40	I:41.5 ± 8.2 (22-50) C:40.8 ± 7.9 (21-49)	I:3 months-6 years C:4 months-5.5 years	Acupuncture + Traditional Chinese medicine	Traditional Chinese medicine	6 months	NR	total clinical efficiency, E2, FSH, LH, P
3	Zhang Y, 2018 (29) (China)	I:35/35 C:33/33	I:38.4 ± 2.5 (31-45) C:38.5 ± 2.5 (31-47)	I:3.0 ± 0.6 C:3.1 ± 0.6	Acupuncture + Traditional Chinese medicine	Traditional Chinese medicine	3 months	NR	total clinical efficiency, the volume of uterine fibroids
4	Zhang X, 2015 (30) (China)	I:40/40 C:40/40	I:44.81 ± 5.66 (20-60) C:47.49 ± 4.36 (20-60)	NR	Acupuncture + Traditional Chinese medicine	Traditional Chinese medicine	3 months	NR	total clinical efficiency, the volume of uterine fibroids
5	Yang Z, 2019 (31) (China)	I:30/30 C:30/30	I:47.8 ± 5.1 (NR) C:48.2 ± 4.5 (NR)	I:1.5 ± 0.4 C:1.9 ± 0.5	Acupuncture + Traditional Chinese medicine	Traditional Chinese medicine	1.4 months	NR	total clinical efficiency, the volume of uterine fibroids, Clinical symptoms, Quality of life
6	Peng YS, 2010 (32) (China)	I:32/32 C:30/30	I:38.6 ± 7.1 (30-57) C:37.9 ± 6.8 (31-59)	NR	Acupuncture + Traditional Chinese medicine	Traditional Chinese medicine	2 months	NR	total clinical efficiency, the volume of uterine fibroids
7	Hu JP, 2018 (33) (China)	I:43/43 C:43/43	I:43.7 ± 3.2 (30-62) C:43.7 ± 3.2 (30-62)	NR	Acupuncture + Traditional Chinese medicine	Traditional Chinese medicine	2 months	NR	total clinical efficiency, the volume of uterine fibroids
8	Zhou QL, 2018 (34) (China)	I:40/40 C:40/40	I:37.69 ± 2.14 (23-51) C:35.88 ± 2.26 (19-54)	I:1.7 ± 0.27 C:1.6 ± 0.24	Acupuncture + Traditional Chinese medicine	Traditional Chinese medicine	3 months	NR	total clinical efficiency, the volume of uterine fibroids
9	Wan LX, 2013 (35) (China)	I:32/32 C:32/32	38.5(30-49)	NR	Acupuncture + Traditional Chinese medicine	Traditional Chinese medicine	3 months	NR	total clinical efficiency, the volume of uterine fibroids

1: estradio (E2); 2: follicle-stimulating hormone (FSH); 3: Luteinizing Hormone (LH); 4: Progesterone (P).

10.3389/fonc.2024.1456809

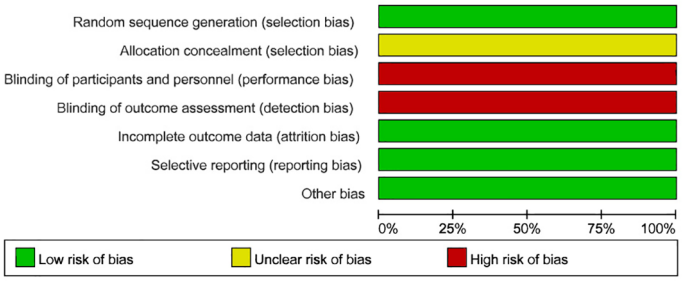

FIGURE 1
Risk of bias summary.

they were judged as low risk of bias. 7) None of them had any other sources of bias, judged as low risk of bias. (Table 2).

Main results

Size of uterine fibroids

Eight studies used fibroid volume to assess the effectiveness of treatment, involving a total of 573 participants, with 288 in the treatment group and 285 in the control group. After treatment in both groups, fibroid volume was used as the joint effect measure. The heterogeneity test revealed substantial heterogeneity, so the random-effects model was selected for the meta-analysis [Z=2.95, P=0.003, SMD= -0.82,95%CI - 1.36 to -0.27, P<0.00001, I^2=90%] (Figure 6), Sensitivity analyses were performed by excluding the studies by Zhang X (2015) and Zhou QL (2018), which resulted in P = 0.14 and I^2 = 40%. To further explore the cause of heterogeneity, we excluded the two aforementioned studies and conducted a subgroup analysis based on the publication year of the studies. The results showed P = 0.41 and I^2 = 0% for studies published before 2017, and P = 0.13 and I^2 = 46% for those published after 2017. We found that the heterogeneity for studies published before 2017 (I^2 = 0%) was significantly lower than the overall heterogeneity (I^2 = 40%). Therefore, the source of heterogeneity may be related to the publication year of the studies (Figure 7).

The overall clinical efficacy rate

Eight studies used the overall clinical efficacy rate to evaluate treatment outcomes. These studies included 576 participants, with 291 in the treatment group and 285 in the control group. A test for heterogeneity was conducted, revealing low heterogeneity and statistical significance, allowing for meta-analysis using a fixed-effects model [Z=5.00, P=0.74, relative risk(RR)1.20,95%CI 1.12 to 1.30, P<0.00001, I^2=0%]. To ensure the accuracy and stability of the results, a sensitivity analysis was performed, which showed that none of the studies significantly affected the results of the meta-analysis. This indicates that the study had good stability and suggests that the overall treatment effect in the experimental group was better than that in the control group (Figure 8). A funnel plot was generated, which appeared symmetrical, suggesting no significant publication bias in the included studies. However, some data points were located on the lower right side of the funnel, which may indicate that the relative risk (RR) of some findings was

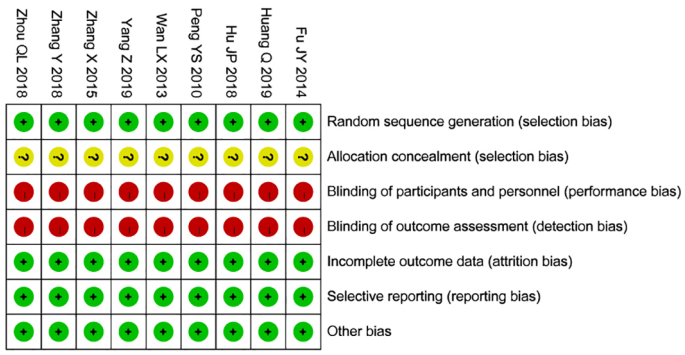

FIGURE 2
Risk of bias graph.

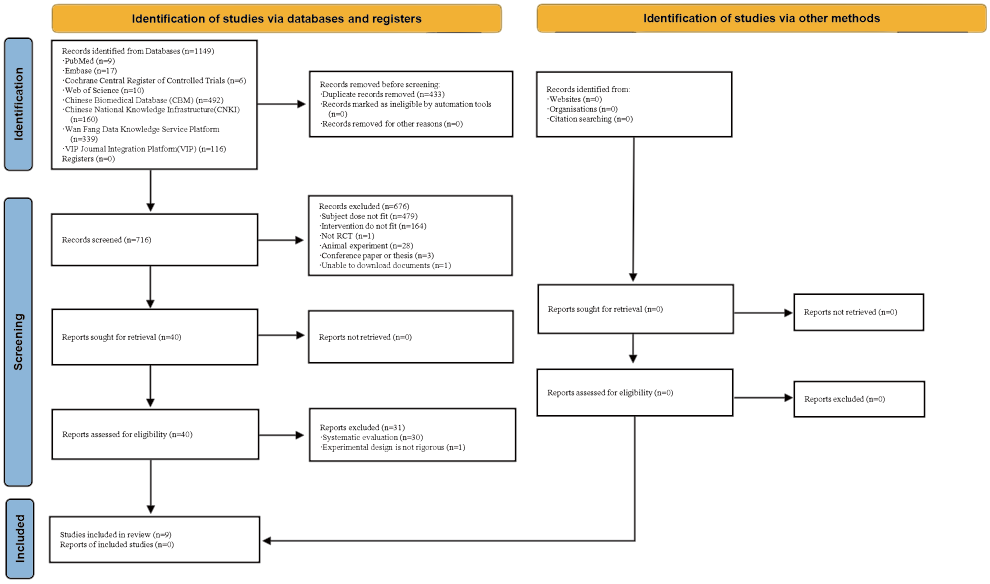

FIGURE 3
Flowchart of the study selection process.

higher than the average. While the funnel plot did not show obvious serious bias, this does not completely rule out the possibility of publication bias. Funnel plots provide only a preliminary visual assessment and cannot guarantee the absence of potential bias. For example, studies with non-significant results may not have been published, leading to a bias favoring studies with positive outcomes. Additionally, the shape of the funnel plot may be influenced by the sample size of the included studies. The relatively small number of studies included in the plot reduces its statistical power. (Figure 9).

Other outcome indicators

Only a few studies mentioned uterine volume, hormone levels, clinical symptoms, quality of life, and adverse effects, but these will not be analyzed due to incomplete data.

Discussion

Summary of main results

The meta-analysis included data from nine randomized controlled trials and 640 participants to compare the efficacy and safety of acupuncture combined with Chinese herbs versus Chinese herbs alone in the treatment of uterine fibroids. The results showed that acupuncture combined with Chinese herbs significantly increased the overall clinical effectiveness for uterine fibroids compared with Chinese herbs alone [Z=5.00, P=0.74, relative risk (RR)1.20,95%CI 1.12 to 1.30, P<0.00001, I^2=0%] (27–34), and also reduced the size of uterine fibroids [Z=2.95, P=0.003, SMD= -0.82,95%CI - 1.36 to -0.27, P<0.00001, I^2=90%] (27, 29–35). Additionally, a few studies have shown that acupuncture combined with Chinese herbs can reduce uterine size (30), lower hormone levels (E2, FSH, LH, P) (28), and improve quality of life (31).

Author(s):
Date: 2024-04-20
Question: Uterine fibroid volume for uterine fibroids
Settings:
Bibliography: . Acupuncture combined with traditional Chinese medicine versus traditional Chinese medicine for uterine fibroids. Cochrane Database of Systematic Reviews [Year], Issue [Issue].

Quality assessment							No of patients		Effect		Quality	Importance
No of studies	Design	Risk of bias	Inconsistency	Indirectness	Imprecision	Other considerations	Uterine fibroid volume	Control	Relative (95% CI)	Absolute		
Uterine fibroid volume (Better indicated by lower values)												
8	randomised trials	serious[1]	very serious[2]	no serious indirectness	serious[3]	none	288	285	-	SMD 0.82 lower (1.36 to 0.27 lower)	⊕OOO VERY LOW	CRITICAL

[1] Allocation of concealment is not clear
[2] P≥75%
[3] Small sample size

FIGURE 4
Quality of evidence assessment scale for uterine fibroid volume.

Author(s):
Date: 2024-04-20
Question: Total effective rate for uterine fibroids
Settings:
Bibliography: . Acupuncture combined with traditional Chinese medicine versus traditional Chinese medicine for uterine fibroids. Cochrane Database of Systematic Reviews [Year], Issue [Issue].

Quality assessment							No of patients		Effect		Quality	Importance
No of studies	Design	Risk of bias	Inconsistency	Indirectness	Imprecision	Other considerations	Total effective rate	Control	Relative (95% CI)	Absolute		
Total effective rate												
8	randomised trials	serious[1]	no serious inconsistency	no serious indirectness	serious[2]	none	267/291 (91.8%)	217/285 (76.1%)	RR 1.2 (1.12 to 1.3)	152 more per 1000 (from 91 more to 228 more)	⊕⊕OO LOW	IMPORTANT
								75.8%		152 more per 1000 (from 91 more to 227 more)		

[1] Allocation of concealment is not clear
[2] Small sample size

FIGURE 5
Quality of evidence assessment scale for total effective rate.

Subgroup analysis of uterine leiomyoma volume indicated that the source of heterogeneity was related to the publication date of the studies. Several factors may account for this. First, the increased heterogeneity between studies conducted before and after 2017 may be related to changes in diagnostic and treatment standards. In China, the diagnostic criteria and treatment protocols for uterine fibroids have evolved in recent years due to advances in medicine and updated guidelines. For example, starting in 2017, new diagnostic equipment and techniques, such as more precise ultrasound and MRI, were widely adopted, likely leading to more accurate measurements of fibroid volume. This suggests that studies conducted after 2017 reported more accurate data on fibroid volume, whereas pre-2017 studies relied on more basic measurement techniques, resulting in a wider range of data and reducing comparability. Second, earlier treatments primarily involved surgery and traditional Chinese medicine, while newer combination therapies, such as acupuncture, moxibustion, and acupoint catgut embedding, have gradually become more prevalent in clinical studies over time. The introduction of these newer therapies may have introduced additional variables between studies. For instance, acupoint catgut embedding combined with Chinese herbal medicine significantly reduced leiomyoma size, whereas Chinese herbal medicine alone had a relatively weaker effect. These differences in treatment regimens likely contributed to increased heterogeneity in outcomes, particularly as newer therapies became more commonly studied after 2017. Finally, studies conducted before 2017 may have employed simpler statistical methods, while more recent studies, benefiting from advancements in study design and statistical analysis—such as the wider use of random-effects models—are better able to capture data variability. As a result, post-2017 studies may display greater heterogeneity due to the use of more sophisticated analytical methods.

These findings are consistent with previous systematic reviews and randomized controlled trials. Additionally, several studies have demonstrated that acupuncture, either alone or in combination with traditional Chinese medicine, can more effectively improve various clinical symptoms in patients with uterine fibroids. These studies further validate our results.

Secondly, acupuncture works to reduce the size of fibroids by selecting appropriate acupuncture points based on the patient's specific symptoms. While acupuncture therapy does not directly

TABLE 2 Cochrane risk of bias assessment.

NO.	Author	Publication year	Baseline comparability	Random allocation	Allocation concealment	Blinding	Integrity of results data	Selective reporting of findings	Other sources of bias
NO.1	Huang Q	2019	√	①	Inaccurate	Non-blind	√	×	×
NO.2	Fu JY	2014	√	②	Inaccurate	Non-blind	√	×	×
NO.3	Zhang Y	2018	√	②	Inaccurate	Non-blind	√	×	×
NO.4	Zhang X	2015	√	②	Inaccurate	Non-blind	√	×	×
NO.5	Yang Z	2019	√	①	Inaccurate	Non-blind	√	×	×
NO.6	Peng YS	2010	√	②	Inaccurate	Non-blind	√	×	×
NO.7	Hu JP	2018	√	②	Inaccurate	Non-blind	√	×	×
NO.8	Zhou QL	2018	√	③	Inaccurate	Non-blind	√	×	×
NO.9	Wan LX	2013	√	②	Inaccurate	Non-blind	√	×	×

1: Random number—①; Randomized control methods, but no specific random assignment method described—②; Totally random—③.

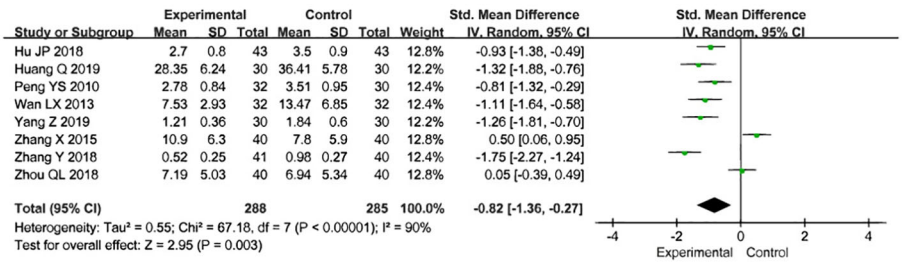

FIGURE 6
Meta analysis results of acupuncture combined with traditional Chinese medicine in the treatment of uterine fibroid volume reduction.

cause fibroids to disappear, it can help shrink them by regulating the body's endocrine system, improving the circulation of qi and blood, and exerting an inhibitory effect on fibroid growth.

Clinical trials have shown that acupuncture has a positive effect on endometriosis, significantly reducing pain levels, shortening the duration of pain, relieving anxiety and depression, and improving patients' quality of life, as indicated by the Visual Analog Scale (VAS) score. However, its efficacy diminishes once treatment is stopped (36). Additionally, acupuncture has been shown to reduce the size of ectopic cysts, lower serum carbohydrate antigen 125 (CA125) levels, regulate serum sex hormones, improve ovarian reserve function, increase pregnancy rates, and reduce recurrence rates and adverse effects. The mechanisms of acupuncture primarily involve the inhibition of angiogenesis, suppression of estrogen and its receptors, regulation of immune function, and pain relief (37). Animal experiments have demonstrated that electroacupuncture promotes the transition of the uterus to the active phase in late-pregnant rats by altering hormone levels in serum and uterine tissues, and it enhances coordinated uterine contractions by increasing the expression of uterine gap junction proteins (38).

Overall, these findings suggest that acupuncture provides more effective treatment for uterine diseases compared to herbal medicine alone.

Overall completeness and applicability of evidence

None of the nine studies reported follow-up or withdrawal data, making it difficult to assess the long-term effects of treatment and relapse rates. Additionally, no violations of assigned treatments were noted. None of the studies specified whether the trial investigator and outcome assessor were the same person, which introduces potential bias. Bias may arise when the trial investigator also assesses participants' outcomes. Furthermore, only one study reported adverse effects (31). Although the benefits of acupuncture appear to outweigh its drawbacks, we are not entirely confident about its safety. The total sample size of 640 patients across nine trials results in a small average sample size per trial, which may have led to a lack of statistical power and an increased likelihood of false-negative results. Even if the treatment effect is significant, the study may not detect it due to insufficient sample size. Trials with small sample sizes are more susceptible to the influence of individual data points, leading to unstable results. For example, an individual patient's response may disproportionately impact the overall findings, making conclusions vulnerable to being skewed by outliers. Additionally, rare adverse reactions may go undetected due to the limited statistical data. The limited number of

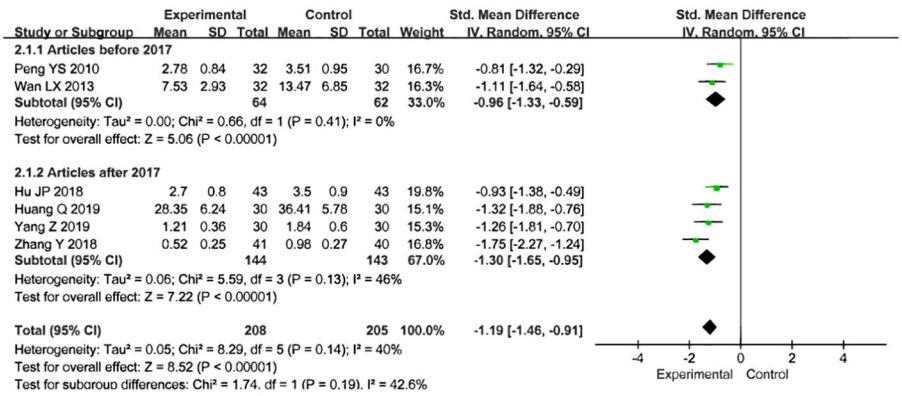

FIGURE 7
Subgroup analysis of uterine fibroid volume.

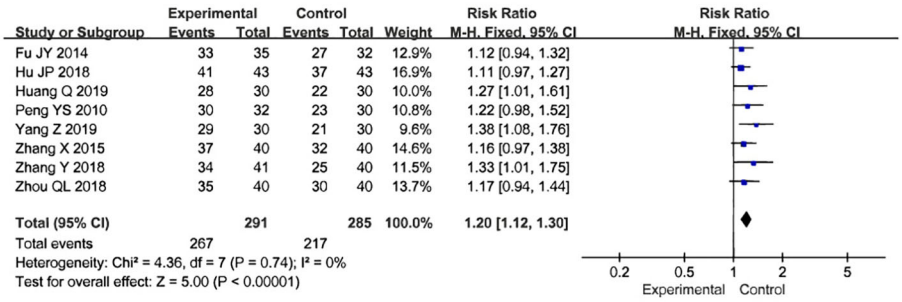

FIGURE 8
Forest map of total efficiency of acupuncture combined with traditional Chinese medicine in the treatment of uterine fibroids.

randomized controlled trials and participants means that the available evidence on the effectiveness of acupuncture combined with Chinese herbs for treating uterine fibroids remains incomplete. Future research should focus on conducting multicenter randomized controlled trials to increase sample sizes and improve statistical power. Multicenter studies can cover broader regions and populations, enhancing the generalizability of the results. For instance, recruiting patients from different racial and geographic backgrounds—such as populations in Asia, Europe, and Africa—could help validate the treatment's applicability across diverse groups. International collaborations could also expand patient recruitment and facilitate resource sharing. Collaborating with hospitals and research institutions in other countries would help validate the global efficacy of acupuncture and herbal medicine for uterine fibroids.

Quality of the evidence

Overall, this meta-analysis had a low risk of bias (Figures 1, 2), but was rated as high risk in terms of blinding, as all trials were unblinded. This lack of blinding may lead to several issues: (1) When researchers know which treatment participants received, they may unintentionally influence their evaluation or recording of the results; (2) When participants know they are receiving a particular treatment, their expectations and attitudes may influence the results. This phenomenon is known as the placebo effect or the nocebo effect (anti-placebo effect); (3) Participants' compliance may be affected when they are aware of receiving either a new drug or a control treatment. If participants know they are assigned to the control group, they may lose motivation to continue participating, leading to decreased adherence or even withdrawal. This may affect data integrity and the accuracy of the analysis; (4) In some cases, non-blinded trials are designed for ethical reasons, such as ensuring participants are fully informed. However, researchers, aware of the treatment allocation, may unintentionally alter their care or treatment of participants, affecting the objectivity of the trial; (5) Bias may lead to overestimation or underestimation of effect sizes. It becomes difficult to discern whether the observed effects are genuine results of the treatment or artifacts of the researchers' and participants' expectations. While statistical models can adjust for potential bias, they cannot entirely eliminate its effects. Moreover, none of the studies mentioned whether allocation concealment was implemented. The source of bias may also be related to participant characteristics (e.g., age, diagnostic criteria, severity of uterine fibroids), the method of acupuncture (e.g., needling, electroacupuncture, moxibustion, or acupoint catgut embedding), the selection and dosage of Chinese herbs, specific symptoms, and the course of treatment. Some studies also had limited reporting due to small sample sizes and differences in interventions. Therefore, the results of this meta-analysis should be interpreted with caution.

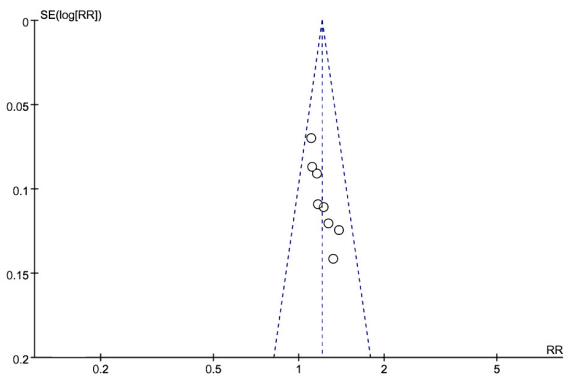

FIGURE 9
Funnel map of total effective rate of acupuncture combined with traditional Chinese medicine in the treatment of uterine fibroids.

Potential biases in the review process

We conducted an extensive search across multiple databases to reduce the likelihood of missing relevant studies. We also recognized the potential for publication bias, as this systematic review did not include trials with negative results. However, all the randomized controlled trials included in this study were conducted in China, with the study population primarily consisting of Chinese women. These participants were treated with acupuncture and herbal medicine, both of which are traditional Chinese therapies. This geographic and demographic limitation may affect the

generalizability of the findings, particularly when applying them to non-Asian populations. Different ethnic groups and regions may exhibit significant variations in genetics, environment, lifestyle, and disease manifestation. As a result, the applicability and effectiveness of acupuncture combined with Chinese herbal treatments for uterine fibroids in non-Asian populations remain uncertain, necessitating further research across diverse regions and ethnicities to validate the broader relevance of these findings. Despite our efforts to search both Chinese and English databases, all the eligible studies were conducted in China, and the trial reports were brief, with some critical information either unclear or missing. Additionally, we were unable to obtain further clarification from the trial investigators despite attempts via email and phone. These factors may introduce bias into the current review.

The actual contribution and impact of clinical practice

The contribution of this meta-analysis to clinical practice lies in its provision of systematic, quantitative evidence supporting the effectiveness of acupuncture combined with Chinese herbs in treating uterine fibroids. Compared with Chinese herbs alone, the combination of acupuncture and Chinese herbs enhanced the overall treatment effectiveness and significantly reduced the size of uterine fibroids. This finding serves as an important reference for physicians when selecting appropriate treatment options in clinical settings.

First, for clinicians, integrating acupuncture with Chinese herbs offers a more comprehensive treatment option for patients with uterine fibroids. Based on the results of this study, clinicians can consider acupuncture combined with herbal medicine as a safe and effective non-invasive treatment option for patients who prefer to avoid surgery or are not eligible for surgical interventions.

Secondly, for patients with large fibroids or severe symptoms, acupuncture combined with Chinese herbs can help reduce the size of fibroids by regulating the endocrine system and improving blood circulation, thereby alleviating associated symptoms and enhancing overall quality of life. This approach allows the therapy to play an active role in symptom management and long-term treatment.

In conclusion, the findings of this study provide a strong scientific basis for the integration of Chinese and Western medicine in the treatment of uterine diseases. Specifically, for uterine fibroids—a chronic condition—acupuncture combined with Chinese herbs offers a more comprehensive therapeutic option, underscoring the importance of individualized treatment. Selecting the appropriate acupoints and herbal formulas based on clinical symptoms can further improve the precision and effectiveness of treatment.

Despite the positive findings of this study regarding the effectiveness of acupuncture, clinicians should remain mindful of its limitations, such as the small sample size and insufficient follow-up data. Therefore, in clinical practice, it is recommended that patient symptom changes be regularly monitored when incorporating acupuncture into treatment, and that other conventional therapies be combined to maximize efficacy. Additionally, more high-quality clinical trials with long-term follow-up are needed to strengthen the reliability and broader applicability of the evidence.

Conclusion

Implications for practice

We cannot rule out the possibility of clinically relevant differences between acupuncture combined with Chinese herbs and Chinese herbs alone in terms of overall clinical efficacy, reduction in the size of uterine fibroids, levels of E2, FSH, LH, and P, as well as improvements in clinical symptoms and quality of life. Compared with Chinese herbs alone, acupuncture combined with Chinese herbs was found to improve overall clinical efficacy, reduce fibroid size, and positively affect hormone levels (E2, FSH, LH, P), clinical symptoms, and quality of life. However, due to the low quality of evidence in this field and the limited number of clinical trials available, we could only conclude that acupuncture combined with Chinese herbs appears more effective than Chinese herbs alone in treating uterine fibroids.

Implications for research

It is hoped that acupuncture combined with Chinese herbs will improve the overall clinical outcomes for patients with uterine fibroids. Under unified diagnostic criteria, a standardized set of acupoints and stimulation methods should be used, and the control group should receive the same herbal treatment as the acupuncture group.

Data availability statement

The original contributions presented in the study are included in the article/supplementary material. Further inquiries can be directed to the corresponding author.

Author contributions

TC: Conceptualization, Data curation, Formal analysis, Investigation, Methodology, Software, Writing – original draft, Writing – review & editing. XC: Project administration, Supervision, Validation, Writing – original draft, Writing – review & editing. WH: Investigation, Methodology, Visualization, Writing – original draft, Writing – review & editing. XM: Formal analysis, Investigation, Methodology, Writing – original draft, Writing – review & editing. ZZ: Funding acquisition, Resources, Supervision, Writing – original draft, Writing – review & editing.

Funding

The author(s) declare financial support was received for the research, authorship, and/or publication of this article. This work was supported by the National Key Basic Research Program (Grant numbers: 202301AZ070001-009).

Acknowledgments

The authors thank to the National Key Basic Research Program for their financial support.

Conflict of interest

The authors declare that the research was conducted in the absence of any commercial or financial relationships that could be construed as a potential conflict of interest.

Publisher's note

All claims expressed in this article are solely those of the authors and do not necessarily represent those of their affiliated organizations, or those of the publisher, the editors and the reviewers. Any product that may be evaluated in this article, or claim that may be made by its manufacturer, is not guaranteed or endorsed by the publisher.

References

1. Donnez J, Dolmans MM. Uterine fibroid management: from the present to the future. *Hum Reprod Update*. (2016) 22:665–86. doi: 10.1093/humupd/dmw023

2. Ciebiera M, Włodarczyk M, Ciebiera M, Zaręba K, Łukaszuk K, Jakiel G. Vitamin D and uterine fibroids-review of the literature and novel conce-pts. *Int J Mol Sci*. (2018) 19:2051. doi: 10.3390/ijms19072051

3. Baker JM, Chase DM, Herbst-Kralovetz MM. Uterine microbiota: residents, Tourists, or invaders? *Front Immunol*. (2018) 9:1874. doi: 10.3389/fimmu.2018.01874

4. Lee G, Kim S, Bastiaensen M, Malarvannan G, Poma G, Caballero Casero N, et al. Exposure to organophosphate esters, phthalates, and alternative pl-asticizers in association with uterine fibroids. *Environ Res*. (2020) 189:109874. doi: 10.1016/j.envres.2020.109874

5. Wong JY, Chang PY, Gold EB, Johnson WO, Lee JS. Environmental tobacco smoke and risk of late-diagnosis incident fibroids in the Study of Women's Health across the Nation (SWAN). *Fertil Steril*. (2016) 106:1157–64. doi: 10.1016/j.fertnstert.2016.06.025

6. Stewart EA, Laughlin-Tommaso SK, Catherino WH, Lalitkumar S, Gupta D, Vollenhoven B. Uterine fibroids. *Nat Rev Dis Primers*. (2016) 2:16043. doi: 10.1038/nrdp.2016.44

7. Zhang Y, Peng W, Clarke J, Liu Z. Acupuncture for uterine fibroids. *Coc-hrane Database Syst Rev*. (2010) 1):CD007221. doi: 10.1002/14651858.cd007221.pub2

8. Liu T, Yu J, Kuang W, Wang X, Ye J, Qiu X, et al. Acupuncture for ut-erine fibroids: Protocol for a systematic review of randomized controlled tr-ials. *Med (Baltimore)*. (2019) 98:e14631. doi: 10.1097/md.0000000000014631

9. Van Voorhis B. A 41-year-old woman with menorrhagia, anemia, and fibroids: review of treatment of uterine fibroids. *JAMA*. (2009) 301:82–93. doi: 10.1001/jama.2008.791

10. Drayer SM, Catherino WH. Prevalence, morbidity, and current medical management of uterine leiomyomas. *Int J Gynaecol Obstet*. (2015) 131:117–22. doi: 10.1016/j.ijgo.2015.04.051

11. Bukulmez O, Doody KJ. Clinical features of myomas. *Obstet Gynecol Clin North Am*. (2006) 33:69–84. doi: 10.1016/j.ogc.2005.12.002

12. Donnez J, Jadoul P. What are the implications of myomas on fertility? A need for a debate? *Hum Reprod*. (2002) 17:1424–30. doi: 10.1093/humrep/17.6.1424

13. Lumsden MA, Hamoodi I, Gupta J, Hickey M. Fibroids: diagnosis and management. *BMJ*. (2015) 351:h4887. doi: 10.1136/bmj.h4887

14. Stewart EA. Clinical practice. Uterine fibroids. *N Engl J Med*. (2015) 372:1646–55. doi: 10.1056/nejmcp1411029

15. Zupi E, Centini G, Sabbioni L, Lazzeri L, Argay IM, Petraglia F. Nonsurgical alternatives for uterine fibroids. *Best Pract Res Clin Obstet Gynaecol*. (2016) 34:122–31. doi: 10.1016/j.bpobgyn.2015.11.013

16. Celik H, Sapmaz E. Use of a single preoperative dose of misoprostol is efficacious for patients who undergo abdominal myomectomy. *Fertil Steril*. (2003) 79:1207–10. doi: 10.1016/s0015-0282(03)00076-1

17. Frederick J, Hardie M, Reid M, Fletcher H, Wynter S, Frederick C. Opera-tive morbidity and reproductive outcome in secondary myomectomy: a pros-pective cohort study. *Hum Reprod*. (2002) 17:2967–71. doi: 10.1093/humrep/17.11.2967

18. Chwalisz K, Taylor H. Current and emerging medical treatments for uter-ine fibroids. *Semin Reprod Med*. (2017) 35:510–22. doi: 10.1055/s-0037-1606302

19. Garland SN, Xie SX, DuHamel K, Bao T, Li Q, Barg FK, et al. Acupuncture versus cognitive behavioral therapy for insomnia in cancer survivors: A randomized clinical trial. *J Natl Cancer Inst*. (2019) 111:1323–31. doi: 10.1093/jnci/djz050

20. Wen Q, Hu M, Lai M, Li J, Hu Z, Quan K, et al. Effect of acupuncture and metformin on insulin sensitivity in women with polycystic ovary syndrome and insulin resistance: a three-armed randomized controlled trial. *Hum Reprod*. (2022) 37:542–52. doi: 10.1093/humrep/deab272

21. Cakmak YÖ, Akpınar IN, Yoldemir T, Cavdar S. Decreasing bleeding due to uterine fibroid with electroacupuncture. *Fertil Steril*. (2011) 96:e13–5. doi: 10.1016/j.fertnstert.2011.03.110

22. Cruz J, Carrington L, Hong H. A feasibility study on treatment of uterine fibroids with tung's acupuncture. *Med Acupunct*. (2019) 31:384–91. doi: 10.1089/acu.2019.1385

23. Stener-Victorin E, Kobayashi R, Watanabe O, Lundeberg T, Kurosawa M. Effect of electro-acupuncture stimulation of different frequencies and intensi-ties on ovarian blood flow in anaesthetized rats with steroid-induced polyc-ystic ovaries. *Reprod Biol Endocrinol*. (2004) 2:16. doi: 10.1186/1477-7827-2-16

24. Farris M, Bastianelli C, Rosato E, Brosens I, Benagiano G. Uterine fibroids: an update on current and emerging medical treatment options. *Ther Clin Risk Manage*. (2019) 15:157–78. doi: 10.2147/tcrm.s147318

25. Page MJ, Mckenzie JE, Bossuyt PM, Boutron I, Hoffmann TC, Mulrow CD, et al. The PRISMA 2020 statement: an updated guideline for reporting systematic reviews. *bmj*. (2021) 372:n71. doi: 10.1371/journal.pmed.1003583

26. Sterne JAC, Savović J, Page MJ, Elbers RG, Blencowe NS, Boutron I, et al. RoB2: a revised tool for assessing risk of bias in randomised trials. *BMJ*. (2019) 366:l4898. doi: 10.1136/bmj.l4898

27. Huang Q. Clinical efficacy of electroacupuncture combined with Shaofuzhuyu Tang in the treatment of uterine fibroids and its effect on the volume of fibroids. *J Electrocardiogram (Electronic Edition)*. (2019) 8:88–9.

28. Fu JY, Chen X, Fu K. Clinical study on the treatment of uterine fibroids with Gui Zhi Fu Ling capsule combined with moxibustion. *Chin J Traditional Med Sci Technol*. (2014) z1:6–7.

29. Zhang Y. Clinical observation on the treatment of uterine fibroid by combi-ning moxibustion with Gui Zhi Fu Ling Wan. *J Pract Trad-itional Chin Med*. (2018) 34:290–1. doi: 10.3969/j.issn.1004-2814.2018.03.017

30. Zhang X. Clinical observation on the efficacy of acupoint burrowing combined with Gui Zhi Fu Ling capsule on uterine fibroids. *New Mom New Born*. (2015) 22):57–7.

31. Yang Z, Li XX, Li QP. Clinical study on the treatment of uterine fibroids by acupuncture with traditional Chinese medicine formulas of Huo Xue Xiao Zheng. *Traditional Chin Med Rehabil*. (2019) 10:30–2. doi: 10.19787/j.issn.1008-1879.2019.14.013

32. Peng YS, Qian X, Peng GJ. Study on the theraputic effect of comprehensi-ve treatment by Acupuncture with Chinese herbs on hysteromyoma. *Ch-ina Med Herald*. (2010) 7:82–3. doi: 10.3969/j.issn.1673-7210.2010.02.050

33. Hu JP. Study on the theraputic effect of comprehensive treatment by Acupuncture with Chinese herbs on hysteromyoma. *psychol Doctor*. (2018) 24:62.

34. Zhou QL, Liu J, Du YJ. A randomized controlled study on the treatment of uterine fibroids with a combination of acupuncture and traditional Chinese medicine. *Hebei J Traditional Chin Med*. (2018) 40:1245–7. doi: 10.3969/j.issn.1002-2619.2018.08.028

35. Wan LX. Analysis of the efficacy of combined treatment of uterine f-ibroids with traditional Chinese medicine and electroacupuncture and moxib-ustion. *J Mudanjiang Med Univ*. (2013) 34:69–71. doi: 10.13799/j.cnki.mdjyxyxb.2013.06.013

36. Li PS, Peng XM, Niu XX, Xu L, Hung Yu Ng E, Wang CC, et al. Efficacy of acupuncture for endometriosis-associated pain: a multicenter randomized single-blind placebo-controlled trial. *Fertil Steril*. (2023) 119:815–23. doi: 10.1016/j.fertnstert.2023.01.034

37. Mu YF, Song CH, Xie LZ, Fu Y, Yu Y, Wang Y, et al. Progress in clinical and mechanistic research on acupuncture treatment for endometriosis. *Inf Traditional Chin Med*. (2024) 41:85–90. doi: 10.19656/j.cnki.1002-2406.20240115

38. Yuan HW, Su FZ, Chen YR, Li CH, Liu YQ, Ma LX, et al. Effect of conventional midwifery prescription on coordinated contraction of uterine smooth muscle in late trimester rats. *China J Traditional Chin Med Pharm*. (2013) 28:1207–11.

Frontiers in Medicine

Translating medical research and innovation into improved patient care

A multidisciplinary journal which advances our medical knowledge. It supports the translation of scientific advances into new therapies and diagnostic tools that will improve patient care.

Discover the latest Research Topics

See more →

Frontiers

Avenue du Tribunal-Fédéral 34
1005 Lausanne, Switzerland
frontiersin.org

Contact us

+41 (0)21 510 17 00
frontiersin.org/about/contact